Letter from the Editors

Research in the field of Living Systems is unthinkable without international cooperation. One of the important sections in our journal is now devoted to reviews penned by leading domestic and foreign scientists. These authors represent the leading scientific schools of Russia, Europe, and the U.S..

In addition, we publish the results of work conducted by international research groups in the experimental section of our journal. Hence, this issue contains an article written in collaboration with our Japanese colleagues that focuses on the study of the enzyme deacylation process for the family of penicillin-binding proteins. Another experimental paper written by a team of German scientists highlights the possibility of using 2D-gel electrophoresis to study a receptor complex.

Some of the materials in the section "Forum" are devoted to an important aspect of international cooperation in the field of Living Systems: the article is about customs tariffs as barriers to the development of biotechnology and possible ways to overcome them.

Taking further the topic of state support of science initiated in the previous issue (*Acta Naturae*, 2010, Volume 2, № 1 (4)), we are offering material on the implementation of the Federal Target Program Research and Scientific-Pedagogical Human Resources.

We are also exited to share with our readers some good news: the journal *Acta Naturae* has been entered into the list of the leading periodicals of the Higher Attestation Commission of the Russian Ministry of Education and Science. We hope this distinction will steer more and more young researchers in our direction.

Editorial Board

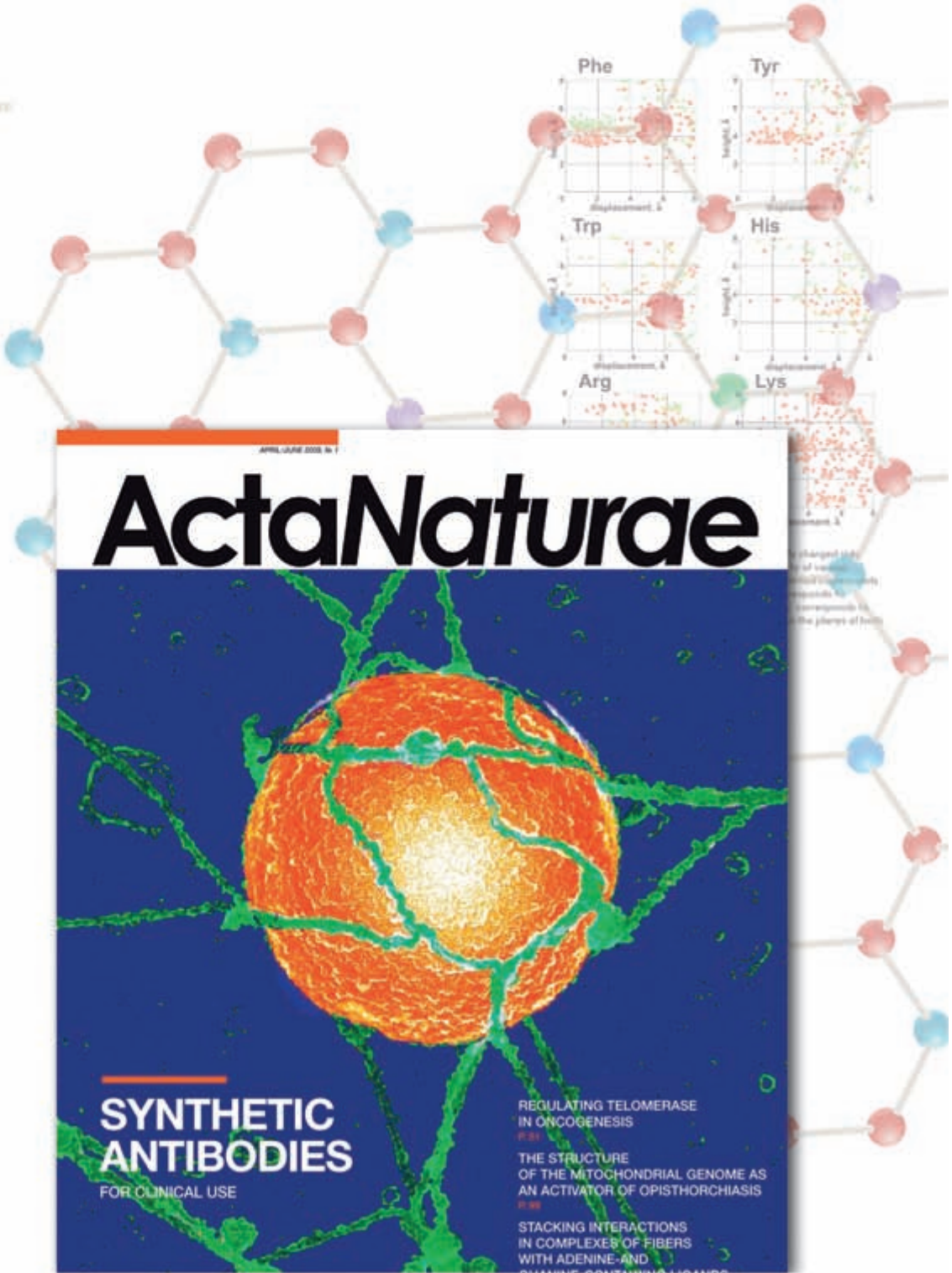

D. Riess, I. Lavrik

2D-gel Electrophoresis As a Tool to Investigate the Composition of CD95 DISC

In this work, the composition of the CD95 DISC in two different cell types was analyzed using proteomics approaches. Using 2D gels, the composition of the CD95 DISC was analyzed in the so-called Type I and Type II cells, which are characterized by different kinetics of apoptosis. The detailed analysis of the CD95 DISC demonstrated that, besides the well-established components of the CD95 DISC, which are present in both cell types (CD95, FADD and procaspase-8), there are a number of differential spots detected at the CD95 DISC of Type I *versus* Type II cells. Taken together, this work demonstrates the differential composition of the CD95 DISC of Type I *versus* Type II cells.

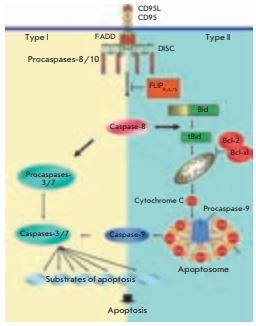

Scheme of Type I and Type II apoptotic pathways

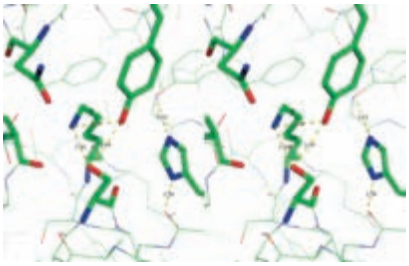

Stereo view of the D-aminopeptidase active site and spatial organization of catalytic triad.

I.G. Khaliullin, D.A. Suplatov, D.N. Shalaeva, M. Otsuka, Y. Asano, V.K. Švedas

Bioinformatic Analysis, Molecular Modeling of Role of Lys65 Residue in Catalytic Triad of D-aminopeptidase from *Ochrobactrum anthropi*

The resulting data have been used to elucidate the role of Lys65 in the catalytic mechanism of D-aminopeptidase as a general base for proton transfer from catalytic Ser62 to Tyr153, and vice versa, during the formation and hydrolysis of the acylenzyme intermediate.

S. P. Medvedev, A. A. Malakhova, E. V. Grigor'eva, A. I. Shevchenko, E. V. Dementyeva, I. A. Sobolev, I. N. Lebedev, A .G. Shilov, I. F. Zhimulev, S. M. Zakian

Derivation of Induced Pluripotent Stem Cells from Fetal Human Skin Fibroblasts

In this study we reprogrammed fetal human skin fibroblasts by transduction with retroviral vectors carrying murine *Oct4*, *Sox2*, *Klf4*, and *c-Myc* cDNAs. As a result, cells with the protein expression and gene transcription pattern characteristic of human embryonic stem cells were derived.

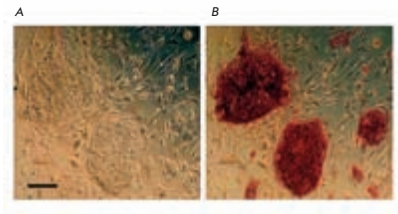

Morphology of iPSC colonies derived from human embryonic fibroblasts

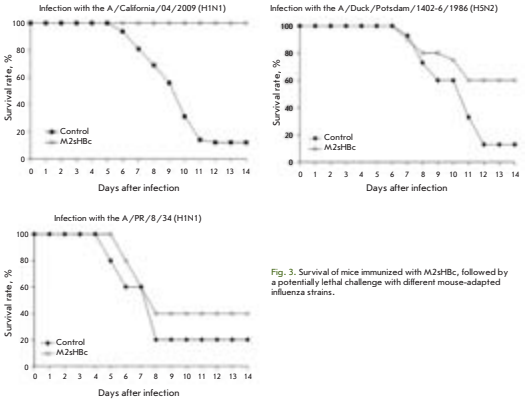

Fig. 3. Survival of mice immunized with M2sHBc, followed by a potentially lethal challenge with different mouse-adapted influenza strains.

Survival of mice immunized with M2sHBc, followed by a potentially lethal challenge with mouse-adapted influenza strains.

R.Y. Kotlyarov, V.V. Kuprianov, A.I. Migunov, L.A. Stepanova, L.M. Tsybalova, O.I. Kiselev, N.V. Ravin, K.G. Skryabin

Development of Recombinant Vaccine against A(H1N1) 2009 Influenza Based on Virus-like Nanoparticles Carrying the Extracellular Domain of M2 Protein

We constructed recombinant nanosized virus-like particles based on a nuclear antigen of the hepatitis B virus. These particles expose on the surface the extracellular domain of the M2 protein of the highly pathogenic A(H1N1) 2009 influenza virus. Experiments on animals show that M2sHBc particles are highly immunogenic in mice and provide complete protection against the lethal influenza challenge.

ActaNaturae
APRIL–JUNE 2010, VOL. 2 № 2 (5)

Founders
Russian Federation Agency
for Science and Innovation,
Lomonosov Moscow State University,
Park Media Ltd

Address: 119991 Moscow, Russia, Leninskiye Gory, Nauchny
Park MGU, vlad.1, stroeniye 75G.
Phone/Fax: +7 (495) 930 80 06
E-mail: knorrevd@gmail.com, enovoselova@strf.ru, biomem@mail.ru

Номер подписан в печать 18 июня 2010 г.
Тираж 300 экз. Цена свободная.
Отпечатано в типографии «МЕДИА-ГРАНД»

CONTENTS

RESEARCH ARTICLES

SHORT REPORTS

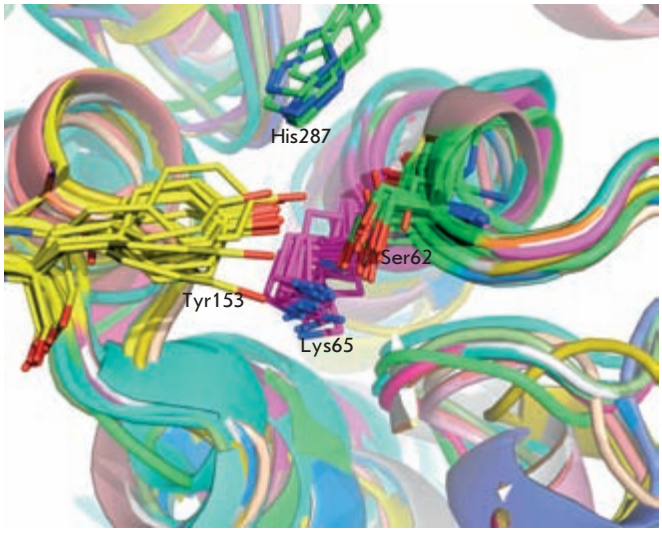

IMAGE ON THE COVER PAGE
An active site fragment of the structural alignment of penicillin-binding proteins – structural homologs of D-aminopeptidase from *Ochrobactrum anthropi*.

Russian Federation State Prize in Science and Technology for 2009

The Russian Federation State Prize in Science and Technology for 2009 honoring scientists for "A Set of Scientific Works on the Development of Laser and Information Technologies in Medicine" (Presidential Decree no. 678, June 6, 2010) was awarded to V.Ya. Panchenko, doctor of physical and mathematical sciences, academician of the Russian Academy of Sciences, director of the Institute of Laser and Information Technologies, Russian Academy of Sciences; to A.A. Potapov, doctor of medical sciences, Russian Academy of Medical Sciences, deputy director of the Burdenko Neurosurgery Research Institute, Medical Academy of Medical Sciences; and to V.I. Chissov, doctor of medical sciences, academician of the Russian Academy of Medical Sciences, director of Herzen's Cancer Research Institute, Moscow.


V.Ya. Panchenko


A.A. Potapov


V.I. Chissov

In the work of these scientists, a system for the remote production of individual implants and biomodels based on tomography data of the evaluation of pre-surgery patients via the Internet to a center for rapid prototyping and manufacturing was established for the first time ever. Original locally conceived systems for rapid prototyping, namely, laser systems and selective laser sintering of micro-, nano-, and biocompatible materials, were designed and manufactured. Biomodels created based on these materials are being used for pre-surgery planning.

This technology of preoperative biomodeling is being widely used in neurosurgery, oncology, and reconstructive surgery at many hospitals in different regions of Russia and other countries. The effectiveness of operational preplanning using biomodels is demonstrated in the significant reduction in time and in the improvement of treatment outcomes in neurosurgery, maxillofacial surgery, reconstructive surgery, and oncology.

A huge amount of problems related to traumatic brain injury are solved through neurosurgery. For the first time, technology and methods for obtaining and producing stereo lithographic models that are fully congruent to real facial and cranial defects are being developed, therefore radically changing plastic and reconstructive microsurgery and allowing for the accumulation of the largest body of clinical material both in the country and in the world.

Technology to manufacture individual implants from various biocompatible materials and molds for its production using the "symmetric stereo lithography" method, as well as a database of "online donors," are being developed.

For the first time, a special form of traumatic brain injury (crush syndrome of the head) has been described. Several other technologies are being developed and implemented in practice, such as computer simulation of preoperative craniocerebral operations and intraoperative navigation technology, including three-dimensional CT, MRI, and ultrasound images; optical fluorescence; neurophysiologic mapping; and neuromonitoring.

These concepts and technology for reconstructive neurosurgery, which yield restoration of the structural integrity of the brain's functionality and the individual configuration of the skull, as well as the soft covers of the head based on modern laser information technologies, are a priority.

A novel approach is being pursued in the field of cancer surgery in which a complex set of laser technologies, such as spiral CT, MRI, and 3D ultrasound, constitute the foundation for the surgical planning of anatomically complex locations of tumors; the data obtained combine laser information technologies, creating a real three-dimensional model of the diseased organ. This proves that it is possible to successfully surgically treat a tumor that affects the skull's base, cranio-maxillo-facial region, spine, larynx, and trachea. Preoperative planning for the real prototype, obtained by laser stereo lithographic technology, allows to preserve vital organs and improve the radical removal of tumors. For the first time ever mutual dependence between cancer and plastic treatment components has been established; radical tumor removal leads to defects incompatible with life and requires immediate and safe reconstruction, which is impossible without an accurate evaluation of the level and composition of the plastic material with location on real biomodels.

A new generation of intelligent laser surgical systems have been designed and built. The laser installation in real time defines the boundaries of the treated area. Testing of this new installation revealed a new possibility for the use of the surgical laser in different modes, depending on various conditions. The system opens entirely new opportunities for low-traumatic and organ-saving operations.

Laser information technologies are being introduced in other medical fields, such as ophthalmology, cardiac surgery, etc., through the creation of specialized tasks geared to these complexes.

The next issue will contain a detailed publication from the Russian State Prize winners. ●

Scientific Personnel

The federal targeted program (FTP) Scientific and Science-Oriented Educational Personnel started out in 2009. One of its projects was meant to support scientific research conducted by educational scientific centers (ESC). We decided to ask some questions that are regularly of interest to ESC groups applying for grants with the program, and Head of the Department of Programs and Projects at Rosnauka Gennadiy Shepelev agreed to answer them.

Gennadiy Vasilievich, what was the idea behind creating a grant competition for educational scientific centers under the "Personnel" FTP? What were the aims? How would you describe the educational side of these projects?

On the history of the subject, attempts to create ESC were made under the federal targeted scientific and technical program Research and Development in the Priority Fields of Science and Technology in 2005-2006. The results of these attempts showed that training of scientific personnel is in itself an important and difficult endeavor, and the federal targeted program Scientific and Science-Oriented Educational Personnel of Innovational Russia is one of the instruments designed to solve this problem.

Educational scientific centers are a part of the network of training institutions for scientific personnel; it is one of the instruments that allow to fuse scientific research and education. One of the tasks of ESCs is to involve scientists in the training of young specialists. ESCs train young specialists through direct practice by involving them in scientific research. This allows to supplement the theoretical base with practical skills, which are learned during experimental research.

In turn, the educational activities of an ESC are aimed at incorporating the new knowledge learned during research into the educational process, such as educational programs, lectures, practical courses, and seminars.

It is obvious that modern education must be based not only on classical knowledge, but also on novel discoveries. For example, we can look into discussions in the IT industry on whether textbooks and educational programs should contain obsolete information. This kind of information does not seem to spur a student's interest in science, since in their life outside education young people most often find themselves face to face with new technologies and knowledge which have not been covered in their education. Obsolete textbooks provide a skewed view of the level of scientific knowledge in a certain field. ESCs are supposed to solve these problems as well.

A new wave of projects were launched in 2010. Does the level of the applications differ from that of last year? We are asking because last year more projects were funded then was planned, do you see fewer good projects this year?

Last year the program planned to fund 450 projects, each receiving up to 15 million rubles during the course of 3 years. Since the budget of the "Personnel" FTP was cut by 15%, we could only fund 383 projects. However, since the average size of a contract turned out to be lower than planned, we managed to sign 502 contracts.

Despite the fact that more projects than was planned received support, there is no sign that researchers are running out of good projects. This year there were more applications in the competition. The first 8 stages of the competition received more than 2,800 applications, and we expect more than 5,000 by the end of the year. However, we must remember that some applications are repeated – the losers in one stage take part in the next stages. Thus, the number of first-time applications will be lower than the overall number of applications.

How much was the average amount in a contract reduced compared to the initial estimate? Could this influence the quality of the projects and the list of winners in the competition?

Gennadiy Shepelev

One opinion is that reduction of the amount on the contract is a negative factor, but we must remember that the number of competitors increased, and we managed to fund more scientific groups, which is likely a positive outcome. On the subject of the amount, the initial amount of a contract was 15 million rubles or approximately 500, 000 US dollars. Last year the average amount on a contract was approximately 11.4 million rubles, this year the first stages show an average of 8.6 million rubles. We can compare this to the average size of an NSF (National Science Foundation) grant in the USA, which is about 300-350, 000 US dollars during the course of 3 years. This is about the same range that we are seeing in our program. We must also keep in mind the difference in average salaries in the U.S. and in Russia. This means that

the value of our contract is in line with world standards.

Of course some applications were cheaper, but then again, others were more expensive. There is no single "correct" amount to allocate for every project. Some projects use expensive materials, others use cheaper ones. Also, the amount on a contract must be weighed against the results that can be obtained. There is a possibility for two errors here; one is when a project is overfunded, and another is when it is underfunded, because competitors in one competition state a lower price in order to win. As we know, the Federal Law on Government Purchases № 94 prohibits the buyer to ask for an itemized cost sheet, which means that in this case the legislation prevents us from obtaining this information.

On the subject of whether the list of winners was substantially influenced by the amounts allocated and terms, the Russian Institute of Economics, Politics and Law has analyzed whether the 2009 winner list was to change if the amount on a contract and the term of the project were not taken into account (Recently, the term parameter has been practically removed, since a serious advantage in score can only be achieved by reducing the duration by 25%, which will have an obvious negative effect on the work. Because of this, the role of the amount of funds allocated has increased even more). The conclusion was that the list of winners would experience a 15% change. Whether this is a significant change or not is debatable. However, the difference between the scoring by different experts varies in about the same range. In other words, there are other comparable factors except from the completion dates and size of grants which have the same relevance and have a similar effect on the final results of the competition.

With all this in mind, is there a way to prevent weak, "price dumping" applications from winning the competition?

Once again, the question assumes that "price dumping" applications are bad. Price and quality are two different parameters which are both weighed during expert assessment. We try not to accept bad applications, and there is a mechanism for achieving this. For instance, each project has indicators of whether young specialists will be involved, and meeting these criteria requires that a salary be paid to the appropriate number of employees. Thus, based on the minimum wage we can see that the minimum size of a contract in which these indicators are met is 7-9 million rubles. If the amount is lower, then we understand that some indicators are poor, and thus the project does not conform to competition rules and will not be funded. We are trying to make sure that the quality of projects is the most important factor; however, we cannot completely ignore the size of grants since the Federal Law № 94 is a law, and breaking it results in administrative punishment.

There is another problem here: the number of specialists required for a project can be overestimated, meaning that the project in fact needs less people than are listed in the application. However, it would be a negative trend if we were only aiming at saving money. Moreover, one of our goals is to attract young people into research. Thus, we are actually stimulating groups to inflate their requests by including less qualified personnel into the project. Also, we must keep in mind that research groups often do not conduct work exclusively on the terms in the contract, as science often takes the researcher beyond the boundaries of the technical specifications of the contract. This will of course take up money from the project and human resources. This could be interpreted as a misuse of funds; however, the general logic of science is that this is precisely the way it should be. Scientific groups should have enough room for men in their research.

One of the indicators of ESC projects is the involvement of younger personnel. During the project these people will work in the applying organization, what happens after the contract is over? Is there any mechanism for keeping these specialists after the project ends?

There are no projects in the world that can guarantee lifetime funding. Keeping scientific personnel in institutions is achieved by permanent slots, which are limited in number. However, there are positions under temporary economic contracts. In order for them to be maintained after the project is finished, the researchers must receive new grants and contracts. Another untapped resource is cooperation with business and industry. In our country approximately 65% of all research is funded by the government and the remaining 35% receive non-budgetary funding. In foreign countries, this ratio is exactly the reverse. However, there are examples when a Russian college receives 50% of its funds from businesses. Currently, the government is pressuring businesses to direct a certain percentage of their income towards scientific research, especially those companies that are partially owned by the government. Moreover, Decree 218 for the support of cooperation between colleges and industrial companies has recently come into force, and it is also a resource that can provide additional funding for scientific groups.

What if an organization attracts young specialists without aiming to keep them in the organization after the ESC funding runs out and gets rid of them after the completion of the project?

Of course some organizations will choose this route, get rid of the personnel after the project is completed. But administrative regulation of these processes would be outside the priorities supported by the FTPs. The projects under the ECS program are a chance for young specialists to test their abilities, not a ploy to keep them working at a certain ESC for the rest of their lives. In the latter case, the centers should not have been called "educational." Some of the involved specialists will leave, but we cannot really say that this is either good or bad. We assume that the people involved in the project have received higher qualification and will use these new skills and knowledge in some other organization (not necessarily the same ESC or an ESC at all). If the economy gets a better trained specialist, then this is a good outcome, irrespective of whether or not this specialist continues to work in the organization that trained him.

In some cases a research group uses a paper that was in press before the start of a project as an indicator of a project's progress in their report. What is your opinion of this practice?

Again, there is no "black or white" answer here. If an ESC is there for

work, not to write a report, then it must have a head start in research which began before the start of a contract – this is one of the criteria for selecting the best ESCs. If one adopts this point of view, it does not really matter when the article was planned. Delaying articles so as to send them to a journal during the course of the project is of course nonsense. Of course if there are no other articles during the course of the project then this is another matter, but this has to be controlled by the authority that oversees progress in the project.

Can you comment on the overall situation with scientific personnel turnover in Russia?

No serious studies of the scientific personnel process have been conducted as of now. There is only general statistical data which lack details. This leads to speculation and pessimistic prognoses and various interpretations of the situation with varying comments depending on the position of the commenting party.

The following example illustrates this point. The drain of scientific personnel was at its highest in the relatively prosperous year of 2008, the reduction in scientific personnel was 5%, even though the overall number of people involved in science increased in 2007. The reduction was spread out fairly evenly among all organizations, both governmental and non-governmental. However, the proportion of research scientists involved in science has increased. Possibly people moved over to the realm of business, which promised a considerable increase in income at the time, some role might have been played by the cutbacks because of the crisis near the end of the year. This is the most we can say on the issue, because no more specific information is available.

But, as I have said earlier, these facts cannot be interpreted in terms of good or bad; there are different facets to every problem. We need to ask ourselves several questions – how many people are needed in the scientific field? What do we want from them? Just scientific papers? Of course not. One of the reasons for personnel leaving the scientific sector may be increased competition from industry; production requires technologies as well as qualified specialists.

Let me give an example. In the Soviet Union I worked at an institute which was among other things involved in the development of laser crystals. When the technology was transferred from the developing institute to the manufacturing plant, the quality of the crystals was considerably worse. Why did this happen? One of the possible reasons is the human factor, which in this case was the lower qualification of the manufacturing plant's personnel as compared to the staff at the research facility.

What can ESCs expect in the following year?

This year there will be approximately 300 more contracts for ECSs in addition to the contracts that are currently running. The plans for next year will be formulated after the program's budget for next year is set. We hope to sign no less than 500 contracts. ●

Interview by Ivan Ohapkin

What is the situation with Personnel in Life Sciences?

The field of "Living Systems" is a priority in the Scientific and Science Education Personnel FTP, which is evident from the statistical data on the event Conduct of Scientific Research by Educational Scientific Center Staff (Table 1).

The overall level of competition in 2009 was 5.1 applications per grant. For comparison, in 2009 the average level of competition in the "nanotechnology and nanomaterials" field was 8 applications per grant.

Interestingly, judging by the first stages of the "Living Systems" in 2010, competition has increased as compared to 2009; however, the average size of a contract in 2010 is much smaller (this is probably because of the inadequacies in the governmental purchases legislature). The increased competition is due to the increasing phenomenon of "price dumping" applications which use the flaws of the Federal Law № 94 on Government Purchases and which leads to the breaking-up of government funds into ever smaller grants. In practice, the average amount of a grant in 2010 is 1.5-2 times smaller than was planned

Table 1.

Name of the indicator	Event 1.1	
	2009	2010*
Number of application (Life Sciences)	421	333
Number of supported ESC projects (Life Sciences)	82	43
Overall amount of funds, million rubles	986.0	377.9
In 2009	312.6	-
In 2010	353.0	126.0
Average size of contract, million rubles	12.0	8.8
In 2009	3.8	-
In 2010	4.3	2.9
Maximum size of contract, million rubles	15.0	12.5
In 2009	5.0	-
In 2010	5.0	4.2
Minimum size of contract, million rubles	6.0	4.5
In 2009	0.5	-
In 2010	2.0	1.5
*The 2010 competitions are still in progress.		

Table 2

Theme groups	Competition		Number of projects		Number of applications	
	2009	2010	2009	2010	2009	2010
141 General biology and genetics	2.4	7.8	12	4	29	31
142 Physico-chemical biology	2.6	6.2	12	5	31	31
143 Fundamental medicine	4.9	5.5	19	14	94	77
201 Biocatalytic technology	4.5	11.5	4	2	18	23
202 Biomedical protection technologies	9.0	9.3	20	14	179	130
203 Genomic technology	5.0	10.3	3	4	15	41
204 Cellular technology	5.0		3	-	15	-
205 Bioengineering	3,3		4	-	13	-
206 Bioinformatic technology	7,0		2	-	14	-
209 Creation of biocompatible materials	4,3		3	-	13	-
Average \ Amount	5.1	7.7	82	43	421	333

by the authors of the FTP project during its development.

Table 2 shows the distribution of applications and contracts between fields in the section of Living Systems.

Data on the affiliation of the winning organizations are also of some interest. If it were not for the flaws of the law on governmental purchases, these data could be considered to be a realistic rating of Life Sciences centers affiliated with various agencies. However, the current data are not as valuable as that.

Notably, MSU, which won 7 ESC grants in 2009, won only one in 2010. Nevertheless, this university is still the leader in the number of ESCs among all participating organizations.

Table 4 shows the 15 most active participants in the ESC grant competition in the field of Living Systems in 2009-2010.

As we can see, 11 of the 15 organizations which applied for more than 8 grants are higher educational institutions. However, the success ratio (which indirectly reflects the quality and scientific level of the presented projects) is higher for research institutes of the Biology Division of RAS as compared to universities, research institutes of the other RAS divisions and other agencies. The RAS Institute of Molecular Biology and RAS Institute of Gene Biology won two grants each after having applied for three each. Identical results (2 contracts per 3 applications) were also obtained by other acknowledged biological centers: The Pushkino State University, Research Institute of Physico-Chemical Medicine, and others.

In conclusion, we list the organizations with the most funding for their contracts according to the results of the completed competitions in 2010 (Table 5):

Table 3.

Higher educational facilities of the Ministry of Education (RosObr)	42
RAS	38
RAMS	18
Higher educational facilities of the Ministry of Health and institutions of its agencies	16
Lomonosov MSU	8
Russian Academy of Agricultural and Livestock Sciences	1
Ministry of Agriculture and Livestock	1
Others (Karpov Scientific Research Institute of Physical Chemistry)	1
Overall	125

* The listed numbers are the number of supported ESC applications, not the number of winning organizations

Table 4.

Organization	Number of applications	Number of contracts
Novosibirsk State University	11	3
South Federal University	10	1
Immanuel Kant Russian Governmental University	10	1
RAS Institute of Theoretical and Experimental Biophysics	9	2
Peoples Friendship University of Russia	9	2
Siberian State Medical University of the Federal Health and Social Development Agency	9	3
Tomsk State University	9	1
Saint-Petersburg State Polytechnical University	8	0
Saint-Petersburg State University	8	2
RAMS Cardiology Research instate of the Siberian branch of RAMS	8	1
RAS institute of chemical biology and fundamental medicine of the Siberian Branch of RAS	8	3
National nuclear research university of the Moscow Engineering and Physics Institute	8	1
Department of Biology of the M.V. Lomonosov Moscow State University	8	1
RAS Institute of Molecular Genetics	8	3
N.G. Chernishevsky Saratov State University	8	2

Table 5.

Organization	Project	Size of contract (in millions of rubles).
Research Institute of Physico-Chemical Medicine of the Federal Medico-biological agency	Study of the paracrine mechanisms behind the effect of mesenchimal stem cells on the regeneration of tissues using proteome analysis	12.5
Research Institute of Urology of the Federal Agency for Highly Technological Medical Assistance	Development of a comprehensive diagnostic and metric system for studying the functional activity of the higher an lower urinary ducts	12.0
Moscow Energetic Institute (Technical University)	Study of the condition and evolutionary change of biological objects using remote laser diagnostics	11.0
K.I. Skryabin Moscow State Academy of Veterinary Medicine and Biotechnology	Development of innovational diagnostic methods using animal physiology and biochemistry as a model for medical use	10.8
Department of Chemistry of the M.V. Lomonosov Moscow State University	Development of a method for the molecular monitoring of the spread of viral infections and for determining the effectiveness of antiviral compounds in order to create the next generation of therapeutic drugs	10.8

This material was prepared by Ivan Sterligov using materials from the National Personnel Training Foundation (NPTF) – Analytical Administration Board of FTPs. The editors thank Alexander Kalyagin (NPTF).

Customs Barriers in the Way of Progress in Biotechnology

S. Sinyavskaya, specially for Acta Naturae

Scientific research in the field of Life Sciences is impossible without international cooperation, which means that no research is possible without foreign equipment, reagents, laboratory animals and biological materials. Yet, customs regulations in the field of biotechnology are raising more and more questions from scientists. Passing customs control takes up a lot of time, energy and funds. Can these bureaucratic procedures be simplified for the international transportation of goods for scientific research?

The 21st century is the century of biotechnology; these technologies are the foundation for the 6th technological stage. The importance of this field of knowledge for the development of modern society is understood by the government: *living systems technologies* were deemed priorities in scientific and technical development in 2002 and 2006; a presidential modernization committee has designated *medical technology* as one of the five priorities in economic development; the FTP (Federal Target Program) Research and Development in Priority Fields for the Development of the Russian Scientific and Technological Complexes in the years 2007-2012 and the field of Living systems are among the leading fields in the country. More than 30% of funds in this program are directed into this particular field.

It is clear that as the government favors this field of knowledge among others, it needs to create specific work conditions that will promote effective usage of the funds of scientific organizations and the time of their employees. If such a requirement is not met, then hardly any results adequate to the allocated funds can be expected. Work environment issues are precisely the ones that hamper the work of Russian life sciences researchers most of all. One of the most annoying problems is customs barriers, which prevent Russian science from integrating the worldwide network of scientific and agricultural interactions. In the words of corresponding RAS member **Alexander Gabibov**, an "artificial iron curtain" seems to have been put in place. An international parcel can seldom pass through customs on time and legally, and for a reasonable amount of money.

For instance, if you engage the services of a company which specializes in shipping equipment, reagents, and other goods, then the cost of the goods (and these can be very expensive materials) increases approximately 2.5-3 fold. Under these conditions, all the work needed to clear customs control is outsourced by the scientific organization. Obviously, this path is seldom chosen, as purchasing of equipment and reagents takes up from 10 to 50% of grant money as it is. Most often, scientists go through customs themselves or engage the services of a shipping company. In the latter case, not only do you have to pay for the shipping company's services and customs duties, but also to collect the appropriate documentation which is needed to pass customs. For instance, shipment by DHL requires the following:

– a letter requiring the release of the shipment;
– a translation of the invoice into Russian;
– a detailed description of the goods;
– a copy of the free release agreement between the sender and the recipient;
– registration with the Sheremetyevo or Moscow Customs Office (this can be done by DHL using the provided documentation);
– approval documents, the number of which depends on the specific code of the goods to be imported. The code is selected based on the detailed description (permission from the Ministry of Health and Social Development or a veterinary certificate may be needed, depending on the description).

Importing biological materials for scientific research requires permission from the Ministry of Health and Social Development and the government's Drug Control Department, and these papers are very difficult to obtain and take up a large amount of time (the list of documents requested is shown in appendix 1.2).

The amount to be paid in customs duties is calculated according to the following guidelines:

– the import customs duty ranges from 0%-20% (depending on the code of the goods) of the customs value of the goods (the customs value is the price of the goods according to the invoice + shipping);
– VAT of 18% of the customs value + customs duty;
– the minimal customs duty for a corporation or any other legal entity is 500 rubles;
– the minimum price charged for broker services is 7,000 rubles (without VAT; it is a standard tariff if the goods will be shipped via the DHL Express network with doorstep delivery), and

Svetlana Senotrusova, Doctor of Biological Sciences, Professor at the Organization of Customs Control department at the Russian Customs Academy.

Are the difficulties in the import of compounds needed for scientific research warranted in your opinion?

– I think that the existing procedures for customs regulation of the import of chemical reagents are to some extent warranted, since this is a special group of goods which can be extremely poisonous. Separating the import of goods for scientific purposes and for other needs may be a difficult task, since most of the import is accomplished by intermediary companies.

Spokespeople from the scientific community have been talking about the need for a single code (3822 00 000 0) for goods used only for research and development purposes, which is by the way how it is done in Europe and the USA. Why does not Russia introduce a single code for this group of goods?

– Group 3822 000000 includes reagents for diagnostics or laboratory use mounted on a support sheet, ready-made diagnostic or laboratory-use reagents with or without a support sheet, excluding goods which fall under the 3002 and 3006 categories; certified etalon materials. Goods that fall under this category are indeed not import-restricted. But even this category is burdened by the need for a number of supporting documents. But two other large groups of goods, which include organic and inorganic chemical compounds, rare-earth metals, radioactive elements and their isotopes cannot be folded into the 3822 group, since this may be harmful to national security. The majority of these chemicals and compounds require the use of nontariff means of control. A thorough diversification of the goods in groups 28, 29, and 38 of the Goods Nomenclature for the Foreign Trade is required.

The nomenclature lacks classification for many types of biological materials used in scientific research. Here is an example: a plasmid with all the required support documentation was sent from La Sapienza University in Rome via TNT express-mail. However, customs officials could not find the appropriate code and thus had to send the plasmid back to Rome.

– Of course the nomenclature lacks classifications for some types of biomaterial used in scientific research; this is not news, since science develops much faster than changes in the Nomenclature can be made. Declaration of such goods requires a qualified approach, especially from a foreign economic entity, a customs control specialist, or a broker. Unfortunately, the qualification of experts in the customs control of special-group goods is currently insufficient. Indeed, the declaring entity has priority in establishing the code of the goods and thus the amount to be paid in customs duties, and customs authorities only oversee this process. In the case of the returned plasmid, the mistake was due to the declarant and the customs broker. Such situations do no occur very often.

What changes should be made to the statutes to simplify customs control for research purposes?

My view is that optimizing customs duties which involve reagents for scientific research would be effective, since this will not affect the fiscal functions of the customs tariff of the Customs Authorities but will promote the development of science in Russia. Another import-optimization issue may be reducing the number of importers of these types of products; however, exemptions or simplifications of customs control procedures are out of the question.

Goods which can easily spoil are prioritized during customs control. These goods include living animals and the like (art. 67 of the Russian Customs Code). This prioritization must be carefully used.

Changes in the legislation aimed at the simplification of the export and import of goods used in scientific research require very thorough substantiation, which in turn requires significant, time-consuming work. We are working on this issue, but the problem is a difficult one.

the amount also depends on the need for additional services.

In theory, a shipment can be processed without professional assistance; however, customs services do not give consultations on the telephone. You need to show up and to present a 10-digit code for the goods in question (which is pretty difficult to figure out on one's own) in order to get the complete documentation package. Here, more difficulties await an applicant on his journey as an unassisted customs check:

– The longest delays usually occur when obtaining the so-called "refusal letters" issued by five government departments: the Ministry of Health and Social Development, Ministry of Agriculture, Governmental Drug Control Department, Russian Technical Supervision Department, and the Federal Technical and Export Control Department. The letters must acknowledge that the imported goods are not listed as medical or veterinary drugs, narcotic or potent drugs, dangerous waste or dual-use goods, and that they do not require certification or licensing. Obtaining this type of documentation can take up to 2-3 months.

– Combersome customs declaration process.

– Currently, because of the ill-conceived set of customs codes, the legal import of animals and biomaterials into the country is very difficult. This includes cell lines, DNA (such as plasmids), and bacteria. The nomenclature also lacks many of the biomaterial types which are commonly used in scientific research.

– Customs duties are not designed to tell the difference between goods shipped for sale or for scientific research. Because of this, scientists need to prepare lots of documentation that confirms their "good intentions."

Getting only one permission from the Ministry of Health and Social Development, which is valid for 30 days, requires an extensive package of documents (see more in Appendix 1), which includes a permission from the permanent committee on drug control for the export (import) of biological materials (the list of documents for a review of this committee is presented in Appendix 2).

– Moreover, it must be noted that some types of biological materials may spoil if the transportation and storage requirements in the customs storage

Alexander Gabibov, head of the Biocatalysis Laboratory at the M.M. Shemyakin and Yu. A. Ovchinnikov Institute of Bioorganic Chemistry (IBC RAS), corresponding member of RAS, Doctor of Chemical Sciences, professor:

During Soviet times, we used to order reagents from abroad a year ahead. Nowadays, some reagents take more than a year to arrive. Also, these reagents cost much more after passing through customs than they are for users in western countries. How can we even discuss priorities, market development and progress in nano- and biotechnology when we use up to 50% of our grant money on purchasing equipment? Can any world-class research take place when both animals and derivatives (such as human or animal blood) are virtually impossible to import legally? For instance, we need to transport certain genetic lines of mice into our Pushchino branch of IBC. We can only transport them as a present. However, we have to pay large sums of money to transport companies and customs authorities even for this "present." This is why we much prefer to conduct our animal experiments in our branch laboratories in Israel and France. This means that, even though we have all the technology, the administrative restrictions are so excruciating that we are forced to move our operations to western countries. Also, western researchers can transport animal blood, while Russian scientists need to obtain permission from the Drug Control Committee, which has to certify that the blood is free of narcotic compounds. But the thing is we carry blood in miniscule amounts, so drugs could not be extracted even if the blood did have drugs in it. It is unacceptable to prevent us from working just because bureaucratically it is easier to restrict than to allow. For example, we need spider toxins for studying cellular electric potentials. A western researcher can buy these compounds after signing several papers that state that the toxins will be used for such and such purposes. A Russian researcher just cannot cross the border with these toxins. Also, we cannot buy any spoilable reagents, even though companies such as Fedex and DHL ship these reagents all over the world in dry ice. The reason for this is that Russian customs control takes so much time that everything will thaw before it is released.

In order to open this "iron curtain" a whole series of legislative acts needs to be drawn up and the scientific community needs to be involved in their drafting. My opinion is that customs officials, who are highly qualified specialists, need to work on a single-window basis. Also, the veterinary service could be located inside the customs offices as opposed to being located in the other part of the city.

facility are not observed (for instance cell lines need to be stored in dry ice or at -80°C).

As we can see, obtaining materials for scientific research takes months, lots of efforts, and a large amount of funds.

We were unsuccessful in trying to play this game on our own; i.e., trying to pass customs control without assistance, and we could not get any broker or company to agree to do their job in the presence of reporters by the time this issue went to print, even though we did have preliminary arrangements. We also could not get any answers from the Federal Customs Authorities, who claimed to be busy with signing the Customs Agreement between Russia and Kazakhstan, and thus declined to comment. In short, all our attempts to prepare an objective article on the customs control of biological materials were very much reminiscent of the stories of the scientists who attempted to get their materials through customs.

However, we were able to find someone with a different opinion. Prominent lawyer Sergei Zhorin says that most of the problems associated with customs control can be avoided if "the performance of the appropriate tasks is not procrastinated." "Scientific research is usually conducted according to a plan, which means that a) knowing that certain materials will be needed during the following 3-6 months, one needs to consult customs authorities on the documentation needed for successful customs processing; b) the appropriate documents can be obtained at a reasonable pace with no rush; c) the goods should be pre-declared, which means that a customs declaration is filed before the goods arrive on the territory of the Russian Federation; d) after which the sender is notified that the recipient is ready to receive the previously ordered goods. In such a case, the completion of customs formalities will not take a large amount of time."

One way to ease customs formalities for scientists would be to assign a single code to all the goods needed in scientific research (3822 00 000 0), which is the case in Europe and the United States. According to Sergei Zhorin, the issue of putting certain goods in a specific position in the Goods Nomenclature (GN) is the sole domain of the Government of the Russian Federation. Zhorin himself believes that "the current concept for developing the customs authorities of the Russian Federation warrants the creation of a specialized customs post (or customs department) which would perform customs registration of these goods in the shortest possible time."

According to customs broker **Andrei Kirienkov**, the government will probably not assign a single code to this group of goods, since different goods have appropriate duties and customs in western countries are "much more oriented at targeted usage than the customs authorities in our country." The main problem is that scientific facilities have no priority over any others: "Such preferences need to be won as a first step. Then some other things can be fought over. The Federal Customs Authority does have a practice of granting privileges and permissions, scientific institutions need to team up and lobby their interests and solve this problem on their own and not put all their hopes into the government."

However, in this case the government then should not put too much hope into getting adequate results from the money it puts into biotechnology.

We thank Upravlyaushaya Kompania "Bioprocess Capital Partners" LLC and Olga Golub personally for the presented analytical materials and appendices. ●

Appendix 1

MINISTRY OF HEALTH
OF THE RUSSIAN FEDERATION

LETTER
Dated October 17, 2000, N 2510/11197-32

ON THE IMPLEMENTATION OF A TEMPORARY PROCEDURE FOR THE IMPORT (EXPORT) OF BIOLOGICAL MATERIALS

This material is forwarded as a guideline and procedure for the temporary procedure of document review, as submitted by organizations (institutions) to the Ministry of Health of the Russian Federation, for obtaining permission for import into the Russian Federation and export abroad of biological materials during the course of international scientific cooperation. This temporary procedure was approved on October 12, 2000, in accordance with the Decree of the Ministry of Health of the Russian Federation dated July 14, 2000, N 259.

This temporary procedure regulates the documentation process involved in the import and export of biological materials in the course of international cooperation in various aspects of medical science and creates a single organizational and methodological basis for the fulfillment of this task.

First Deputy Minister of Health
Of the Russian Federation
A.I. Vyalkov

Hereby Confirm
First Deputy Minister of Health
Of the Russian Federation
A.I. Vyalkov
October 12, 2000

THE TEMPORARY PROCEDURE OF DOCUMENT REVIEW, AS SUBMITTED BY ORGANIZATIONS (INSTITUTIONS) TO THE MINISTRY OF HEALTH OF THE RUSSIAN FEDERATION, FOR OBTAINING PERMISSION FOR THE IMPORT INTO THE RUSSIAN FEDERATION AND EXPORT ABROAD OF BIOLOGICAL MATERIALS DURING THE COURSE OF INTERNATIONAL SCIENTIFIC COOPERATION.

This temporary procedure is implemented in accordance with the Decree of the Ministry of Health of the Russian Federation dated 07.14.2000 N 259 (art. 1.7) in order to regulate the issue of permissions for organizations (institutions) for the import into the Russian Federation and export abroad of biological materials during the course of international scientific cooperation.

I. General provisions for the drawing up of documentation by organizations (institutions) for the import (export) of biological materials

1. The organization (institution) must send a petition addressed to the administration of the Ministry of Health of the Russian Federation drafted according to the attached form and with the required package of documentation as listed in Section II of this temporary procedure.

2. Notarized originals of the documents or, in specific cases, their copies (also notarized) must be presented. Documents which have more than one page must be sewn together. Documents which have not been notarized or do not have all the required signatures will not be accepted. Documents (agreements, contracts, conventions, etc.) must be signed and have printed names under the signatures, and also bear clear seals of the involved parties.

4. Documents must be submitted in the Russian language. Documentation in foreign languages must have an attached translation signed by the head of the organization (institution) according to the established procedure, which also indicates the person who performed the translation.

5. Permissions for the export of biological materials can only be granted to Russian organizations (institutions) which have the legal right to conduct scientific and/(or) technical research in cooperation with foreign legal entities.

6. A permission from the Ministry of Health of the Russian Federation is a single-use document and is to be obtained for each instance of export (import) of biological materials used in the course of international scientific cooperation and is issued to the applying organization (institution).

7. Permission for the import (export) of biological materials is issued to the organization (institution) as a single copy and cannot be passed on to other organizations (institutions).

8. The permission document (permit) for the export (import) of biological materials is valid for 30 days from the date set by the registration number of the Ministry of Health of the Russian Federation.

9. The original of the permit issued by the Ministry of Health of the Russian Federation is presented by the organization (institution) to the customs authority of the Russian Federation at the place of registration, according to the procedure set by the National Customs Committee of the Russian Federation.

10. Changes in the legal status of the organization (institution), changes in the agreement (contract, convention) between the parties require a new application with a full set of documentation.

11. The person who signed the documents is responsible for the truthfulness of the information and correctness of the data presented to the Ministry of Health of the Russian Fed-

eration in the course of the procedure for obtaining a permit for the export (import) of biological materials in the course of international scientific cooperation, in accordance with laws of the Russian Federation.

12. The Ministry of health has the right to deny an organization (institution) an export (import) permit for biological materials in the following cases:

12.1. Incorrect drafting of the documentation by the organization (institution).

12.2. Incomplete presentation of the required materials, and also failure to conform to the requirements set by this temporary procedure.

12.3. False or distorted information in the documentation.

II. Documents required from the organization (institution) in order to obtain a permit for the import (export) of biological materials.

1. An application from the organization (institution), drafted according to the attached form.

2. Agreement [contract, convention, grant (a description of the grant and its main points must be included)] stipulating international scientific cooperation.

Scientific research performed in collaboration under intergovernmental agreements is to be documented by a copy of the appropriate document or an extract, certified in due manner.

3. Corporate charter and registration documents of the applying organization (institution).

4. Copies of the licenses of the parties named in the agreement (convention, contract), confirming their rights to conduct scientific research in the biological and medical fields.

5. A conclusion from the administration of a medical institution confirming that the subjects from which the biological samples were obtained did not have any infectious illnesses.

6. Documents from the cooperating party which state that the biological materials in question will be used only for scientific purposes, and that these materials will not be passed on to any third party without prior consent from the Russian party named in the agreement.

Note. This document must be drafted only if the above-said condition is not addressed in the agreement (contract, convention).

7. A foreign party importing biological materials into the Russian Federation must present an official letter of confirmation from the appropriate Health Ministry (Department) that the biological materials in question do not bear any infectious agents, addressed to the Ministry of Health of the Russian Federation.

8. Scientific research in the fields of infectious diseases (AIDS, HIV, hepatitis, etc.) must provide to the Ministry of Health of the Russian Federation a permit (consent) of the appropriate Health Ministry (Department) of the country into which the biological materials in question will be imported.

9. Biological materials that need to be imported into the Russian Federation to be used in scientific research in the field of infectious diseases must be reviewed in advance by the Ministry of Health of the Russian Federation, which makes the appropriate decision.

10. A permit for the import (export) of biological materials from the Permanent Drug Control Committee.

11. Reports on the conducted scientific research and a list of publications in Russian and foreign journals.

Head of the Medical Scientific
Research Facility Control Unit
S.B. TKACHENKO

Appendix to the temporary procedure of document review, as submitted by organizations (institutions) to the Ministry of Health of the Russian Federation, for obtaining permission for the import into the Russian Federation and export abroad of biological materials during the course of international scientific cooperation.
October 12, 2000.

I. APPLICATION FROM THE ORGANIZATION (INSTITUTION)

1. The application must be drafted on the organization's (institution's) official letterhead signed by the head of the organization (institution) and have the contact telephone and fax numbers of the executor, together with his/her last name. The application must include:

1.1. The location (country, city) and full title of the organization (institution) to which the biological materials will be exported in the course of international scientific cooperation.

1.2. Type of exported biological material (blood or blood fractions, serum, urine, spittle, other biological fluids, bioptates, etc.).

1.3. Number of units for each type of biological material.

1.4. Packaging type.

1.5. Mode of transportation:

a) package – mode of shipping must be described;

b) hand carry – full name of the person to transport the biological material, number of his foreign passport.

II. AGREEMENT (CONTRACT, CONVENTION)

Agreements (contracts, conventions) must have the following articles:

1. Subject of the agreement.

2. Agreement conditions.

3. Responsibilities and liabilities of the parties in the agreement.

4. Results of the scientific research and their use by the parties.

5. Duration of the agreement.

6. Description of the experiments to be conducted, and work plans and timetables of the research should be presented as an attachment to the agreement (contract, convention).

Appendix 2

List of documents to be submitted by the applicant for the expert assessment procedure in issuing a permit for the import/export of biological materials

A letter from the applicant to the Head of the Federal Agency for Healthcare and Social Development Control (Roszdravnadzor) requesting a permit for the import (export) of biological materials. The letter must be on the applying organization's letterhead, indicating the address of incorporation, and signed by the head of the organization – 1 copy.

An appendix to the above-mentioned letter with a list of the biological materials to be imported (exported), signed by the head of the organization, bearing a note from the Permanent Drug Control Committee certifying that there are no narcotic or psychotropic drugs or their precursors in the biological materials to be imported (exported), whose circulation is controlled by the Russian Federation (if the Appendix is more than one page, then each page must bear this note) – 2 copies.

A copy of the contract [agreement, convention, grant (the grant must be indicated by its full title and have a brief description of its main points)] on international scientific cooperation, certified by the applying organization's seal – 1 copy.

Copies of the founding and registry documentation of the applying organization, notarized – 1 copy.

Extract from the charter of the organization confirming that the organization is involved in research and development activities, notarized by the applying organization's seal – 1 copy.

Conclusion from the administration of a healthcare institution certifying that the person(s) who provided the samples does (do) not carry any infectious diseases – 1 copy.

Document from the cooperating party certifying that the biological materials will be used only for scientific purposes and that they will not be passed on to third parties without prior permission from the Russian party in the Agreement (this document is required if this issue is not covered in the contract).

A foreign party importing biological materials into the Russian Federation is required to supply an official confirmation from the appropriate Healthcare Ministry's (Department) that the biological materials in question do not harbor any infectious diseases.

In case of studies involving infectious diseases (AIDS, HIV, hepatitis, etc.), Roszdravnadzor requires a permit (consent) from the appropriate Healthcare Ministry's (Department) of the country into which the biological materials in question will be imported.

Import of biological materials for studies involving infectious diseases involves a review procedure by Roszdravnadzor, which decides whether or not to grant its consent.

Reports of the conducted scientific research and a list of publications in Russian and foreign journals.

Induced Pluripotent Stem Cells: Problems and Advantages when Applying them in Regenerative Medicine

S. P. Medvedev[1], A. I. Shevchenko[1], S. M. Zakian[1,2]*
[1] Institute of Cytology and Genetics, Siberian Branch, Russian Academy of Sciences
[2] Research Center of Clinical and Experimental Medicine, Siberian Branch, Russian Academy of Medical Sciences
* E-mail: zakian@bionet.nsc.ru
Received 10. 04. 2010

ABSTRACT **Induced pluripotent stem cells (iPSCs) are a new type of pluripotent cells that can be obtained by reprogramming animal and human differentiated cells. In this review, issues related to the nature of iPSCs are discussed and different methods of iPSC production are described. We particularly focused on methods of iPSC production without the genetic modification of the cell genome and with means for increasing the iPSC production efficiency. The possibility and issues related to the safety of iPSC use in cell replacement therapy of human diseases and a study of new medicines are considered.**
KEYWORDS **cell reprogramming, induced pluripotent stem cells, directed stem cell differentiation, cell replacement therapy**
ABBREVIATIONS **ESC – embryonic stem cells, iPSCs – induced pluripotent stem cells, NSCs – neural stem cells, ASCs – adipose stem cells, PDFs – papillary dermal fibroblasts, CMs – cardiomyocytes, SMA – spinal muscular atrophy, SMA-iPSCs – iPCSs derived from fibroblasts of SMA patients, GFP – green fluorescent protein, LTR – long terminal repeat**

INDUCED PLURIPOTENCY

Pluripotent stem cells are a unique model for studying a variety of processes that occur in the early development of mammals and a promising tool in cell therapy of human diseases. The unique nature of these cells lies in their capability, when cultured, for unlimited self-renewal and reproduction of all adult cell types in the course of their differentiation [1]. Pluripotency is supported by a complex system of signaling molecules and gene network that is specific for pluripotent cells. The pivotal position in the hierarchy of genes implicated in the maintenance of pluripotency is occupied by *Oct4*, *Sox2*, and *Nanog* genes encoding transcription factors [2, 3]. The mutual effect of outer signaling molecules and inner factors leads to the formation of a specific expression pattern, as well as to the epigenome state characteristic of stem cells. Both spontaneous and directed differentiations are associated with changes in the expression pattern and massive epigenetic transformations, leading to transcriptome and epigenome adjustment to a distinct cell type.

Until recently, embryonic stem cells (ESCs) were the only well-studied source of pluripotent stem cells. ESCs are obtained from either the inner cell mass or epiblast of blastocysts [4–6]. A series of protocols has been developed for the preparation of various cell derivatives from human ESCs. However, there are constraints for ESC use in cell replacement therapy. The first constraint is the immune incompatibility between the donor cells and the recipient, which can result in the rejection of transplanted cells. The second constraint is ethical, because the embryo dies during the isolation of ESCs. The first problem can be solved by the somatic cell nuclear transfer into the egg cell and then obtaining the embryo and ESCs. The nuclear transfer leads to genome reprogramming, in which ovarian cytoplasmic factors are implicated. This way of preparing pluripotent cells from certain individuals was called therapeutic cloning. However, this method is technology-intensive, and the reprogramming yield is very low. Moreover, this approach encounters the abovementioned ethic problem that, in this case, is associated with the generation of many human ovarian cells [7].

In 2006, the preparation of pluripotent cells by the ectopic expression of four genes – *Oct4*, *Sox2*, *Klf4*, and *c-Myc* – in both embryonic and adult murine fibroblasts was first reported [8]. The pluripotent cells derived from somatic ones were called induced pluripotent stem cells (iPSCs). Using this set of factors (Oct4, Sox2, Klf4, and c-Myc), iPSCs were prepared later from various differentiated mouse [9–14] and human [15–17] cell types. Human iPSCs were obtained with a somewhat altered gene set: *OCT4*, *SOX2*, *NANOG*, and *LIN28* [18]. Induced PSCs closely resemble ESCs in a broad spectrum of features. They possess similar morphologies and growth manners and are equally sensitive to growth factors and signaling molecules. Like ESCs, iPSCs can differentiate *in vitro* into derivatives of all three primary germ layers (ectoderm, mesoderm, and endoderm) and form teratomas following their

subcutaneous injection into immunodeficient mice. Murine iPSCs injected into blastocysts are normally included in the development to yield animals with a high degree of chimerism. Moreover, murine iPSCs, when injected into tetraploid blastocycts, can develop into a whole organism [19, 20]. Thus, an excellent method that allows the preparation of pluripotent stem cells from various somatic cell types while bypassing ethical problems has been uncovered by researchers.

THE PROBLEM OF IPSC PRODUCTION EFFICIENCY AND APPLICATION SAFETY IN CELL REPLACEMENT THERAPY

In the first works on murine and human iPSC production, either retro- or lentiviral vectors were used for the delivery of *Oct4*, *Sox2*, *Klf4*, and *c-Myc* genes into somatic cells. The efficiency of transduction with retroviruses is high enough, although it is not the same for different cell types. Retroviral integration into the host genome requires a comparatively high division rate, which is characteristic of the relatively narrow spectrum of cultured cells. Moreover, the transcription of retroviral construct under the control of a promoter localized in 5'LTR (long terminal repeat) is terminated when the somatic cell transform switches to the pluripotent state [21]. This feature makes retroviruses attractive in iPSC production. Nevertheless, retroviruses possess some properties that make iPSCs that are produced using them improper for cell therapy of human diseases. First, retroviral DNA is integrated into the host cell genome. The integration occurs randomly; i.e., there are no specific sequences or apparent logic for retroviral integration. The copy number of the exogenous retroviral DNA that is integrated into a genome may vary to a great extent [15]. Retroviruses being integrated into the cell genome can introduce promoter elements and polyadenylation signals; they can also interpose coding sequences, thus affecting transcription. Second, since the transcription level of exogenous *Oct4*, *Sox2*, *Klf4*, and *c-Myc* in the retroviral construct decreases with cell transition into the pluripotent state, this can result in a decrease in the efficiency of the stable iPSC line production, because the switch from the exogenous expression of pluripotency genes to their endogenous expression may not occur. Third, some studies show that the transcription of transgenes can resume in the cells derived from iPSCs [22]. The high probability that the ectopic *Oct4*, *Sox2*, *Klf4*, and *c-Myc* gene expression will resume makes it impossible to apply iPSCs produced with the use of retroviruses in clinical trials; moreover, these iPSCs are hardly applicable even for fundamental studies on reprogramming and pluripotency principles. Lentiviruses used for iPSC production can also be integrated into the genome and maintain their transcriptional activity in pluripotent cells. One way to avoid this situation is to use promoters controlled by exogenous substances added to the culture medium, such as tetracycline and doxycycline, which allows the transgene transcription to be regulated. iPSCs are already being produced using such systems [23].

Another serious problem is the gene set itself that is used for the induction of pluripotency [22]. The ectopic transcription of *Oct4*, *Sox2*, *Klf4*, and *c-Myc* can lead to neoplastic development from cells derived from iPSCs, because the expression of *Oct4*, *Sox2*, *Klf4*, and *c-Myc* genes is associated with the development of multiple tumors known in oncogenetics [22, 24]. In particular, the overexpression of *Oct4* causes murine epithelial cell dysplasia [25], the aberrant expression of *Sox2* causes the development of serrated polyps and mucinous colon carcinomas [26], breast tumors are characterized by elevated expression of *Klf4* [27], and the improper expression of *c-Myc* is observed in 70% of human cancers [28]. Tumor development is oberved in ~50% of murine chimeras obtained through the injection of retroviral iPSCs into blastocysts, which is very likely associated with the reactivation of exogenous *c-Myc* [29, 30].

Several possible strategies exist for resolving the abovementioned problems:

- The search for a less carcinogenic gene set that is necessary and sufficient for reprogramming;
- The minimization of the number of genes required for reprogramming and searching for the nongenetic factors facilitating it;
- The search for systems allowing the elimination of the exogenous DNA from the host cell genome after the reprogramming;
- The development of delivery protocols for nonintegrated genetic constructs;
- The search for ways to reprogram somatic cells using recombinant proteins.

POSSIBLE GENE SUBSTITUENTS FOR *C-MYC* AND *KLF4* IN IPSC PREPARATION

The ectopic expression of *c-Myc* and *Klf4* genes is the most dangerous because of the high probability that malignant tumors will develop [22]. Hence the necessity to find other genes that could substitute *c-Myc* and *Klf4* in iPSC production. It has been reported that these genes can be successfully substituted by *NANOG* and *LIN28* for reprogramming human somatic cells [18]. iPSCs were prepared from murine embryonic fibroblasts by the overexpression of *Oct4* and *Sox2*, as well as the *Esrrb* gene encoding the murine orphan nuclear receptor beta. It has already been shown that *Esrrb*, which acts as a transcription activator of *Oct4*, *Sox2*, and *Nanog*, is necessary for the self-renewal and maintenance of the pluripotency of murine ESCs. Moreover, *Esrrb* can exert a positive control over *Klf4*. Thus, the genes causing elevated carcinogenicity of both iPSCs and their derivatives can be successfully replaced with less dangerous ones [31].

MEANS FOR INCREASING THE PRODUCTION EFFICIENCY OF IPSCS

The Most Effectively Reprogrammed Cell Lines

Murine and human iPSCs can be obtained from fibroblasts using the factors Oct4, Sox2, and Klf4, but without *c-Myc*. However, in this case, reprogramming decelerates and an essential shortcoming of stable iPSC clones is observed [32, 33]. The reduction of a number of necessary factors without any decrease in efficiency is possible when iPSCs are produced from murine and human neural stem cells (NSCs) [12, 34, 35]. For instance, iPSCs were produced from NSCs isolated from adult murine brain using two factors, Oct4 and Klf4, as well as even Oct4 by itself [12, 34]. Later, human iPSCs were produced by the reprogramming of fetal NSCs transduced with a retroviral vector only carrying *OCT4* [35]. It is most likely

that the irrelevance of Sox2, Klf4, and c-Myc is due to the high endogenous expression level of these genes in NSCs.

Successful reprogramming was also achieved in experiments with other cell lines, in particular, melanocytes of neuroectodermal genesis [36]. Both murine and human melanocytes are characterized by a considerable expression level of the *Sox2* gene, especially at early passages. iPSCs from murine and human melanocytes were produced without the use of Sox2 or c-Myc. However, the yield of iPSC clones produced from murine melanocytes was lower (0.03% without Sox2 and 0.02% without c-Myc) in comparison with that achieved when all four factors were applied to melanocytes (0.19%) and fibroblasts (0.056%). A decreased efficiency without Sox2 or c-Myc was observed in human melanocyte reprogramming (0.05% with all four factors and 0.01% without either *Sox2* or *c-Myc*). All attempts to obtain stable iPSC clones in the absence of both Sox2 and c-Myc were unsuccessful [36]. Thus, the minimization of the number of factors required for iPSC preparation can be achieved by choosing the proper somatic cell type that most effectively undergoes reprogramming under the action of fewer factors, for example, due to the endogenous expression of "pluripotency genes." However, if human iPSCs are necessary, these somatic cells should be easily accessible and well-cultured and their method of isolation should be as noninvasive as possible.

One of these cell types can be adipose stem cells (ASCs). This is a heterogeneous group of multipotent cells which can be relatively easily isolated in large amounts from adipose tissue following liposuction. Human iPSCs were successfully produced from ASCs with a twofold reprogramming rate and 20-fold efficiency (0.2%), exceeding those of fibroblasts [37].

However, more accessible resources for the effective production of human iPSCs are keratinocytes. When compared with fibroblasts, human iPSC production from keratinocytes demonstrated a 100-fold greater efficiency and a twofold higher reprogramming rate [38].

It has recently been found that the reprogramming of murine papillary dermal fibroblasts (PDFs) into iPSCs can be highly effective with the overexpression of only two genes, *Oct4* and *Klf4*, inserted into retroviral vectors [39]. PDFs are specialized cells of mesodermal genesis surrounding the stem cells of hair follicles. One characteristic feature of these cells is the endogenous expression of *Sox2*, *Klf4*, and *c-Myc* genes, as well as the gene-encoding alkaline phosphatase, one of the murine and human ESC markers. PDFs can be easily separated from other cell types by FACS (fluorescence-activated cell sorting) using life staining with antibodies against the surface antigens characteristic of one or another cell type. The PDF reprogramming efficiency with the use of four factors (Oct4, Sox2, Klf4, and c-Myc) retroviral vectors is 1.38%, which is 1,000-fold higher than the skin fibroblast reprogramming efficiency in the same system. Reprogramming PDFs with two factors, *Oct4* and *Klf4*, yields 0.024%, which is comparable to the efficiency of skin fibroblast reprogramming using all four factors. The efficiency of PDF reprogramming is comparable with that of NSCs, but PDF isolation is steady and far less invasive [39]. It seems likely that human PDF lines are also usable, and this cell type may appear to be one of the most promising for human iPSC production in terms of pharmacological studies and cell replacement therapy. The use of such cell types undergoing more effective reprogramming, together with methods providing the delivery of "pluripotency genes" without the integration of foreign DNA into the host genome and chemical compounds increasing the reprogramming efficiency and substituting some factors required for reprogramming, is particularly relevant.

Chemical Compounds Increasing Cell Reprogramming Efficiency

As was noted above, the minimization of the factors used for reprogramming decreases the efficiency of iPSC production. Nonetheless, several recent studies have shown that the use of genetic mechanisms, namely, the initiation of ectopic gene expression, can be substituted by chemical compounds, most of them operating at the epigenetic level. For instance, BIX-01294 inhibiting histone methyltransferase G9a allows murine fibroblast reprogramming using only two factors, Oct4 and Klf4, with a fivefold increased yield of iPSC clones in comparison with the control experiment without BIX-01294 [40]. BIX-01294 taken in combination with another compound can increase the reprogramming efficiency even more. In particular, BIX-01294 plus BayK8644 elevated the yield of iPCSs 15 times, and BIX-01294 plus RG108 elevated it 30 times when only two reprogramming factors, Oct4 and Klf4, were used. RG108 is an inhibitor of DNA methyltransferases, and its role in reprogramming is apparently in initiating the more rapid and effective demethylation of promoters of pluripotent cell-specific genes, whereas BayK8644 is an antagonist of L-type calcium channels, and its role in reprogramming is not understood very well [40]. However, more considerable results were obtained in reprogramming murine NSCs. The use of BIX-01294 allowed a 1.5-fold increase in iPSC production efficiency with two factors, Oct4 and Klf4, in comparison with reprogramming with all four factors. Moreover, BIX-01294 can even substitute Oct4 in the reprogramming of NSCs, although the yield is very low [41]. Valproic (2-propylvaleric) acid inhibiting histone deacetylases can also substitute c-Myc in reprogramming murine and human fibroblasts. Valproic acid (VPA) increases the reprogramming efficiency of murine fibroblasts 50 times, and human fibroblasts increases it 10–20 times when three factors are used [42, 43]. Other deacetylase inhibitors, such as TSA (trichostatin A) and SAHA (suberoylanilide hyroxamic acid), also increase the reprogramming efficiency. TSA increases the murine fibroblast reprogramming efficiency 15 times, and SAHA doubles it when all four factors are used [42]. Besides epigenetic regulators, the substances inhibiting the protein components of signaling pathways implicated in the differentiation of pluripotent cells are also applicable in the substitution of reprogramming factors. In particular, inhibitors of MEK and GSK3 kinases (PD0325901 and CHIR99021, respectively) benefit the establishment of the complete and stable pluripotency of iPSCs produced from murine NSCs using two factors, Oct4 and Klf4 [41, 44].

It has recently been shown that antioxidants can considerably increase the efficiency of somatic cell reprogramming. Ascorbic acid (vitamin C) can essentially influence the efficiency of iPSC production from various murine and human somatic cell types [45]. The transduction of murine embry-

onic fibroblasts (mEFs) with retroviruses carrying the *Oct4*, *Sox2*, and *Klf4* genes results in a significant increase in the production level of reactive oxygen species (ROS) compared with that of both control and Efs tranduced with *Oct4*, *Sox2*, *c-Myc*, and *Klf4*. In turn, the increase in the ROS level causes accelerated aging and apoptosis of the cell, which should influence the efficiency of cell reprogramming. By testing several substances possessing antioxidant activity such as vitamin B1, sodium selenite, reduced glutathione, and ascorbic acid, the authors have found that combining these substances increases the yield of GFP-positive cells in EF reprogramming (the *Gfp* gene was under the control of the *Oct4* gene promoter). The use of individual substances has shown that only ascorbate possesses a pronounced capability to increase the level of GFP-positive cells, although other substances keep their ROS-decreasing ability. In all likelihood, this feature of ascorbates is not directly associated with its antioxidant activity [45]. The score of GFP-positive iPSC colonies expressing an alkaline phosphatase has shown that the efficiency of iPSC production from mEFs with three factors (Oct4, Sox2, and Klf4) can reach 3.8% in the presence of ascorbate. When all four factors (Oct4, Sox2, Klf4, and c-Myc) are used together with ascorbate, the efficiency of iPSC production may reach 8.75%. A similar increase in the iPSC yield was also observed in the reprogramming of murine breast fibroblasts; i.e., the effect of vitamin C is not limited by one cell type. Moreover, the effect of vitamin C on the reprogramming efficiency is more profound than that of the deacetylase inhibitor valproic (2-propylvaleric) acid. The mutual effect of ascorbate and valproate is additive; i.e., these substances have different action mechanisms. Moreover, vitamin C facilitates the transition from pre-iPSCs to stable pluripotent cells. This feature is akin to the effects of PD0325901 and CHIR99021, which are inhibitors of MEK and GSK3 kinases, respectively. This effect of vitamin C expands to human cells as well [45]. Following the transduction of human fibroblasts with retroviruses carrying *Oct4*, *Sox2*, *Klf4*, and *c-Myc* and treatment with ascorbate, the authors prepared iPSCs with efficiencies reaching 6.2%. The reprogramming efficiency of ASCs under the same conditions reached 7.06%. The mechanism of the effect that vitamin C has on the reprogramming efficiency is not known in detail. Nevertheless, the acceleration of cell proliferation was observed at the transitional stage of reprogramming. The levels of the p53 and p21 proteins decreased in cells treated with ascorbate, whereas the DNA repair machinery worked properly [45]. It is interesting that an essential decrease in the efficiency of iPSC production has been shown under the action of processes initiated by p53 and p21 [46–50].

METHODS FOR IPSC PRODUCTION WITHOUT MODIFICATION OF THE CELL GENOME

As was mentioned above, for murine and human iPSC production, both retro- and lentiviruses were initially used as delivery vectors for the genes required for cell reprogramming. The main drawback of this method is the uncontrolled integration of viral DNA into the host cell's genome. Several research groups have introduced methods for delivering "pluripotency genes" into the recipient cell which either do not integrate allogenic DNA into the host genome or eliminate exogenous genetic constructs from the genome.

Cre-loxP-Mediated Recombination

To prepare iPSCs from patients with Parkinson's disease, lentiviruses were used, the proviruses of which can be removed from the genome by *Cre*-recombinase. To do this, the *loxP*-site was introduced into the lentiviral 3'LTR-regions containing separate reprogramming genes under the control of the doxycycline-inducible promoter. During viral replication, *loxP* was duplicated in the 5'LTR of the vector. As a result, the provirus integrated into the genome was flanked with two *loxP*-sites. The inserts were eliminated using the temporary transfection of iPSCs with a vector expressing *Cre*-recombinase [51].

In another study, murine iPSCs were produced using a plasmid carrying the *Oct4*, *Sox2*, *Klf4I,* and *c-Myc* genes in the same reading frame in which individual cDNAs were separated by sequences encoding 2A peptides, and practically the whole construct was flanked with *loxP*-sites [52]. The use of this vector allowed a notable decrease in the number of exogenous DNA inserts in the host cell's genome and, hence, the simplification of their following excision [52]. It has been shown using lentiviruses carrying similar polycistronic constructs that one copy of transgene providing a high expression level of the exogenous factors Oct4, Sox2, Klf4, and c-Myc is sufficient for the reprogramming of differentiated cells into the pluripotent state [53, 54].

The drawback of the *Cre-loxP*-system is the incomplete excision of integrated sequences; at least the *loxP*-site remains in the genome, so the risk of insertion mutations remains.

Plasmid Vectors

The application of lentiviruses and plasmids carrying the *loxP*-sites required for the elimination of transgene constructs modifies, although insignificantly, the host cell's genome. One way to avoid this is to use vector systems that generally do not provide for the integration of the whole vector or parts of it into the cell's genome. One such system providing a temporary transfection with polycistronic plasmid vectors was used for iPSC production from mEFs [29]. A polycistronic plasmid carrying the *Oct4*, *Sox2*, and *Klf4* gene cDNAs, as well as a plasmid expressing *c-Myc*, was transfected into mEFs one, three, five, and seven days after their primary seeding. Fibroblasts were passaged on the ninth day, and the iPSC colonies were selected on the 25th day. Seven out of ten experiments succeeded in producing GFP-positive colonies (the *Gfp* gene was under the control of the *Nanog* gene promoter). The iPSCs that were obtained were similar in their features to murine ESCs and did not contain inserts of the used DNA constructs in their genomes. Therefore, it was shown that wholesome murine iPSCs that do not carry transgenes can be reproducibly produced, and that the temporary overexpression of *Oct4*, *Sox2*, *Klf4*, and *c-Myc* is sufficient for reprogramming. The main drawback of this method is its low yield. In ten experiments the yield varied from 1 to 29 iPSC colonies per ten million fibroblasts, whereas up to 1,000 colonies per ten millions were obtained in the same study using retroviral constructs [29].

Episomal Vectors

Human iPSCs were successfully produced from skin fibroblasts using single transfection with polycistronic episomal

constructs carrying various combinations of *Oct4*, *Sox2*, *Nanog*, *Klf4*, *c-Myc*, *Lin28*, and *SV40LT* genes. These constructs were designed on the basis of the oriP/EBNA1 (Epstein-Barr nuclear antigen-1) vector [55]. The oriP/EBNA1 vector contains the IRES2 linker sequence allowing the expression of several individual cDNAs (encoding the genes required for successful reprogramming in this case) into one polycistronic mRNA from which several proteins are translated. The oriP/EBNA1 vector is also characterized by low-copy representation in the cells of primates and can be replicated once per cell cycle (hence, it is not rapidly eliminated, the way common plasmids are). Under nonselective conditions, the plasmid is eliminated at a rate of about 5% per cell cycle [56]. In this work, the broad spectrum of the reprogramming factor combinations was tested, resulting in the best reprogramming efficiency with cotransfection with three episomes containing the following gene sets: *Oct4* + *Sox2* + *Nanog* + *Klf4*, *Oct4* + *Sox2* + *SV40LT* + *Klf4*, and *c-Myc* + *Lin28*. *SV40LT* (*SV40 large T gene*) neutralizes the possible toxic effect of *c-Myc* overexpression [57]. The authors have shown that wholesome iPSCs possessing all features of pluripotent cells can be produced following the temporary expression of a certain gene combination in human somatic cells without the integration of episomal DNA into the genome. However, as in the case when plasmid vectors are being used, this way of reprogramming is characterized by low efficiency. In separate experiments the authors obtained from 3 to 6 stable iPSC colonies per 10^6 transfected fibroblasts [55]. Despite the fact that skin fibroblasts are well-cultured and accessible, the search for other cell types which are relatively better cultured and more effectively subject themselves to reprogramming through this method is very likely required. Another drawback of the given system is that this type of episome is unequally maintained in different cell types.

PiggyBac-Transposition

One promising system used for iPSC production without any modification of the host genome is based on DNA transposons. So-called *PiggyBac*-transposons containing 2A-linkered reprogramming genes localized between the 5'- and 3'-terminal repeats were used for iPSC production from fibroblasts. The integration of the given constructs into the genome occurs due to mutual transfection with a plasmid encoding transposase. Following reprogramming due to the temporary expression of transposase, the elimination of inserts from the genome took place [58, 59]. One advantage of the *PiggyBac* system on *Cre-loxP* is that the exogenous DNA is completely removed [60].

However, despite the relatively high efficiency of exogenous DNA excision from the genome by *PiggyBac*-transposition, the removal of a large number of transposon copies is hardly achievable.

Nonintegrating Viral Vectors

Murine iPSCs were successfully produced from hepatocytes and fibroblasts using four adenoviral vectors nonintegrating into the genome and carrying the *Oct4*, *Sox2*, *Klf4*, and *c-Myc* genes. An analysis of the obtained iPSCs has shown that they are similar to murine ESCs in their properties (teratoma formation, gene promoter DNA methylation, and the expression of pluripotent markers), but they do not carry insertions of viral DNA in their genomes [61]. Later, human fibroblast-derived iPSCs were produced using this method [62].

The authors of this paper cited the postulate that the use of adenoviral vectors allows the production of iPSCs, which are suitable for use without the risk of viral or oncogenic activity. Its very low yield (0.0001–0.001%), the deceleration of reprogramming, and the probability of tetraploid cell formation are the drawbacks of the method. Not all cell types are equally sensitive to transduction with adenoviruses.

Another method of gene delivery based on viral vectors was recently employed for the production of human iPSCs. The sendai-virus (SeV)-based vector was used in this case [63]. SeV is a single-stranded RNA virus which does not modify the genome of recipient cells; it seems to be a good vector for the expression of reprogramming factors. Vectors containing either all "pluripotency factors" or three of them (without *c-Myc*) were used for reprogramming the human fibroblast. The construct based on SeV is eliminated later in the course of cell proliferation. It is possible to remove cells with the integrated provirus via negative selection against the surface HN antigen exposed on the infected cells. The authors postulate that reprogramming technology based on SeV will enable the production of clinically applicable human iPSCs [63].

Cell Transduction with Recombinant Proteins

Although the methods for iPSC production without gene modification of the cell's genome (adenoviral vectors, plasmid gene transfer, etc.) are elaborated, the theoretical possibility for exogenous DNA integration into the host cell's genome still exists. The mutagenic potential of the substances used presently for enhancing iPSC production efficiency has not been studied in detail. Fully checking iPSC genomes for exogenous DNA inserts and other mutations is a difficult task, which becomes impossible to solve in bulk culturing of multiple lines. The use of protein factors delivered into a differentiated cell instead of exogenous DNA may solve this problem. Two reports have been published to date in which murine and human iPSCs were produced using the recombinant OCT4, SOX2, KLF4, and C-MYC proteins [64, 65]. The method used to deliver the protein into the cell is based on the ability of peptides enriched with basic residues (such as arginine and lysine) to penetrate the cell's membrane. Murine iPSCs were produced using the recombinant OCT4, SOX2, KLF4, and C-MYC proteins containing eleven C-terminal arginine residues and expressed in *E. coli*. The authors succeeded in producing murine iPSCs during four rounds of protein transduction into embryonic fibroblasts [65]. However, iPSCs were only produced when the cells were additionally treated with 2-propylvalerate (the deacetylase inhibitor). The same principle was used for the production of human iPSCs, but protein expression was carried out in human HEK293 cells, and the proteins were expressed with a fragment of nine arginins at the protein C-end. Researchers have succeeded in producing human iPSCs after six transduction rounds without any additional treatment [64]. The efficiency of producing human iPSC in this way was 0.001%, which is one order lower than the reprogramming efficiency with retroviruses. Despite some drawbacks, this method is very promising for the production of patient-specific iPSCs.

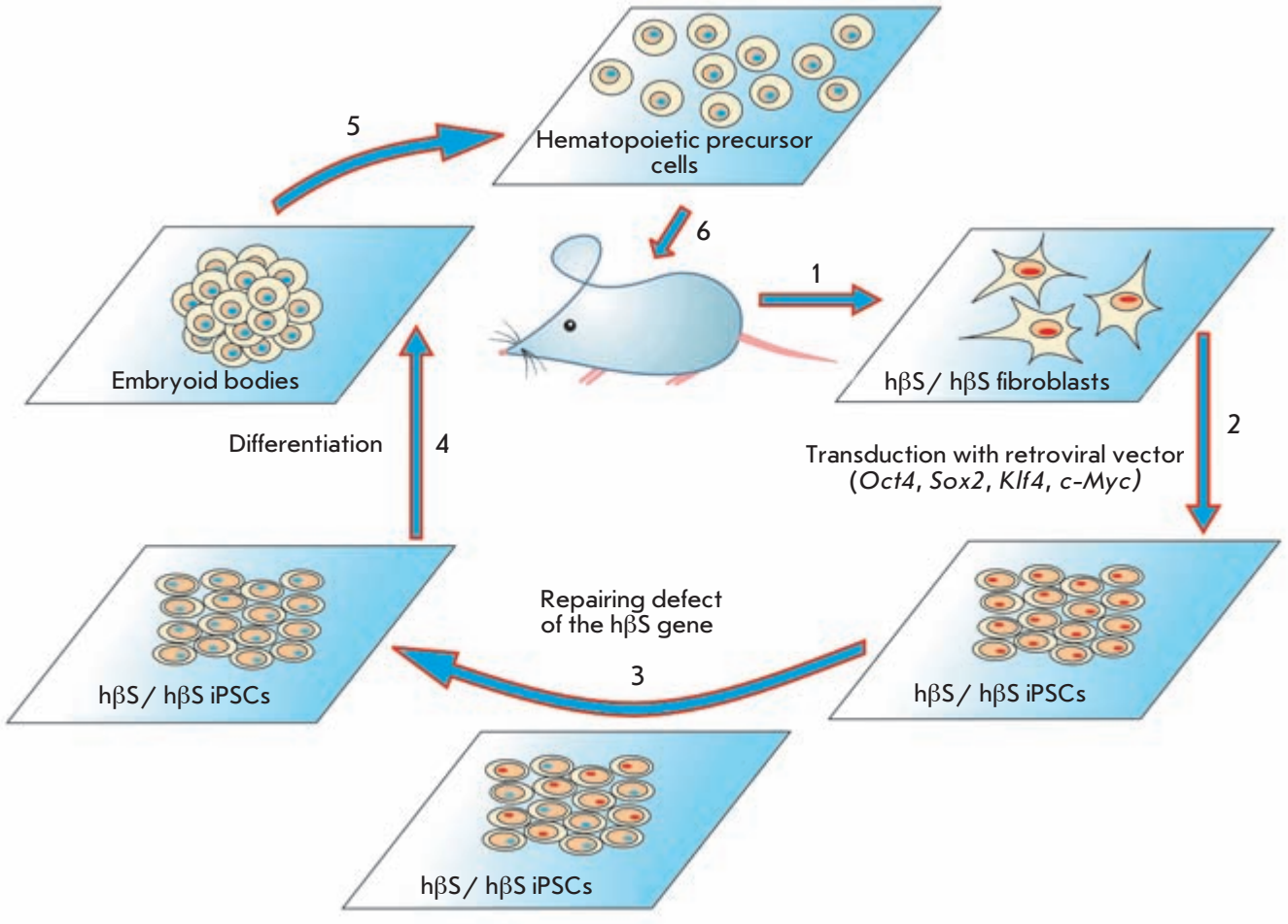

Design of an experiment on repairing the mutant phenotype in mice modeling sickle cell anemia development [2]. Fibroblasts isolated from the tail of a mouse (*1*) carrying a mutant allele of the gene encoding the human hemoglobin β-chain (hβs) were used for iPSC production (*2*). The mutation was then repaired in iPSCs by means of homological recombination (*3*) followed by cell differentiation via the embryoid body formation (*4*). The directed differentiation of the embryoid body cells led to hematopoietic precursor cells (*5*) that were subsequently introduced into a mouse exposed to ionizing radiation (*6*).

INDUCED PLURIPOTENT STEM CELLS AS A MODEL FOR PATHOGENESIS STUDIES AND A SOURCE OF CELL REPLACEMENT THERAPY

The first lines of human pluripotent ESCs were produced in 1998 [6]. In line with the obvious fundamental importance of embryonic stem cell studies with regard to the multiple processes taking place in early embryogenesis, much of the interest of investigators is associated with the possibility of using ESCs and their derivatives as models for the pathogenesis of human diseases, new drugs testing, and cell replacement therapy. Substantial progress is being achieved in studies on directed human ESC differentiation and the possibility of using them to correct degenerative disorders. Functional cell types, such as motor dopaminergic neurons, cardiomyocytes, and hematopoietic cell progenitors, can be produced as a result of ESC differentiation. These cell derivatives, judging from their biochemical and physiological properties, are potentially applicable for the therapy of cardiovascular disorders, nervous system diseases, and human hematological disorders [66]. Moreover, derivatives produced from ESCs have been successfully used for treating diseases modeled on animals. Therefore, blood-cell progenitors produced from ESCs were successfully used for correcting immune deficiency in mice. Visual functions were restored in blind mice using photoreceptors produced from human ESCs, and the normal functioning of the nervous system was restored in rats modeling Parkinson's disease using the dopaminergic neurons produced from human ESCs [67–70]. Despite obvious success, the full-scale application of ESCs in therapy and the modeling of disorders still carry difficulties, because of the necessity to create ESC banks corresponding to all HLA-haplotypes, which is practically unrealistic and hindered by technical and ethical problems.

Table. iPSC lines produced by reprogramming somatic cells from patients with various diseases

Disease	Causative factor	Reprogrammed cell type	Means of reprogramming	Ref. No
Adenosine deaminase deficiency	Replacement of GGG with AGG in exon 7 resulting in G216R substitution or deletion of GAAGA in exon 10 of the *ADA* (*adenosine deaminase*) gene	Skin fibroblasts, karyotype 46,XY	Transduction with retroviruses carrying the *OCT4*, *SOX2*, *KLF4*, and *c-MYC* cDNAs	[91]
Type 3 Gaucher's disease	Replacement of AAC with AGC in exon 9 or insertion of G at position 84 of the *GBA* (*β-acid glucosidase*) gene cDNA	Skin fibroblasts, karyotype 46,XY	Transduction with retroviruses carrying the *OCT4*, *SOX2*, *KLF4*, and *c-MYC* cDNAs	[91]
Duchenne muscular dystrophy	Deletion of exons 45-52 of the *DMD* (*dystrophin*) gene	Skin fibroblasts, karyotype 46,XY	Transduction with retroviruses carrying the *OCT4*, *SOX2*, *KLF4*, and *c-MYC* cDNAs	[91]
Becker muscular dystrophy	Unidentified mutation in the *DMD* gene	Skin fibroblasts, karyotype 46,XY	Transduction with retroviruses carrying the *OCT4*, *SOX2*, *KLF4*, and *c-MYC* cDNAs	[91]
Down syndrome	Trisomy of chromosome 21	Skin fibroblasts, karyotype 47,XY,+21	Transduction with retroviruses carrying the *OCT4*, *SOX2*, *KLF4*, and *c-MYC* cDNAs	[91]
Parkinson's disease	Multifactorial disease	Skin fibroblasts, karyotype 46,XY	Transduction with retroviruses carrying the *OCT4*, *SOX2*, *KLF4*, and *c-MYC* cDNAs	[91]
		Fibroblasts; the age of the patient at the moment of biopsy was 53–85 years, karyotypes: 46,XY (six lines) and 46,XX (one line)	Transduction with lentiviruses carrying the *OCT4*, *SOX2*, and *KLF4* or *OCT4*, *SOX2*, *KLF4* and *c-MYC* genes. Viral LTRs contained *LoxP* sites required for the excision of the exogenous construct from the cell genome	[51]
Diabetes mellitus type 1 (juvenile diabetes)	Multifactorial disease	Skin fibroblasts, karyotype 46,XX	Transduction with retroviruses carrying the *OCT4*, *SOX2*, *KLF4*, and *c-MYC* cDNAs	[91]
Shwachman–Bodian–Diamond syndrome	Point mutations in the *SBDS* (*Shwachman–Bodian–Diamond Syndrome*) gene	Bone marrow mesenchymal cells, karyotype 46,XY	Transduction with retroviruses carrying the *OCT4*, *SOX2*, *KLF4*, and *c-MYC* cDNAs	[91]
Huntington's disease	CAG repeat expansion in the *Huntington* gene from normal 11–34 copies to 37–100 and more	Skin fibroblasts, karyotype 46,XX	Transduction with retroviruses carrying the *OCT4*, *SOX2*, *KLF4*, and *c-MYC* cDNAs	[91]
Lesch–Nyhan syndrome	Mutations in the *HPRT* (*hypoxanthine-guanine phosphoribosyltransferase*) gene	Skin fibroblasts, karyotype 46,XX	Transduction with retroviruses carrying the *OCT4*, *SOX2*, *KLF4*, and *c-MYC* cDNAs. One line was produced by transduction with doxycyclin-controlled lentiviral vectors carrying the *OCT4*, *SOX2*, *KLF4*, *c-MYC*, and *NANOG* cDNAs	[91]
		Fibroblasts, karyotype 46,XX	Transduction with lentiviruses carrying the *OCT4*, *SOX2*, and *KLF4* genes. Viral LTRs contained *LoxP* sites required for the excision of exogenous construct from cell genome	[51]
Dyskeratosis congenita (Zinsser-Engman-Cole syndrome)	Mutations in the *DKC1* (*Dyskeratosis congenita*) gene	Fibroblasts, karyotype 46,XX	Transduction with lentiviruses carrying the *OCT4*, *SOX2*, and *KLF4* genes	[51]
Spinal muscular atrophy	Mutations in the *SMN1* (*Survival Motor Neuron 1*) gene resulting in a decreased level of the SMN protein	Skin fibroblasts, karyotype 46,XY	Transduction with lentiviruses carrying the *OCT4*, *SOX2*, *NANOG*, and *LIN28* cDNAs	[89]
Familial dysautonomia	Mutation in the *IKBKAP* (*inhibitor of kappa light polypeptide gene enhancer in B-cells; IkB kinase complex associated protein*) gene resulted in shift splicing that generates a transcript lacking exon 20	Lung and skin fibroblasts, karyotypes 46,XX and 46,XY	Transduction with lentiviruses carrying the *OCT4*, *SOX2*, *KLF4*, and *c-MYC* cDNAs	[90]
β-Thalassemia	Mutations in the *HBB* (*haemoglobin beta*) gene	Skin fibroblasts, karyotype 46,XY	Transduction with retroviruses carrying the *OCT4*, *SOX2*, *KLF4*, and *c-MYC* cDNAs	[92]
Diabetes mellitus type 1 (juvenile diabetes)	Multifactorial disease	Skin fibroblasts, karyotype 46,XY	Transduction with retroviruses carrying the *OCT4*, *SOX2*, and *KLF4* cDNAs	[93]
Amyotrophic lateral sclerosis	L144F substitution in superoxide dismutase encoded by the dominant allele of the *SOD1* (*Superoxide dismutase 1*) gene; this mutation is associated with slow disease progression	Skin fibroblasts, karyotype 46,XX	Transduction with retroviruses carrying the *OCT4*, *SOX2*, *KLF4*, and *c-MYC* cDNAs	[94]
Fanconi anemia	At present, 13 genes whose mutations cause Fanconi anemia are known	Skin fibroblasts and epidermal keratinocytes	Transduction with retroviruses carrying the *OCT4*, *SOX2*, *KLF4*, and *c-MYC* cDNAs. iPSCs from keratinocytes were produced without *c-MYC*	[87]

Induced pluripotent stem cells can become an alternative for ESCs in the area of clinical application of cell replacement therapy and screening for new pharmaceuticals. iPSCs closely resemble ESCs and, at the same time, can be produced in almost unlimited amounts from the differentiated cells of each patient. Despite the fact that the first iPSCs were produced relatively recently, work on directed iPSC differentiation and the production of patient-specific iPSCs is intensive, and progress in this field is obvious.

Dopamine and motor neurons were produced from human iPSCs by directed differentiation *in vitro* [71, 72]. These types of neurons are damaged in many inherited or acquired human diseases, such as spinal cord injury, Parkinson's disease, spinal muscular atrophy, and amyotrophic lateral sclerosis. Some investigators have succeeded in producing various retinal cells from murine and human iPSCs [73–75]. Human iPSCs have been shown to be spontaneously differentiated *in vitro* into the cells of retinal pigment epithelium [76]. Another group of investigators has demonstrated that treating human and murine iPSCs with WNT and NODAL antagonists in a suspended culture induces the appearance of markers of cell progenitors and pigment epithelium cells. Further treating the cells with retinoic acid and taurine activates the appearance of cells expressing photoreceptor markers [75].

Several research groups have produced functional cardiomyocytes (CMs) *in vitro* from murine and human iPSCs [77–81]. Cardiomyocytes produced from iPSC are very similar in characteristics (morphology, marker expression, electrophysiological features, and sensitivity to chemicals) to the CMs of cardiac muscle and to CMs produced from differentiated ESCs. Moreover, murine iPSCs, when injected, can repair muscle and endothelial cardiac tissues damaged by cardiac infarction [77].

Hepatocyte-like cell derivatives, dendritic cells, macrophages, insulin-producing cell clusters similar to the duodenal islets of Langerhans, and hematopoietic and endothelial cells are currently produced from murine and human iPSCs, in addition to the already-listed types of differentiated cells [82–85].

In addition to directed differentiation *in vitro*, investigators apply much effort at producing patient-specific iPSCs. The availability of pluripotent cells from individual patients makes it possible to study pathogenesis and carry out experiments on the therapy of inherited diseases, the development of which is associated with distinct cell types that are hard to obtain by biopsy: so the use of iPSCs provides almost an unlimited resource for these investigations. Recently, the possibility of treating diseases using iPSCs was successfully demonstrated, and the design of the experiment is presented in the figure. A mutant allele was substituted with a normal allele via homologous recombination in murine fibroblasts representing a model of human sickle cell anemia. iPSCs were produced from "repaired" fibroblasts and then differentiated into hematopoietic cell precursors. The hematopoietic precursors were then injected into a mouse from which the skin fibroblasts were initially isolated (see figure). As a result, the initial pathological phenotype was substantially corrected [86]. A similar approach was applied to the fibroblasts and keratinocytes of a patient with Fanconi's anemia. The normal allele of the mutant gene producing anemia was introduced into a somatic cell genome using a lentivirus, and then iPSCs were obtained from these cells. iPSCs carrying the normal allele were differentiated into hematopoietic cells maintaining a normal phenotype [87]. The use of lentiviruses is unambiguously impossible when producing cells to be introduced into the human body due to their oncogenic potential. However, new relatively safe methods of genome manipulation are currently being developed; for instance, the use of synthetic nucleases containing zinc finger domains allowing the effective correction of genetic defects *in vitro* [88].

The induced pluripotent stem cells are an excellent model for pathogenetic studies at the cell level and testing compounds possessing a possible therapeutic effect.

The induced pluripotent stem cells were produced from the fibroblasts of a patient with spinal muscular atrophy (SMA) (SMA-iPSCs). SMA is an autosomal recessive disease caused by a mutation in the *SMN1* (*survival motor neuron 1*) gene, which is manifested as the selective nonviability of lower α-motor neurons. Patients with this disorder usually die at the age of about two years. Existing experimental models of this disorder based on the use of flatworms, drosophila, and mice are not satisfactory. The available fibroblast lines from patients with SMA cannot provide the necessary data on the pathogenesis of this disorder either. It was shown that motor neurons produced from SMA-iPSCs can retain the features of SMA development, selective neuronal death, and the lack of *SMN1* transcription. Moreover, the authors succeeded in elevating the SMN protein level and aggregation (encoded by the *SMN2* gene, whose expression can compensate for the shortage in the SMN1 protein) in response to the treatment of motor neurons and astrocytes produced from SMA-iPSCs with valproate and torbomycin [89]. iPSCs and their derivatives can serve as objects for pharmacological studies, as has been demonstrated on iPSCs from patients with familial dysautonomia (FDA) [90]. FDA is an inherited autosomal recessive disorder manifested as the degeneration of sensor and autonomous neurons. This is due to a mutation causing the tissue-specific splicing of the *IKBKAP* gene, resulting in a decrease in the level of the full-length IKAP protein. iPSCs were produced from fibroblasts of patients with FDA. They possessed all features of pluripotent cells. Neural derivatives produced from these cells had signs of FDA pathogenesis and low levels of the full-length *IKBKAP* transcript. The authors studied the effect of three substances, kinetin, epigallocatechin gallate, and tocotrienol, on the parameters associated with FDA pathogenesis. Only kinetin has been shown to induce an increase in the level of full-length *IKBKAP* transcript. Prolonged treatment with kinetin induces an increase in the level of neuronal differentiation and expression of peripheral neuronal markers.

Currently, a broad spectrum of iPSCs is produced from patients with various inherited pathologies and multifactorial disorders, such as Parkinson's disease, Down syndrome, type 1 diabetes, Duchenne muscular dystrophy, β-talassemia, etc., which are often lethal and can scarcely be treated with routine therapy [51, 87, 89, 91–94]. The data on iPSCs produced by reprogramming somatic cells from patients with various pathologies are given in the table.

One can confidently state that both iPSCs themselves and their derivatives are potent instruments applicable in

biomedicine, cell replacement therapy, pharmacology, and toxicology. However, the safe application of iPSC-based technologies requires the use of methods of iPSCs production and their directed differentiation which minimize both the possibility of mutations in cell genomes under *in vitro* culturing and the probability of malignant transformation of the injected cells. The development of methods for human iPSC culturing without the use of animal cells (for instance, the feeder layer of murine fibroblasts) is necessary; they make a viral-origin pathogen transfer from animals to humans impossible. There is a need for the maximum standardization of conditions for cell culturing and differentiation. ●

This study was supported by the Russian Academy of Sciences' Presidium Program "Molecular and Cell Biology."

REFERENCES

1. Smith A.G. // Annu. Rev. Cell. Dev. Biol. 2001. V. 17. P. 435–462.
2. Boyer L.A., Lee T.I., Cole M.F., et al. // Cell. 2005. V. 122. P. 947–956.
3. Loh Y.H., Wu Q., Chew J.L., et al. // Nat. Genet. 2006. V. 38. P. 431–440.
4. Martin G.R. // Proc. Natl. Acad. Sci. USA. 1981. V. 78. P. 7634–7638.
5. Evans M.J., Kaufman M.H. // Nature. 1981. V. 292. P. 154–156.
6. Thomson J.A., Itskovitz-Eldor J., Shapiro S.S., et al. // Science. 1998. V. 282. P. 1145–1147.
7. Hochedlinger K., Jaenisch R. // Nature. 2006. V. 441. P. 1061–1067.
8. Takahashi K., Yamanaka S. // Cell. 2006. V. 126. P. 663–676.
9. Aoi T., Yae K., Nakagawa M., et al. // Science. 2008. V. 321. P. 699–702.
10. Eminli S., Utikal J., Arnold K., et al. // Stem Cells. 2008. V. 26. P. 2467–2474.
11. Hanna J., Markoulaki S., Schorderet P., et al. // Cell. 2008. V. 133. P. 250–264.
12. Kim J.B., Zaehres H., Wu G., et al. // Nature. 2008. V. 454. P. 646–650.
13. Stadtfeld M., Brennand K., Hochedlinger K. // Curr. Biol. 2008. V. 18. P. 890–894.
14. Wernig M., Meissner A., Foreman R., et al. // Nature. 2007. V. 448. P. 318–324.
15. Takahashi K., Tanabe K., Ohnuki M., et al. // Cell. 2007. V. 131. P. 861–872.
16. Park I.H., Zhao R., West J.A., et al. // Nature. 2008. V. 451. P. 141–146.
17. Lowry W.E., Richter L., Yachechko R., et al. // Proc. Natl. Acad. Sci. USA. 2008. V. 105. P. 2883–2888.
18. Yu J., Vodyanik M.A., Smuga-Otto K., et al. / // Science. 2007. V. 318. P. 1917–1920.
19. Kang L., Wang J., Zhang Y., et al. / // Cell Stem Cell. 2009. V. 5. P. 135–138.
20. Zhao X.Y., Li W., Lv Z., et al. / // Nature. 2009. V. 461. P. 86–90.
21. Hotta A., Ellis J. // J. Cell Biochem. 2008. V. 105. P. 940–948.
22. Okita K., Ichisaka T., Yamanaka S. // Nature. 2007. V. 448. P. 313–317.
23. Carey B.W., Markoulaki S., Hanna J., et al. // Proc. Natl. Acad. Sci. USA. 2009. V. 106. P. 157–162.
24. Ben-Porath I., Thomson M.W., Carey V.J., et al. // Nat. Genet. 2008. V. 40. P. 499–507.
25. Hochedlinger K., Yamada Y., Beard C., Jaenisch R. // Cell. 2005. V. 121. P. 465–477.
26. Park E.T., Gum J.R., Kakar S., et al. // Int. J. Cancer. 2008. V. 122. P. 1253–1260.
27. Ghaleb A.M., Nandan M.O., Chanchevalap S., et al. // Cell Res. 2005. V. 15. P. 92–96.
28. Kuttler F., Mai S. // Genome Dyn. 2006. V. 1. P. 171–190.
29. Okita K., Nakagawa M., Hyenjong H., et al. // Science. 2008. V. 322. P. 949–953.
30. Duinsbergen D., Salvatori D., Eriksson M., Mikkers H. // Ann. N. Y. Acad. Sci. 2009. V. 1176. P. 197–204.
31. Feng B., Jiang J., Kraus P., et al. // Nat. Cell. Biol. 2009. V. 11. P. 197–203.
32. Nakagawa M., Koyanagi M., Tanabe K., et al. // Nat. Biotechnol. 2008. V. 26. P. 101–106.
33. Wernig M., Meissner A., Cassady J.P., Jaenisch R. // Cell Stem Cell. 2008. V. 2. P. 10–12.
34. Kim J.B., Sebastiano V., Wu G., et al. // Cell. 2009. V. 136. P. 411–419.
35. Kim J.B., Greber B., Arauzo-Bravo M.J., et al. // Nature. 2009. V. 461. P. 649–643.
36. Utikal J., Maherali N., Kulalert W., Hochedlinger K. // J. Cell Sci. 2009. V. 122. P. 3502–3510.
37. Sun N., Panetta N.J., Gupta D.M., et al. // Proc. Natl. Acad. Sci. USA. 2009. V. 106. P. 15720–15725.
38. Aasen T., Raya A., Barrero M.J., et al. // Nat. Biotechnol. 2008. V. 26. P. 1276–1284.
39. Tsai S.Y., Clavel C., Kim S., et al. // Stem Cells. 2010. V. 28. P. 221–228
40. Shi Y., Desponts C., Do J.T., et al. // Cell Stem Cell. 2008. V. 3. P. 568–574.
41. Shi Y., Do J.T., Desponts C., et al. // Cell Stem Cell. 2008. V. 2. P. 525–528.
42. Huangfu D., Maehr R., Guo W., et al. // Nat. Biotechnol. 2008. V. 26. P. 795–797.
43. Huangfu D., Osafune K., Maehr R., et al. // Nat. Biotechnol. 2008. V. 26. P. 1269–1275.
44. Silva J., Barrandon O., Nichols J., et al. // PLoS Biol. 2008. V. 6. P. e253.
45. Esteban M.A., Wang T., Qin B., et al. // Cell Stem Cell. 2010. V. 6. P. 71–79.
46. Hong H., Takahashi K., Ichisaka T., et al. // Nature. 2009. V. 460. P. 1132–1135.
47. Utikal J., Polo J.M., Stadtfeld M., et al. // Nature. 2009. V. 460. P. 1145–1148.
48. Marion R.M., Strati K., Li H., et al. // Nature. 2009. V. 460. P. 1149–1153.
49. Li H., Collado M., Villasante A., et al. // Nature. 2009. V. 460. P. 1136–1139.
50. Kawamura T., Suzuki J., Wang Y.V., et al. // Nature. 2009. V. 460. P. 1140–1144.
51. Soldner F., Hockemeyer D., Beard C., et al. // Cell. 2009. V. 136. P. 964–977.
52. Kaji K., Norrby K., Paca A., et al. // Nature. 2009. V. 458. P. 771–775.
53. Shao L., Feng W., Sun Y., et al. // Cell Res. 2009. V. 19. P. 296–306.
54. Sommer C.A., Stadtfeld M., Murphy G.J., et al. // Stem Cells. 2009. V. 27. P. 543–549.
55. Yu J., Hu K., Smuga-Otto K., et al. // Science. 2009. V. 324. P. 797–801.
56. Nanbo A., Sugden A., Sugden B. // EMBO J. 2007. V. 26. P. 4252–4262.
57. Hahn W.C., Counter C.M., Lundberg A.S., et al. // Nature. 1999. V. 400. P. 464–468.
58. Woltjen K., Michael I.P., Mohseni P., et al. // Nature. 2009. V. 458. P. 766–770.
59. Yusa K., Rad R., Takeda J., Bradley A. // Nat. Methods. 2009. V. 6. P. 363–369.
60. Elick T.A., Bauser C.A., Fraser M.J. // Genetica. 1996. V. 98. P. 33–41.
61. Stadtfeld M., Nagaya M., Utikal J., et al. // Science. 2008. V. 322. P. 945–949.
62. Zhou W., Freed C.R. // Stem Cells. 2009. V. 27. P. 2667–2674.
63. Fusaki N., Ban H., Nishiyama A., et al. // Proc. Jpn. Acad. Ser. B. Phys. Biol. Sci. 2009. V. 85. P. 348–362.

64. Kim D., Kim C.H., Moon J.I., et al. // Cell Stem Cell. 2009. V. 4. P. 472–476.
65. Zhou H., Wu S., Joo J.Y., et al. // Cell Stem Cell. 2009. V. 4. P. 381–384.
66. Murry C.E., Keller G. // Cell. 2008. V. 132. P. 661–680.
67. Rideout W.M., 3rd, Hochedlinger K., Kyba M., et al. // Cell. 2002. V. 109. P. 17–27.
68. Lamba D.A., Gust J., Reh T.A. // Cell Stem Cell. 2009. V. 4. P. 73–79.
69. Yang D., Zhang Z.J., Oldenburg M., et al. // Stem Cells. 2008. V. 26. P. 55–63.
70. Kim J.H., Auerbach J.M., Rodriguez-Gomez J.A., et al. // Nature. 2002. V. 418. P. 50–56.
71. Karumbayaram S., Novitch B.G., Patterson M., et al. // Stem Cells. 2009. V. 27. P. 806–811.
72. Chambers S.M., Fasano C.A., Papapetrou E.P., et al. // Nat. Biotechnol. 2009. V. 27. P. 275–280.
73. Carr A.J., Vugler A.A., Hikita S.T., et al. // PLoS One. 2009. V. 4. P. e8152.
74. Meyer J.S., Shearer R.L., Capowski E.E., et al. // Proc. Natl. Acad. Sci. USA. 2009. V. 106. P. 16698–16703.
75. Hirami Y., Osakada F., Takahashi K., et al. // Neurosci. Lett. 2009. V. 458. P. 126–131.
76. Buchholz D.E., Hikita S.T., Rowland T.J., et al. // Stem Cells. 2009. V. 27. P. 2427–2434.
77. Nelson T.J., Martinez-Fernandez A., Yamada S., et al. // Circulation. 2009. V. 120. P. 408–416.
78. Tanaka T., Tohyama S., Murata M., et al. // Biochem. Biophys. Res. Commun. 2009. V. 385. P. 497–502.
79. Kuzmenkin A., Liang H., Xu G., et al. // FASEB J. 2009. V. 23. P. 4168–4180.
80. Mauritz C., Schwanke K., Reppel M., et al. // Circulation. 2008. V. 118. P. 507–517.
81. Gai H., Leung E.L., Costantino P.D., et al. // Cell. Biol. Int. 2009. V. 33. P. 1184–1193.
82. Song Z., Cai J., Liu Y., et al. // Cell Res. 2009. V. 19. P. 1233–1242.
83. Senju S., Haruta M., Matsunaga Y., et al. // Stem Cells. 2009. V. 27. P. 1021–1031.
84. Tateishi K., He J., Taranova O., et al. // J. Biol. Chem. 2008. V. 283. P. 31601–31607.
85. Choi K.D., Yu J., Smuga-Otto K., et al. // Stem Cells. 2009. V. 27. P. 559–567.
86. Hanna J., Wernig M., Markoulaki S., et al. // Science. 2007. V. 318. P. 1920–1923.
87. Raya A., Rodriguez-Piza I., Guenechea G., et al. // Nature. 2009. V. 460. P. 53–59.
88. Zou J., Maeder M.L., Mali P., et al. // Cell Stem Cell. 2009. V. 5. P. 97–110.
89. Ebert A.D., Yu J., Rose F.F., Jr., et al. // Nature. 2009. V. 457. P. 277–280.
90. Lee G., Papapetrou E.P., Kim H., et al. // Nature. 2009. V. 461. P. 402–406.
91. Park I.H., Arora N., Huo H., et al. // Cell. 2008. V. 134. P. 877–886.
92. Wang Y., Jiang Y., Liu S., et al. // Cell Res. 2009. V. 19. P. 1120–1123.
93. Maehr R., Chen S., Snitow M., et al. // Proc. Natl. Acad. Sci. USA. 2009. V. 106. P. 15768–15773.
94. Dimos J.T., Rodolfa K.T., Niakan K.K., et al. // Science. 2008. V. 321. P. 1218–1221.

Bioglycans and Natural Glycosides As a Promising Research Topic in Bioorganic Chemistriy

Yu. S. Ovodov
Institute of Physiology, Komi Science Center, The Urals Branch, Russian Academy of Sciences
E-mail: ovoys@physiol.komisc.ru
Received 18.03.2010

ABSTRACT **This review defines bioorganic chemistry as one of the most important constituents of physico-chemical biology, which is a fundamental life science. The problems and goals of bioorganic chemistry are examined through a comparatively small number of examples. Bioorganic chemistry is supposed to be a logical continuation of the chemistry of the natural substances that arose many years ago. Bioorganic chemistry has contributed some achievements in solving the problems of the chemical structure, biological function, and physiological activity of biopolymers and low-molecular-weight bioregulators, as well as in the elucidation of the molecular mechanisms of different life processes. The most striking achievements in bioorganic chemistry are discussed in this paper. However, this review discusses not only the general achievements in this field of science, but also research data obtained by scientists from the Pacific Institute of Bioorganic Chemistry, Far East Branch, Russian Academy of Sciences (Vladivostok, Russia), and the Institute of Physiology, Komi Science Centre, The Urals Branch, Russian Academy of Sciences (Syktyvkar, Russia). Particular attention is focused on comprehensive research into polysaccharides and biopolymers (bioglycans) and some natural glycosides that the author of this review has studied for a long time. The author has worked in these institutes for a long time and was honored by being chosen to head one of the scientific schools in the field of bioorganic chemistry and molecular immunology.**
KEYWORDS **bioglycans, natural glycosides, low-molecular-weight bioregulators.**
ABBREVIATIONS **LPS – lipopolysaccharide, PSA – prostate specific antigen, LPPC - lipopolysaccharide-protein complex, CEA – carcino-embryonic antigen, PC – prostate cancer.**

INTRODUCTION

The chemical structure of biopolymers and bioregulators with low molecular weight, their biological activity, and their role in the organism are what bioorganic chemistry studies. Bioorganic chemistry also studies the physiological effects of different chemicals isolated from a particular source in a human or nonhuman organism. According to N.E. Spichenkov and V.E. Vas'kovsky [1], the term "bioorganic chemistry" was first mentioned in 1967 in an article by M.M. Shemyakin and A.S. Khokhlov [2]. All aspects of bioorganic chemistry were thoroughly reviewed by Yu.A. Ovchinnikov in his classical work [3] widely used by specialists in this scientific field.

Since the middle of the 20th century, bioorganic chemists have been interested in marine organisms [4–6], including seaweeds, marine animals, and bacteria. Many marine organisms are sources of unusual secondary metabolites with peculiar structures and unique properties [7]. Studies of the polysaccharides of seaweeds began in the 19th century and successfully continue today [8].

Bioorganic chemistry plays a crucial role in the development of pharmacological drugs, nutritional supplements, pharmacological chemistry, and medicine. This scientific branch rests on the basis of the chemistry of the natural compounds used in ethnomedicine, which has existed for thousands of years and helps in the choice of biological compounds as origins and sources of valuable biopharmaceuticals, nutritional supplements, and drugs. A detailed review of low-molecular-weight bioregulators of different types was recently published by scientists from Irkutsk [9–11]. Thus, in a historical perspective, a structural analysis of the ginseng and trepang extracts [4] used in Chinese medicine as active biostimulators shows that both extracts contain similar low-molecular-weight ingredients (bioregulators), which are triterpene glycosides lacking carbohydrate branches (aglicons and genins). Similar compounds were also found in birch and alder leaves, which in some cases can serve as raw material for the artificial synthesis of an effective agent of ginseng (*Panax gingeng*, C.A. May) and its glycosides (panaxosides) (Fig. 1). To trigger the physiological activity of these glycosides, a carbohydrate component (glycon) is needed, and it must contain oligosaccharides and comparatively short hydrocarbon chains.

PLANTS AND FUNGI POLYSACCHARIDES

Plants are known to contain polysaccharides with long carbohydrate chains, linear or branched. Such polysaccharides make up 80% of the chemical compounds of the cell. They have different functions in the cell; many of them possess a

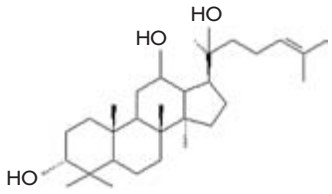

Fig. 1. Betulafolientriol from the leaves of birch and alder, one of the panaxosides' genines, and the triterpenic glycosides of ginseng.

marked physiological activity. Physiologically active polysaccharides contain glycuronic acids in their structure: mainly D-galacturonic and D-glucuronic acids. Plant polysaccharides such as pectic substances, gums, and mucilages [12, 13] demand special attention. Alginic acid, the main polysaccharide of marine brown seaweeds, consists of D-mannuronic and L-guluronic acids [14].

For a long period of time, pectic substances, which are the principium of so-called plant dietary fibers and biopolymers with high and polypotent biological activity [15], have been the object of special attention from researchers. The 1,4-linked residues of α-D-galacturonic acid form the backbone of pectic substances. The linear regions of this chain are interlinked by L-rhamnose residues involved into the chain by 1,2- α-glycoside linkages. The side chains of different lengths are made mainly of the arabinose and galactose residues which attached to the rhamnose residues. Pectic substances are considered a complicated polysaccharide complex composing the basis of the plant cell and including protopectin, an insoluble pectin complex with cellulose and hemicellulose; pectin polysaccharides of irregular structures; and concomitant branched polysaccharides: arabinans, galactans, and arabinogalactants (Fig. 2) [16].

A general scheme of pectin polysaccharides is shown in Fig. 3 [16, 17].

Pectin polysaccharides were shown to possess a wide spectrum of physiological activity [17–19]. Therein, we should first mention their immunomodulating effect (phagocytosis stimulation); pronounced antiulcerous and antidotal action; and the ability to remove salts of heavy metals, organic toxins, and poisons from the organism. This is why, in hot shops and during chemical production, workers usually receive some pectins instead of milk as a preventive antidote. Apple pectins are also good for human health. Regular apple consumption (one in the morning and one in the evening) can prolong a human's life by 10 years. Apple jam is supposed to be healthier because of its higher relative pectin content when compared to fresh apples. Galacturonans lacking side chains were found to possess pronounced antiinflammatory activity [20].

Several fungi should be mentioned, which are the sources and origins of other physiologically active polysaccharides. Lentinan and pachimaran are of great interest to researchers. Lentinan was first isolated by a Japanese research team headed by G. Chihara in 1969 [21] from the mushroom *Lentinus edodes*, which is widespread in the Pacific region and popular in Japan. Another active fungi glucan, called pachiman, was isolated from fungus *Poria cocos* [22, 23]. The mild periodate oxidation of pachiman leads to the generation of the more active pachimaran. Moreover, the latter fungus is a source of a series of physiologically active 1,3-β-D-glucans [24, 25]. Lentinan and pachimaran belong to the group 1,3-β-,

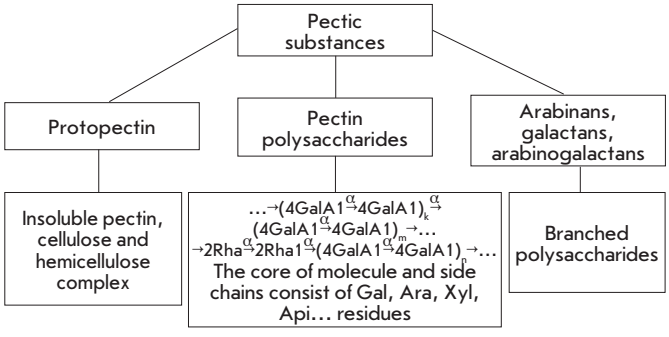

Fig. 2. Components of pectic substances.

1,6- β-D-glucans, the backbone of which consists of D-glucopyranose residues linked by β-1,3-glycosidic linkages; the side chains of β-D-glucopyranose are attached to the backbone by the β-1,6-glycoside linkage [21–26].

Both polysaccharides possess high antitumor activity, which, as was shown by Chihara and other Japanese researchers, can be explained directly by their immunomodulating effect on the immune system of an organism with a tumor [21, 27, 28].

Thus, lentinan almost completely breaks the growth of a number of experimental tumors such as Gauss sarcoma, Ehrlich carcinoma, etc. Lentinan's antitumor activity was shown to be caused by stimulation of T-lymphocyte killers, while no effect on B-lymphocytes and, thus, on the antibody development (humoral response) was observed. The high molecular weight of the fungi glucans (1 MDa) was shown to be a significant factor of their immunomodulating activity. However, the partial removal of the side chains of lentinan without a significant decrease in its molecular weight failed to affect immunomodulating activity; moreover, the transformation of pachiman into pachimaran leads to a noticeable increase in physiological activity [27].

Lentinan is widely used in medicine as an effective means for preventing and curing a number of malignancies.

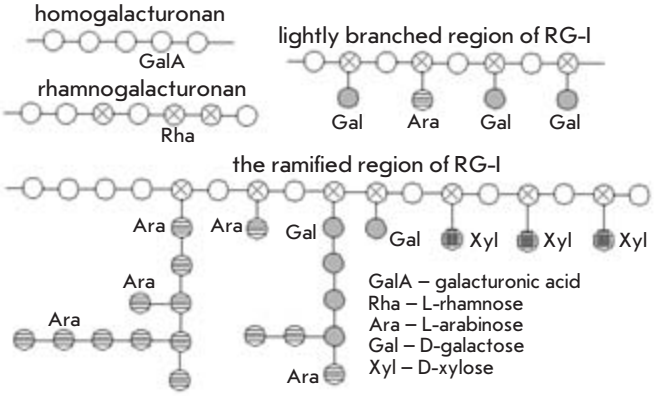

Fig. 3. General scheme of the structure of pectin polysaccharides.

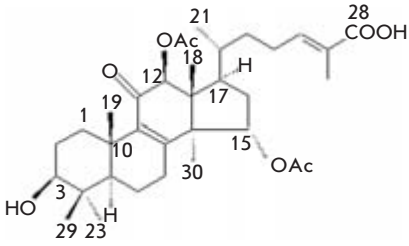

Fig. 4. Ganodermic acid: the lanostanic triterpen of *G. lucidum*, *G. applanatum*.

The fungi of different species of *Ganoderma* genus and first of all of *G. lucidium*, which is widely used in ethnomedicine in Japan and China in particular, are widespread sources of 1,3-β-D-glucans [29, 30]. Over the last several years, comprehensive research into this group of fungi has been carried out [30–35]. 1,3-β-D-glucan was found to be one of the main components of *G. lucidium* [35], which possesses immunostimulating activity and, first and foremost, intensified phagocytosis and increased interleukin-1 (IL-1) production. Moreover, 1,3-β-D-glucans were shown to increase the production of an intensive immunomodulator, interferon (IFN-γ) [36]. Therefore, fungus extracts are used to cure the impaired immune system, digestive tract ulcer, and cancer. A preparation based on the dry powder of *G. lucidium*, particularly, is used to cure sarcoma [37].

Moreover, lanostanic triterpenoids found and isolated from different species of fungi [38, 39], ganodermic acid in particular, are being studied (Fig. 4). The presence of ganodermic acid in the aqueous ethanolic extract of *G. lucidium* was found to cause various physiological activities. The Ling-Zhi preparation based on *G. lucidium* (aqueous ethanolic extract) produced in China is used to cure nerve diseases, insomnia, vertigo, asthma, and other allergic manifestations [39].

A large body of data concerning the structure and physiological activity of 1,3-β-D-glucans from a number of fungi has been accumulated over the last several years [40–43].

BIOGLYCANS OF MARINE INVERTEBRATES

The substantial bioglycan group of immunomodulators representing carbohydrate-protein biopolymers with a branched D-glucan was isolated from marine invertebrates. Branched D-glucan forms stable noncovalent bonds with the protein component representing lectin, which specifically binds polysaccharides. Immunomodulating activity was shown to need the presence of both bioglycan constituents [44, 45].

We have systematically studied many different marine invertebrates [45], and almost all of them were found to contain immunomodulating bioglycans. Our results led us to conclude that marine invertebrates produce immunomodulating bioglycans, which are responsible for their well-known resistance to arising neoplasma [45].

Mytilan is the most thoroughly studied immunomodulating bioglycan; it is isolated from different species of mussels of the Mytilidae family (*Crenomytilus grayanus*, *Mytilus edulis*, and *M. galloprovinciales*), which are widespread in the seas [44, 45]. Mytilan significantly increases phagocytic activity and factors of the humoral immunity. This substance is obtained from the so-called mussel juice, which was considered as waste in processing mussel as food stuff [6, 44, 45].

The property of mytilan behind the increase in the immune response to influenza has attracted the most interest. Because of that, mytilan has been widely used for influenza prevention and curation, especially at the early stage of the disease. The antiviral effect of mytilan is due to its ability to increase the biosynthesis of endogenous interferon, which plays a determinative role in the organism's resistance to viral infection. Interestingly, mytilan has been found to double the mean lifetime of experimental animals [6, 45].

LYPOPOLYSACCHARIDES OF GRAM-NEGATIVE BACTERIA

Since the middle of the 1930s, the attention of researchers has focused studies of the structural features and physiological activity of the antigens of gram-negative bacteria, the so-called O-somatic antigens, representing lipopolysaccharides (LPS) [46].

In the beginning, the French scientists A. Boivin and L. Mesrobeanu [47] isolated the immunogenic lipopolysaccharide-protein complex (LPPC) which is known up to now as the Boivin antigen [48]. Later, a huge number of works were devoted to the study of the structure and properties of LPS, which were not only O-somatic antigens of gram-negative bacteria, but also active endotoxins [49]. LPS were found to consist of three main regions bound to each other as follows:

Lipid A – Core of the macromolecule – O-Specific polysaccharide.

A significant contribution to the study of the structure and properties of LPS has been made by the German Westphal-Luderitz school in Freiburg (FRG) since the 20th century. Since the 1960s, studies of the structure and properties of LPS have multiplied. In 1970 [50] at the Pacific Institute for Bioorganic Chemistry (Vladivostok), we started studying the antigenic composition of the pseudotuberculous microbe *Yersinia pseudotuberculosis* which causes a specitic disease, the so-called Far East scarlatinous fever (in Primorsky region). Research of LPS continues up to now. The most well-known works devoted to the study of LPS were carried out by the N.K. Kochetkov's scientific school [51] especially by his pupil Yu.A. Knirel [52].

The structural features of the numerous LPS of gram-negative bacteria have been elucidated as a resut of these Research. Lipid A was shown to be responsible for the endotoxic properties of LPS, namely to cause the main symptoms of various diseases. The pattern of the immune response is determined by the O-specific polysaccharide, which is a matrix for the antibody production and differentiation. Therefore, this polysaccharide is in charge of the organism's immune response during the development of the disease. The structure of O-specific polysaccharides can vary significantly. They have been found to contain the residues of many unusual monosaccharides. Such monosaccharides are often located at the terminal points of the macromolecule, and they determine its serospecificity, being immunodeterminant or immunodominant sugars [51–53].

As a rule, LPSs are not used for curation because of their high toxicity and, thus, low therapeutic index. However, on the basis of LPSs, many diagnostic techniques have been developed which make it possible to diagnose a disease at the earliest stage. Moreover, O-specific polysaccharides often

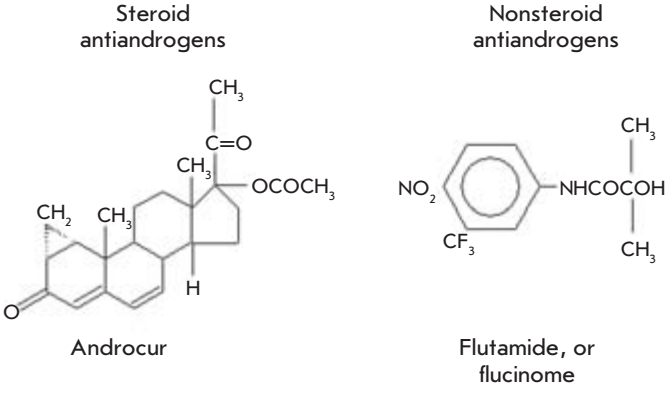

Fig. 5. The inhibitors of transformation of testosterone into dihydro testosterone.

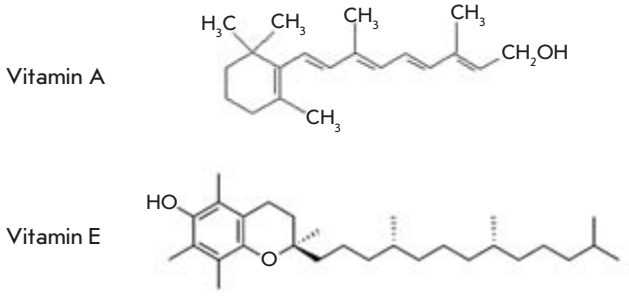

Fig. 6. Vitamins A (retinol) and E (α-tocopherol), powerful antioxidants used for curing oncological diseases.

possess an immunoadjuvant property; i.e., they can boost the effect of a vaccine against a certain disease [52, 54].

The LPSs of blue-green algae known also as cyanobacteria appear to hold much promise. Such LPSs are nontoxic, while they possess pronounced immunoadjuvant properties; on their basis we developed a powerful adjuvant lacking the side effects characteristic of classic adjuvants, such as the Freund's adjuvant, which often causes abscess to develop at the injection site [55].

ONCOFETAL ANTIGENS

The oncofetal antigens discovered by Yu.S. Tatarinov and G.I. Abelev in the beginning of the 1960s [56, 57] are of great research interest today [58–61]. Oncofetal antigens appear in the human organism during prenatal development, making the organism tolerant to these antigens. Later, they disappear and can appear again only during the development of an oncological disease. Thus, the cancer cell hides from the immune system of the host organism, which in this case cannot recognize the cancer cell as a foreign antigen. Therefore, oncofetal antigens are important markers of cancer (neoplasma) and are used to reveal tumors at the early stages of their development [44, 62, 63].

In this relation, the carcino-embryonic antigen (CEA) [63, 64], which does not differ in high specificity and is not revealed in the bodily fluids of a healthy human, is of great interest. Its appearance and accumulation in blood (more than 5 ng/ml) evidence the presence of almost any oncological disease in the organism, like neoplasias of the digestive tract and respiratory system or carcinoma of the breast, head, or neck [63]. Like all the oncofetal antigens CEA is a complicated glycoprotein, the protein part of which plays the determinative role. A study of its spatial structure showed that the carbohydrate moiety stabilizes the CEA conformation [64, 65].

It should be noted that many oncofetal antigens possess high enough, although not absolute specificity. Among them, the prostate-specific antigen (PSA) is one of the main markers of prostate cancer (PC), namely adenocarcinoma of prostate [66]. The PC is a male tumor, hormone-dependent at its early stages (androgen-dependent) [67–70], and widespread among men (second after lung cancer). Later, PC transforms into an androgen-independent metastasizing stage. Its lethality is usually due to metastases in bones and lymphnodes, as well as to switch of the tumor into the androgen-independent stage of tumor growth, which aggravates the process curing PC. Any effective curation of PC with metastases is absent in the present time. This disease is especially widespread among men in the United States. Official data show that PC was responsible for the death of more than 37,000 men in 1999 and about 30,000 men in 2005 in the U.S.A. Studies of PC are being pursued intensively there. An analysis of the PSA level in blood is widely used for PC diagnostics. Though this test often yields a false-positive reaction, it accurately determines the risk level. PSA is a single-stranded glycoprotein containing 240 a.a. with a molecular weight of 33–34 kDa [66]. There are several markers for the existence of PC, nevertheless an exact diagnosis remains difficult, although modern techniques for measuring PSA in blood have recently been developed [71–73].

A cure for PC includes a sharp increase in physical activity, leading to the normalization of metabolic processes and to decongestion [69, 71]. Pharmaceutical treatment is based on the use of antioxidants, anti-inflammatory compounds, and antiandrogens (Fig. 5) inhibiting testosterone transformation into dihydrotestosteron. Antiandrogens are important when curing at the first androgen-dependent stage of the disease [66, 74–79].

Strategies for curing any tumor, PC in particular, include the wide use of antioxidants. Increased oxygen consumption is a characteristic of tumor cells. Therefore, antioxidants, for instance, apigenin, an active component of green tea, effectively block tumor development (Figs. 6, 7).

Licopene (Fig. 7), a lipophilic hydrocarbon with a linear chain consisting of 40 carbon atoms and containing 11 conju-

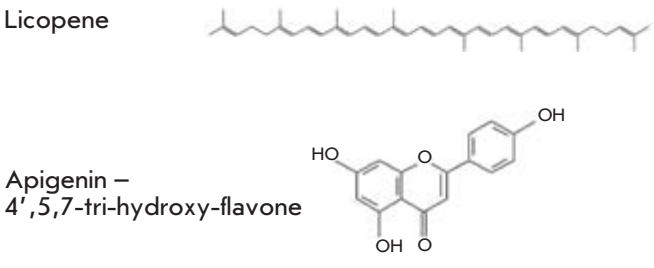

Fig. 7. Antioxidants used for curing oncological diseases.

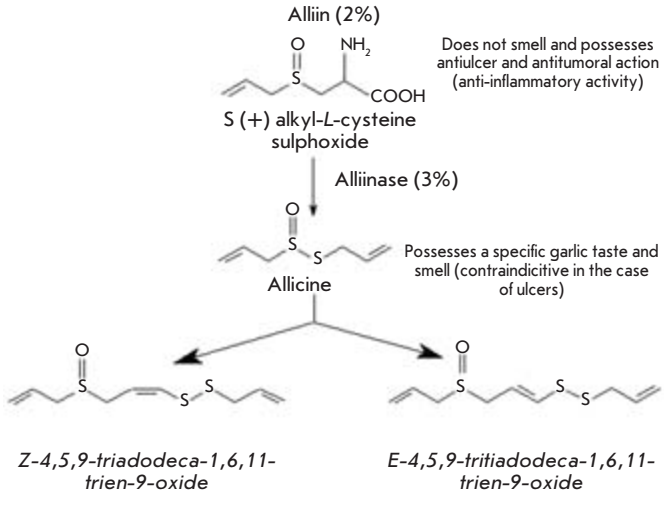

Fig. 8. Active components of garlic (*Allium sativum L.*).

gated and 2 nonconjugated olefinic linkages, possesses high antitumor activity [80]. Fresh tomatoes contain the licopene *trans*-form, which, after the tomatoes are processed, transforms into the *cis*-form. Licopene bioavailability for humans is 2.5-fold higher in tomato paste when compared to fresh tomatoes. Tomato consumption decreases the PC risk by 20%, while the use of tomato paste or tomato sauce leads to a 66% decline of this parameter. Therefore, the consumption of food containing tomato significantly decreases the risk of PC. Simultaneously, the cancer risk in the digestive tract, lung, and breast also declines [80].

Licopene has been shown to be an antioxidant and possesses a protective effect against lipid peroxygenation and DNA oxidative cleavage. These properties are behind the protective role played by licopene against tumors [81]. Licopene is used in medicine as a component of biologically active supplements such as licoprophit and licolam.

Thus, a number of medications exist that are used for curing oncological diseases. Many of them were offered by experts in bioorganic chemistry. However, more than any medications, the desire of a patient to resist the disease, constant cheertul mood, and an active way of life (which promotes metabolism normalization and intensifies immunity) are the main factors enhancing the organism's resistance to oncological diseases.

ACTIVE COMPONENTS OF GARLIC

Garlic, *Allium sativum L.* (Fig. 8), contains very interesting compounds with different physiological functions [82]. The average content of alliin, a sulfoxide S(+)-alkyl-L-cystein, is about 2%. Alliin possesses a marked physiological action against gastric ulcer and is useful for curing oncological diseases due to its anti-inflammatory activity.

However, garlic contains about 3% of a highly active enzyme, alliinase, which strongly intensifies in the presence of atmospheric oxygen, as was demonstrated by Japanese researchers [83]. This explains the fast alliin digestion on grinding garlic leading to allicin and the formation of other sulphur compounds, which are responsible for the specific smell and taste of garlic. These compounds possess a powerful bactericidal effect against gram-positive (e.g., *Staphylococcus aureus*) and gram-negative (e.g., *Salmonella sp.*) microorganisms, but they markedly irritate mucous membranes and are contraindicated in case of gastric ulcer [83]. Sulphur compounds were also shown to decrease carcinogen-induced cancer development in several organs due to their high antioxidative activity and ability to stimulate the immune response [84].

FLAVONOIDS AND ALKALOIDS

Flavonoids are a large class of active natural compounds widespread in the plant world. They appear to be different derivatives of chromane and isochromane and are found in nature as glycosides and aglycons [9–11].

Quercetin bioside (Fig. 9), called rutin after the plant rue from where it was first isolated, can be such an example [9, 10]. Rutinose, a disaccharide, is a constituent of rutin. Rutin was isolated from buckwheat leaves and belongs to the group P of vitamins. In the mammalian organism, rutin strengthens blood capillaries and increases blood coagulation. The presence of the vitamin C increases the effect of rutin. Rutin is used for curing diseases connected with blood strokes caused by increased capillary fragility and a defect in the blood coagulation system. Such a physiological action is characteristic of many flavonoids, which more or less possess P-vitamin activity.

Flavonoids are powerful antioxidants and can bind free radicals damaging the cell walls of normal cells.

Of all the other low-molecular-weight bioregulators, only alkaloids will be mentioned [3], which are various, highly active compounds containing nitrogen. Many of them are strong narcotics and analgesics. Morphine (Fig. 10), the main alkaloid of the poppy (*Papaver somniferum*), is one of the most famous alkaloids [3, 85]. Bioorganic chemists have elucidated not only the structure of this very complicated natural compound, but also succeeded in synthesizing it. In addition, ajmaline and allopinine are alkaloids with a strong antiarrhythmic effect.

POISONS AND TOXINS

Poisons and toxins, small doses of which cause the death of an organism, possess the highest physiological activity. The terms *poison* and *toxin* are very similar, though poisons are

Fig. 9. Rutin (vitamin P), quercetin's rutinoside.

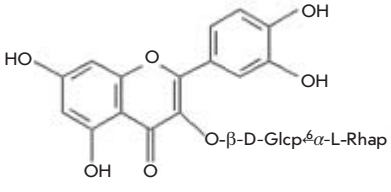

Fig. 10. Morphine, poppy (*Papaver somniferum*) alkaloid, strong narcotic, and powerful analgesic.

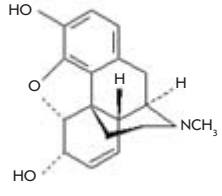

Fig. 11. Tetrodotoxin.

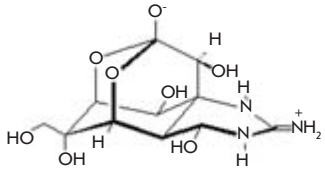

any toxic substance irrespective its origin, e.g., cianide, arsenic, and cobra poison. Toxins are poisons of a biological nature only [3].

Poisons and toxins are substances of the highest physiological activity and selectivity. Botulinotoxin, the protein toxin of the anaerobic bacteria *Clostridium botulinum,* is the most toxic among poisons and toxins [3, 86]. Other clostridium toxins possess the same high toxicity. A lethal dosage of botulinotoxin is equal to 10^{-5} μg/kg, while the toxicity of potassium cyanide is 10^{4} μg/kg. Botulinotoxin is synthesized by clostridia in strictly anaerobic conditions. This is a powerful neurotoxin blocking the transduction of neural impulses, which leads to paralysis and death. Humans and domestic animals are the most sensitive subjects to botulinotoxin. Humans are usually affected by botulinotoxin after eating poorly preserved food, like meat; fish; and, more frequently, agarics. Clostridium endospores are well preserved on unpeeled mushrooms. Endospores are stable to the tough condition of sterilization. During home conservation, conditions are often nonsterile, which promotes the survival and reproduction of clostridium endospores in an anaerobic medium, leading to the generation of the active form of clostridia, which produces botulinotoxin. Botulism is a severe disease and leads to death. This is why buying canned mushrooms of unknown origin and eating underboiled preserved mushrooms are not recommended. It is recommended to boil even homemade canned goods before eating to destroy the synthesized botulinotoxin in case it formed in the conserved product. Using anatoxin, i.e. a toxin treated previously with formalin, or using a serum against anatoxin gives good results in curing botulism at all stages of the disease's development.

Cyclopeptide toxins of the death cup *Amanita phalloides* [3, 76], amanitine and phalloidin, are other powerful toxins of a protein nature which were first isolated as individual substances in 1937 by the German researchers F. Linen and G. Viland. Poisoning by death cup toxins is widespread. These toxins are distinguished by their prolonged latent period (up to 36 hours) as the liver is painlessly destroyed. By the time the symptoms emerge, any kind of cure appears to be ineffective, which explains the high percentage of mortality by intoxication. Interestingly, eating even one death cup can be fatal. At the same time, the death cup contains peptide antamadine, a 1 mg/kg concentration of which protects the organism from the destructive action of the toxin. Hepatoprotective medication (carsil, isolated from *Silybum marianum* and available in any pharmacy) has a positive effect, which is especially preventive against amanitine intoxication.

Among the nonprotein toxins, we will mention shortly toxins produced by marine organisms.

Tetrodotoxin, contained in fish of the Tetraodontidae family (Fig. 11), is one of the most well-known nonprotein toxins. The most famous of the family goes by the names hogfish, swell fish, or puffer fish *Fugu niphobles* and *F. rubripes.* Tetrodotoxin was also isolated from the Corsican frog *Atelopus sp.*, the crab *Atergatis floridis*, and the Californian triton *Taricha torosa.*

The puffer fish is considered a delicacy in Japan. Tetrodotoxin is accumulated in different fugu organs, but mainly in roe, liver, and skin. Special chefs carefully remove these organs before cooking. However, in some seasons, tetrodotoxin accumulates in all of the fugu body, making it completely toxic, which often leads to fatal consequences. In some years, hundreds of people die in Japan after eating puffer fish. This is why the puffer fish is served only in special restaurants displaying signs that read "Want to try fugu? Write your last will."

Tetrodotoxin is a powerful neurotoxin causing the paralysis of human and mammalian skeletal muscle, a sharp decline in blood pressure, and death by respiratory arrest. The lethal dosage is equal to 7 μg/kg.

Tetrodotoxin is widely used in laboratory practice to study the mechanisms of neural transduction.

Palytoxin is another nonprotein toxin of marine origin with a complicated structure (Fig. 12). It was first isolated in 1971 by the American scientists R.E. Moore and P. Scheuer [87] from the soft corall *Polytoa toxica.* The results of numerous studies of palytoxin have been described in a detailed review [88]. While the toxin was being isolated by Drs. Moore and Scheuer, a conflagration appeared in the laboratory. Everybody who dealt with the toxin suffered; particularly the cardiovascular system of the researchers was injured. Consequently, this powerful toxin was named "messenger of Satan." The complex structure of palytoxin was determined a decade later, in 1981, by two independent research groups, one from Japan headed by Prof. Y.Hirata [89, 90] and another by Prof. R.E. Moore [91]. The determination of the palytoxin structure became a significant event in bioorganic chemistry. Its molecule possesses a unique structure [3] (Fig. 12). A stereochemical study of palytoxins was successfully carried out by the above-mentioned groups of Japanese and American researchers [92, 93]. In spite of the existence of a huge number of possible stereoisomers, a group of Japanese researchers headed by Prof. Y. Kishi [94] in 1989 successfully synthesized several palytoxin derivatives. A comparison with the natural palytoxin showed that synthetic substances were identical to natural ones in biological activity, chromatographic behavior, and spectral characteristics obtained by NMR spectroscopy and mass spectrometry [94]. Several years later, in 1994, a palytoxin specimen completely identical to the natural one was synthesized [95]. However, the complete chemical synthesis of palytoxins includes 65 stages [96], which makes it impossible to use in every day practice. The physiological action of palytoxin is quite significant [3]; being injected intravenously, it is LD_{50} = 0.15 μg/kg for mice and 0.08 μg/kg for monkeys. The lethal outcome takes 5–30 minutes as a result of deep injury to the cardiovascular system and respiratory arrest. The toxic dose for different animals varies from 0.01 to 0.1 μg/kg of LD_{50} [96]. The toxic dose for human was not measured experimentally of course, though an extrapolation of the data obtained in studies on different animals makes it possible to conclude that it takes LD_{50} of about 0.04 μg/kg [97]. In spite of the high toxicity, palytoxin was found in a number of marine invertebrates [88, 97]. Interestingly, palytoxin in

Fig. 12. Palytoxin.

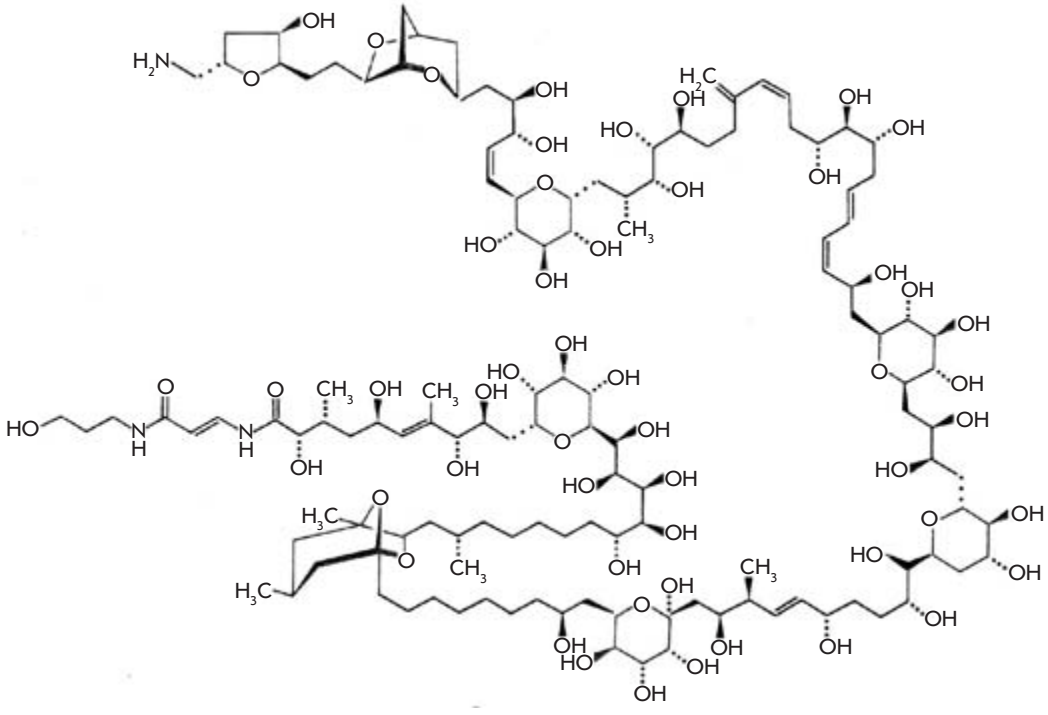

the sublethal dose demonstrated a high antitumoral activity.

In tropical seas, "red tides" are often observed causing the massive death of various marine organisms as a result of the intensive multiplication of toxic microalgae (dinoflagellates). These microalgae release a number of strong toxins, including the most powerful of the known nonprotein toxins, maitotoxin [98]. This toxin was first found in 1976 [99] in the intestine of the surgeonfish *Ctenochaetus striatus* as the main component of siguatera, the famous food toxin of dinoflagellates *Gambierdicus toxicus*, which is included in the food chain of herbivorous fish. The toxicity of maitotoxin is the highest, LD_{50} is equal to near 0.05 μg/kg for mice. Maitotoxin was first isolated as an individual substance in 1988 by a group of Japanese researchers headed by Prof. T. Yasumoto from Tochoku University [100]. The structure of this complicated substance, including the elements of stereochemistry, was elucidated in 1992–1994 [101] by this research group using spectral analysis, NMR spectroscopy, and mass spectrometry techniques, in particular. They also determined the absolute configuration of maitotoxin in 1996 [102]. The data obtained were confirmed later, when maitotoxin was artificially synthesized by a group of Japanese scientists headed by Y. Kishi [103].

These data demonstrate clearly that bioorganic chemistry has assumed a prominent place among the sciences that study basic life processes and the substances playing an active role in those processes. Bioorganic chemists continue to study the chemical structure of new biopolymers and low-molecular-weight bioregulators and to shed light on their biological functions and physiological activity. Special attention is focused on unveiling the interrelations between the structural features and biological activities of different chemical substances. Bioorganic chemists, together with biochemists, biotechnologists, physiologists, and doctors, are obtaining new results that help extend productive human life. ●

REFERENCES

1. Spichenkova N.E., Vaskovsky V.E. //Bioorg. Khimiya. 2009. V. 35. №2. P. 279-288.
2. Shemyakin M.M., Khokhlov A.S. //J. General Chem. 1967. V. 37. P. 2369-2370.
3. Ovchinnikov Yu.A. Bioorganic Chemistry //M.: Prosveshcheniye. 1987. 815 p.
4. Elyakov G.B., Stonik V.A. Marine Organisms' Terpenoids /Ed. Kamernitsky A.V., M.: Nauka, 1986. 270 p.
5. Elyakov G.B., Stonik V.A. Marine Organisms' Steroids /Ed. Kamernitsky A.V., M.: Nauka, 1988. 208 p.
6. Zaporozhets T.S., Besednova N.N. Immunoactive Biopolymers of Marine Hydrobionts //Vladivostok, 2007. 218 p.
7. Stonik V.A. //Acta Naturae. 2009. V. 1. №2. P. 16-27.
8. Usov A.I. //Uspekhi Khim. 1999. V. 78. P. 846-862.
9. Semyonov A.A. Essays of Natural Compound Chemistry /Ed. Tolstikov G.A. Novosibirsk: Nauka, 2000. 664 p.
10. Semenov A.A., Kartcev V.G. The Basics of Natural Substances Chemistry. V. 2. Moscow: MBFNP, 2009. 642 p.
12. Kochetkov N.K., Bochkov A.F., Dmitriev B.A., et al. The Carbohydrate Chemistry //M.: Khimiya, 1967. 672 p.
13. Aspinall G.O. //Adv. Carbohydr. Chem. Biochem. 1969. V. 24. P. 333-379.
14. Painter T.J. Algal Polysaccharides //The Polysaccharides. V. 2 / Ed. Aspinall G.O. NY, L.: Acad. Press, 1983. V. 2. P. 263-273.
15. Ovodov Yu.S., Golovchenko V.V., Günter E.A., et al. Pectic Substances of Plants of the European North of Russia /Ed. Kutchin A.V. Ekaterinburg, 2009. 112 p.
16. Ovodov Yu.S. Biologically Active Pectin Polysaccharides of Komi Republic Plants in the North /Ed. Lazhentsev V.N. Syktyvkar, 2006. P. 236-257.
17. Ovodov Yu.S. //Bioorg. Khimiya. 2000. V. 35. P. 293-310.
18. Popov S.V. Interaction of mammalian phagocytes with plant polysaccharides /Ed. Ovodov Yu.S. Syktyvkar, 2002. 97 p.
19. Ovodov Yu.S. //Bioorg. Khimiya. 1998. V. 24. P. 483-501.
20. Popov S.V., Ovodova R.G., Popova G.Yu., et. al. //Bioorg. Khimiya. 2007. V. 33. P. 187-192.

21. Chihara G., Namuro J., Maeda Y. ET AL. //Cancer Res. 1970. V. 30. P. 2776-2781.
22. Kanayama H., Adachi N., Togami M. //Chem. Pharm. Bull. 1983. V. 31. P. 1115-1118.
23. Wang Y., Cheng Z., Mao J., et. al. //Carbohydr. Polym. 2009. V. 77. P. 713-717.
24. Wang Y.F., Zhang M., Ruan D., et. al. //Carbohydr. Res. 2004. V. 339. P. 327-334.
25. Chen X., Xu X., Zhang L., et al. //Carbohydr. Polym. 2009. V. 76. P. 586-591.
26. Stone B.A., Clarke A.E. Chemistry and Biology of (1→3)-β-Glucans //Victoria, Australia: LaTrobe Univ. Press, 1992. 803 p.
27. Chihara G. Cancer Detection and Prevention /Ed. Maltoni C. NY.: Acad. Press, 1987. Suppl. 1. P. 423-443.
28. Minato K., Mizuno M., Ashida H., et. al. //Int. J. Med. Mushrooms. 1999. V. 1. P. 265-272.
29. The Alternative Advisor //Time-Life Inc. USA, 1997.
30. Evseyenko M.S., Shashkov A.S., Avtonomova A.V. et al. //Biochemistry (Moscow). 2009. V. 74. P. 657-667.
31. Bao X., Liu C., Fang J., et al. //Carbohydr. Res. 2001. V. 332. P. 67-74.
32. Bao X., Zhen Y., Ruan L., et al. //Chem. Pharm. Bull. 2002. V. 50. P. 623-629.
33. Lin Z., Zhang H. //Acta Pharmacol. Sin. 2004. V. 25. P. 1387-1395.
34. Paterson R.R.M. //Phytochemistry. 2006. V. 67. P. 1985-2001.
35. Wang J., Zhang L. //Carbohydr. Res. 2009. V. 344. P. 105-112.
36. Kohguchi M., Kunikata T., Watanabe N., et. al. //Biosci. Biotechnol. Biochem. 2004. V. 68. P. 881-887.
37. Nonaka Y., Shibata H., Nakai M., et. al. //Biosci. Biotechnol. Biochem. 2006. V. 70. P. 2028-2034.
38. El Dine R.S., El Halawany A.M., Nakamura N., et. al. //Chem. Pharm. Bull. 2008. V. 56. P. 642-646.
39. Wang F., Liu J-K. //Chem. Pharm. Bull. 2008. V. 56. P. 1035-1037.
40. Yang L., Zhang L.-M. //Carbohydr. Polym. 2009. V. 76. P. 349-361.
41. Sun Z., He Y., Liang Z. et. al. //Carbohydr. Polym. 2009. V. 76. P. 628-633.
42. Moradali M.-F., Mostafavi H., Ghods S., et al. //Int. Immunopharmacol. 2007. V. 7. P. 701-724.
43. Chen J., Seviour R. //Mycological Res. 2007. V. 111. P. 635-652.
44. Ovodov Yu.S., Ovodova R.G., Popov S.V. // Phytotherapy, Biologically Active Substances of Natural Origins. Chernogolovka: Bioprogress, 2003. P. 348-362.
45. Ovodov Yu.S., Ovodova R.G., Loyenko Yu.N. //Khimiya Prirodn. Soedin. 1983. P. 675-694.
46. Lüderitz O., Westphal O., Staub A.M., Nikaido H. Isolation and Chemical and Immunological Characterization of Bacterial Lipopolysaccharides //Microbial Toxins /Eds. Weinbaum G., Kadis S., Ajl S.J. NY.- Lnd, 1971. IV. P. 145-233.
47. Boivin A., Mesrobeanu L. //Compt. Rend. Soc. Biol. 1933. V. 113. P. 490-492.
48. Solov'eva T.F., Ovodov Yu.S. //Bioorg . Khimiya. 1983. V. 9. P. 725-733.
49. Lüderitz O. //Microbiology. 1977. P. 239-251.
50. Ovodov Y.S., Gorshkova R.P., Tomshich S.V. //Immunochemistry. 1971. V. 8. P. 1071-1079.
51. Knirel Yu.A., Kochetkov N.K. //Biochemistry (Moscow). 1994. V. 59. P. 1784-1851.
52. Knirel Yu.A. O-Specific polysaccharides of Gram-negative bacteria //Microbial Glycobiology: Structures, Relevance and Applications /Eds. Moran A., et al. Amsterdam: Elsevier, 2009. P. 57-73.
53. Kalmykova E.N., Gorshkova R.P., Ovodov Yu.S. //Khimiya Prirodn. Soedin. 1989. P. 743-763.
54. Rietschel E.T., Kirikae T., Schade F.U. et. al. //Immunobiology. 1993. V. 187. P. 169-178.
55. Mikheyskaya L.V., Ovodova R.G., Ovodov Yu.S. // Khimiya Prirodn. Soedin. 1985. P. 493-496.
56. Tatarinov Yu.S. The Past and Future of Oncofetal Proteins // M.: Russian State Med. Univ., 1988. 23 p.
57. Tatarinov Y.S. Human alpha-fetoprotein //M.: Russian State Med. Univ., 1994. 90 p.
58. Abelev G.I. //Int. Contra Cancer. 1963. V. 19. P. 80-92.
59. Tatarinov Yu.S. //The Thesis of I Allunion Biochemical Congress, M-L., 1963. V. 2. P. 274.
60. Ttatrinov Yu.S. //Vopr. Med. Khimii. 1964. V. 10. P. 584-589.
61. Tatarinov Yu.S. //Nature (Lond.) 1968. V. 217. P. 964-965.
62. Ovodov Yu.S. The Chemistry of Immunity //Syktyvkar, 1997. 159 p.
63. Elistratova E.V., Laktionov P.P., Shelestyuk P.I. et. al. //Biomed. Khimiya. 2009. V. 55. №1. P. 15-31.
64. Pavlenko A.F., Kurika A.V., Ovodov Yu.S. //Usp. Sovremen. Biol. 1988. V. 106. P. 412-425.
65. Pavlenko A.F., Chikalovets I.N., Kurika A.V. et. al. //Tumor. Biol. 1990. V. 11. P. 306-318.
66. Ablin R.J. //J. Cancer Res. Clin. Oncol. 1997. V. 123. P. 583-594.
67. Vorob'ev A.V. //Voprosy Onkol. 2009. V. 55. №2. P. 241-249.
68. Kostin A.A., Kaprin A.D., Tsybul'sky A.D. //Voprosy Onkol. 2009. V. 55. №2. P. 187-191.
69. Kaprin A.D., Kostin A.A., Tsybul'sky A.D. //Voprosy Onkol. 2009. V. 55. №3. P. 285-290.
70. Kaprin A.D., Gafanov R.A., Fastovets S.V. //Voprosy Onkol. 2009. V. 55. №3. P. 474-476.
71. Bukharin B.V. //Sovremen. Onkol. 1998. V. 334. P. 667-694.
72. Lyubavina I.A., Zinchenko A.A., Lebedin Yu.S., et al. //Bioorgan Khimiya. 2007. V. 33. P. 550-554.
73. Lokhov P.G., Dashtiev M.I., Bondartsov L.V., et. al. //Biomed. Khimiya. 2009. V. 55. №3. P. 247-254.
74. Friedenreich C.M., Thune I. //Cancer Causes and Controls. 2001. V. 12. P. 461-475.
75. Reid P., Kantoff P., Oh W. //Invest. New Drugs. 1999. V. 17. P. 271-284.
76. Bruckheimer E.M., Kyprianou N. //Cell Tissue Res. 2000. V. 301. P. 153-162.
77. So A.I., Hurtado-Coll A., Gleave M.E. //World J.Urol. 2003. V. 21. P. 325-337.
78. Sonpavde G., Hutson T.E., Berry W.R. //Cancer Treatment Rev. 2006. V. 32. P. 90-100.
79. Han H.-Y., Wen P., Liu H.-W., et. al. //Chem. Pharm. Bull. 2008. V. 56. P. 1338-1341.
80. Omoni A.O., Aluko R.E. //Trends Food Sci. Technol. 2005. V. 16. P. 344-350.
81. Kucuk O., Sarnar F.H., Sakr W., et. al. //Cancer Epidemiol. Biomarkers Prevention. 2001. V. 10. P. 861-868.
82. Yoshida H., Iwata N., Katzuzaki H., et. al. //Biosci. Biotechnol. Biochem. 1998. V. 62. P. 1014-1017.
83. Fujisawa H., Suma K., Origuchi K., et. al. //Biosci. Biotechnol. Biochem. 2008. V. 72. P. 2877-2883.
84. Youn H.-S., Lim H.J., Lee H.J., et. al. //Biosci. Biotechnol. Biochem. 2008. V. 72. P. 368-375.
85. Mashkovsky M.D. The Remedies /Ed. Yuzhakov S.D., M.: Novaya Volna, 15 Ed., 2005. P. 146-147.
86. Ovodov Yu.S. The Selected Topics of Bioorganic Chemistry // Syktyvkar, 1998. 222 p.
87. Moore R.E., Scheuer P.J. //Science. 1971. V. 172. P. 495-498.
88. Katikou P. Chemistry of Palytoxins and Ostreocins //Phytotoxins: Chemistry and Biochemistry /Ed. Botana L.M. Ames: Blackwell Publ., 2007. P. 75-93.
89. Hirata Y., Uemura D., Ueda K., et al. //Pure Appl. Chem. 1979. 51. 1875-1883.
90. Uemura D., Ueda K., Hirata Y., et. al. //Tetrahedron Lett. 1981. V. 22. P. 2781-2784.
91. Moore R.E., Bartolini G. //J. Am. Chem. Soc. 1981. V. 103. P. 2491-2494.
92. Moore R.E., Bartolini G., Barchi J. //J. Am. Chem. Soc. 1982. V. 104. P. 3776-3779.
93. Cha J.K., Christ W.J., Finan J.M., et. al. //J. Am. Chem. Soc. 1982. V. 104. P. 7369-7371.
94. Kishi Y. //Pure Appl. Chem. 1989. V. 61. P. 313-324.
95. Suh E.M., Kishi Y. //J. Am. Chem. Soc. 1994. V. 116. P. 11205-11206.
96. Wiles J.S., Vick J.A., Christensen M.K. //Toxicon. 1974. V. 12. P. 427-433.
97. Taniyama S., Mahmud Y., Terada M., et. al. //J. Nat. Toxins. 2002. V. 11. P. 277-282.
98. Satake M. Chemistry of Maitotoxin //Phytotoxins: Chemistry and Biochemistry /Ed. Botana L.M. Ames: Blackwell Publ., 2007. P. 47-54.
99. Yasumoto T., Baginis R., Vernoux J.P. //Bull. Jpn. Soc. Sci. Fish. 1976. V. 42. P. 359-365.
100. Yokoyama A., Murata M., Oshima Y., et. al. //J. Biochem. 1988. V. 104. P. 184-187.
101. Murata M., Naoki H., Matsunaga S., et. al. //J. Am. Chem. Soc. 1994. V. 116. P. 7098-7107.
102. Nokomura T., Sasaki M., Matsumori N., et. al. //Angew. Chem. Inter. Ed. Engl. 1996. V. 35. P. 1675-1678.
103. Zheng W., DeMattei J.A., Wu J.-P., et. al. //J. Am. Chem. Soc. 1996. V. 118. P. 7946-7968.

New Trends in Nucleoside Biotechnology

I.A. Mikhailopulo[1*], A.I. Miroshnikov[2]
[1]Institute of Bioorganic Chemistry, National Academy of Sciences, Belarus
[2]Shemyakin and Ovchinnikov Institute of Bioorganic Chemistry, Russian Academy of Sciences
*E-mail: igor_mikhailo@yahoo.de
Received 29.04.2010

ABSTRACT **This review focuses on new trends in nucleoside biotechnology, which have emerged during the last decade. Continuously growing interest in the study of this class of compounds is fueled by a number of factors: (*i*) a growing need for large-scale production of natural 2'-deoxy-β-D-ribonucleosides as well as their analogs with modifications in the carbohydrate and base fragments, which can then be used for the synthesis and study of oligonucleotides, including short-interfering RNA (siRNA), microRNA (miRNA), etc.; (*ii*) a necessity for the development of efficient practical technologies for the production of biologically important analogs of natural nucleosides, including a number of anticancer and antiviral drugs; (*iii*) a need for further study of known and novel enzymatic transformations and their use as tools for the efficient synthesis of new nucloside analogs and derivates with biomedical potential. This article will review all of these aspects and also include a brief retrospect of this field of research.**
KEYWORDS **nucleosides, nucleic acid metabolism enzymes, chemoenzymaticsynthesis, bio-mimetic synthesis.**

INTRODUCTION

Nucleosides are a large family of natural compounds and their chemically modified analogs, which are characterized by great structural diversity. The four 2'-deoxy-β-D-ribonucleosides of adenine (**1**) and guanine (**2**), and thymine (**3**) and cytosine (**4**), along with the related four β-D-ribonucleosides (**5**-**8**), are the main constituents of DNA and RNA, respectively (Scheme 1). Analogs of these natural nucleosides with variously modified carbohydrate and/or aglycon fragments have been found in RNA's and are also included into a sub-family of nucleoside antibiotics which is also characterized by great structural diversity. 5'-Phosphorylated nucleosides, called nucleotides, are important metabolites of DNA and RNA biosynthesis, and they also act as co-substrates and cofactors of a large number of biochemical transformations.

The first identified natural representative of this family, inosine-5'-monophosphate (**9**; IMP; the name inosine originates from the Greek word *inos* – muscle), was isolated from beef extract by J.F. von Liebig in 1847. He also described its taste intensifier property; synthesis of IMP from inosine and its structure as ribofuranoside 5'-monophosphate was described by P.A. Levene & R.S. Tipson 88 years later (Scheme 1) [1]. It is interesting to note that it was P.A. Levene who coined the general term "nucleotide" for phosphoric acid derivatives formed as the result of nucleic acid hydrolysis, and suggested the term "nucleoside" for dephosphorylated nucleotides, and also identified *D*-ribose and later 2-deoxy-*D*-ribose as constituents of RNA and DNA, respectively [2 – 7].

Pioneering structural studies on nucleosides and nucleotides during the last decade of the 19th and first decade of the 20th centuries showed that DNA and RNA consist of five heterocyclic bases and two pentoses. The first chemical condensation of these two of two components was reported by E. Fischer & B. Helferich in 1914 [8]; condensation of a silver salt of 2,8-dichloroadenine with 2,3,4,5-tetra-*O*-acetyl-α-*D*-glucopyranosyl bromide followed by deprotection and hydrodehalogenation yielded a nonnatural nucleoside N^9-(β-*D*-glucopyranosyl)adenine (**10**), whose structure was unequivocally proved by J.M. Gulland & L.F. Story 24 years later (Scheme 1) [9]. Between World War I and II, a number of very important studies dedicated to the chemical synthesis of pyrimidine and purine nucleosides were published, but systematic studies on the chemical synthesis of nucleosides, nucleotides, and oligomers were started by A. Todd and his co-workers in 1942 at Cambridge University in England and somewhat later in the USA. Since then, numerous books and reviews have been published on the subject, summarizing the enormous progress achieved (see [10 – 12]).

Systematic studies of the biological properties of nucleosides began in the second half of the 1940s. Somewhat earlier, P. Fildes & D.D. Woods formulated the antimetabolite theory and a resulting approach to the design of natural compound analogs with biomedical potential sparked an enormous amount of research in this area (for the relevant reviews, see [13, 14]). Despite the moderate predictive power of this theory, synthesis of a large variety of natural nucleoside analogs and data on their biological properties yielded (*i*) very useful tools for studying biochemical transformations, which facilitated understanding of the mechanism of functioning of enzymes of nucleic acids metabolism; (*ii*) an analysis of the structure-activity relationships, which allowed rational design of new analogs with improved activity-toxicity ratios; and (*iii*) a number of anticancer and antiviral drugs.

Thirty years of systematic studies resulted in the discovery of several major structures of great biological and medicinal importance, such as heterocyclic bases (6-mercaptopurine **(11)**, thioguanine **(12)**, 5-fluorouracil **(13)**), analogues of thymidine modified at C5 of an aglycone (2'-deoxy-5-iodouridine **(14),** Idoxuridine,; Iduviran;; 2'-deoxy-5-fluorouridine **(15),** FUDR, Floxuridine; (*E*)-5-(2-bromovinyl)-2'-deoxyuridine **(16)**, BVDU, Brivudine) and at C3' of the carbohydrate moiety (3'-deoxy-3'-fluorothymidine **(17),** FLT, Alovudine and

Scheme 1

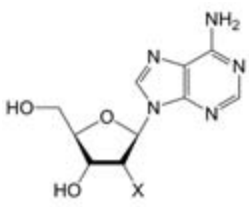

(1), X = H
(2'-Deoxyadenosine; dAdo)
(5), X = OH
(Adenosine; Ado)

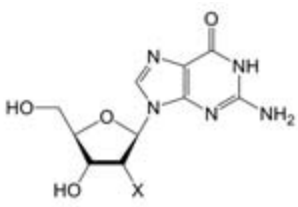

(2), X = H
(2'-Deoxyguanosine; dGuo)
(6), X = OH
(Guanosine; Guo)

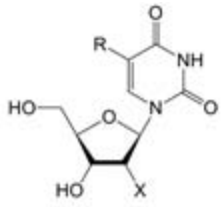

(3), X = H;
R = Me (Thymidine; Thd)
(7), X = OH;
R = H (Uridine; Urd)

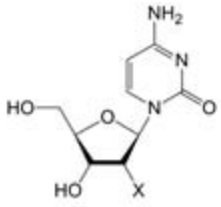

(4), X = H
(2'-Deoxycytidine; dCyd)
(8), X = OH
(Cytidine; Cyd)

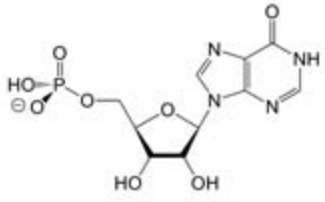

(9)

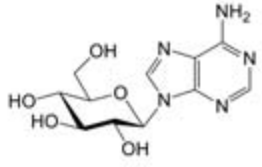

(10)

3'-deoxy-3'-azidothymidine **(18),** AZT, Zidovudine), β-D-arabinofuranosyl nucleosides (1-(β -*D*-arabinofuranosyl)-cytosine **(19),** aC, Cytarabine; -adenine **(20),** aA, Vidarabine; -guanine **(21),** aG), 3-carboxamido-1-(β -*D*-ribofuranosyl)-1,2,4-triazole **(22),** Virazole, Ribavirin, hyper-modified purine acyclonucleosides, and also analogs in which the sugar moiety of a nucleoside is replaced with an aliphatic chain mimicking the carbohydrate fragment, such as Aciclovir **(23),** ACV, Zovirax; Gancyclovir **(24),** DHPG, Cytovene; Buciclovir **(25)**, Penciclovir **(26),** and Famciclovir **(27)** (Scheme 2).

Discovery of a number of compounds that displayed strong antiviral and/or anticancer activities, some of which were later approved by the FDA (Food and Drug Administration, USA), as well as isolation of nucleoside antibiotics from natural sources [15], stimulated extensive synthesis of a wide variety of modified nucleosides. Studies aimed at shedding light on the mechanisms behind the antiviral and antitumor activities of these compounds yielded extensive data regarding the metabolic transformations of modified nucleosides, including their metabolic activation and deactivation. Moreover, these studies identified the enzymatic reactions involved in these activities, and also led to the discovery of the role of nucleoside utilization mechanisms ("salvage" synthesis) and the involvement of virus-encoded nucleoside kinases in a key step of nucleoside activation via intracellular 5'-monophosphorylation. The nucleoside-5'-monophosphates are then further metabolized into 5'-di- and 5'-triphosphates, which can then take part in various metabolic transformations [14, 16 – 19].

It was established that the majority of nucleoside analogs exhibiting antiviral and/or antitumor activities are not active as such but gain activity after being transformed into nucleotides by intracellular enzymes. In the case of antiviral agents, nucleoside-5'-triphosphates are often true inhibitors of viral DNA or RNA polymerases. In some cases, polymerases introduce an analog of the natural substrate into the growing chain, thus blocking or severely impeding the chain's growth or producing a functionally incompetent biopolymer [16, 17].

In cancer cells, synthesis of the active species is initiated either by the transformation of a heterocyclic base into the respective ribonucleoside-5'-monophosphate, catalyzed by nucleoside phosphoribosyl transferase or by direct 5'-monophosphorylation of nucleosides by cellular nucleoside kinases [14, 20 – 22]. On the contrary, in virus-infected cells, the first critical step of antiviral nucleoside activation involves 5'-monophosphorylation catalyzed by virus-encoded kinases [16, 17, 23].

Catabolic deactivation of biologically active nucleosides often involves deamination of cytosine and adenine nucleosides by the respective deaminases, which usually yield inactive derivatives [14, 24, 26], and phosphorolytic cleavage of the glycoside bond by nucleoside phosphorylases, which results in the formation of heterocyclic bases and α-*D*-pentofuranose 1-phosphates [24, 27 and works cited in 27].

New data on the metabolism of nucleosides and their mechanism of action towards their targets allowed improvement of the activity of the originally discovered compounds by protecting them from catabolic transformations and facilitating their targeted delivery, and also stimulated the search for new biologically active molecules [18, 19, 28]. The first approach can be illustrated by the anticancer drugs Ftorafur® **(28)**, 5-fluoro-5'-deoxyuridine **(29),** and Capecitabine **(30)**; by nucleosides similar to aA, such as Cladribine **(31)**, Fludarabine **(32)** and Clofarabine **(33)**, which are highly active against various forms of leukemia and are resistant to deamination by adenosine deaminase [21, 22]; and by the antileukemic drug Nelarabine **(34),** "prodrug" aG, which has better solubility and stronger activity as compared to the parent aG drug [29] (Scheme 3).

Elucidation of the mechanism of AZT action and establishment of viral-encoded reverse transcriptase as an important

Scheme 2

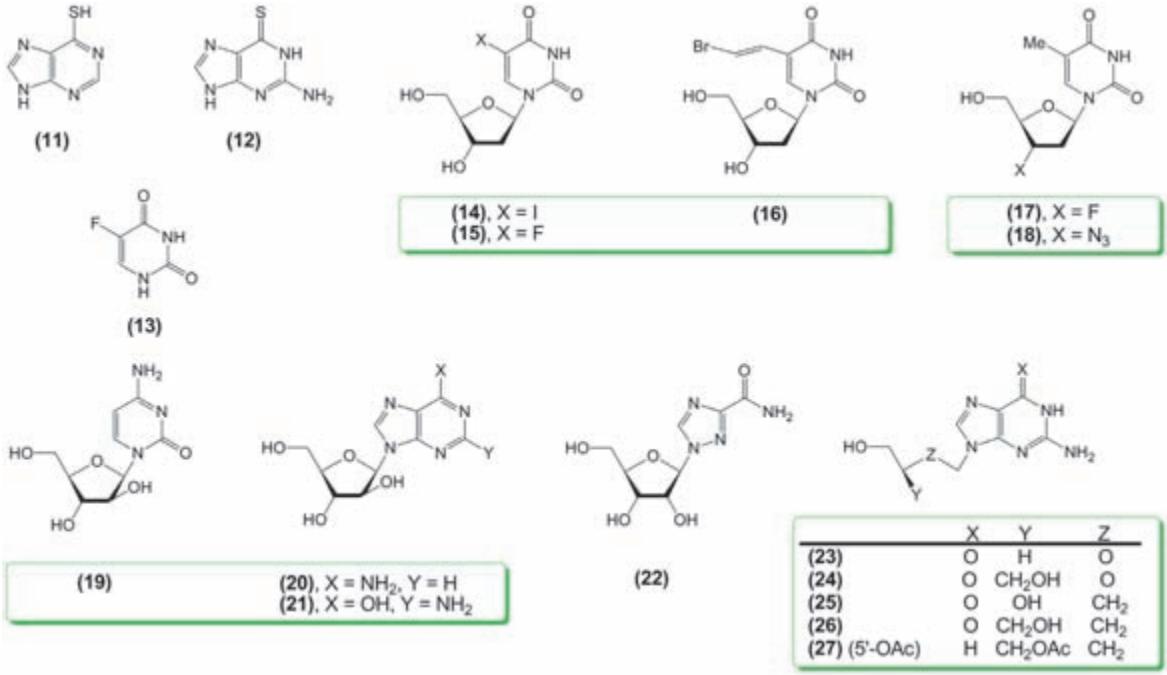

biochemical target for anti-HIV drugs stimulated extensive synthesis of various 2',3'-dideoxy nucleosides, *e.g.*, Zalcitabine (**(41)**; Hivid®), Didanosine **(42)** and related nucleosides with a C2'-C3' double bond, 2',3'-didehydro-2',3'-dideoxythimidine (**(35)**, Stavudine, Zerit®) and its cytosine analogs (**(36), (37)**; Reverset™), nucleosides with oxygen or sulfur atoms substituting the C3' carbon atom of the pentofuranose ring (**(38),** Amdoxovir; **(39),** Lamivudine, Epivir®; **(40)**, Emtricitabine, Emtriva®), as well as a number of hypermodified acyclic nucleosides with phosphonate function and their prodrugs (**(43),** Cidofovir; **(44),** Tenofovir) [30 – 34] (Scheme 3).

Notably, pioneering studies by H. Schaeffer and co-workers on the synthesis and study of the biochemical properties of acyclic nucleosides led to the discovery of 9-[2-hydroxy(ethoxymethyl)]guanine (**(23)**, Acyclovir) as an effective antiviral drug [35 – 38] and stimulated extensive synthesis of a wide variety of acyclic nucleosides modified either in the aglycone or in the acyclic fragment, including phosphonate analogs of nucleoside 5'-phosphates and their numerous prodrugs, some of which manifested a broad spectrum of biological activities [39].

Up to the present, a vast majority of the modified nucleosides have been synthesized by chemical methods. Most of the developed synthetic approaches can be divided into three main groups: (*i*) convergent synthesis, employing the suitable sugar or sugar-mimicking derivatives as glycosylating agents, (*ii*) chemical transformations of natural nucleosides, and (*iii*) rational combinations of both aforementioned approaches. Despite the impressive progress achieved in the development of chemical methods, production of many antiviral and anticancer drugs, as well as other biologically active compounds, remains a challenge. This leads to high drug costs and consequently prevents extensive biological trials and studies, as well as broad therapeutic application. The need for the development of new strategies became apparent in the late 1970s.

CHEMO – ENZYMATIC STRATEGY FOR THE SYNTHESIS OF NUCLEOSIDES (NUCLEOSIDE BIOTECHNOLOGY)

Amidst the great number of nucleic acid metabolism enzymes, approximately 20 are promising in relation to the development of novel effective strategies for the production of biologically important nucleosides. These are foremostly enzymes that catalyze the condensation of heterocyclic bases and sugars, thus forming glycoside bonds, and also enzymes that are involved in various transformations of nucleosides. These enzymes are of utmost importance for the research and development of novel approaches for nucleoside synthesis.

In parallel with the pioneering chemical studies and investigation of the biochemical properties of modified nucleosides, researchers began attempting the isolation of enzymes involved in nucleic acid metabolism from natural sources and to study the mechanisms of their functioning (for a review, see [24]). The first reports by P. Levene and co-workers [40 – 44] and W. Jones [45, 46] on the activities involved in nucleic acid hydrolysis and nucleoside disassembly were published in 1911; later on, Levene and co-workers described a procedure for the isolation of "nucleosidase" from the spleen, kidney, and pancreas of cattle. The isolated enzyme was able to hydrolyze adenosine and inosine in phosphate buffer with similar efficiency, thus yielding the respective bases and ribose (formation of ribose-1-phosphate was not discovered at that time!). The authors also investigated the properties of this enzyme [47 – 49]. They determined the optimal temperature (37 °C) and pH (7.5) of the reaction and found that (*i*) ribose and adenine exert "an impeding influence on the progress of the reaction," (*ii*) kaolin completely adsorbs the partially purified enzyme from the solution, and the enzyme-kaolin complex is stable within pH 4.0 – 8.0 values at 40 °C for 15 h and shows the same level of activity, (*iii*) a chemically prepared adenine nucleoside containing hexose (the structure was not established) could not act as a substrate for this enzyme.

Scheme 3

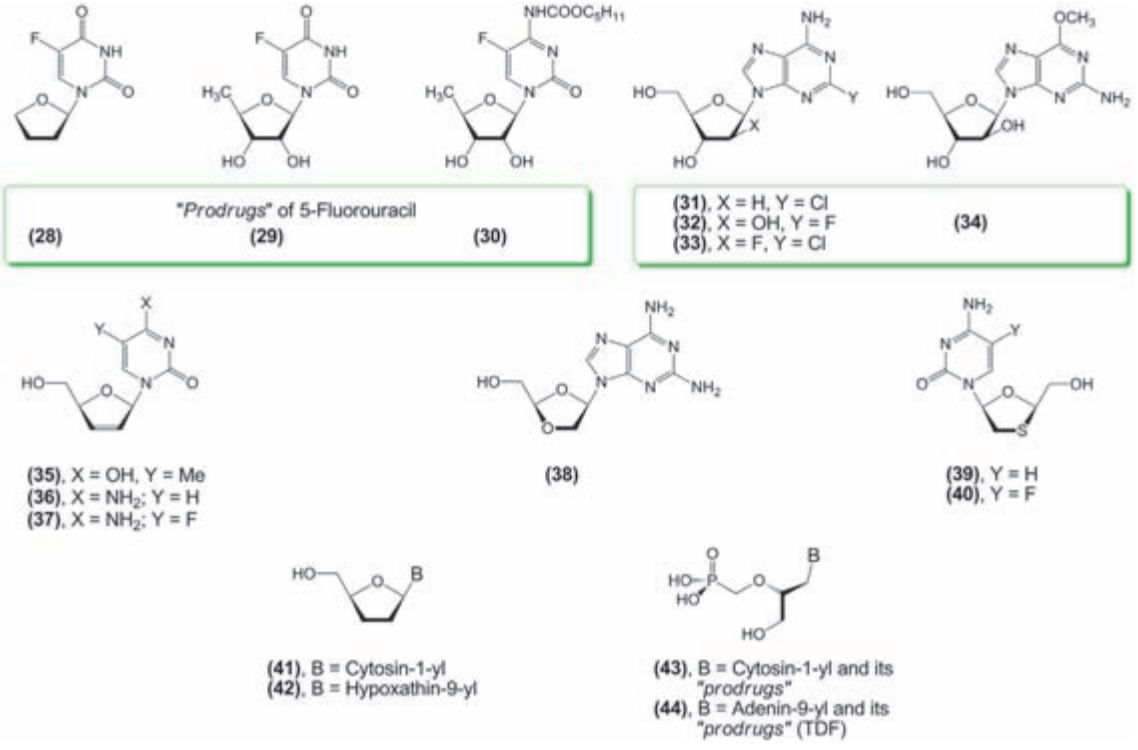

Later on, H. Kalckar investigated nucleosidase extracted from rat liver and found that (*i*) this enzyme was in fact a purine nucleoside phosphorylase (PNP; EC 2.4.2.1), which hydrolyzed inosine or guanosine via phosphorolysis, thus yielding ribose-1-phosphate (structure was later determined to be α-*D*-ribofuranose-1-*O*-phosphate; RP; **(47)**; for reviews, see [24, 50]) and the corresponding purine bases, hypoxanthine or guanine; (*ii*) when RP is incubated with hypoxanthine or guanine in the presence of PNP, a rapid formation of inosine or guanosine takes place [51, 52]. Kalkar's paper was the first report on the isolation of pure RP. Shortly after this publication, L. Manson & J. Lampen showed that quiescent *Escherichia coli* cells, as well as a cell-free extract, contain enzymes which can hydrolyze 2'-deoxyinosine and thymidine in the presence of inorganic phosphate down to free bases and a deoxyribose ester whose structure was later established to be 2-deoxy-α-*D*-ribofuranose-1-phosphate **(48)** [24, 53]. It was suggested that this extract contains purine and pyrimidine nucleoside phosphorylases, whose specificity was later found to be similar to that of mammalian enzymes. Moreover, evidence was presented that these bacterial enzymes reversibly catalyze the synthesis of nucleosides and their phosphorolytic degradation (Scheme 4).

Subsequent studies have corroborated and extended these fundamental findings, and it was found that purine nucleoside phosphorylase is specific to 9-(β-D-pentofuranosyl)purines, whereas mammalian PNP is specific to 6-oxopurines (compared with data by Levene *et al.* [47 – 49]; *vide supra*) and their nucleosides, as well as some analogs, whereas PNP from bacterial sources displays very broad specificity, accepting both 6-oxo- and 6-aminopurines and their nucleosides as substrates, along with many analogs.

Thymidine phosphorylase (TP; EC 2.4.2.4) reversibly catalyzes the phosphorolysis of thymidine **(7)** and 2'-deoxyuridine but not uridine **(7)** or 1-(β-*D*-arabinofuranosyl)-thymine and –uracil, whereas uridine phosphorylase (UP; EC 2.4.2.3) does not distinguish between β-*D*-ribofuranose and 2'-deoxy-β-*D*-ribofuranose in pyrimidine nucleosides and accepts 1-(β-*D*-arabinofuranosyl)-pyrimidines as substrates as well. Cytosine and its nucleosides are not substrates either for TP or UP; however, we must note two peculiar observations. Firstly, PNP exhibited cytidine phosphorylase activity in some experiments [54]. Secondly, it was shown that human deoxycytidine kinase is a cytosolic enzyme that plays a key role in the activation of therapeutically relevant nucleoside analogs via their 5'-monophosphorylation, accomplishes phosphorolytic cleavage of 2'-deoxynuclosides, including 2'-deoxycytidine into free heterocyclic bases and 2-deoxy- α-*D*-ribofuranose-1-phosphate [55].

The results of pioneering research unequivocally indicated a possibility for the enzymatic synthesis of nucleotides using purine or pirimidine heterobases as a starting point and

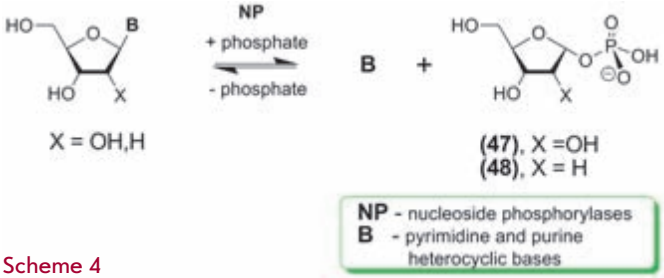

Scheme 4

Scheme 5

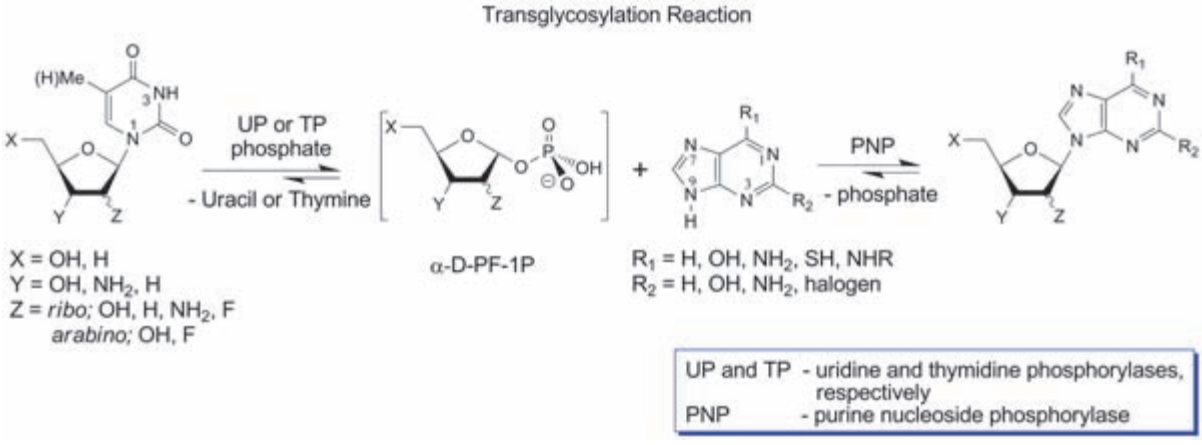

α-*D*-pentofuranose-1-phosphate or another nucleoside as a carbohydrate fragment donor (see [24, 56] for a review). The first attempts to use enzymes for the synthesis of pyrimidine nuclesides were made by M. Friedkin & D. Roberts, who attempted to synthesize thymidine and related nucleosides [57, 58], and by R. Duschinsky & C. Heidelberger for the synthesis of 5-fluoro-2'-deoxyuridine (FUDR, (**15**)) and 2'-deoxy-β-*D*-ribofuranosil-5-trifluoromethyl-urcail (CF_3-dUrd) [59–64]. Interestingly, the first report of FUDR synthesis via enzymatic transfer of the 2-deoxyribofurnaose residues of thymidine onto 5-fluoro-uracil **(13)** was published in 1957 [59]. A preparative-scale enzymatic process was later patented [60]. The same group of researchers described a chemical method for the synthesis of 5-fluoro-2'-deoxyuridine (**15**), and a low-yield enzymatic process for the synthesis of another anti-cancer nucleoside – CF_3-dUrd using a cell-free extract of *E. coli* as a source of thymidine phosphorylase [36] (See [24, 56, 65–68] for reviews). Later on, a number of 5-modified uracil nucleosides, including 2'-deoxy-5-iodouridine ((**14**); 55%), 5-fluoro-2'-deoxyuridine ((**15**); 65%), and *E*-5-(2-bromovinyl)-2'-deoxyuridine ((**16**); 61%), were obtained by using thymidine (**3**) or 2'-deoxyguanisone (**2**) as donors of 2-deoxyribofuranose, the appropriate heterobases as acceptors, and selected BM-11 *E. coli* as a biocatalyst [69].

Transfer of a pentofuranose moiety from pyrimidine nucleosides to purine bases and *vice versa* (transglycosylation reaction) catalyzed by bacterial nucleoside phosphorylases (NP) was shown to be a very efficient method for the synthesis of a number of analogs of natural purine and pyrimidine nucleosides of biological and pharmaceutical importance. The most exploited pathway includes the transfer of a pentofuranase moiety from pyrimidine nucleosides to purine bases (Scheme 5).

This transglycosylation approach is based on numerous efficient chemical transformations of readily available natural pyrimidine nucleosides into diverse nucleosides modified in their carbohydrate component through the intermediate formation of O^2,2'(3';5')-*anhydro* derivatives, followed by opening of the *anhydro* ring upon treatment with nucleophilic agents. Unfortunately, a similar approach is not practical for the production of related purine nucleosides. Moreover, distinctions in the substrate specificity of TP and UP extend the number of the pentofuranose donors of the transglycosylation reaction that can be used with the optimal efficiency. Thus, 1-(2-deoxy-2-fluoro-β-*D*-ribofuranosyl)uracil (Scheme 5, X = Y = OH; Z = *ribo*F) and 1-(2-deoxy-2-fluoro-β-*D*-arabinofuranosyl)thymine (Scheme 5, X = Y = OH; Z = *arabino*F) display no substrate activity towards UP: thus it cannot be employed as a biocatalyst; on the contrary, both nucleosides have been found to be (although very poor) substrates for TP, allowing their use for TP-catalyzed transglycosylation of purine bases [70, 71].

The successful employment of nucleoside phosphorylases as biocatalysts for the synthesis of purine arabinosides and a multitude of base- and carbohydrate-modified nucleosides has been described in numerous publications (for reviews, see [24, 56]).

Three types of biocatalysts have been successfully employed for transglycosylation reactions: (*i*) selected intact bacterial cells, which display UP and/or TP and PNP activities, (*ii*) intact bacterial cells overexpressing recombinant nucleoside phosphorylases, and (*iii*) purified recombinant enzymes.

Intact bacterial cells as a biocatalyst represent a kind of naturally immobilized enzyme, which can be used for the transformation of interest. Use of this type of biocatalysts offers some advantages (relatively low cost) over the application of purified enzymes or immobilized (encapsulated) enzymes. However, intact bacterial cells may display activities which will catalyze the transformation of the substrate and/or the desired product of the transglycosylation reaction into an undesirable form (see further). On the other hand, considerable progress has been achieved in the practical production of recombinant enzymes during the last decade, which makes these biocatalysts available for broad application, including the development of biotechnological processes for the production of drugs. In case of very low substrate activity of a pentofuranose donor or an acceptor base, use of purified enzymes as biocatalysts may be a rational alternative to the use of intact bacterial cells.

Notably, the off-pathway activities displayed by intact cells can be rationally involved in the synthesis of the desired nucleosides. For example, selected *E. coli* BM-11 cells displaying high cytidine deaminase (CDase) activity, along with UP

Scheme 6

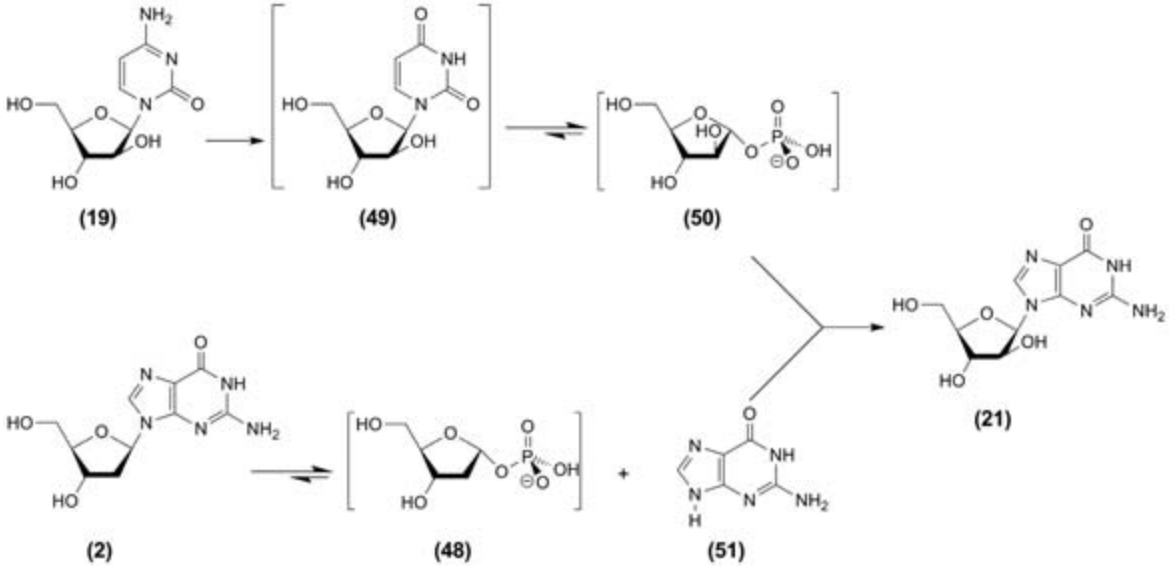

Scheme 7

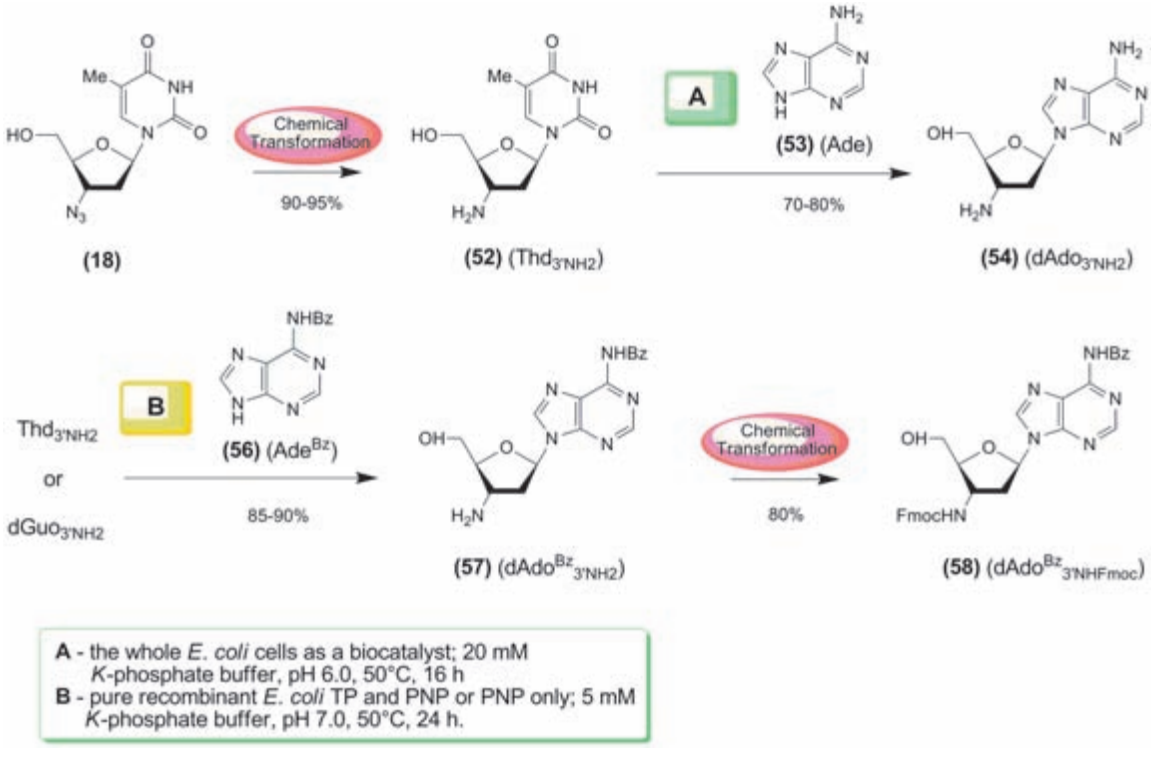

and PNP activities, were employed as a biocatalyst for the synthesis of aG **(21)** (isolated yield 48-53%) using aC **(19)** and 2'-deoxyguanosine (**(2);** dGuo) as donors of *D*-arabinofuranose residue and *in situ* formed guanine (**(51)**; Gua), respectively (Scheme 6). Deamination of aC to aU **(49)** by cytidine deaminase precedes the formation of α-*D*-arabinofuranose-1-phosphate **(50)** from aU catalyzed by UP.

A similar approach was employed for the synthesis of 2'-deoxy-2'-fluoroguanosine using 2'-deoxy-2'-fluorocytidine as a donor of 2-deoxy-2-fluoro-α-*D*-ribofuranose-1-phosphate [73]; note that the use of selected *E. coli* BMT-4D/1A cells for the synthesis of 2'-deoxy-2'-fluoroguanosine [73] appears to be preferable over the use of purified UP and PNP [70, 71].

The use of the selected *E. coli* cells was found to be very efficient for chemoenzymatic syntheses of purine 3'-amino-2',3'-dideoxy-β-*D*-ribonucleosides (Scheme 7) [74]. Notably, AZT **(18)** is neither a substrate for TP or UP and cannot, therefore, be used as a donor of the pentofuranose moiety. Reduction of the azido group of AZT produces 3'-amino-2',3'-dideoxythymidine (**(52)**; $dThd_{3'NH2}$) that is a satisfactory substrate for TP and can be used as a donor of the carbohy-

Scheme 8

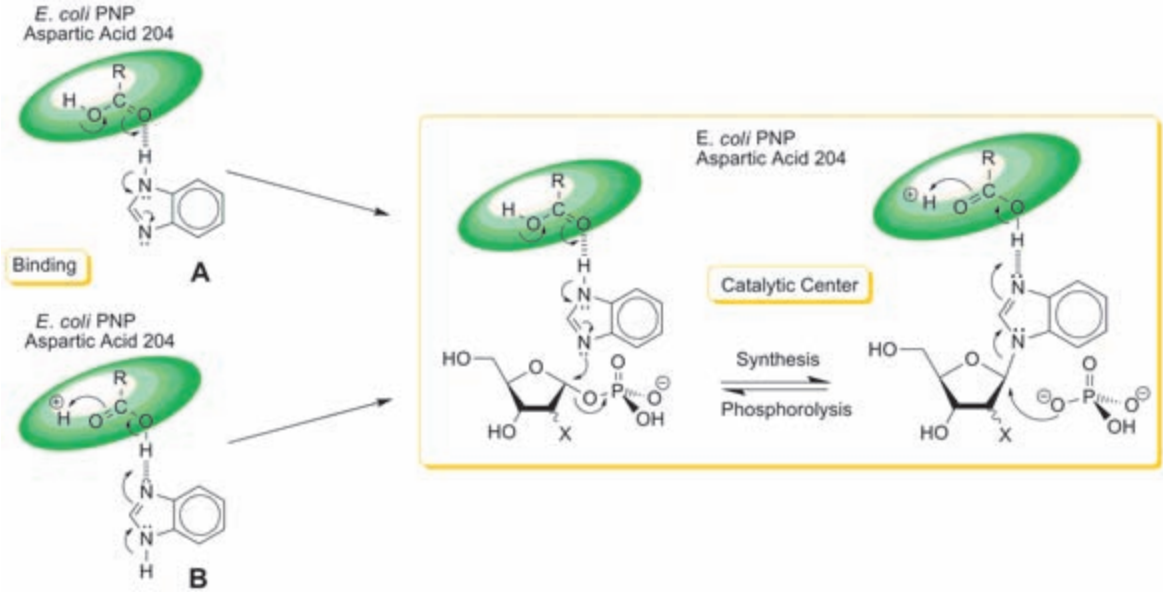

drate moiety. Transfer of the pentofuranose moiety from $dThd_{3'NH2}$ to adenine catalyzed by intact *E. coli* cells proceeds smoothly, and the desired 3'-amino-2',3'-dideoxyadenosine (**(54)**; $ddAdo_{3'NH2}$) can be isolated with good yields. However, replacement of adenine **(53)** by N^6-benzoyladenine **(56)** in the aforementioned reaction produces 3'-amino-2',3'-dideoxyadenosine **(54)** instead of the expected N^6-benzoyl derivative of $ddAdo_{3'NH2}$ **(57),** owing to the off-pathway activity present in the intact cells.

Taking into account that $ddAdo_{3'NH2}$ with orthogonally protected amino functions **(58)** is of interest for oligonucleotide synthesis, we recently investigated transglycosylation reactions using pure recombinant *E. coli* TP and PNP [75]. It was found that the use of $Thd_{3'NH2}$ as a donor of the pentofuranose residue and TP and PNP as biocatalysts or a $dGuo_{3'NH2}$ / PNP combination (5 mM K-phosphate buffer (pH 7.0), 50 °C, 24 h) produced the desired N^6-benzoyl derivative of $ddAdo_{3'NH2}$ **(57)** in high yield (Scheme 7) [76]. Standard treatment of the latter with Fmoc-OSU yielded the desired $ddAdo^{Bz}_{3'NHFmoc}$ **(58)** with orthogonally protected amino groups.

The possible areas of application of nucleoside phosphorylases for the synthesis of nucleosides, as well as the limitations of this methodology, have been investigated in detail; however, several very interesting enzymatic synthetic reactions deserve special attention, because they are crucial for understanding the mechanism of synthetic reactions catalyzed by these enzymes and may expand the scope of their practical use.

It is well documented that the N^7-atom of purine plays a very important role in the phosphorolytic cleavage of the glycosyl bond of purine nucleosides ([77, 78] and works cited in [77]) and, it seems, in the reversed synthetic reaction catalyzed by *E. coli* PNP as well, even though the mechanism of this reaction has not been adequately studied. The finding that 3-deazapurines [79 – 81] and 1-deaza-, 3-deaza- and 1,3-dideazapurines (benzimidazoles, including fluoro-, chloro- and bromo-substituted) [82 – 84] are good substrates for *E. coli* PNP allows the authors to suggest a key role for two nitrogen atoms of the imidazole ring in the above-mentioned reaction. Namely, one of them is involved in the binding of the heterocyclic base in the enzyme's active site, which may in turn increase the nucleophilicity of the second nitrogen atom. This facilitates an attack by this atom on the electrophilic C^1 carbon atom of α-*D*-pentofuranose-1-phosphate and eventually results in the formation of a glycosidic bond (Scheme 8).

Remarkably, the mechanism of this synthetic reaction catalyzed by nucleoside phosphorylases did not attract the attention of researchers and many important details were left unclear. Thus, the mode of initial binding of the substrate or inhibitor of *E. coli* PNP (see binding types **A** and **B** in Scheme 8) might have shed light on the mechanism of the enzyme's functioning and provided a clue for the explanation of some unusual observations. Participation of two nitrogen atoms in this reaction seems obvious taking into account the fact that 7-deazahypoxanthine (**(61)**; 7-DAH) is a very potent inhibitor of PNP (Scheme 8) [50, 85]. Tubercidine **(59)** and 7-deazainosine **(60)** are not substrates for PNP and showed very low affinity for the active site of the enzyme. On the contrary, the free base, 7-deazahypoxanthine **(61)**, is recognized by the enzyme and forms a very strong PNP-phosphate-base complex, which results in complete inhibition of the enzyme [85].

The mechanism of 7-DAH binding in the *E. coli* PNP binding site still remains unknown; two types of interactions can be proposed – **A** and **B**. The first (type **A**) is similar to one of the two possible modes of binding of the natural substrate in the PNP active site via a hydrogen bond with the carboxyl moiety of aspartic acid-204 (type **A** on Scheme 8 and type **A** on Scheme 9). Obviously, type **A** binding of 7-DAH in the *E. coli* PNP binding site cannot result in the formation of a nucleoside, since there is no N^9-nitrogen atom (purine numbering). Type **B** binding involves the formation of an unusual hydrogen bond between the OH-group of the tautomeric form of the cyclic amide. This hypothetic bond can seemingly stabilize the PNP–phosphate–7-DAH complex

Scheme 9

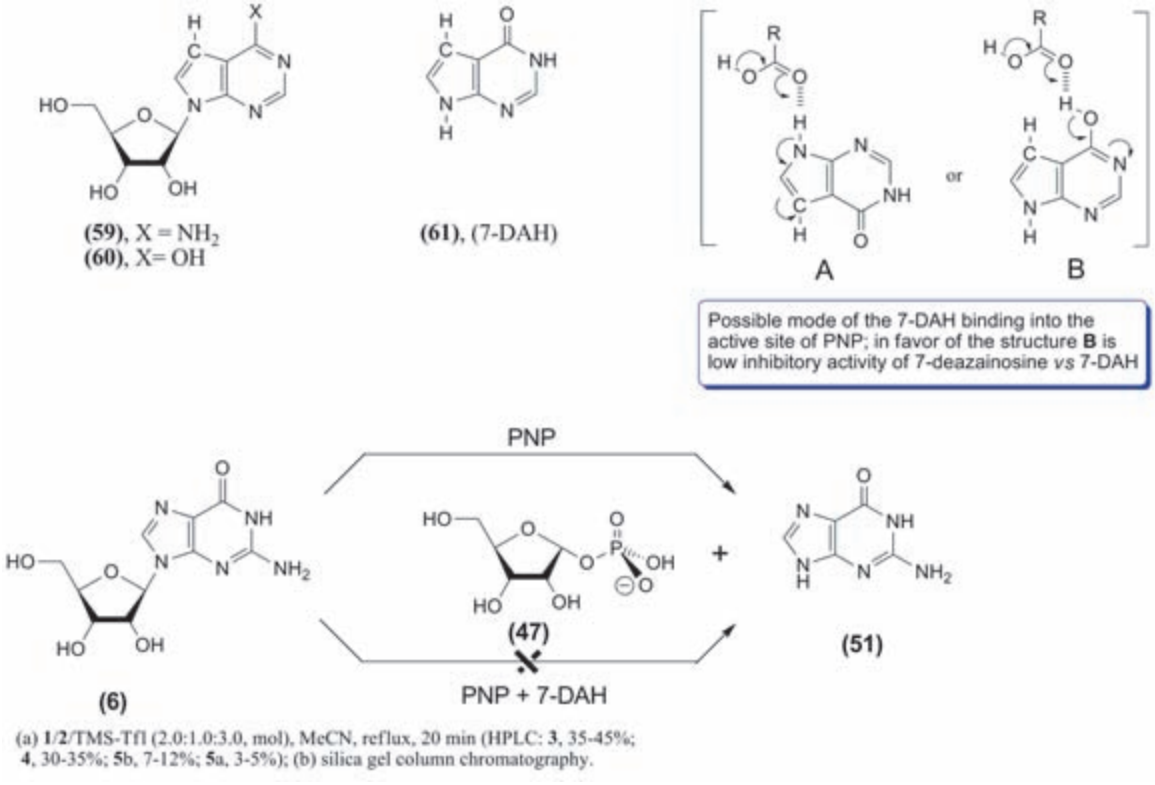

(N^9-H-structure), whose electron or spatial structure either impedes or prevents a nucleophilic attack of the C 1-atom of α-*D*-pentofuranose-1-phosphate (**47**) (Scheme 9). The hypothetical possibility of the existence of a **B**-type structure is unexpectedly supported by the moderate acceptor activity of 5-aza-7-deazaguanine (**62**) during a glycosylation reaction involving PNP (bovine spleen extract; Sigma) and 2-deoxy-β-*D*-pentofuranose-1-phosphate (**48**) as a carbohydrate donor (see [86] and other works cited in this article). Indeed, the heterobase can exist in three tautomeric forms (**62-I–III**), and one of them, a (**62-III)** structure, can be recognized by PNP and thus result in the formation of a nucleoside via a nucleophilic attack of the free N^9-nitrogen atom on the C 1-carbon atom of the carbohydrate substrate (Scheme 10). Notably, analysis of tautomeric structures involving *ab inito* (6-31G**) and semi-empirical methods (PM3, in water) (HyperChem 8.1) show that structure **II** is the most stable in terms of thermodynamics, while structures **III** and **I** are less stable (I.A. Mikhailopulo, unpublished).

Obviously, the binding mechanism of 7-DAH and 5-aza-7-deazaguanine (**62**) in the PNP active site and also the possible ways of using this information for the production of some 7-deazopurine-derived nucleosides deserve further thorough research.

Other examples of unusual biotransformations are the metabolic and enzymatic transformations of the anti-influenza agent *N*-(1,3,4-thiadiazol-2-ylc)yanamide (**(64)**; LY217896) (Scheme 11) [87, 88]. This compound shows a degree of structural similarity with the heterocyclic bases of the antiviral nucleoside Virazole (**(22)**; Ribavirin) and of the anticancer C-nucleoside tiazofurin **(65).** It was found to be active against the influenza A and B viruses both *in vitro* and in animal models but was ineffective in clinical trials against an experimental influenza A (H1N1) virus. A number of its metabolites were detected in experiments with mammalian cells and animals as well, and the structures of three metabolites were established (Scheme 11).

It was found that purine nucleoside phosphorylases isolated from calf spleens and human erythrocytes, as well as the bacterial enzyme (Sigma, N-8265), catalyze the transformation of *N*-(1,3,4-thiadiazol-2-yl)cyanamide in the presence of α-*D*-ribofuranose-1-phosphate **(47)** into N^4- and N^3-ribosides (37 ˚C, 20-70 h, 2 – 200 units of PNP; the ratio between the N^4- and N^3-ribosides (**(66)** and **(67))** was found to be ~ 1:3 (60-65% combined yield) at high concentrations of PNP and ~ 3:1 (12-14% combined yield) at low concentrations of PNP) [89]. Interestingly, the formation of the mesoionic [88] or ionic (as

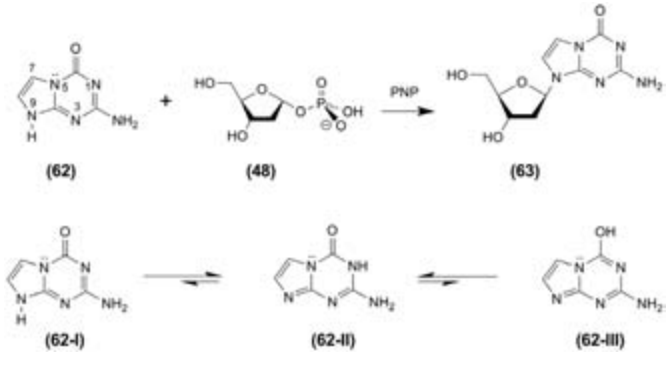

Scheme 10

Scheme 11

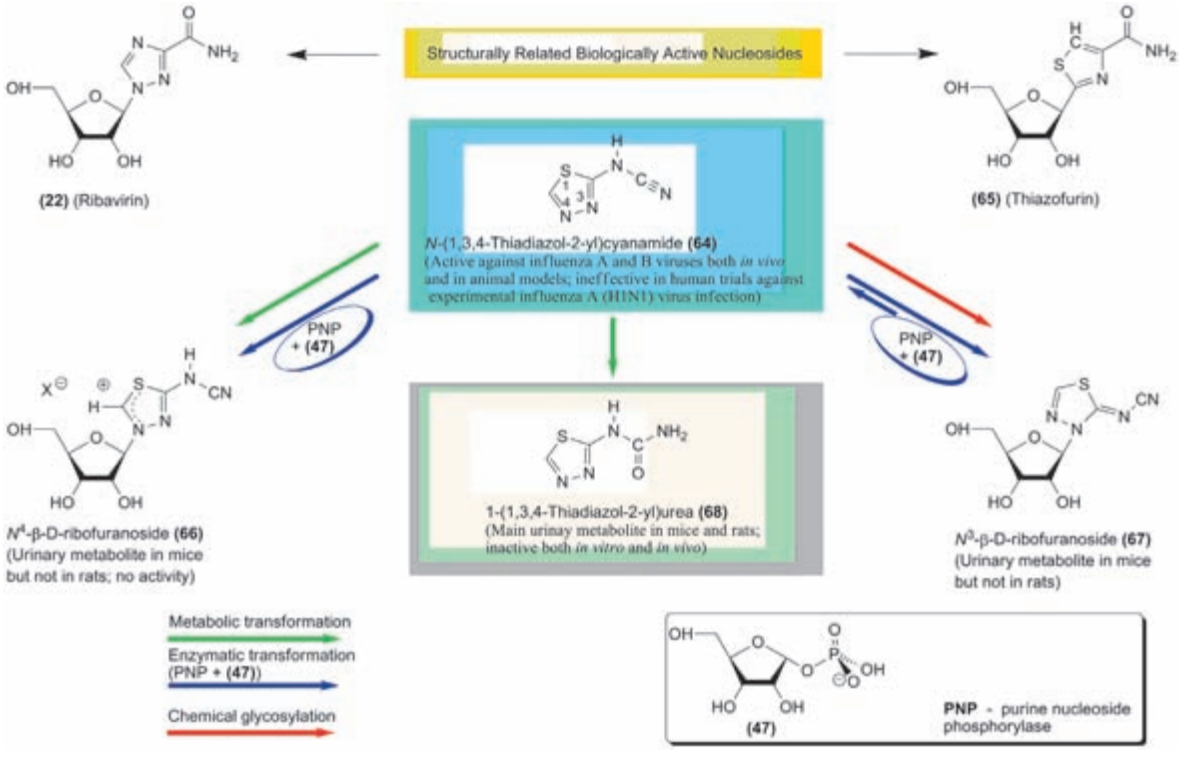

shown in Scheme 11) N^4-riboside **(66)** apparently proceeded in an irreversible manner, whereas the N^3-riboside **(67)** was found to be a substrate of PNP.

We must also mention several extremely interesting observations made in this excellent study. Firstly, 1,3,4-thiadiazol-2-ylcyanamide displayed broad antiviral activity *in vitro* and in animal models against orthomyxo- and paramyxoviruses. Oral, intraperitoneal or aerosol administration of the drug protected mice against lethal influenza A or B virus infections; however, it did not show either toxicity or anti-influenza activity in phase I trials on healthy volunteers [89]. Secondly, the data on the pharmacokinetics of the thiadiazol base also show considerable diversity. Thirdly, contrary to the above, PNP of mammalian and bacterial origin manifested close catalytic similarity in the ribosylation of this base, despite the well-known differences between the substrate preferences of these two types of PNP for natural substrates. These data imply that *N*-(1,3,4-thiadiazol-2-yl)cyanamide **(64)**, which does not have any common features with natural substrates of PNP, still possesses functionality that is sufficient for the synthetic reaction catalyzed by both types of PNP. Testing new heterocyclic bases as substrates of PNP may help understand this functionality, providing further insight into the mechanism of the enzyme's function and also opening new possibilities for its practical use.

The use of intact bacterial cells as a biocatalyst for transglycosylation reactions (Scheme 5) implies that the cells contain uridine, thymidine, and purine nucleoside phosphorylases. Besides the aforementioned nucleoside phosphorylases, other phosphorylases have been found in bacteria that may be useful for the enzymatic synthesis of nucleosides. For instance, the nucleoside phosphorylase purified from the *Klebsiella* sp. strain LF1202 demonstrated very interesting properties [90]. It consists of five identical subunits with a molecular weight of 25 000 Da (based on the results of SDS-PAGE) and shows pyrimidine and purine nucleoside phosphorylase activities. Inosine, adenosine **(5)**, 2'-deoxyadenosine **(1)**, guanosine **(6)**, and 2'-deoxyguanosine **(2)** showed similar substrate activity (relative activity ~100%) in phosphorolysis (K_m values for inosine and inorganic phosphate (P_i) were calculated to be 0.66 and 0.56 mM, respectively); substrate activity for 2'-deoxyinosine was 2.5-fold higher (254%); xanthosine and its 2'-deoxy counterpart did not act as substrates. In the synthetic reaction, the substrate activity of hypoxanthine and adenine was similar (K_m values for hypoxanthine and α-D-ribofuranose-1-phosphate (**(47)**; α-*D*-RF-1P) were calculated to be 0.45 and 0.14 microM, respectively); guanine showed somewhat decreased substrate activity in the synthetic reaction. As for pyrimidine nucleosides, uridine was found to be the best substrate (relative activity 368%) as opposed to 2'-deoxyuridine (95%) and thymidine (29%); the K_m values for uridine (0.38 mM) during phosphorolytic cleavage and for uracil (0.44 mM) during the synthetic reaction were similar. The substrate activity of uracil in the synthetic reaction with α-*D*-RF-1P (82%) and 2-deoxy-α-*D*-ribofuranose-1-phosphate (**48**) was found to be 82 and 39%, respectively; thymine showed decreased activity (17%); neither cytidine, nor 2'-deoxycytidine, nor cytosine demonstrated any substrate activity in the enzymatic reactions.

The *Klebsiella* sp. nucleoside phosphorylase was employed for the synthesis of aA from aU and adenine (3:1 molar ratio) under optimized reaction conditions (0.1 M *K*-phosphate buffer, pH = 8.0; 6.7 mM concentration of adenine; 50 °C, 30 h; 0.86 units of enzyme) and converted approximately 90% of

Scheme 12

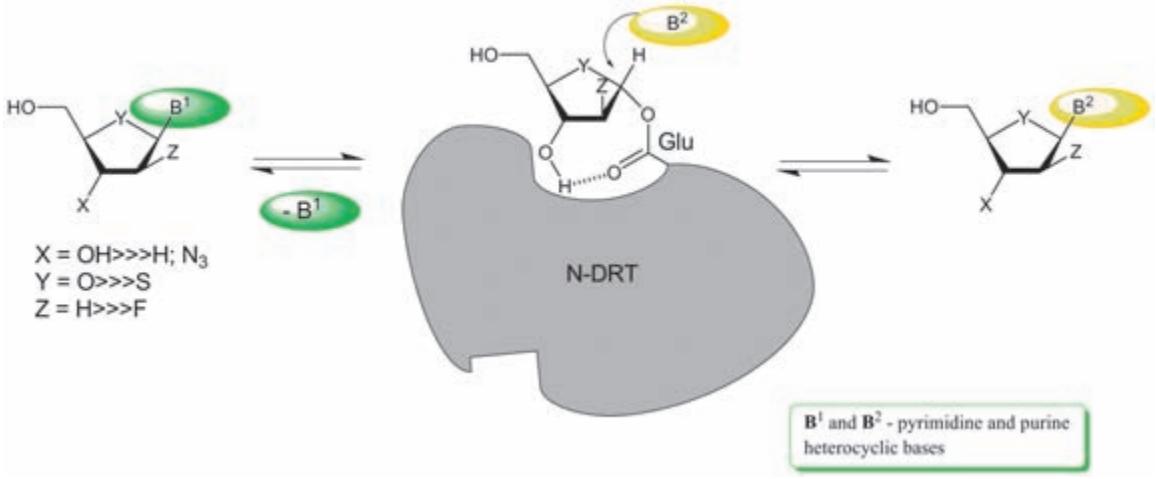

the adenine into aA, as assayed by TLC analysis of the reaction mixture [90].

H. Shirae & K. Yokozeki isolated an orotidine-phosphorolysing enzyme (OrP) from *Erwinia carotovora* AJ 2992 and investigated its properties [91]. Orotidine ~~(OrP)~~ was irreversibly phosphorolysed into orotic acid and 1-phosphate **(47)** by OrPE, and the enzyme showed no strict specificity. Indeed, the substrate activity of uridine was found to be two orders of magnitude higher as opposed to orotidine (relative activity of 100% and 1% for uridine and orotidine, respectively); moreover, 5-methyluridine (10%), aU (11%), 2'-deoxyuridine (22%), 3'-deoxyuridine (11%), and 2',3'-dideoxyuridine (1%) were also found to be substrates for the OrP preparation. At each purification step, OrPE was always co-purified with uridine phosphorylase (UP) and the researchers were unable to separate these two activities. Both activities corresponded to a single band on SDS-PAGE, suggesting that both activities are present in the same protein. The purified enzyme had a molecular weight of 68 000 ± 2 000 Da, which suggests a dimeric structure. The most interesting finding is that the optimal temperatures and the pH values of the phosphate buffer were found to be 60 °C and 6.0 for orotidine phosphorylase activity and 70 °C and 7.0 for the uridine phosphorylase activity. On the whole, despite the differences in the optimal conditions for these two activities, it appears that the enzyme preparation from *Erwinia carotovora* AJ 2992 consists of a UP with broad substrate specificity.

N-Deoxyribosyltransferases (DRT's; nucleoside: purine(pyrimidine)deoxyribosyl transferases; EC 2.4.2.6) represent another type of enzymes, which are considerable interest as biocatalysts for nucleoside synthesis (for a review of pioneering studies, see [92]). As opposed to nucleoside phosphorylases, DRTs catalyze the direct transfer of the deoxyribofuranosyl moiety between a nucleoside and an acceptor base without intermediary formation of 2-deoxyribofuranose phosphate. The reaction proceeds through the intermediate formation of a covalently bound 2-deoxy-α-*D*-ribofuranosyl moiety, whose glycosidic hydroxyl forms a complex ester bond (Scheme 12) [93 and works cited in this paper].

DRTs are mainly present in some bacterial species of the *Lactobacillus* genus and were first discovered by W.S. MacNutt [94] in *Lactobacillus helveticus* and isolated by A. Roush & R. Betz [95]; later, DRT was purified from *L. leichmannii* by W. Beck & M. Levin, and its properties were thoroughly studied [96]. *Lactobacillus* bacteria contain DRT enzymes with two types of enzymatic activity, and these were first isolated by L. Holguin & R. Cardinaud from *L. helveticus* using affinity chromatography: DRT class I (also called purine deoxyribosyltransferase, PDT), which specifically transfer 2-deoxyribofuranose moieties from purine nucleosides to purine bases, and DRT class II (also called nucleoside deoxyribosyltransferase, NDT), which catalyze the transfer of 2-deoxyribofuranose between purines and pyrimidines in any combination [97]. Early reports on DRT substrate specificity revealed (*i*) strict specificity for the 2-deoxyribofuranose moiety, the absence of β-*D*-ribonucleoside substrate activity[92]; (*ii*) rather broad tolerance regarding various modifications of natural purines [96, 98, 99]; (*iii*) good substrate activity of cytosine as an acceptor of the 2-deoxy- and 2,3-dideoxyribofuranose residues, and the corresponding purine and pyrimidine nucleosides as donors of carbohydrate moieties [100] (for a review, see [24]).

A number of very interesting observations concerning the possible practical applications of DRT were made during the last two decades. Thus, D.A. Carson & D.B. Wasson investigated the substrate specificity of NDT isolated from *L. helveticus* (ATCC, #8018) (purified according to [96]) and found that the enzyme displays broad specificity both for pentofuranose residue donors and for purine and pyrimidine acceptors [100]. Testing the pentofuranose donor activity of 2',3'-dideoxy-β-*D*-nucleosides (ddN) in acetate buffer (pH 6.0) with an equimolar ratio between the donor and acceptor molecules at 37 °C revealed an exceptionally high activity of cytosine as an acceptor (16-60 $nmol \cdot min^{-1} \cdot mg^{-1}$ of enzyme with the following preference for donors: dT > ddG > ddC > ddA > ddI); donor activity of 2',3'-dideoxycytidine (ddC) and 3'-deoxythymidine (dT) was found to be approximately 2.2-11.6 $nmol \cdot min^{-1} \cdot mg^{-1}$ of enzyme for adenine, guanine, and hypoxanthine acceptors.

The first recombinant *L. leichmanii* NDT (DRT II) was prepared by W. Cook *et al.* [101]. These authors also studied the biochemical properties of this enzyme [102-104] and es-

Scheme 13

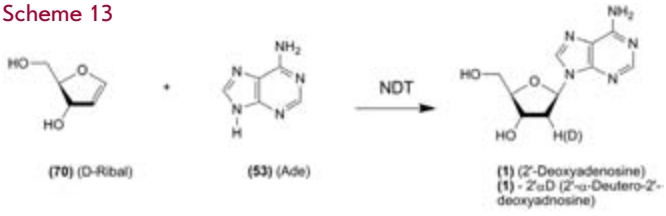

NDT - nucleoside deoxyribosyltransferase from *Lactobacillus leichmannii*; D-ribal (0.155 mmol) + adenine (0.093 mmol) + enzyme (2.84 mg) in 0.1 M *K*-phosphate buffer (2.9 mL, pH 5.7); 37°C. H_2O - 3 h; D_2O - 32 h.

tablished the architecture of the enzyme's active site [105]. In its native state, the enzyme turned out to be a hexamer composed of identical subunits with one active site per subunit, and two subunits forming a complete catalytic center. R. Wolfenden and co-workers discovered a lyase activity of *L. leichmanii* NDT and found that an interim 1-*O*-glutamyl derivative of 2-deoxy-*D*-ribofuranose is broken down in the absence of a heterocyclic base, yielding *D*-ribal. The latter reacts with adenine in a stereospecific manner under NDT catalysis, forming 2'-deoxyadenosine in aqueous solution and its 2'-α-deuterium derivative in D_2O (Scheme 13) [102]. Formation of thymidine and 2'-deoxyuridine from *D*-ribal and the respective bases could also be performed in a similar manner. The practical implications of this study of the chemoenzymatic synthesis of 2'-β-*D*-deoxynucleosides have not yet been investigated; however, further studies in this direction seem practical, as *D*-ribal can readily be produced by chemical methods (see [106, 107]), and the recombinant enzyme is also available.

Notably, recombinant *L. leichmanii* NDT catalyzes the stero- and regioselective transfer of 3-azido-2,3-dideoxyribofuranose from AZT to various 2-amino-6-substituted purine bases (50 mM *Na*-citrate buffer, pH 6.0; 50 °C, 21-28 days) yielding the corresponding purine N^9-β-*D*-nucleosides with moderate yields. The same enzyme was also employed as a biocatalyst for the synthesis of purine 4'-thionucleosides [104]. 2'-Deoxy-4'-thiouridine (used as an anomere mixture obtained via chemical glycosylation of uracil) was used as a carbohydrate moiety donor for the transglycosylation of a number of purine bases, with NDT as a catalyst (50 mM citrate buffer, pH 6.0; 50 °C, 5 days). Individual 9-(2'-deoxy-4'-thio-β-*D*-ribofuranosyl) purines were isolated with yields in the range of 5-48% after laborious treatment and chromatography of the reaction mixtures. It is worth noting that the use of thymidine and purine nucleoside phosphorylases as biocatalysts for the transglycosylation reaction yielded negative results.

Identification of glutamic acid 98 as the active site nucleophile of recombinant *L. leichmanii* NDT (the DRT II class) was made by D. Porter *et al.* [108]. The authors thoroughly investigated the interaction of the enzyme with 4 isomeric pairs of nucleosides, namely 9-(2-deoxy-2-fluoro-β-*D*-ribo(arabino)furanosyl)adenine (**(71)** and **(72)**), 2-amino-9-(2-deoxy-2-fluoro-β-*D*-ribo(arabino)furanosyl)adenine (**(73)** and **(74)**), 1-(2-deoxy-2-fluoro-β-*D*-ribo(arabino)furanosyl) thymine (**(75)** and **(76)**), and 9-(β-*D*- arabinofuranosyl)guanine **(21;** aG**)**. Incubation of the enzyme (2 microM) with arabinosyl nucleosides **(72)**, **(74),** or aG **(21)** (100 microM) at 25 °C for 20 min resulted in inhibition of transferase activity by 91, 72, and 21%, respectively; thymine nucleosides did not inhibit the enzyme. The inhibited enzyme contained stoichiometric amounts of covalently bound 2-deoxy-2-fluoro-*D*-arabinose, and its activity could be restored upon treatment with adenine, which simultaneously yielded adenine arabinoside **(72)**. Proteolysis of the inhibited enzyme yielded data that suggest that the γ-carboxylate of Glu-98 is esterified during catalysis (Scheme 14). Finally, a recombinant enzyme, in which the Glu-98 residue is replaced by alanine, showed a decrease in activity by 3 orders of magnitude as compared to the wild-type recombinant enzyme.

Later on, P.A. Kaminski obtained recombinant *L. helveticus* PDT and NDT and determined that the polypeptides

Scheme 14

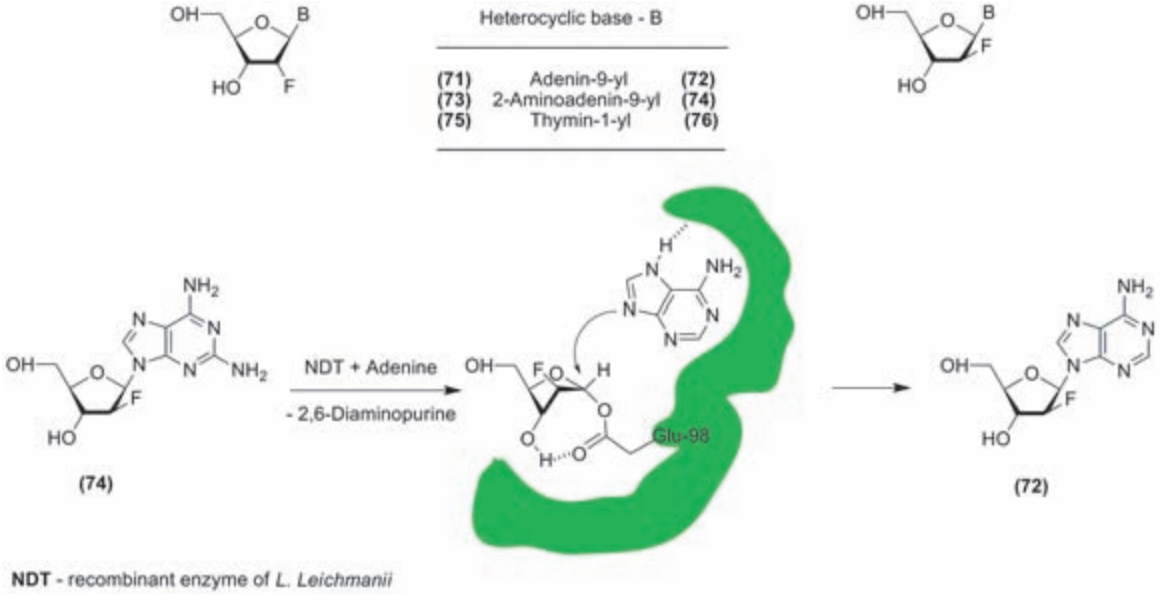

display 25.6% identity in the region involved in the binding of substrate to the Glu-98 residue of the enzyme's active site [109]. Both enzymes catalyzed the transformation of 2-aminopurine and 2,6-diaminopurine into the corresponding 2-deoxy-β-*D*-ribonucleosides at a rate comparable to that of natural purine bases. 4-Aminoimidazole-5-carboxamide (AICA) and imidazole-5-carboxamide (ICA) turned out to be poor substrates, and their trans-2-deoxyribosylation required large quantities of enzyme and extended incubation times. It is worth noting that the specific activity of PDT was higher than that of NDT in all four studied transglycosylation reactions (no experimental details were given).

The structure of the recombinant purine 2'-deoxyribosyltransferase of *L. helveticus* (PDT) was determined by X-ray crystallography [93], and the structure was found to be somewhat similar to that of NDT from *L. leichmanii* [105]. It was determined that, in the case of *L. helveticus* PDT, Glu-101 serves as the nucleophile in the active site, which attacks the glycoside carbon atom of the nucleoside, while the C3' oxygen atom of the furanose moiety forms a hydrogen bond with one of the oxygen atoms in the carboxogroup of Glu-101 (Scheme 12). Glycosylated PDT, which is formed after treatment with adenine arabinoside **(72),** contains a 2-deoxyfluoro-α-*D*-arabinofuranose residue covalently bound to one of the oxygen atoms of Glu-101. Comparison of the PDT-2'-deoxyadenosine and PDT-6-selenoinosine complex structures [105] allows to explain the specificity of the enzymes for 2'-deoxynucleosides: namely that the C2' and C3' oxygen atoms of the ribonucleoside are involved in the formation of a hydrogen bond with Glu-101, making the formation of an intermediate structure with a covalently bound carbohydrate residue impossible (Scheme 12).

Recently, a very interesting study aimed at creating NDT with improved activity in regard to the synthesis of 2',3'-dideoxy purine nucleosides was published by Kaminski and co-workers [110]. The authors constructed random mutant libraries of *ndt* genes from *L. leichmanii* (*Ll*) and *L. fermentum* (*Lf*) with a variable frequency of nucleotide substitutions (between 1 and 10 per sequence), developed a functional screening method, and selected the mutants, which were suited for the synthesis of 2',3'-dideoxynucleosides. Sequencing of the corresponding genes revealed a single mutation (G3A transition), which caused a small aliphatic amino acid to be replaced by a residue with a hydroxyl group, Ala-15 was substituted for Thr (*L. fermentum*) or Gly-9 for Ser (*L. leichmanii*), respectively. This single amino acid substitution was sufficient to enhance the substrate activity towards dideoxynucleosides. The authors concluded that the 2,3-dideoxyribosyl transfer activity requires an additional hydroxyl group at the 9th (*Ll*) or 15th (*Lf*) position, so as to overcome the absence of such a group in the corresponding substrate. Both artificial enzymes also displayed significantly improved transferase activity in regard to 2',3'-didehydro-2',3'-dideoxy-β-D-ribofuranosyl nucleosides. It was shown (without experimental details) that the *Lf*-NDT A15T enzyme catalyzed the synthesis of 2',3'-didehydro-2',3'-dideoxyadenosine and 2',3'-didehydro-2',3'-dideoxyinosine using 2',3'-didehydro-2',3'-dideoxyuridine (d4U) as a donor of the pentofuranose moiety at the mM scale and with a good yield (up to 70%) [110].

Comparison of transglycosylation reactions catalyzed by a crude enzyme (NDT) preparation from *L. helveticus* [111] and *E. coli* purine nucleoside phosphorylase (PNP; Sigma) yielded rather unexpected results [112, 113]. On the whole, it was shown that NDT-catalyzed reactions proceeded with higher regioselectivity as compared to those catalyzed by PNP, and the difference strongly depended on the structure of the acceptor-base (for details, see [24]).

N-deoxyribosyltransferses are not restricted to *Lactobacilli* and have also been isolated from the protozoan parasites *Critinia lucilliae* (see, *e.g.*, [109]) and *Trypanosoma brucei brucei* [114, 115]. The enzyme from *T. b. brucei* was purified over 400-fold to >95% homogeneity from the bloodstream form of this parasite, and its properties have been investigated [79]; a recombinant enzyme of the same origin was also prepared [80]. As opposed to *Lactobacilli* enzymes, the enzyme from *T. b. brucei* was found to be *N*-ribohydrolase with a preference towards inosine, adenosine, and guanosine as substrates. The k_{cat}/K_m values for the recombinant enzyme and inosine, adenosine, and guanosine as substrates were ($\times 10^6$ $M^{-1}\cdot s^{-1}$) 1.6, 1.4, and 0.7, respectively. Pyrimidine and 2'-deoxynucleosides were poor substrates with k_{cat}/K_m values approximately 10^3 $M^{-1}\cdot s^{-1}$ and 10^2 $M^{-1}\cdot s^{-1}$, respectively. 3-Deazaadenosine, 7-deazaadenosine (Tubercidin), and formicin B were found to be inhibitors with K_i values of 1.8, 59, and 13 microM respectively. To the best of our knowledge, this enzyme has not been used for the synthesis of nucleosides yet.

To sum up all of the above, we must note that chemo-enzymatic (biotechnological) strategies are currently displacing multi-stage chemical processes, and this allows key transformations to be achieved with high selectivity and regio- and stereospecificity. Considerable progress in the production of biologically important analogs of natural nucleosides has been achieved through the rational combination of chemical and biochemical transformations. Use of recombinant nucleoside phosphorylases and *N*-deoxyribosyl transferases as biocatalysts for the synthesis of natural nucleosides and their modified analogs is of considerable importance for the creation of modern technological processes. We must also note that the two enzymatic groups complement one another and allow finding out a straightforward way to the desired compound. The use of chemo-enzymatic methods undoubtedly allows improvement of the price-quality ratio during the production of many medical drugs.

NEW TRENDS IN BIOTECHNOLOGY OF NUCLEOSIDES

A number of studies published over the last decade give new impulse for the development of nucleoside biotechnology. Much attention is given to the use of α-*D*-pentafuranose-1-phosphates as substrates for the enzymatic synthesis of nucleosides. It must be noted that both the enzymatic and chemical syntheses of *D*-pentofuranose-1-phosphates have extensive histories (see [24]). However, only several recently published works are interesting from a practical point of view. There are two main lines of research in this field: (*i*) biochemical (microbiological, enzymatic) *retro*-synthesis of 2'-deoxyribonucleotides and (*ii*) chemical synthesis of *D*-pentofuranose-1-phosphates and their subsequent enzymatic condensation with heterocyclic bases.

Scheme 15

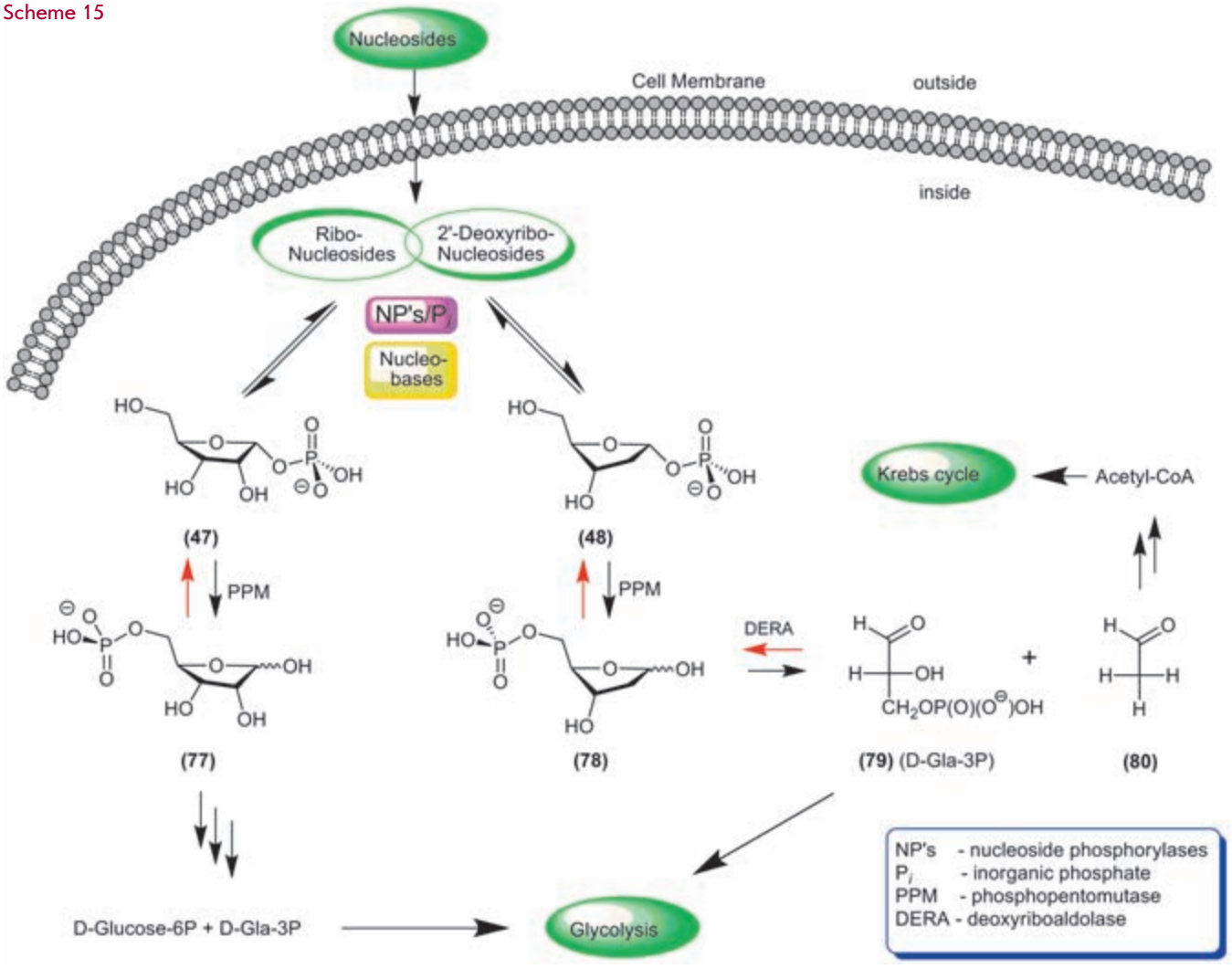

The metabolic transformations of pentoses have been investigated thoroughly (for a review, see, *e.g.*, [116]). Both in bacteria and eukaryotic cells nucleosides are regarded as carriers of carbohydrates, which serve as sources of carbon and energy. α-*D*-Ribofuranose-1-phosphate **(47)** is mainly produced from purine nucleosides via a process catalyzed by PNP. This phosphate is then involved in (*i*) glycolysis, (*ii*) metabolic activation of pyrimidine heterobases, which results in the formation of ribonucleosides (*e.g.* transformation of 5-fluorouracil into 5-fluorouridine catalyzed by UP), and (*iii*) an enzymatic transformation into 5-phospho-D-ribofuranose, catalyzed by phosphopentomutase (PPM). This process is usually in a state of enzymatic equilibrium, and the product of this reaction (5-phospho-D-ribofuranose) is a precursor of 5-phospho-α-*D*-ribofuranosyl-1-pyrophosphate (PRPP). The latter acts as a donor of the 5-phospho-*D*-ribofuranose moiety for both *de novo* and "salvage" synthesis of nucleosides. Catabolic transformations of 2'-deoxynucleosides also proceed under the control of nucleoside phosphorylases and PPM, and the resulting 2-deoxy-*D*-ribofuranose-5-phosphate **(78)** is then irreversibly metabolized into *D*-glyceraldehyde-3-phosphate (**(79)**; Gla-3P) and acetaldehyde **(80)** by bacterial or eukaryotic deoxyriboaldolases (Scheme 15).

The reversed *retro*-pathway for nucleoside synthesis beginning with Gla-3P and acetaldehyde was studied by J. Raap and co-workers [117, 118]. The authors described a one-pot two-step enzymatic reaction involving glycosylation of thymine or uracil (labeled by ^{13}C and ^{15}N atoms) using 2-deoxy-α-*D*-ribofuranose-1-phosphate (**(48)**; also ^{13}C-labeled at the different carbon atoms) and commercially available thymidine phosphorylase (TP). Synthesis of 1-phosphate (**48**) was performed using 2-deoxy-*D*-ribofuranose-5-phosphate (**78**) by stereospecific phosphate C5 → C1 translocation catalyzed by partially purified recombinant phosphopentomutase. The ^{13}C-labeled 5-phosphates were enzymatically prepared from chemically synthesized dihydroxyacetone monophosphate (**81**) in the presence of an excess of acetaldehyde using deoxyriboaldolase (DERA) and commercially available triose phosphate isomerase (TRI; from baker's yeast). The **(78)** → **(48)** transformation and condensation with thymine or ura-

Scheme 16

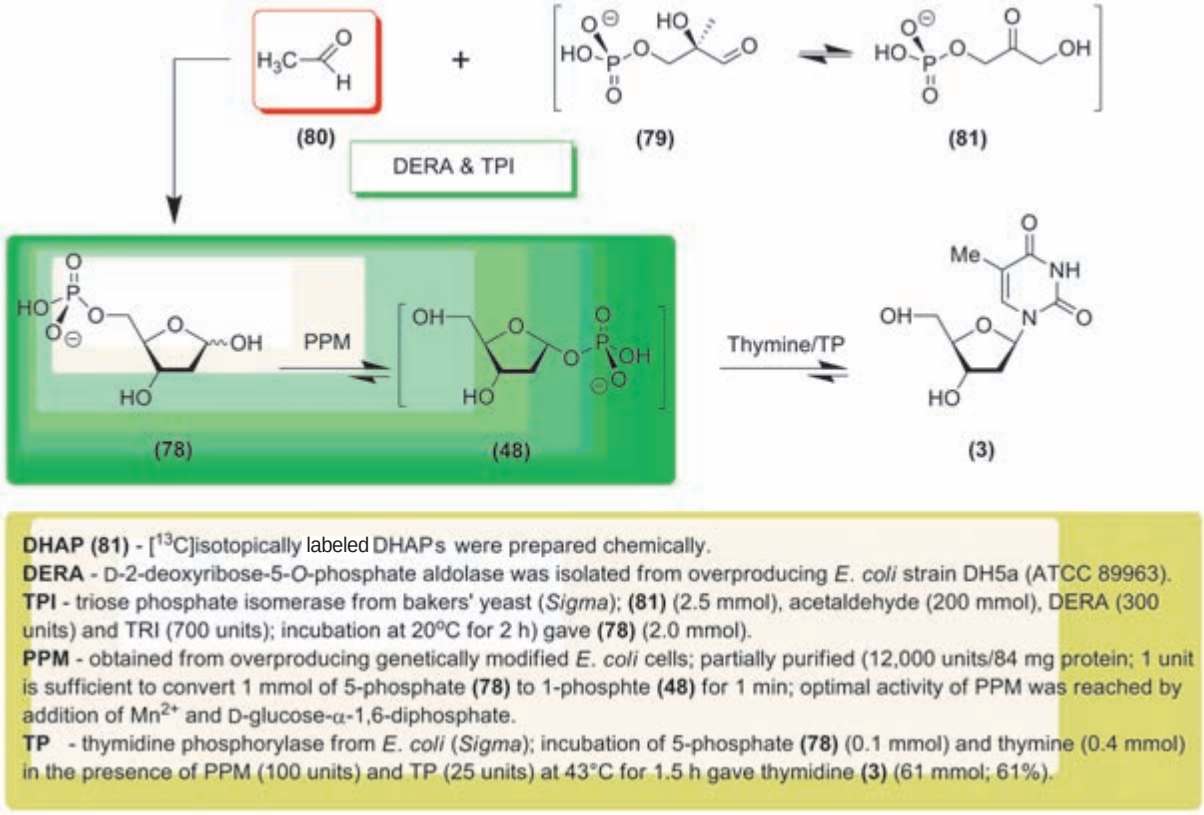

DHAP (81) - [^{13}C]isotopically labeled DHAPs were prepared chemically.
DERA - D-2-deoxyribose-5-O-phosphate aldolase was isolated from overproducing *E. coli* strain DH5a (ATCC 89963).
TPI - triose phosphate isomerase from bakers' yeast (*Sigma*); **(81)** (2.5 mmol), acetaldehyde (200 mmol), DERA (300 units) and TRI (700 units); incubation at 20°C for 2 h) gave **(78)** (2.0 mmol).
PPM - obtained from overproducing genetically modified *E. coli* cells; partially purified (12,000 units/84 mg protein; 1 unit is sufficient to convert 1 mmol of 5-phosphate **(78)** to 1-phosphte **(48)** for 1 min; optimal activity of PPM was reached by addition of Mn^{2+} and D-glucose-α-1,6-diphosphate.
TP - thymidine phosphorylase from *E. coli* (*Sigma*); incubation of 5-phosphate **(78)** (0.1 mmol) and thymine (0.4 mmol) in the presence of PPM (100 units) and TP (25 units) at 43°C for 1.5 h gave thymidine **(3)** (61 mmol; 61%).

cil were carried out in a one-pot system, and the respective 2'-deoxyribonucleosides were then isolated in yields of 50-60% (Scheme 16). It should be stressed that the great excess of acetaldehyde is necessary to prevent the cleavage of Gla-3P and to direct the metabolic reaction in the reverse synthetic direction.

A similar approach was used by J. Ogawa *et al.* for the synthesis of 2'-deoxynucleosides from acetaldehyde and dihydroxyacetone monophosphate through the intermediate formation of 5-phosphate **(78)** [119, 120]. The authors selected the *Klebsiella pneumoniae* B-4-4 strain for clones that could efficiently synthesize 5-phosphate **(78)**, which was then transformed into 1-phosphate **(48)** in the presence of transformed *E. coli* pTS17/BL21 cells, expressing *E. coli* PPM. The 1-phosphate (without any isolation procedures) was then condensed with adenine in the presence of commercially available PNP, which yielded a ~1:16 mixture of 2'-deoxyadenosine **(1)** and 2'-deoxyinosine **(82)**. Formation of the latter as the major product is due to the presence of adenosinedeaminase (ADA) in the *E. coli* pTS17/BL21 cells. This enzyme deaminates the initially formed 2'-deoxyadenosine (**1**). Notably, the *K. pneumoniae* B-4-4 strain tolerated high concentrations of acetaldehyde, which directs the reversible DERA-catalyzed reaction in the direction of 5-phosphate synthesis **(78)**.

Later on, Ogawa and co-workers combined the alcoholic fermentation system of baker's yeast and the DERA-expressing *E. coli* cells for the synthesis of 5-phosphate (**78**) [121 – 124]. The procedure for the synthesis of 2'-deoxyribonucleosides consisted of four steps: ***1*** – baker's yeast synthesize fructose-1,6-diphosphate (FDP) via alcoholic fermentation; ***2*** – the DERA expressing *E. coli* 10B5/pTS8 cells transform FDP into an equilibrated mixture of dihydroxyacetone monophosphate (**81**) and *D*-glyceraldehyde-3-phosphate (**79**); enzymatic condensation of (**79**) and acetaldehyde (the high concentration of acetaldehyde is necessary in order to prevent the reversed reaction!) produces 5-phosphate; ***3*** – the latter is transformed into 1-phosphate (**48**) under catalysis of PPM-expressing *E. coli* BL21/pTS17 cells; and finally step ***4***, accomplished in one pot in the presence of a heterocyclic base and commercially available purine nucleoside phosphorylase or thymidine phosphorylase, since the activity of both enzymes within the used *E. coli* cells was insufficient.

Synthesis of 2'-deoxyadenosine (**1**) was also accompanied by the formation of 2'-deoxyinosine (**82**). Xylene and polyoxyethylenelaurilamine were used in order to improve the permeability of the *E. coli* cells, which in turn improved the yield of 5-phosphate (**78**).

Notably, microbial synthesis [119 – 124] appears to be limited to the production of 2'-deoxy-β-*D*-ribonucleosides (isolation of individual products has not been published as of now). Also, satisfactory solubility of heterocyclic bases in the reaction mixture is an important prerequisite for successful nucleoside synthesis (for instance, low solubility of guanine makes synthesis of 2'-deoxyguanosine highly improbable). It is also important to bear in mind the off-pathway activities present in the employed cells, which can prevent efficient synthesis of the desired product.

The second line of research, chemo-enzymatic synthesis, involves chemical synthesis of α-*D*-pentofuranose-1-phosphates, which are then used for enzymatic condensation with heterocyclic bases. This line of research presents more

Scheme 17

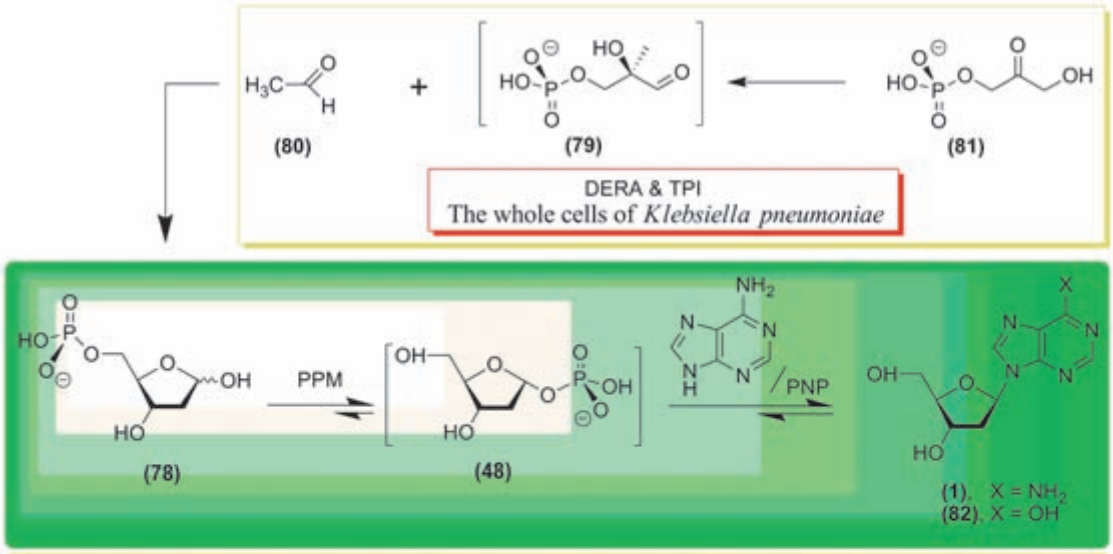

TPI & DERA - triose phosphate isomerase and D-2-deoxyribose-5-*O*-phosphate aldolase of the whole cells *Klebsiella pneumoniae* B-4-4; incubation of **(81)** (117 mmol) and **(80)** in the presence of washed cells (16.6% by weight) at 30°C for 2 h gave 5-phosphate **(78)** (84.3% calculated for **(81)** taken into the reaction)

PPM & PNP - an *E. coli* transformant, *E. coli* pTS17/BL 21, expressing *E. coli* phosphopentomutase and purine nucleoside phosphorylase (*Sigma*) (incubation of the resuted supernatant after centrifugation of the *Klebsiella pneumoniae* cells contained the 5-phosphate **(78)** or commercial **(78)** (*Sigma;* 25 mmol) and adenine (50 mmol) in NH_4Cl/NH_4OH buffer (150 mmol; pH 9.0) in the presence of washed *E. coli* pTS17/BL 21 cells, D-glucose 1,6-diphosphate (0.1 mmol), $MnCl_2$ (1 mmol) at 30°C for 3 h gave (HPLC) 2'-deoxyinosine (**(82)**, 9.7 mmol) and 2'-deoxyadenosine (**(1)**, 0.6 mmol); 2'-deoxyinosine **(82)** resulted from the primaraly formed 2'-deoxyadenosine **(1)** under the action of adenosine deaminase (ADA) that was present in the *E. coli* cells.

Scheme 18

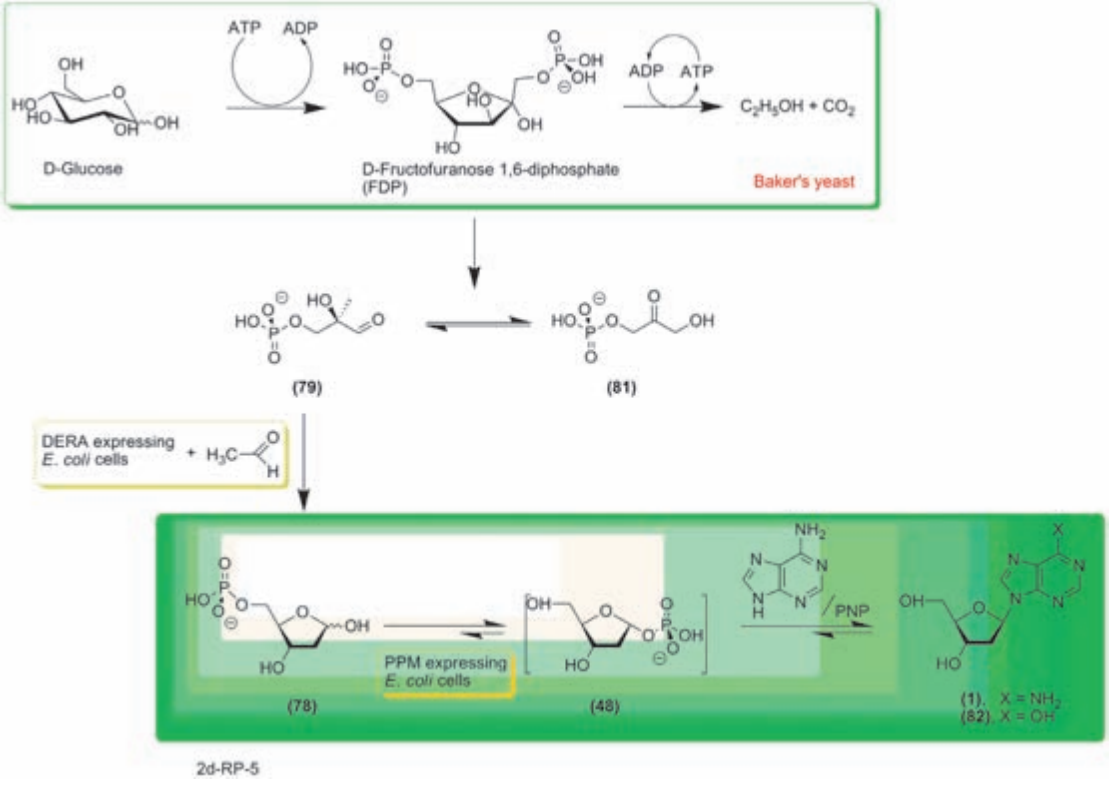

Scheme 19

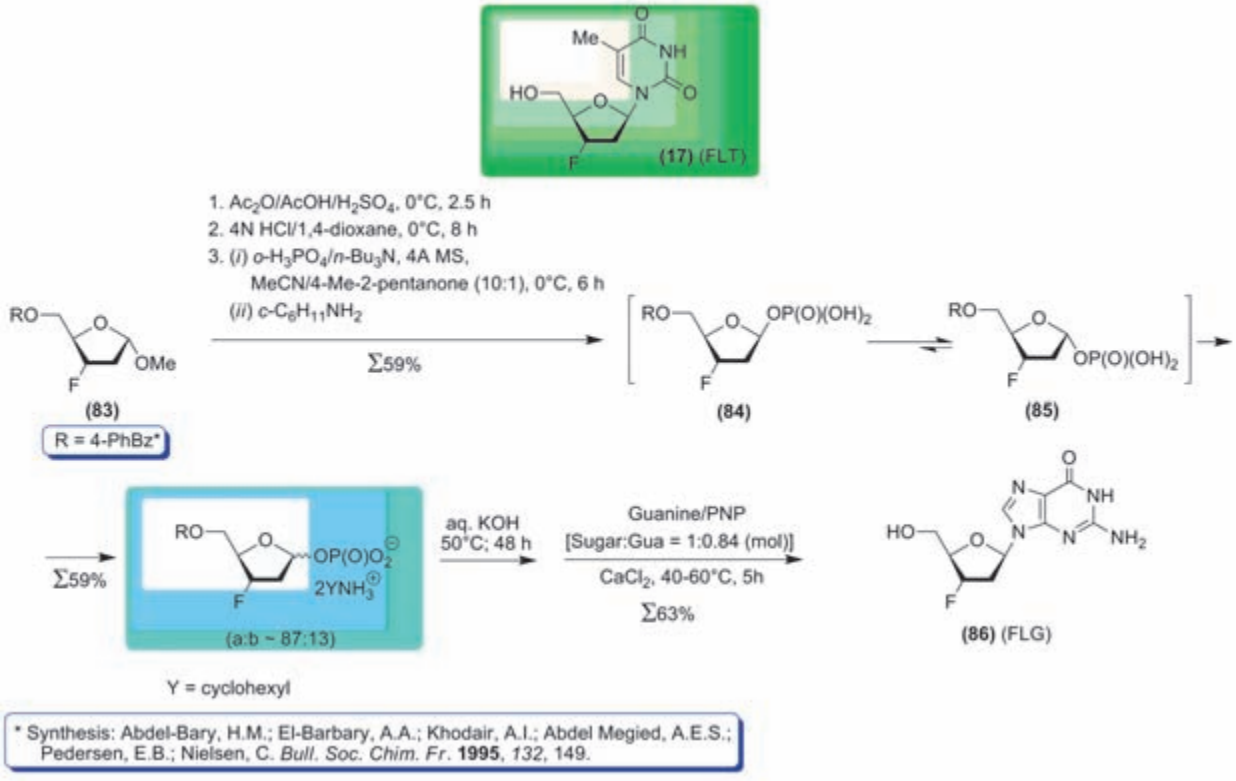

possibilities for variety and is promising for the synthesis of biologically important nucleosides and their analogs with modifications in the carbohydrate and base fragments. Indeed, α-*D*-pentofuranose-1-phosphates are universal glycosylation agents and can be used for the synthesis of both purine and pyrimidine nucleosides, as well as for reactions with any other type of heterocyclic base which can act as a substrate for nucleoside phophorylases.

The effectiveness of this strategy was demonstrated in a very convincing manner almost simultaneously with the discovery of nucleoside phosphorylases and *N*-deoxyribosyl transferases. In this context, we must also note the pioneering studies on phosphorolysis and resynthesis of purine 2'-deoxyribosides involving mammalian nucleoside phosphorylases [40–49], purification of 2'-deoxy-α-*D*-ribofuranose-1-phosphate (**48**) as crystalline cyclohexylammonium salt [24, 53], and the synthesis of thymidine and a number of 5'-modified pyrimidine 2'-deoxyribonucleotides [57, 58]. Further studies also managed to create procedures for the chemical synthesis of α- and β-anomers of *D*-ribofuranose-1-phosphate and 2-deoxy-*D*-ribofuranose-1-phosphate (see [24]).

A group of researchers from Mitsui Chemicals is also investigating the synthesis of nucleosides via condensation of α-*D*-pentofuranose-1-phosphates with heterobases using nucleoside phosphorylases [125–127]. First of all, they have developed "crystallization-induced asymmetric transformation" for the stereoselective synthesis of 2-deoxy-α-*D*-ribofuranose-1-phosphate (**48**) and its β-*D*-anomer [125, 126]. Both anomers have been isolated as pure stable bis(cyclohexylammonium) salts. It was also clearly shown that the former is a substrate for PNP, while the β-*D*-anomer did not show any substrate activity, as was expected. 2-Deoxy-α-*D*-ribofuranose-1-phosphate (**48**) was used for the synthesis of 2'-deoxy-2-chloroadenosine (Cladribine) via one-step condensation with 2-chloroadenine or via a two-step process involving the intermediary formation of 9-(2-deoxy-β-*D*-ribofuranosyl)-2,6-dichloroadenine [128]. This method was then successfully extended to the synthesis of 2,3-dideoxy-3-fluoro-5-*O*-[(4-phenyl)benzoyl]-*D*-ribofuranose-1-phosphate (in the form of a ≈ 87 : 13 mixture of the α- and β-anomers (**85)** and (**84**)) from methyl-2-deoxy-*D*-ribofuranoside (**83**), and the α-anomer from this mixture was then used as the main PNP substrate (after the removal of the 5-*O*-blocking group) for the synthesis of 2',3'-dideoxy-3'-fluoroguanosine (**86**) via enzymatic glycosylation of guanine (Scheme 19) [127, 129].

This study is of vast importance for further development of this field of research, since it gives a clear answer to the following question: if the potential carbohydrate-modified nucleoside donor shows extremely low substrate activity towards the relevant nucleoside phosphorylase (like FLT (**17**) towards TP and UP) does this mean that the corresponding α-*D*-pentofuranose-1-phosphate (such as 2,3-dideoxy-3-fluoro-α-*D*-ribofuranose-1-phosphate) will also be lacking in substrate activity towards the same nucleoside phosphorylase? It is known that a number of pyrimidine nucleosides, which are easily synthesized via chemical methods, cannot act as substrates for TP and/or UP and thus cannot be used as pentose donors. Chemical synthesis of the appropriate α-*D*-pentofuranose-1-phosphates and assaying of their substrate qualities is of vast interest. The study by H. Komatsu *et al.* [127] is very revealing and demonstrates the need for further studies in this direction.

Scheme 20

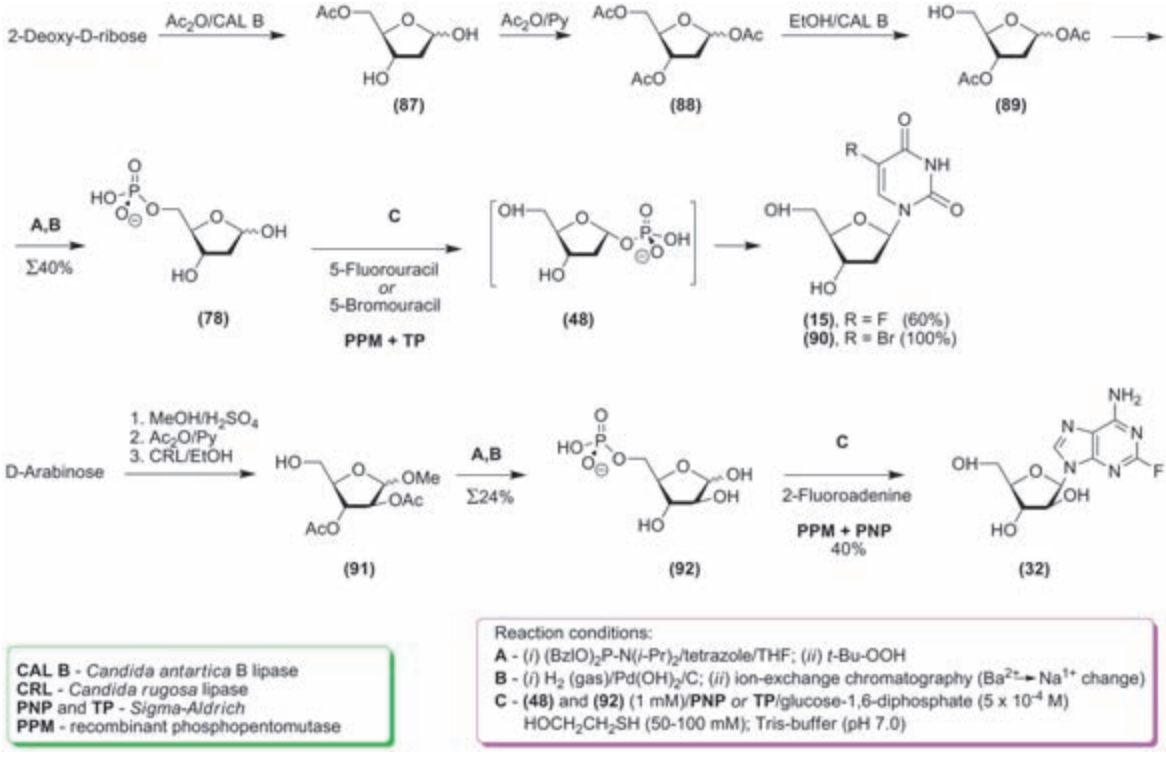

Recently, J.M. Montserrat *et al*. described a chemo-enzymatic approach to the nucleoside synthesis involving *D*-ribose, 2'-deoxy-*D*-ribose, and *D*-arabinose [130]. Pentoses were transformed into 5-phosphates (in the form of sodium salts) using chemical methods which sometimes utilized lypases for the introduction or removal of protective groups. The combined effect of PPM, which catalyzes the transformation of 5-phosphates into 1-phosphates, and condensation of the latter with heterobases in the presence of PNP or TP, leads to the formation of the appropriate nucleosides (*Scheme 20*).

The work of Montserrat *et al*. is very interesting as an example of rational chemo-enzymatic synthesis of *D*-pentofuranose-5-phosphates (compare the above work with [118, 119, 121–123]). We must of course note the universal approach to the synthesis of *D*-pentafuranose-5-phosphates, since the use of lypases for the regioselective introduction and removal of protective groups seems not to be limited to the studied pentoses.

The synthesis of 9-(2-deoxy-2-fluoro-β-*D*-arabinofuranosyl) purines described in the study by K. Yamada *et al*. is also of considerable interest [131, 132]. In this case, there are no easy and simple methods for the synthesis of the potential carbohydrate fragment donor, which is why the chemical synthesis of 2-deoxy-2-fluoro-α-*D*-arabinofuranose-1-phosphate (**96**) and its use as a universal glycosylation agent seems to be a reasonable alternative to the chemical glycosylation of heterobases (Scheme 21). Commercially available 1-*O*-acetyl-

Scheme 21

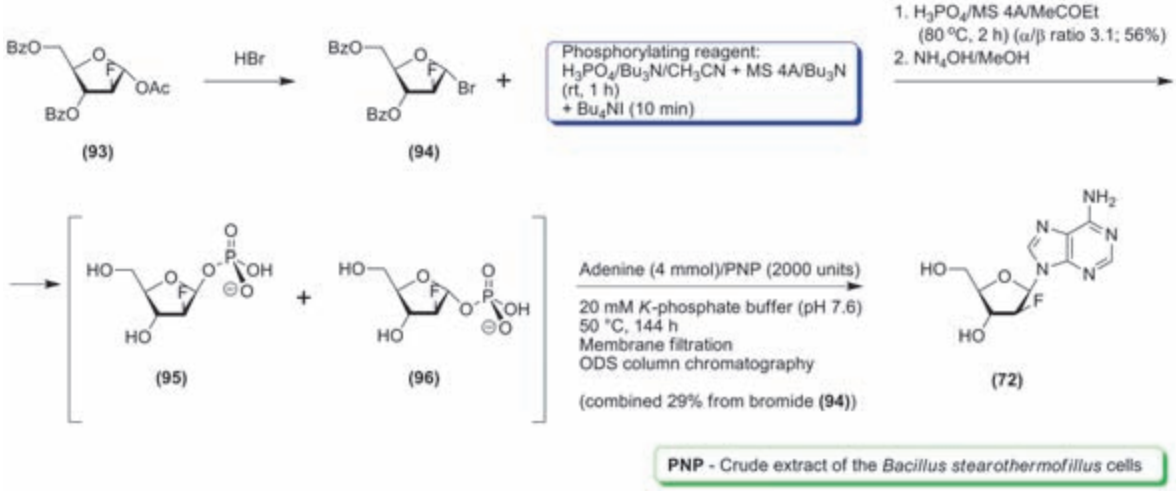

Scheme 22

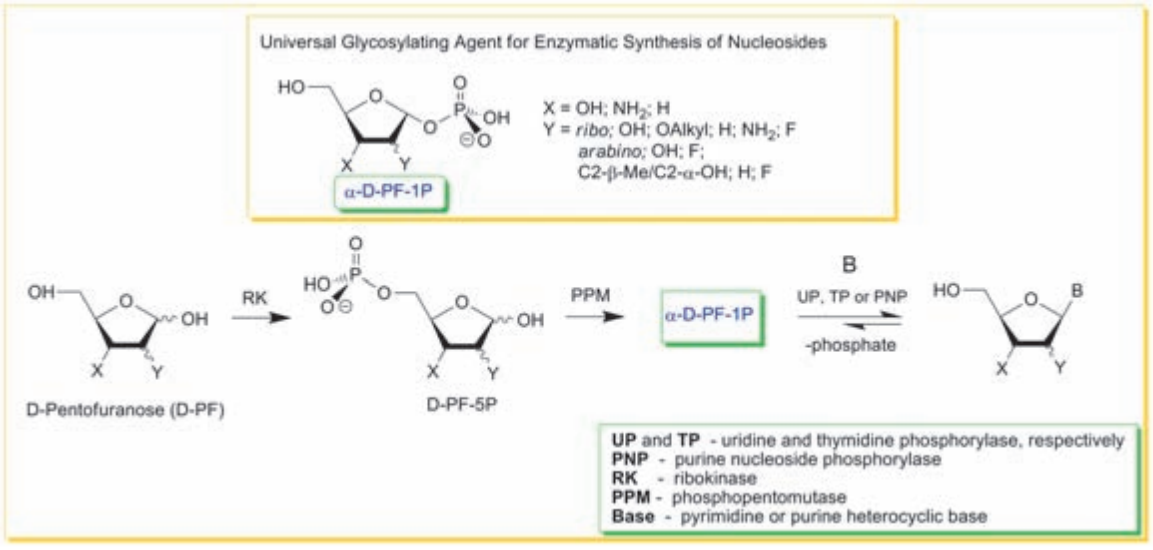

3,5-di-*O*-benzoyl-2-deoxy-2-fluoro-α-*D*-arabinofuranose was used as the initial compound (**93**), which was then transformed into a bromide (**94**) and then into a ≈3 : 1 mixture of α- and β-phosphates (**96**) and (**95**). This mixture was used for the synthesis of N^9-purine 2-deoxy-2-fluoro-β-*D*-arabinofuranosyl nucleosides without isolation of the individual α-anomer (**96**), and the results were satisfactory. We must note that in some cases chemical glycosylation results in the formation of an anomeric mixture (purines and pyrimidines) and regioisomers (purines) [11, 12].

An analysis of the above-mentioned results leads to the conclusion that the laborious and low-yielding preparation of α-*D*-pentofuranosylphosphates is a serious bottleneck of this approach. However, despite this downside, it is an approach to the synthesis of biologically valuable nuclosides that is undoubtedly worthy of further investigation and is a valuable addition to the chemo-enzymatic methods reviewed above.

We recently proposed a novel nucleoside synthesis strategy which consists of the sequential transformation of pentoses into nucleosides in the presence of heterobases. The process is catalyzed by recombinant *E. coli* enzymes, namely ribokinase (RK) (*D*-pentose → *D*-pentose-5-phosphate (*D*-PF-5*P*)), phosphopentomutase (*D*-PF-5*P* → α-*D*-pentofuranose-1-phosphate (*D*-PF-1*P*)), and nucleoside phosphorylases (NP) (*D*-PF-1*P* + heterobase → nucleoside) (Scheme 22) [133].

Production of recombinant RK, as well as that of uridine-, thymidine- and purine-nucleoside phosphorylases, was described in our previous work [134]. We observed that under optimal conditions RK can catalyze the phosphorylation of the primary hydroxyl group not only of *D*-ribose and 2-deoxy-*D*-ribose, but also of *D*-arabinose and *D*-xylose. These data suggest that RK may be used as a biocatalyst for the first step of the cascade transformation of pentoses into nucleosides. Stereospecific C5 →C1-translocation of phosphate by PPM is a reliable bridge within the proposed by us strategy of transformation of pentose into nucleoside, and this was the reason to produce recombinant PPM. The preliminary results of the transformation of *D*-ribose or 2-deoxy-*D*-ribose into pyrimidine and purine nucleosides using purified recombinant *E. coli* RK, PPM, and nucleoside phosphorylases were recently published (Scheme 23) [135].

An analysis of the optimal reaction conditions for RK [133], PPM, and NP [134] showed considerable differences. Bearing this in mind, compromise conditions were chosen for a one-pot cascade transformation of pentoses into nucleosides. These conditions allow for the satisfactory activity of all the used enzymes and are as follows: overall volume of the reaction mix 2 ml; contents of the buffering solution: 2 mM ATP, 50 mM KCl, 3 mM MnCl2, 20 mM Tris-HCl (pH 7.5), 2 mM pentose, 2 mM heterobase; reaction temperature 20 ˚C; and enzymes (in the appropriate units): RK 7.65; PPM 3.9; TP 4.5; UP 5.4; PNP 4.68. The results of the *D*-ribose and 2-deoxy-*D*-ribose transformation into pyrimidine and purine nucleosides are presented in Scheme 23 and Table 1.

Notably, inosine is formed at a faster rate compared to 2'-deoxyinsoine, and the maximum yield is achieved after 30 minutes. Also, the synthesis of purine deoxyribonucleotides was much more effective under transglycosilation conditions as compared to ribonucleside synthesis [82–84]. Obviously, the studied conditions for the cascade transformation of pen-

Table 1. Progress of nucleoside syntheses in cascade one-pot enzymatic reactions at 20°C [content of the corresponding nucleoside (%) in the reaction mixture *vs* time of reaction].

Time of Reaction, h	Inosine (Ino)	2'-Deoxy-inosine (dI)	Thymidine (Thd)/2'-Deoxyuridine (dU)[a]	1-(β-D-Ribofuranosyl)thymine (Rib-Thy)/ Uridine(Urd)[a]
0.5	45.9	18.8	14.5/0.9	4.7/27.6
1	46.1	27.3	17.6/1.1	8.5/26.6
24	38.4	38.3	-	-
44	-	-	34.7/33.2	19.9/17.5
96	29.4	34.4	-	-

[a] Thymidine (TP) and uridine (UP) phosphorylases were employed for the synthesis of thymine and uracil nucleosides, respectively.

Scheme 23

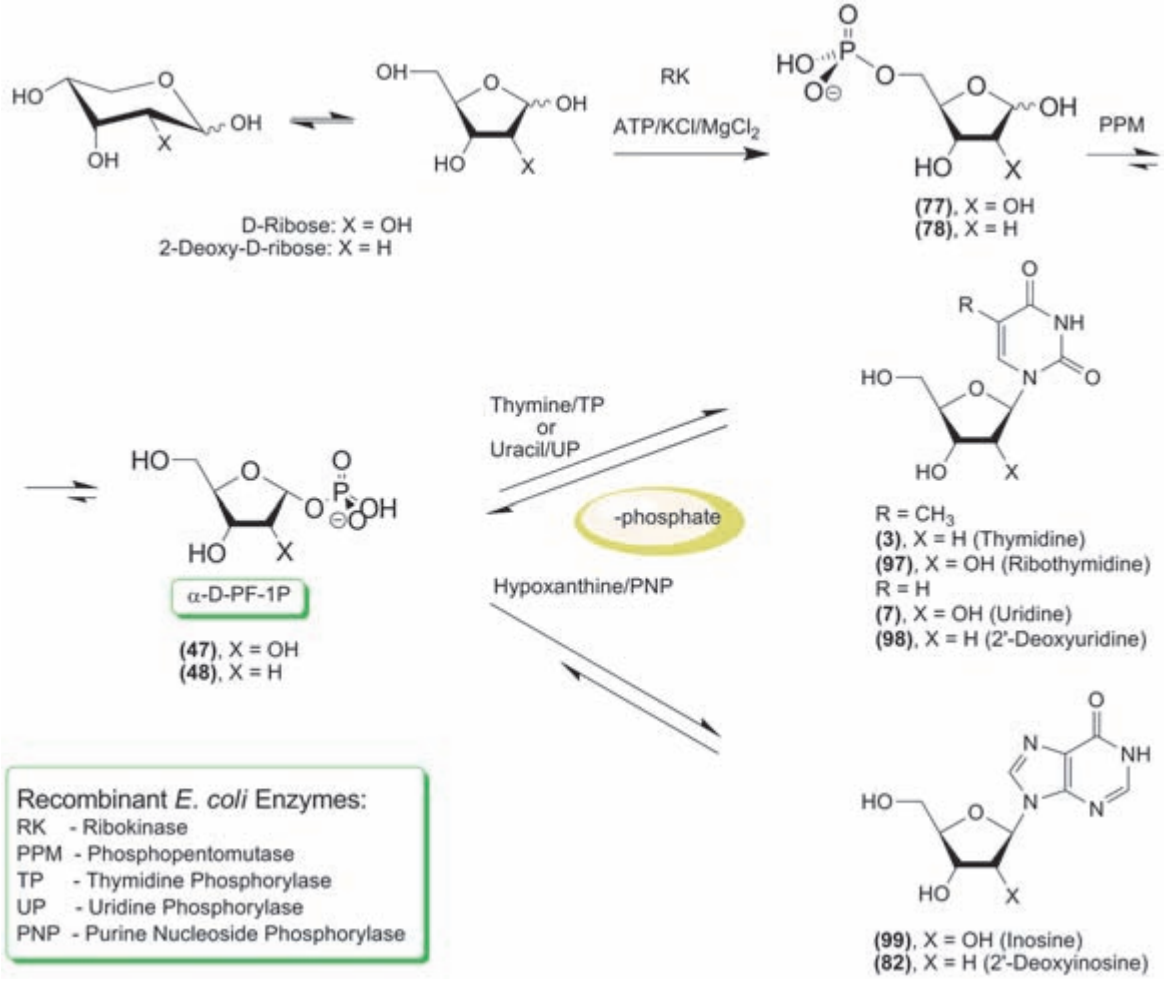

toses into nucleosides require thorough optimization for higher yields of the desired products. Showcase synthesis of Cladribine (**31**) shows that a 1.5 : 1 mixture of 2-deoxy-*D*-ribose and 2-chloroadenine (**100**) (mole/mole) substrates results in a product yield in excess of 90% (Scheme 24) [136].

As was noted earlier, chemical synthesis of α-*D*-pentofurnanose-1-phosphates is relatively complex, which means that these compounds will probably not gain widespread in for the production of preparative amounts of nucleosides. Preliminary results of the cascade transformation of pentoses into nucleosides using three enzymes indicate that this strategy is worth investigating further in terms of its limitations and possibilities for use.

A survey of the chemical methods for the production of pento(hexo)-furanose-1-phosphates [125–132, 137–147] and the methods of anomeric carbon atom activation (see [139]

Scheme 24

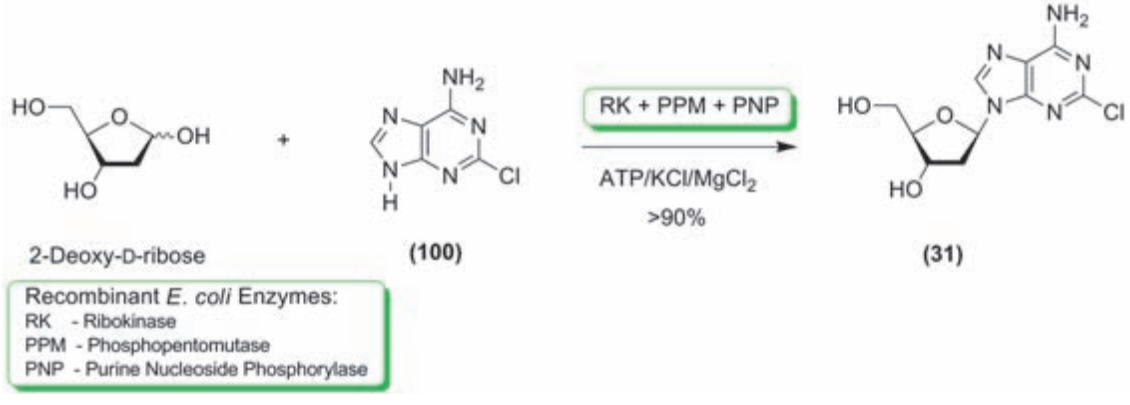

Scheme 25

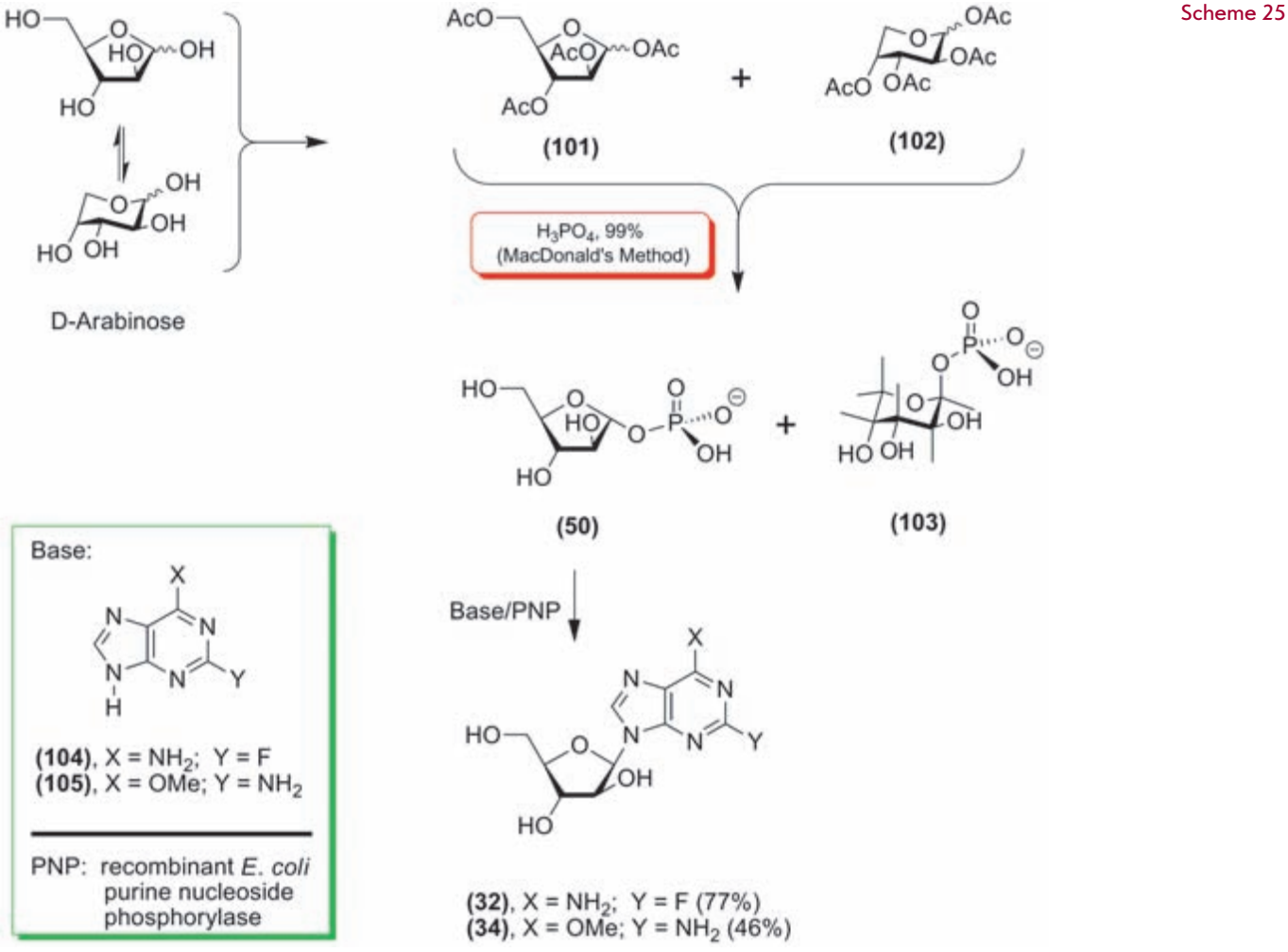

for a review) shows that most of these methods are laborious and low-yielding of the desired phosphates. As can be expected, most of the procedures yield mixtures of anomers, and it seems that only the "crystallization-induced asymmetrical transformation" preferably yields the desired 2-deoxy-α-*D*-pentofuranose-1-phosphates [85].

Because of its relative simplicity, the method proposed by *D.L. MacDonald* [140–144] seems to be the most effective, which is why we chose to use it for the synthesis of α-*D*-pentofuranose-1-phosphates. The method proposed by MacDonald is effective for the synthesis of hexopyranose-1-phosphates and was also used for the synthesis of α-*L*-arabinofuranose-1-phosphate in a study by G.O. Aspinall *et al.*: incubation of a peracetyl-derivative of *L*-arabinofuranose (mixture of α-, β-anomers) in anhydrous phosphoric acid and anhydrous THF at 50°C for 2 h yielded a mixture of *L*-arabinofuranose-1-phosphate (mostly α-*L*-anomer) and *L*-arabinopyranose-1-phosphate (both in the form of cyclohexylammonium salts) in an overall yield of 19% [147]. However, there were no conclusive physico-chemical data in support of the indicated structures.

Bearing in mind that a large number of purine and pyrimidine β-*D*-arabinofuranosides exhibit strong antiviral and antitumor activity (see above and also [18, 19, 148–150]), we chose the MacDonald approach for the synthesis of *D*-arabinofuranose-1-phosphate and used it for the synthesis of purine nucleosides.

A freshly prepared *D*-arabinose tetraacetate was a mixture of α-,β-anomers of furanose (**101**) and pyranose (**102**) forms (compare with [151]); treatment of this mixture according to the MacDonald method yielded an amorphous mixture of α-*D*-arabinofuranose-1-phosphate (**50**) and β-*D*-arabinopyranose-1-phosphate (**103**) (overall yield ≈ 50%; isomer ratio from 1.5 : 8 to 1 : 2, as assayed by ^{1}H-NMR). This mixture was tested in reactions with 2-fluoroadenine (**104**) and 2-amino-6-methoxypurine (**105**), catalyzed by recombinant *E. coli* PNP.

We observed that pyranose 1-phosphate (**102**) does not inhibit the synthesis of 9-(β-*D*-arabinofuranosyl)-2-fluoroadenine ((**32**); Fludarabine) under optimal conditions (water solution, pH 7.0, 55 °C; 1 hour). This procedure had a yield of 77% (Scheme 25) [152]. Unexpectedly, the rate of Fludarabine formation was similar to the rate of 2-fluoroadenosine synthesis from α-*D*-ribofurnaose-1-phosphate (Sigma) and 2-fluoroadenine (**104**) in the presence of recombinant PNP extracted from *E. coli*.

The high rate of Fludarabine formation was unexpected (compare with [130]). In chemical terms, the condensation of α-*D*-pentofuranose-1-phosphates with heterobases is the result of a nucleophilic attack of the heterobase nitrogen atom on the electrophilic anomeric carbon atom of the 1-phosphate. In order to asses the electrophilic properties of the C1-atom, we used an *ab initio* method for the geometry optimization of a number of related phosphate structures, namely α-*D*-ribofuranose-1-phosphates ((**47**); Rib*f*-α1*P*), α-*D*-2-deoxyribofuranose ((**48**); dRib*f*-α1*P*); and ((**50**) Ara*f*-α1*P*) (Table *2*).

It follows from the data in Table 2 that the positive partial charges of the C1-atoms of 2-*deoxyribo*- and *arabino*-phosphates are similar in value and are stronger than the charges of the *ribo*-isomer. The latter has the C-2 hydroxyl and phosphate group in *cis*-conformation and is more stable than the *arabino*-phosphate. The spatial structures of the *ribo*- and 2-*deoxyribo*-phosphates are more favorable for nucleophilic attack, and the C2-hydroxyl of the *arabino*-isomer does not create significant steric barriers for the approach of the base towards the C1-atom [152].

Differences in the partial positive charge of the C1-atoms of *ribo*- and *2-deoxyribo*-phosphates are confirmed by the fact that trans-*deoxyribo*sylation is more effective than trans-*ribo*sylation of deazapurines [24, 82] and benzimidazoles [24, 83, 84]. A similar substrate activity of Rib*f*-α1*P* and Ara*f*-α1*P* in a reaction with 2-fluoroadenine can seemingly be explained by two interacting factors: the high partial positive charge of the C1-atom of Ara*f*-α1*P*, on the one hand, and the negative steric effect of the C2-hydroxyl, on the other (compare this with data from [130]).

It shoud be noted that calculations indicate that both conformers of β-*D*-arabinopyranose-1-phosphate, namely $4C^1$ and $^4C_1$, have higher thermodynamic stability as compared to Ara*f*-α1*P*. These differences seem to account for the preferential formation of pyranose phosphate during the MacDonald reaction.

Unlike 2-fluoroadenine, a reaction between 2-amino-6-methoxypurine (**105**) and Ara*f*-α1*P* (in a mixture with Ara*p*-β1*P*) in the presence of recombinant *E. coli* PNP under conditions specified earlier reached equilibrium at an equimolar ratio between the initial heterobase and reaction product, 2-amino-9-(β-*D*-arabinofuranosyl)-6-methoxypurine ((**34**); Nelarabine), which could then be isolated in a yield of 44%. This result is in accordance with an earlier Nelarabine synthesis in a yield of 53% and involved the transarabinosylation of 2-amino-6-methoxypurine (**105**), using 1-(β-*D*-arabinofuranosyl)uracil (**49**) as a carbohydrate group donor and *E. coli* UP and PNP as biocatalysts [153].

We have observed earlier that trans-2-deoxyribosylation of N^2-acetylguanine with thymidine or 2'-deoxyguanosine as a carbohydrate group donor and TP/PNP or PNP as a biocatalyst initially leads to the formation of N^2-acetyl-7-(2-deoxy-β-*D*-ribofuranosyl)guanine, which eventually rearranges into the more thermodynamically stable N^2-acetyl-9-(2-deoxy-β-*D*-ribofuranosyl)guanine [76]. On the contrary, the Fludarabine and Nelarabine syntheses did not involve similar reaction stages [152]. This result allows us to hypothesize that the electron structure of the heterocyclic base determines the heterobase's mode of binding in the PNP active site, thus determining the regioselectivity of the enzymatic reaction.

Table 2. Results of the *ab initio* geometry optimization procedure (HyperChem, 8.1; *in vacuo*, 6-31G* level) for the spatial structures of α(β)-*D*-pentofuranose(pyranose)-1-phosphates (in mono sodium salt form).

Compound	Positive partial charge at the C1 carbon atom	Total (binding) energy kcal/mol	Conformation of the pento-furanose(pyranose) ring
(**47**); Rib*f*-α1*P*	0.425	-808 850.3	C1-*exo*
(**48**); dRib*f*-α1*P*	0.454	-762 140.7	C3-*endo*
(**50**); Ara*f*-α1*P*	0.464	-808 841.6	O4-*exo*
	0.410	-808 868.5	$_4C^1$ (more stable)
(**103**) Ara*p*-β1*P*	0.451	-808 856.8	$^4C_1$ (less stable)

CONCLUSION

An analysis of the results of the chemoenzymatic syntheses of nucleosides clearly indicates that this methodology is highly effective and very promising for the development of biotechnological processes for the production of biologically important compounds. Glycosylation of heterocyclic bases is catalyzed by two types of enzymes: nucleoside phosphorylases and *N*-deoxyribosyl transferases. These enzymes exhibit varying substrate specificities, which is why they mutually complement in terms of their use as biocatalysts.

Overall, all the above-mentioned results demonstrate the clear advantages of enzymatic methods for nucleoside synthesis as opposed to chemical methods. First of all, enzymatic methods fully conform to the principles of "green chemistry," since routinely they do not use aggressive reagents (apart from acetic aldehyde) or organic solvents. Secondly, the high effectiveness of enzymatic transformations and their stereo- (only β-*D*-nucleosides!) and regioselectivity (apart from some specific cases) simplify the production of the desired compounds and increase the product's quality. All of these factors lower the costs of production of biologically important compounds, making these compounds more available for researchers, and making drugs more available for widespread use. ●

The authors thank the International Scientific and Technology Center (ISTC, project № B-1640) for financial support of this study. I.A. Mikhailopulo thanks the Alexander von Humoboldt Foundation (Bonn, Bad-Godesberg, Germany) for their constant attention and partial financial support.

REFERENCES

1. Levene P.A., Tipson R.S. // J. Biol. Chem. 1935. V. 111 (2). P. 313–323.
2. Levene P.A., Mandel H. // Ber. Deutsch. Chem. Ges. 1908. V. 41 (2). P. 1905–1909.
3. Levene P.A., Jacobs W.A. // Ber. Deutsch. Chem. Ges. 1909. V. 42 (2). P. 2469–2473.
4. Levene P.A., Jacobs W.A. // Ber. Deutsch. Chem. Ges. 1909. V. 42 (2). P. 2474–2478.
5. Levene P.A., Jacobs W.A. //Ber. Deutsch. Chem. Ges. 1911. V. 44 (1). P. 746–753.
6. Levene P.A., London E.S. // J. Biol. Chem. 1929. V. 83 (2). P. 793–802.
7. Levene P.A., Mori T. // J. Biol. Chem. 1929. V. 83 (2). P. 803–816.
8. Fischer E., Helferich B. // Ber. Deutsch. Chem. Ges. 1914. V. 47 (1). P. 210–235.
9. Gulland J.M., Story L.F. // J. Chem. Soc. 1938. P. 259–261.
10. Michelson A.M. The chemistry of nucleosides and nucleotides. London: Acad. Press, 1963. 600 p.
11. Lukevics E., Zablocka A. Nucleoside Synthesis: Organosilicon Methods. Chichester: Ellis Horwood, 1991. 496 p.
12. Vorbrüggen H., Ruh-Pohlenz C. // Organic reactions / Eds Paquette L.A. et al. New York: Wiley, 2000. V. 55. P. 1–630.
13. Bardos Th.J. // Topics Curr. Chem. 1974. V. 52. P. 63–98.
14. Langen P. Antimetabolites of nucleic acid metabolism. New York: Gordon and Breach, 1975. 273 p.
15. Suhadolnik R.J. // Progr. Nucleic Acids Res. Mol. Biol. 1979. V. 22. P. 193–291.
16. De Clercq E. // J. Med Chem. 2010. V. 53 (4). P. 1438–1450.
17. De Clercq E. // Med. Res. Rev. 2009. V. 29 (4). P. 611–645.
18. Modified nucleosides in biochemistry, biotechnology and medicine / Ed. Herdewijn Piet. Wiley–VCH, 2008. 900 p.
19. Famulok M., Hartig J.S., Mayer G. // Chem Rev. 2007. V. 107. P. 3715–3743.
20. Elion G.B. // Science. 1989. V. 244. P. 41–46.
21. Gandhi V., Plunkett W. // Curr. Opinion Oncol. 2006. V. 18. P. 584–590.
22. Bonate P.L., Arthaud L., Cantrell, Jr., W.R., et al. // Nature Rev. Drug Discov. 2006. V. 5. P. 855–863.
23. De Clercq E. // Intern. J. Antimicrob. Agents. 2009. V. 33. P. 307–320.
24. Mikhailopulo I.A. // Current Org. Chem. 2007. V. 11. P. 317–335.
25. Montgomery J.A. // J. Med. Chem. 1980. V. 23 (10). P. 1063–1067.
26. Montgomery J.A. // Heterocycles. 1984. V. 21 (1). P. 137–150.
27. De Crercq E. // Nat. Rev. Drug Discov. 2002. V. 1. P. 13–25.
28. Ftorafur. An anticancer drug. (Pamphlet) / Compiled by Germane S., et al. Riga: Zinatne, 1979. 358 p.
29. Buie L.B., Epstein S.S., Lindley C.M. // Clin. Therapeutics. 2007. V. 29 (9). P. 1887–1899.
30. De Clercq E. // Nature Rev. Drug Discovery. 2007. *V.* 6. P. 1001–1018.
31. De Clercq E. // Antiviral Res. 2010. V. 85 (1). P. 19–24.
32. De Clercq E. // Adv. Virus Res. 2009. V. 73. P. 1–53.
33. Ferir G., Kaptein S., Neyts J., De Clercq E. // Rev. Med. Virol. 2008. V. 18. P. 19–34.
34. Vivet-Boudou V., Didierjean J., Isel C., Marquet R. // Cell. Mol. Life Sci. 2006. V. 63. P. 163–186.
35. Schaeffer H.J., Bhargava P.S. // Biochemistry. 1965. V. 4 (1). P. 71–76.
36. Schaeffer H.J., Vince R. // J. Med. Chem. 1965. V. 8 (1). P. 33–35.
37. Schaeffer H.J., Gurwara S., Vince R., Bittner S. // J. Med. Chem. 1971. V. 14 (4). P. 367–369.
38. Schaeffer H. J., Beauchamp L., de Miranda P., et al. // Nature. 1978. V. 272. P. 583–585.
39. De Clercq E., Holy A. // Nature Rev. Drug Discovery. 2005. V. 4. P. 928–940.
40. Levene P.A., Medigreceanu F. // J. Biol. Chem. 1911. V. 9 (3). P. 375–387.
41. Levene P.A., Medigreceanu F. // J. Biol. Chem. 1911. V. 9 (3). P. 389–402.
42. Levene P.A., Yamagawa M., Weber I. // J. Biol. Chem. 1924. V. 60 (3). P. 693–706.
43. Levene P.A., Weber I. // J. Biol. Chem. 1924. V. 60 (3). P. 707–715.
44. Levene P.A., Weber I. // J. Biol. Chem. 1924. V. 60 (3). P. 717–720.
45. Jones W. // J. Biol. Chem. 1911. V. 9 (2). P. 129–137.
46. Jones W. // J. Biol. Chem. 1911. V. 9 (2). P. 169–180.
47. Levene P.A., Yamagawa M., Weber I. // J. Biol. Chem. 1924. V. 60 (3). P. 693–706.
48. Levene P.A., Weber I. // J. Biol. Chem. 1924. V. 60 (3). P. 707–715.
49. Levene P.A., Weber I. // J. Biol. Chem. 1924. V. 60 (3). P. 717–720.
50. Bzowska A., Kulikowska E., Shugar D. // Pharm. Ther. 2000. V. 88. P. 349–425.
51. Kalckar H.M. // Federation Proc. 1945. V. 4. P. 248–250.
52. Kalckar H.M. // J. Biol. Chem. 1947. V. 167 (2). P. 477–486.
53. Manson L.A., Lampen J.O. // J. Biol. Chem. 1951. V. 193 (2). P. 539–547.
54. Araki T., Ikeda I., Matoishi K., et al. Eur. Pat. Appl. 2002, 32 p. CODEN: EPXXDW EP 1254959 A2 20021106 CAN 137:348820 AN 2002:847552 CAPLUS
55. Usowa E., Maltseva T., Földesi A., et al. // J. Mol. Biol. 2004. V. 344. P. 1347–1358.
56. Lewkowics E.S., Iribarren A.M. // Curr. Org. Chem. 2006. V. 10 (11). P. 1197–1215.
57. Friedkin M., Roberts D. // J. Biol. Chem. 1954. V. 207 (1). P. 245–256.
58. Friedkin M., Roberts D. // J. Biol. Chem. 1954. V. 207 (1). P. 257–266.
59. Duschinsky R., Pleven E., Rlalbica J., Heidelberger C. // Abstracts, 132nd National Meeting of the American Chemical Society. New York, 1957. P. 19–C.
60. Duschinsky R. US Patent 3,168,513 (1965).
61. Hoffer M., Duschinsky R., Fox J.J., Yung N. // J. Am. Chem. Soc. 1959. V. 81 (15). P. 4112–4113.
62. Hoffer M. // Chem. Ber. 1960. V. 93. P. 2777–2781.
63. Heidelberger C., Parsons D.G., Remy D.C. // J. Am. Chem. Soc. 1962. V. 84 (18). P. 3597–3598.
64. Heidelberger C., Parsons D.G., Remy D.C. // J. Med. Chem. 1964. V. 7. P. 1–5.
65. Friedkin M., Kalckar H.M. // The Enzymes, 2nd ed. / Eds Boyer P.D., Lardy H., Myrbäck K. New York: Acad. Press, 1961. V. 5. P. 237–255.
66. Heidelberger C., Ansfield F.J. // Cancer Res. 1963. V. 23. P. 1226–1243.
67. Heidelberger C. // Progr. Nucleic Acid. Res. Mol. Biol. 1965. V. 4. P. l–50.
68. Heidelberger C. // Annu. Rev. Biochem. 1975. V. 44. P. 79–121.
69. Kalinichenko E.N., Barai V.N., Bokut S.B., et al. // Biotechnol. Lett. 1989. V. 11. P. 621–626.
70. Tuttle J.V., Tisdale M., Krenitsky T.A. // J. Med. Chem. 1993. V. 36. P. 119–125.
71. Tuttle J.V., Krenitsky T.A. EP 0285432 B1 (Wellcome Found, GB), Publ. 1988–10–05.
72. Zinchenko A.I., Barai V.N., Bokut S.B., et al. // Appl. Microbiol. Biotechnol. 1990. V. 32. P. 658–661.
73. Zaitsewa G.V., Zinchenko A.I., Barai V.N., et al. // Nucleosides Nucleotides. 1999. V. 18. P. 687–688.
74. Zaitseva G.V., Kvasyuk E.I., Vaaks E.V., et al. // Nucleosides Nucleotides. 1994. V. 13. P. 819–834.
75. Esipov R.S., Gurevich A.I., Chuvikovsky D.V., et al. // Protein Expes. Purif. 2002. V. 24. P. 56–60.
76. Roivainen J., Elizarova T., Lapinjoki S., et al. // Nucleosides, Nucleotides, &.Nucleic Acids. 2007. V. 26. P. 905–909.
77. Bzowska A., Kulikowska E., Shugar D. // Z. Naturforsch. 1990. V. 45c. P. 59–70.
78. Koellner G., Bzowska A., Wielgus-Kutrowska B., et al. // J. Mol. Biol. 2002. V. 315. P. 351–371.
79. Krenitsky T.A., Rideout J.L., Koszalka G.W., et al. // J. Med. Chem. 1982. V. 25. P. 32–35.
80. Krenitsky T.A., Rideout J.L., Chao E.Y., et al. // J. Med. Chem. 1986. V. 29. P. 138–143.
81. Hennen W.J., Wong C.-H. // J. Org. Chem. 1989. V. 54. P. 4692–4695.

82. Mikhailopulo I.A., Zinchenko A.I., Bokut S.B., et al. // Biotechnol. Lett. 1992. V. 14 (10). P. 885–890.
83. Mikhailopulo I.A., Kazimierczuk Z., Zinchenko A.I., et al. // Nucleosides Nucleotides. 1995. V. 14 (3–5). P. 477–480.
84. Mikhailopulo I.A., Kazimierczuk Z., Zinchenko A.I., et al. // Nucl. Acids Symp. Ser. № 31. 1994. P. 83–84.
85. Doskocil J., Holy A. // Coll. Czech. Chem. Commun. 1977. V. 42. P. 370–383.
86. Rosemeyer H., Seela F. // J. Org. Chem. 1987. V. 52. P. 5136–5143.
87. Colacino J. M., DeLong D. C., Nelson J. R., et al. // Antimicrob. Agents Chemother. 1990. V. 34. P. 2156–2163.
88. Ehlhardt W.J., Wheeler W.J., Breau A.P., et al. // Drug Metabolism Disposition. 1993. V. 21. P. 162–170.
89. Hayden F.G., Tunkel A.R., Treanor J.J., et al. // Antimicrob. Agents. Chenther. 1994. V. 38. P. 1178–1181.
90. Ling F., Inoue Y., Kimura A. // Appl. Envirom. Microbiol. 1990. V. 56 (12). P. 3830–3834.
91. Shirae H., Yokozeki K. // Agric. Biol. Chem. 1991. V. 55 (7). P. 1849–1857.
92. Cardinaud R. // Methods Enzymol. 1978. V. 51. P. 446–455.
93. Anand R., Kaminski P.A., Ealick S.E. // Biochemistry. 2004. V. 43. P. 2384–2393.
94. McNutt W.S. // Biochem. J. 1952. V. 50. P. 384–397.
95. Roush A.H., Betz R.F. // J. Biol. Chem. 1958. V. 233. P. 261–266.
96. Beck W.S., Levin M. // J. Biol. Chem. 1963. V. 238. P. 702–709.
97. Holguin L., Cardinaud R. // Eur. J. Biochem. 1975. V. 54. P. 505–514.
98. Huang M.-C., Hatfield K., Roetker A.W., et al. // Biochem. Pharmacol. 1981. V. 30. P. 2663–2671.
99. Holguin L., Cardinaud R., Salemink C.A. // Eur. J. Biochem. 1975. V. 54. P. 515–520.
100. Carson D.A., Wasson D.B. // Biochem. Biophys. Res. Commun. 1988. V. 155. P. 829–834.
101. Cook W.J., Short S.A., Ealick S.E. // J. Biol. Chem. 1990. V. 265. P. 2682–2683.
102. Smar M., Short S.A., Wolfenden R. // Biochemistry. 1991. V. 30. P. 7908–7912.
103. Freeman G.A., Shaver S.R., Rideout J.L., Short S.A. // Bioorg. Med. Chem. 1995. V. 3. P. 447–458.
104. van Draanen N.A., Freeman G.A., Short S.A., et al. // J. Med. Chem. 1996. V. 39. P. 538–542.
105. Armstrong S.R., Cook W.J., Short S.A., Ealick S.E. // Structure. 1996. V. 4. P. 97–107.
106. Cheng J.C.-Y., Hacksell U., Daves G.D., Jr. // J. Org. Chem. 1985. V. 50 (15). P. 2778–2780.
107. Walker J.A., II, Chen J.J., Wise D.S., Townsend L.B. // J. Org. Chem. 1996. V. 61 (6). P. 2219–2221.
108. Porter D.J.T., Merrill B.M., Short S.A. // J. Biol. Chem. 1995. V. 270 (26). P. 15551–15556.
109. Kaminski P.A. // J. Biol. Chem. 2002. V. 277. P. 14400–14407.
110. Kaminski P.A., Dacher P., Dugue L., Pochet S. // J. Biol. Chem. 2008. V. 283. P. 20053–20059.
111. Uerkvitz W. // Eur. J. Biochem. 1971. V. 23. P. 387–395.
112. Chapeau M.-C., Marnett L.J. // Chem. Res. Toxicol. 1991. V. 4. P. 636–638.
113. Müller M., Hutchinson L.K., Guengerich F.P. // Chem. Res. Toxicol. 1996. V. 9. P. 1140–1144.
114. Parkin D.W. // J. Biol. Chem. 1996. V. 271 (6). P. 21713–21719.
115. Pelle R., Schramm V.L., Parkin D.W. // J. Biol. Chem. 1998. V. 273 (4). P. 2118–2126.
116. Tozzi M.G., Camici M., Mascia L., et al. // FEBS J. 2006. V. 273. P. 1089–1101.
117. Ouwerkerk N., van Boom J.H., Lugtenburg J., Raap J. // Eur. J. Org. Chem. 2000. V. 5. P. 861–866.
118. Ouwerkerk N., Steenweg M., De Ruijter M., et al. // J. Org. Chem. 2002. V. 67. P. 1480–1489.
119. Ogawa J., Saito K., Sakai T., et al. // Biosci. Biotechnol. Biochem. 2003. V. 67. P. 933–936.
120. Ishige T., Honda K., Shimizu S. // Curr. Opinion Chem. Biol. 2005. V. 9. P. 174–180.
121. Horinouchi N., Ogawa J., Kawano T., et al. // Appl. Microbiol. Biotechnol. 2006. V. 71. P. 615–621.
122. Horinouchi N., Ogawa J., Kawano T., et al. // Biosci. Biotechnol. Biochem. 2006. V. 70. P. 1371–1378.
123. Horinouchi N., Ogawa J., Kawano T., et al. // Biotechnol. Letters. 2006. V. 28. P. 877–881.
124. Horinouchi N., Kawano T., Sakai T., et al. // New Biotechnol. 2009. V. 26 (1/2). P. 75–82.
125. Komatsu H., Awano H., Tanikawa H., et al. // Nucleosides Nucleotides Nucl. Acids. 2001. V. 20. P. 1291–1293.
126. Komatsu H., Awano H. // J. Org. Chem. 2002. V. 67. P. 5419–5421.
127. Komatsu H., Awano H., Ishibashi H., et al. // Nucl. Acids Res. Suppl. № 3. 2003. P. 101–102.
128. Komatsu H., Araki T. // Nucleosides Nucleotides Nucl. Acids. 2005. V. 24 (5–7). P. 1127–1130.
129. Komatsu H., Araki T. // Tetrahedron Lett. 2003. V. 44. P. 2899–2901.
130. Taverna-Porro M., Bouvier L.A., Pereira C.A., et al. // Tetrahedron Lett. 2008. V. 49. P. 2642–2645.
131. Yamada K., Matsumoto N., Hayakawa H. // Nucl. Acids Symp. Ser. No. 48. 2004. P. 45–46.
132. Yamada K., Matsumoto N., Hayakawa H. // Nucleosides Nucleotides Nucl. Acids. 2009. V. 28. P. 1117–1130.
133. Chuvikovsky D.V., Esipov R.S., Skoblov Y.S., et al. // Bioorg. Med. Chem. 2006. V. 14. P. 6327–6332.
134. Esipov R.S., Gurevich A.I., Chuvikovsky D.V., et al. // Protein Expres. Purif. 2002. V. 24. P. 56–60.
135. Mikhailopulo I.A., Konstantinova I.D., Fateev I.V., et al. // The 2nd International Conference on Drug Discovery & Therapy: Abstracts. Dubai, 2010. P. 123. (ICDDT_AbstractBook.pdf, p. 123).
136. Miroshnikov A.I., Esipov R.S., Konstantinova, I.D., et al. // The Open Conference Proceedings Journal. 2010. V. 1. P. 98-102.
137. de Lederkremer R.M., Nahmad V.B., Varela O. // J. Org. Chem. 1994. V. 59. P. 690–692.
138. Euzen R., Ferrieres V., Plusquellec D. // J. Org. Chem. 2005. V. 70. P. 847–855.
139. Hanessian S., Lou B. // Chem. Rev. 2000. V. 100. P. 4443–4463.
140. MacDonald D.L. // J. Org. Chem. 1962. V. 27. P. 1107–1109.
141. MacDonald D.L. // Carbohyd. Res. 1966. V. 3. P. 117–120
142. MacDonald D.L. // Carbohyd. Res. 1968. V. 6. P. 376–381.
143. Mendicino J., Hanna R. // J. Biol. Chem. 1970. V. 245. P. 6113–6124.
144. Chittenden G.J.F. // Carbohyd. Res. 1972. V. 25. P. 35–41.
145. Wright R.S., Khorana H.G. // J. Am. Chem. Soc. 1958. V. 80. P. 1994–1998.
146. Maryanoff B.E., Reitz A.B., Nortey S.O. // Tetrahedron. 1988. V. 44. P. 3093–3106.
147. Aspinall G.O., Cottrell I.W., Matheson N.K. // Can. J. Biochem. 1972. V. 50. P. 574–580.
148. Larson R.A. // Seminar Oncol. 2007. V. 34 (Suppl. 5). P. S13–S20.
149. Gandhi V., Plunkett W. // Curr. Opinion Oncol. 2006. V. 18. P. 584–590.
150. Bonate P.L., Arthaud L., Cantrell, Jr., W.R., et al. // Nature Rev. Drug Discov. 2006. V. 5. P. 855–863.
151. Kobayashi M. // Tetrahedron. 2002. V. 58. P. 9365–9371.
152. Konstantinova I.D., Antonov K.V., Fateev I.V., et. al. // Int. Roundtable on Nucleosides, Nucleotides and Nucleic Acids. Lyon, 2010. P. 385-386.
153. Averett D.R., Koszalka G.W., Fyfe J.A., et al. // Antimicrob. Agents Chemother. 1991. V. 35. P. 851–857.

Skeletal Muscle Activity and the Fate of Myonuclei

B. S. Shenkman*, O. V.Turtikova, T. L. Nemirovskaya, A. I. Grigoriev
Institute for Biomedical Problems, Russian Academy of Sciences
*E-mail: shenkman@imbp.ru
Received 28.12.2009

ABSTRACT **Adult skeletal muscle fiber is a symplast multinuclear structure developed in ontogenesis by the fusion of the myoblasts (muscle progenitor cells). The nuclei of a muscle fiber (myonuclei) are those located at the periphery of fiber in the space between myofibrils and sarcolemma. In theory, a mass change in skeletal muscle during exercise or unloading may be associated with the altered myonuclear number, ratio of the transcription, and translation and proteolysis rates. Here we review the literature data related to the phenomenology and hypothetical mechanisms of the myonuclear number alterations during enhanced or reduced muscle contractile activity. In many cases (during severe muscle and systemic diseases and gravitational unloading), muscle atrophy is accompanied by a reduction in the amount of myonuclei. Such reduction is usually explained by the development of myonuclear apoptosis. A myonuclear number increase may be provided only by the satellite cell nuclei incorporation via cell fusion with the adjacent myofiber. It is believed that it is these cells which supply fiber with additional nuclei, providing postnatal growth, work hypertrophy, and repair processes. Here we discuss the possible mechanisms controlling satellite cell proliferation during exercise, functional unloading, and passive stretch.**
KEYWORDS **skeletal muscle, myonuclei apoptosis, physical training, working hypertrophy, satellite cells, growth factors, gravitational unloading, muscle stretch.**
ABBREVIATIONS **IGF – insulin-like growth factor, AIF – apoptosis-inducing factor, GFP – green fluorescent protein, BrdU – 5-bromo-2-deoxyuridine, CD34, 45, 54 - clusters of differentiation, c-Met – HGF receptor, HGF – hepatocyte growth factor, FGF fibroblast growth factor, MMPs – matrix metalloproteinases, MGF – mechano-growth factor.**

INTRODUCTION

Skeletal muscle is the most flexible structure in mammalian organisms. High muscle activity and load often lead to an increase in the transverse size (thickness) of the muscle, myofibrils volume, and contractile properties (strength and power). The stable pattern of gene expression underlies such transformation.

A chronic decrease in the functional load on the postural muscles, primarily soleus, under a prolonged change in the action of gravity forces (bed rest, support elimination from all or only hind limbs, or weightlessness) – so-called gravitational unloading – deeply transforms all the structural and functional muscle-tissue machinery [1–3]. One of the most important consequences of muscle transformation under hypogravity is the decrease in the contractile properties (power and working capacity), stiffness of muscle and myofibers, and a significant decline in myofibril and nuclei number, as well as in fiber size (atrophy). It also leads to an overgrowth of the connective tissue and extracellular structures and a shifting of the phenotype of myosin heavy chains towards an increase in the expression of the fast isoforms of the myosin heavy chains. The data obtained in the last years showed that the gravity-dependent transformation of soleus fibers is based on a stable directional change in the expression of a number of genes and the generation of a new integral (the so-called atrophic) expression pattern.

Adult muscle fiber is a symplast ,a multinuclear structure, developed in ontogenesis by the fusion of myoblasts (muscle progenitor cells). Nuclei are located at the periphery of muscle fiber in the space between myofibrils and the cell membrane (sarcolemma). Muscles contain also the nuclei of fibroblasts, endothelial cells, and precursor cells (satellite cells). Thus, in the literature, muscle fiber nuclei are usually called myonuclei. In theory, as a result of disuse or overload, the skeletal muscle mass can change, because of a change in the number of myonuclei or alterations in the rates of transcription, translation, and proteolysis. In this work we review data accumulated in the literature concerning the phenomenology and possible mechanisms of changes in the quantity of muscle fiber nuclei during increased or decreased contractile activity.

The muscle fiber nuclei are postmitotic and cannot divide. Myonuclei quantity is extremely important, since it determines the content of DNA for gene transcription [4]. The interaction between the fiber size and myonuclei number was taken as the basis in the myonuclear domain concept offered by Cheek *et al.* [5]. Myonuclear domain is the volume of muscle fiber cytoplasm regulated by the expression of the genes of one nucleus. The term “myonuclear domain” is quite convenient for describing the mechanisms of muscle plasticity, though it is nominal, and the protein distribution inside muscle fiber depends on many variable parameters. A lot of

studies have analyzed the cross-sectional area per one myonucleus, instead of the domain.

To reveal the myonuclei, DNA-specific dyes are used. The main problem for researchers of the nuclear pool of muscle fiber face is that, in an analysis of the muscle transverse sections without special techniques, it is impossible to distinguish the nuclei located on different sides of the muscle fiber boundary. To solve this problem, different approaches are used; in particular, the double labeling of nuclei and specific proteins of the subsarcolemmal layer, such as dystrophin [6]. Many authors have analyzed the nuclear composition of the isolated muscle fiber [7, 8]. To study an isolated fiber, which is a volumetric structure, a confocal laser microscope should be used. This approach has evident advantages: all of the myofiber nuclei pool can be analyzed (not only the nuclei observed at the cross section); also, the nuclei density distribution along the muscle fiber and its elementary unit, sarcomere, can be traced. However, the number of the fibers is limited in this case by 20–30 fibers per one biological sample.

Allen *et al.* have offered a hypothesis of myonuclear domain constancy during the size changes of the muscle fibers (atrophy and hypertrophy) [4]. The authors showed that the myonuclear domain size remains stable during the acute stage of hypertrophy. A proportional increase in the myonuclei quantity and cytoplasm volume was observed on a model of functional hypertrophy caused by the removal of synergistic muscles [9]. The same authors showed the variability of the myonuclear domain size during a chronic increase or decrease in loads in dogs [10] and under atrophy in rats [7]. Thus, the hypothesis of the myonuclear domain constancy turned out to be indefensible, and it has been further disproved in numerous studies of disuse and training [11–13, 8]. The myonuclear domain has been found to change throughout an animal's lifetime [14–16]. Recent studies by Italian authors have proved the possibility of hypertrophy development without new myonuclei incorporation; i.e., without a myonuclear domain increase under hypertrophy [11].

MYONUCLEAR NUMBER REDUCTION

In a number of cases (during severe muscle and systemic diseases and under gravitational unloading), muscle atrophy is accompanied by a decrease in the myonuclei number per myofiber, along with a corresponding development of apoptotic processes in the myonuclei. Such a reduction in the nuclei number was observed in cosmonauts' quadriceps [17] and rat soleus after space flight [10, 12], under simulated unloading in rats using the so-called hindlimb suspension technique [18, 19], and during soleus immobilization. Myonuclei loss is most intensive in slow fibers [19]. Studies of single fibers have demonstrated a decrease in the myonuclear domain size under disuse in rat soleus, but not in plantaris [12]. The myonuclear domain of rhesus monkeys also tends to decrease after 14 days in space flight [20]. Wang *et al.* showed a reduction of the cross sectional area, myonuclei number (25%), and nuclear domain size of soleus fibers after 16 days of rat hindlimb suspension [21].

Myonuclear number reduction is explained by the nuclei apoptosis in muscle fibers. Apoptotic processes in muscle fibers develop differently than those in other cell types. The changes in contractile activity lead to a weak manifestation of ultrastructural nuclei destruction. At the same time, DNA breaks in the nuclei are accompanied by a number of mitochondrial and extramitochondrial events which are supposed to be components of the interdependent signaling pathways, which cause the apoptotic processes.

Apoptotic nuclei have been observed in the muscle fibers of patients with Duchenne dystrophy (and in its biological model, mdx mice) [22], in fibers affected by chronic heart failure, the development of amyotrophic lateral sclerosis, and in some other cases. Myonuclei apoptosis was also observed after the application of a specific physical load (so-called eccentric exercise) [23]. In this case, muscle fiber strain develops when the fibers are stretched. Such muscle contraction causes numerous destructive changes in the cytoskeletal proteins and sarcolemma. In 1997, Allen *et al.* first reported the presence of apoptotic nuclei during rat hindlimb suspension [18]. The maximum number of apoptotic nuclei was observed in the soleus fibers (according to the TUNEL staining, revealing the DNA breaks) in the 2nd day of soleus disuse [24].

The same data were obtained in experiments on mice, where the maximum apoptosis-inducing factor (AIF) and p53 expression after 24 h of disuse were determined [25]. This was preceded by a marked increase in caspase-3 and caspase-8 after 12 h of suspension. An increased concentration of Bcl-2 was found as early as after 6 h of disuse. During hindlimb suspension for over 24 h, the observed apoptotic manifestations decreased. Soleus immobilization revealed similar dynamics [24]. Seven days of reloading after hindlimb suspension were enough to eliminate apoptosis [26]. Some authors were unable to find caspase cascade activation in soleus under hindlimb unloading or spinal isolation [27], but they observed endonuclease G translocation to the nucleus. Endonuclease G is the mitochondrial enzyme degrading nuclear DNA. Recently, a group of authors suspended animals under decreased temperature, which is supposed to slow down the mitochondria-dependent processes. In this case, apoptotic nuclei and significant caspase activation were also observed [28].

As was mentioned previously, a single exercise bout caused different apoptotic manifestations (DNA fragmentation, increased caspases activity, etc.); however, regular physical training not only decreased such apoptosis manifestations, but it also had an antiapoptotic effect that eliminated the nuclear changes that take place when muscle activity is reduced [18].

Unlike the other cell structures, in a skeletal muscle fiber apoptosis of the individual nuclei does not lead to immediate fiber death, though pathological consequences develop.

Recently, the Bruusgaard group [29] cast doubt on the complex of described observations of nuclear losses and apoptosis during atrophy. The authors studied mice transfected with the GFP-encoding plasmid. GFP was localized in the myonuclei, the quantity of which was analyzed under prolonged (14 days) denervation and disuse of extensor digitorum longus (caused by antagonists' tenotomy). The authors observed a significant decrease in the cross-sectional area of the muscle fibers, but no myonuclei decline. Fixed apoptotic changes were found in the satellite and connective tissue cells only; they were not revealed in muscle fibers. The same results were observed during the detraining of the Japanese quail wing: all the nuclei with apoptosis features were labeled

with bromdeoxyuridine (BrdU), the DNA synthesis indicator, which revealed the satellite cell nuclei [30]. At the same time, the conclusion made by Bruusgaard and Gundersen [29] was based on the denervation experiment and a study of the blockade of nerve impulse conduction to muscles predominantly with the fast fibers (those fibers undergo apoptosis less; see above). The authors dispelled any doubt about the data testifying to apoptosis and myonuclei number reduction using an animal microgravity model of antiorthostatic hindlimb suspension (and, consequently, the results of analogous experiments on volunteers; see above). They assumed that, in this case, systemic manifestations of gravitational unloading favored myonuclei apoptosis. Unfortunately, this hypothesis has no experimental support.

An increase in myonuclei in adult muscle fiber was observed during a power exercise, experimental working hypertrophy (during synergistic muscles dissection), and postatrophic reloading [26, 31–33]. The new nuclei in a fiber can be provided only by the fusion of satellite cells with the muscle fiber. The satellite cells are supposed to provide new nuclei for the muscle fiber during the postnatal period and for the local regeneration of the injured muscle fibers [34].

PRECURSOR CELLS IN SKELETAL MUSCLE. THE MARKERS OF THE MYOSATELLITE CELLS.

Satellite cells in a skeletal muscle are small mononucleate resting cells (remaining in the G_0 phase of the cell cycle) which proliferate and fuse with muscle fibers when activated, being an essential source of myonuclei during postembryonic development under tissue hypertrophy and recovery [12]. They can also fuse with each other, forming new muscle fibers [16]. Satellites may be myoblasts resting in the muscle tissue. According to another opinion, satellites are also believed to derive from some endothelial precursors associated with the embryonic vascular system. They can rest in the skeletal muscle interstitial space and express CD 34 [35]. However, skeletal muscle myogenic precursors are more numerous than satellite cells, because of the migration or recruitment of the undifferentiated stem cells from other sources. The precursor cell population from skeletal muscle was shown to originate from virgin mesenchymal stem cells of bone marrow and differs from satellite cells. Unlike satellites, precursor cells of the side population express Sca-1 (stem cell antigen-1) and CD-45. Evidently, they take part in injured or transplanted muscle regeneration and potentially form myocytes and myosatellite cells [36, 37]. Myosatellites can be identified in a muscle by their location (between the sarcolemma and fiber basal lamina) and by the immunohistochemical identification of different proteins expressed by these cells at different stages of their cell cycles. Desmin, myf5, and MyoD were found in the activated proliferating satellite cells, which normally express the regulatory muscle factors, such as Pax-7 and c-Met. Myogenin and MRF4 synthesis is characteristic of the final stage of differentiation [38]. c-Met, the HGF receptor, is expressed in skeletal muscle not only by satellites, but also by other myogenic precursor cells. Like resting cells, active and proliferating satellite cells usually synthesize such cell adhesion molecules as m-cadherin (Mcad) and NCAM (CD 56, Leu-19, neural cell adhesion molecule), which are located in the narrow space between the satellite cell and muscle fiber. NCAM is expressed in the activated satellite cells (myoblasts), in myotubes during muscle regeneration, and in neuromuscular junctions. Recent data showed that NCAM is the earliest marker of committed myoblasts; i.e., it determins their univocal transition from the proliferation to the differentiation phase [39].

The key molecule of the myogenic morphogenesis is Mcad. Using the combined labeling of Mcad, NCAM, laminin, desmin, and cell nuclei, Irintchev *et al.* [40] demonstrated that Mcad occurs in the satellite cells and myoblasts of normal and regenerating muscle. Simultaneous staining of the regenerating muscle with Mcad and BrdU led the authors to conclude that Mcad is expressed predominantly in mitotically inactive (resting) satellite cells. The myoblast fusion suppressed Mcad expression. NCAM and Mcad simultaneous expression is often observed in the muscles with an innervation failure [40]. As was shown later [41], skeletal muscle hypertrophy caused by overloading and the number of myosatellites expressing Mcad at the early stages of stimulus application increased, while at the later stages the number of cells positively stained against Mcad and NCAM rose. Thus, the Mcad staining was found in the resting myosatellites similarly as in the proliferation and differentiation stages.

MYOSATELLITE CELLS UNDER GRAVITATIONAL UNLOADING

Three days of hindlimb unloading lead to an irreversible transformation in the muscles of young rats. Therefore, the satellite cell number and their proliferative potential (according to the BrdU incorporation data) declined in soleus in the same way as in extensor digitorum longus. In this case, the program of muscle fiber development in growing animals can change irreversibly, leading to a failure of the myonuclei number increase even after reloading [42, 43]. Satellite cell mitotic activity decreased after 24 h of disuse and completely deceased 3–5 days later. The most pronounced decline was observed in soleus. Morphological atrophy features were revealed 48 h later [43]. The increase in the proliferative processes in mice gastrocnemius appeared after one week of hindlimb suspension [44]. The quantity of the resting and mitotically active satellites in muscle fiber fell by 57% when compared to the control group [29]. In the other work by the same authors, 3 months of unloading caused no decrease in the satellite cell quantity or muscle fiber length in young animals, but it led to an apoptosis-independent decrease in the satellite cell and myonuclei contents and a decrease in the satellite mitotic activity [45]. However, Ferreira *et al.* [44] observed unexpected proliferation reinforcement in mice gastrocnemius after one week of suspension.

POSSIBLE WAYS OF ACTIVATING MYOSATELLITES

Myosatellites are supposed to rest when skeletal muscle is not active. Their activation provides muscle mass maintenance, hypertrophy development, or the recovery of injured muscle. Myosatellite activation can also be caused by strengthening exercise [46, 47].

A significant increase in the total number of satellites was shown on several models of compensatory hypertrophy in animals, after eccentric exercise in humans [13, 48], and during muscle stretching [49]. Physical activity, such as resistive exercise or muscle functional overload (chronic stretch, syn-

ergistic muscle removal, and tenotomy), injures muscle tissue [50], stimulating muscle regeneration. Muscle damage causes an inflammatory response. Therefore, in the injured area, the number of neutrophils and macrophages increases. Then, the inflammatory infiltrate is released by immune cells, or the injured fibers release the growth factors regulating the proliferation and differentiation of myosatellites. Cytokines (IL-4, IL-6, IL-15, TNF-α etc.) were shown to affect the satellite cells *in vitro* and during the regeneration of injured muscle [51]. The role of the fibroblast growth factor (FGF) in myosatellite activation has been shown previously [52]. The hepatocyte growth factor (HGF) is supposed to be the key regulator of satellite cells activity during regeneration [18, 53] (Fig. 1). HGF was established to stimulate satellite cell activation in culture and *in vivo* during muscle stretch. HGF release is induced by nitric oxide (NO) synthesis, and it is regulated by matrix metalloproteinases (MMPs) [55]. HGF affects a satellite through its binding to the c-met receptor, stimulating further the signaling cascade, including the PI3K-Akt pathway, which stimulates cell survival and protection against apoptosis. The results of numerous experiments have shown the important role of the insulin-like growth factor in muscle hypertrophy development. In *in vivo* studies on animals, data were obtained demonstrating the role of an insulin-like growth factor (IGF) in the growth processes mediated by myosatellite activity [56, 57]. IGF can stimulate myosatellite proliferation and differentiation in culture [58]. Myosatellite cells of mice with IGF-1 gene overexpression possess increased proliferative potential, which can be due to the activation of a PI3K-Akt signaling pathway and the decline of the blocker of the cyclin-dependent kinase-2 [59], which is a result of FOXO transcription factor inhibition [57]. This is why the IGF-1-activated signaling pathways, which stimulate translation, are also supposed to be activated in myosatellite cells [60]. However, IGF-1EA (the growth factor form expressed in liver cells and skeletal muscle fibers which releases into the blood flow) is not the only IGF-1 gene product.

Physical training or mechanical muscle damage results in IGF-1 gene splicing, leading to the appearance of a splice-variant called the mechano-growth factor (MGF) after 1–2 days. During splicing, the translational frame shift occurs, resulting in a C-terminal sequence change. This leads to the appearance of the so-called E-domain, which differs from the other IGF-1 splice-variant sequences [61]. This unique C-terminal peptide functions as an autocrine growth factor with a short half-life. One of the functions of the peptide is to increase the precursor-cell pool in skeletal muscle (satellite cells) by initiating stem-cell proliferation, however, without myogenic differentiation. After initial splicing leading to MGF formation, the IGF-1 gene product undergoes further splicing, generating the IGF-1EA isoform. IGF-1EA is supposed to stimulate myosatellite differentiation and fusion with muscle fiber [38, 49, 62]. However, according to Wozniak *et al.* [38], only HGF and NO have been proven to activate resting myosatellites. IGF, FGF, and other growth factors were shown to effectively stimulate proliferation and growth following satellite activation. Some other growth factors (in particular, FGF) can also activate satellite cell proliferation [52]. Myosatellite cell activation can be suppressed by myostatin, which is supposed to maintain myosatellites at rest [63]. However,

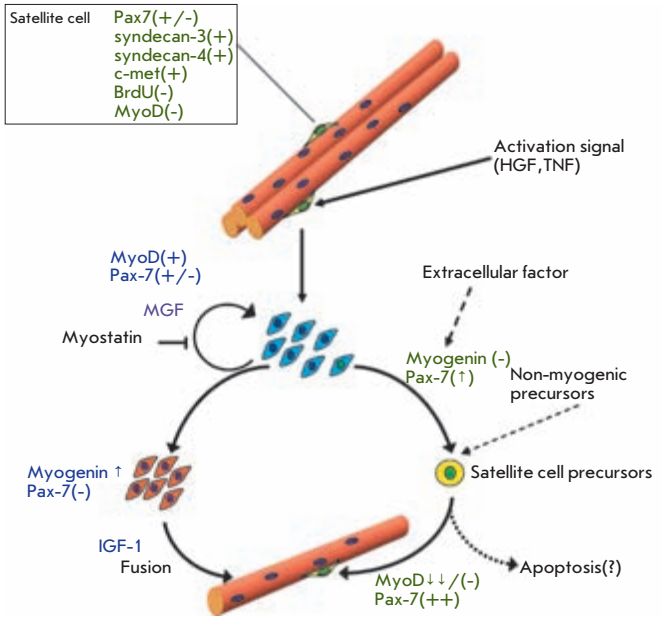

Fig. 1. The hypothetical role of IGF-1 and MGF in satellite cell physiology. Modified scheme of Olguin and Olwin, 2004 [54].

the mechanisms inducing satellite cell activation, proliferation, and their fusion with injured or growing muscle fibers remain poorly understood.

THE ROLE OF PRECURSOR CELLS IN MUSCLE GROWTH

Satellite cells possess high proliferative potential and are supposed to be important for skeletal muscle regeneration and hypertrophy. Different stimuli, such as functional overload during synergist removal, testosterone, clenbuterol, muscle stretch, and exercise can activate the satellites, stimulate their entry to the cell cycle and their proliferation in both fast and slow muscles. An increase in satellite proliferation was observed in the first days after stimulus application. Cramery *et al.* [46] and Kadi *et al.* [13, 31] showed that a series of intensive exercises stimulated an increase in the number of cells expressing NCAM. However, this and other studies did not show proliferating cells fusing with muscle fibers. The question of whether myosatellite nuclei incorporation into the fiber is necessary for muscle growth or mass maintenance remains unanswered. Different points of view exist. Many authors deny the necessity of incorporating myosatellite nuclei for muscle hypertrophy development [64], which has been proven by numerous studies with β2-adrenoceptor agonists application, leading to muscle hypertropy without an increase in DNA or the myonuclear number. According to Kadi *et al.* [13], muscle fiber size can change moderately without the incorporation of new myonuclei. As was shown earlier, the myonuclear number is not normally the determining factor for muscle fiber size; the myonuclear domain size varies during an animal's lifetime [16] and is unstable under muscle atrophy [65]. Despite the lack of dividing myosatellites after ionizing radiation treatment, Lowe [32]

observed hypertrophy of the stretched slow anterior latissimus dorsi of the Japanese quail. Dupont-Versteegden *et al.* [66] showed that in spinalized animals, after myosatellite activation (during resistive exercise), the latter did not fuse with the muscle fibers. Thus, training did not promote the maintenance of the myonuclear number in the soleus of spinal animals. The number of activated myosatellites was higher than that of divided ones. The physiological role of activation of such a huge number of myosatellites without their incorporation into the growing muscle fibers is unclear. Recently, Italian researchers showed that proteinkinase B activation for 3 weeks caused muscle hypertrophy and a doubling of muscle weight, which was not accompanied by satellite activation or the incorporation of new nuclei [11].

The possibility of muscle fiber growth without incorporation of satellite cells, which is one of the ways protein synthesis intensifies, can be due to an increase in DNA matrices because of the incorporation of myosatellite nuclei into the fiber. The supporters of the concept of myonuclear domain constancy theorize that the initial stages of muscle growth are linked with transcription and translation intensification until the myonuclear domain reaches a definite threshold. However, it was established that moderate hypertrophy in human muscles can happen without additional genetic material [13]; from the point of view of the concept mentioned above, this can be explained by the existence of a hypertrophy threshold sensitive to the new nuclei incorporation. Thus, at later stages, the incorporation of new myosatellite nuclei is obligatory for maintaining muscle fiber hypertrophy and the nuclear domain size [9, 33, 64]. The necessity of myosatellites for muscle hypertrophy development was first shown by Rosenblatt *et al.* [9], who observed a decrease in hypertrophy under functional overload after averting satellite proliferation by γ-irradiation. The authors determined that satellite cell death under the irradiation and obviation of their nuclei's incorporation into muscle fibers can completely neutralize the hypertrophy of rat extensor digitorum longus, soleus, and plantaris caused by the removal of synergistic muscles and physical training [67]. Mitchell and Pavlath [33] showed that, after rat hindlimb suspension and irradiation, the prevention of myosatellite proliferation muscle recovery was normal only at the stage where new myonuclei were not necessary, but then the process slowed. Kawano *et al.* [45] showed that, during 3 months of reloading young animals suspended for 3 months, the fiber cross-sectional area did not differ from that of the control animals, while the satellites and myonuclei number increased. The authors concluded that satellite cells were important for soleus growth processes [45]. As was shown earlier, the proliferation, differentiation, and fusion of myosatellites with muscle fibers are induced by growth factor IGF-1 [68]. In the muscle fiber culture, IGF-1 caused myosatellite fusion resulting in hypertrophy [62]. The IGF-1-stimulated hypertrophy was accompanied by an increase in DNA content in the muscle fibers and the appearance of new myonuclei [69]. The irradiation was shown to decrease the hypertrophy of the extensor digitorum longus caused by the intramuscular IGF-1 incorporation twice, inasmuch as in hypertropy induced by the incorporation of myosatellites nuclei into the muscle fibers [70]. These data showed that the loading-stimulated increase in the IGF-1 level can cause hypertrophy, particularly due to the stimulation of myosatellites proliferation and fusion with the maternal fiber.

Data has appeared recently showing that the myosatellite nuclei can incorporate into a fiber under low-intensity chronic training: during low-frequency chronic electro stimulation and voluntary animal activity ("voluntary wheel") [71]. Such a regime of contractile activity usually does not lead to working hypertrophy. However, myosin phenotype actively shifts to the slow direction. As was shown previously [72], an increase in the slow fiber number during the slow-frequency stimulation of rat fast muscles cannot be explained by the change in the myosin isoforms expression inside a fiber. The suppression of myosatellites multiplication prevented by irradiation was established recently to prevent the transformation of fibers to the slow type during low-frequency chronic stimulation [73]. It is of interest that pharmacological stimulation of PPARβ (peroxisome proliferator-activated receptor β) is one of the components of the signaling system switching myosin isoform expression to the slow type in the myonuclei and favors myosatellite fusion with a muscle fiber [74].

Thus, the incorporation of myosatellite nuclei (evidently with a slow pattern of myosin isoform expression) into muscle fiber during prolonged low-frequency stimulation leads to myosin phenotype adaptive changes in the skeletal muscle.

MYOSATELLITE CELLS OF SKELETAL MUSCLE DURING STRETCH AND STRETCH COMBINED WITH DISUSE

Gravitational unloading is a particular type of muscle contractile activity reduction. A sharp decrease in the electric activity of soleus (to the zero level) is observed, as a rule, immediately after support elimination and continues for 2–3 days of disuse. Then electric activity begins its restoration slowly and reaches the control level by the 14th day of real or simulated microgravity [75]. However, gradually increased muscle activity does not prevent muscle atrophy development. Evidently, the decreased contractile activity has an affect alongside with the the significantly declined (to zero under microgravity) resistance to muscle contraction (weight bearing), which has a significant influence on atrophy development [76]. One approach to studying this factor is chronic or repeated passive stretch of the muscle. This stretch compensates for the lack of gravity loading and certainly prevents the development of muscle regeneration [77].

The interrelation between stretch and myosatellite activation in culture was demonstrated in the experiments conducted by Tatsumi *et al.* [78]. Resting satellite cells under periodic stretch activated and entered the cell cycle, probably being stimulated by HGF synthesis in the stretched cells. The same authors showed that, during a short stretch (1 h) combined with the hindlimb suspension of rats, mechanical stretch caused nitric oxide (NO) synthesis. The latter induced HGF linked with the muscle fiber surface. HGF binds the c-Met-receptor of the myosatellite cells, leading to their activation. On the other hand, data exist indicating that, during compensatory hypertrophy caused by the synergistic-muscle removal, myonuclei activation can occur independently from the NOS inhibitor [79]. In the model of Wozniak *et al.* [38], isolated muscle stretch, such as during a single fibers stretch, activated myosatellites, which were determined by BrdU incorporation into the dividing cell nuclei. In our study, 3 days of simulated

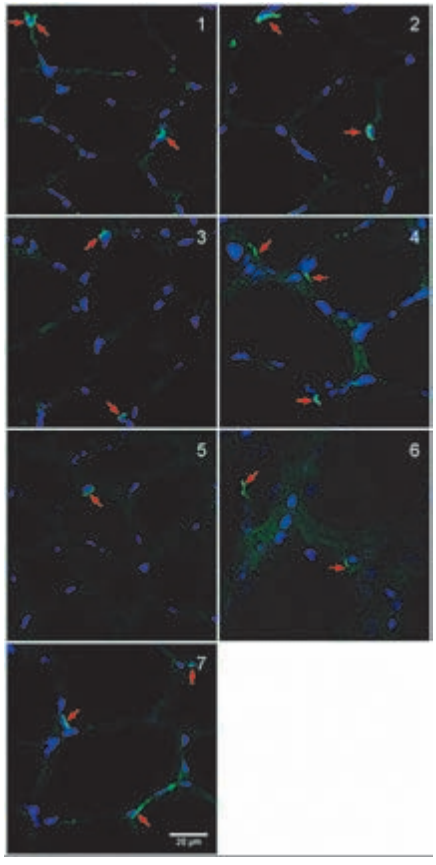

Fig. 2. Satellite cells in rat m.soleus transverse section. M-cadherin staining. (1) "Hindlimb suspension 3 days," (2) "Hindlimb suspension + stretch 3 days," (3) "Hindlimb suspension 7 days", (4) "Hindlimb suspension + stretch 7 days", (5) "Hindlimb suspension 14 days", (6) "Hindlimb suspension + stretch 14 days", (7) Control.

gravitational unloading (hindlimb suspension model) caused no change in the satellite cells expressing m-cadherin in rat soleus, while 7 and 14 days of disuse caused a 30 and 50% decrease in the number of myosatellites, correspondingly, as compared to the control. Passive soleus stretch combined with gravitational unloading made it possible to maintain the amount of satellites 30% higher than in the control at the 3rd and 7th days of disuse, and at the control level until the 14th day of unloading (Fig. 2). We surmised that, after the elimination of the proliferative potential of precursor cells by γ-irradiation, muscle fibers partially lose their ability to maintain fiber size during stretch combined with disuse. A study of local irradiation of a rat shin with a dosage of 2500 rad followed by hindlimb suspension or suspension combined with stretch showed that irradiation did not influence the countermeasure effect of passive stretch (atrophy prevention, fibers transformation, and myonuclei number decrease), which was observed under suspension [80]. Recent *in vivo* experiments demonstrated that L-arginine (NO donor) administration under disuse decreased muscle atrophy and maintained the number of myonuclei and myosatellites at the control level. Moreover, NO-synthetase inhibitor, L-NAME, significantly decreased myosatellite proliferation during stretch combined with animal hindlimb suspension. Thus, one can assume that, in the studied model, NO significantly influences myosatellites proliferation. However, an administration of NO-synthetase blocker did not affect the efficiency of maintaining muscle mass during the stretch (see the significance of myosatellite proliferation during hypertrophy above) [81].

Myotube stretch in culture leads to the release of other endocrine factors, including IGF. The studies conducted by the Goldspink laboratory [49, 61] showed that, during stretch combined with the electro stimulation of the tibialis anterior and during mechanical injury, myosatellite activation occurred along with IGF-1 mRNA expression. The authors linked the resting myosatellite activation and proliferation during muscle stretch to the expression of MGF (the maximal expression of the splice-variant MGF was observed in the first 4 days after the stretch), while their differentiation and fusion with the muscle fibers depended on the subsequent IGF-1Ea (5–12 days after applying the stretch) [49].

Interestingly, in our studies IGF-1 expression stimulation was observed only on the 7th day of stretch combined with gravitational unloading, while the myosatellite-cell number increased on the 3rd day. The proliferation of these cells during stretch combined with disuse can probably be explained by the earlier MGF expression. Further studies should shed more light on the question.

Thus, we can assume that myosatellite proliferation during stretch combined with gravitational unloading, which is stimulated by different mechanisms, is unnecessary for preventing the atrophy of muscle fibers. The myonuclear number is probably maintained in this case due to the antiapoptotic effect of the stretch. However, the concomitant myosatellite activation prevents a decrease in the muscle-regeneration potential.

Therefore, in this review we have discussed one of the most controversial issues surrounding skeletal muscle plasticity: the effect of the contractile activity on the myonuclear pool. The perspectives of pharmacological and gene-therapeutic regulation of myonuclei apoptosis and myosatellite activity are also of importance. NO donors and the recombinant analogues of the growth factors as countermeasures to the atrophy changes in skeletal muscle during posthypokinetic recovery and the rehabilitation of injured athletes need further study. ●

This work was supported by RFBR grants 07-04-00763, 08-04-01557, 10-04-00504. The authors are grateful to Professor G. Goldspink (Royal Free and University College, London) for helpful comments in our discussions of the main statements in this review.

REFERENCES

1. Grigoriev A.I., Kozlovskaya I.B., Shenkman B.S. // Russian journal of physiology. 2004. V. 90 (5). P. 508-521.
2. Grigoriev A.I., Shenkman B.S. // Herald of the Russian Academy of Sciences. 2008. V. 78 (4). P. 337-345.
3. Shenkman B.S., Nemirovskaya T.L., Shapovalova K.B., et al. // Acta Astronautica. 2007. V. 60. P. 307–313.
4. Allen D.L., Roy R.R., Edgerton V.R. // Muscle Nerve. 1999. V. 22 (10). P. 1350–1360.
5. Cheek D.B.// Early Hum. Dev. 1985. V. 12. P. 211 – 239.
6. Ishido M., Kami K., Masuhara M. // Acta Physiol. Scand. 2004. V. 180 (3). P. 281–289.
7. Allen D.L., Monke S.R., Talmadge R.J., et al. // J. Appl. Physiol. 1995. V. 78 (5). P. 1969–1976.

8. Ohira Y., Yoshinaga T., Ohara M., et al. // J. Appl. Physiol. 1999. V. 87 (5). P. 1776–1785.
9. Rosenblatt J.D., Yong D., Parry D.J. // Muscle Nerve. 1994. V. 17 (6). P. 608–613.
10. Allen D.L., Yasui W., Tanaka T., et al. // J. Appl. Physiol. 1996. V. 81 (1). P. 145–151.
11. Blaauw B., Canato M., Agatea L., et al. // FASEB J. 2009. 23 (11). P. 3896–905.
12. Hikida R., Nostran S., Murray J., et al. // Anat. Rec. 1997. V. 247. P. 350–354.
13. Kadi F., Schjerling P., Andersen L.L., et al. // J. Physiol. 2004. V. 558. P. 1005–1012.
14. Aravamudan B., Mantilla C.B., Zhan W.Z., Sieck G.C. // J. Appl. Physiol. 2006. V. 100 (5). P. 1617–1622.
15. Mantilla C.B., Sill R.V., Aravamudan B., et al. // J. Appl. Physiol. 2008. V. 104 (3). P. 787–794.
16. Schultz E., McCormick K.M. // Rev. Physiol. Biochem. Pharmacol. 1994. V. 123. P. 213–257.
17. Day M.K., Allen D.L., Mohajerani L., et al. // J. Gravit. Physiol. 1995. V. 2 (1). P. 47–50.
18. Allen D.L., Linderman J.K., Roy R.R., et al. // Am. J. Physiol. 1997. V. 273. P. 579–587.
19. Ohira M., Hanada H., Kawano F., et al. // Japan. J. Phisiol. 2002. V. 52. P. 235–245.
20. Roy R.R., Zhong H., Talmadge R.J., et al. //J. Gravit. Physiol. 2001. V. 8 (2). P. 49–56.
21. Wang X.D., Kawano F., Matsuoka Y., et al. // Am. J. Physiol. Cell. Physiol. 2006. V. 290 (4). P. 981–989.
22. Reimann J., Irintchev A., Wering A. // Neuromuscular Disorders. 2000. V. 10. P. 276–282.
23. Koçtürk S., Kayatekin B.M., Resmi H., et al. // Eur. J. Appl. Physiol. 2008. V. 102 (5). P. 515–524.
24. Smith H.K., Maxwell L., Martyn J.A., Bass J.J. // Cell. Tissue. Res. 2000. V. 302 (2). P. 235–241.
25. Ferreira R., Neuparth M.J., Vitorino R., et al. // Physiol. Res. 2008. V. 57 (4). P. 601–611.
26. Oishi Y., Ogata T., Yamamoto K.I., et al. // Acta Physiol. (Oxf). 2008. V. 192 (3). P. 381–395.
27. Dupont-Versteegden E.E., Strotman B.A., Gurley C.M., et al. // Am. J. Physiol. Regul. Integr. Comp. Physiol. 2006. V. 291 (6). P. 1730–1740.
28. Nagano K., Suzaki E., Nagano Y., et al. // Acta Histochem. 2008. V. 110 (6). P. 505–518.
29. Bruusgaard J.C., Gundersen K. // J. Clin. Invest. 2008. V. 118 (4). P. 1450–1457.
30. Carson J.A., Alway S.E. // Am. J. Physiol. 1996. V. 270 (2 Pt 1). P. 578–584.
31. Kadi F., Thornell L.E. // Histochem. Cell. Biol. 2000. V. 113 (2). P. 99–103.
32. Lowe D.A., Alway S.E. // Cell Tissue Res. 1999. V. 296 (3). P.531–539.
33. Mitchell P.O., Pavlath G.K. // Am. J. Physiol. Cell. Physiol. 2001. V. 281 (5). P. 1706–1715.
34. Grounds M.D. // Pathol. Res. Pract. 1991. V. 187 (1). P. 1–22.
35. Seale P., Rudnicki M.A. // Dev. Biol. 2000. V. 218 (2). P. 115–224.
36. Asakura A., Seale P., Girgis-Gabardo A., Rudnicki M.A. // J. Cell. Biol. 2002. V. 159 (1). P. 123–134.
37. Parise G., O'Reilly C.E., Rudnicki M.A. // Appl. Physiol. Nutr. Metab. 2006. V. 31 (6). P. 773–781.
38. Wozniak A.C., Kong J., Bock E., et al. // Muscle Nerve. 2005. V. 31 (3). P. 283–300.
39. Capkovic K.L., Stevenson S., Johnson M.C., et al. // Exp. Cell. Res. 2008. V. 314 (7). P. 1553–1565.
40. Irintchev A., Zeschnigk M., Starzinski-Powitz A., Wernig A. // Dev. Dyn. 1994. V. 199 (4). P. 326–337.
41. Ishido M., Uda M., Masuhara M., Kami K. // Acta Physiol. (Oxf). 2006. V. 187 (3). P.407–418.
42. Mozdziak P.E., Pulvermacher P.M., Schultz E. // J. Appl. Physiol. 2000. V. 88. P. 158–164.
43. Schultz, E., Darr K. C., Macius A. // J. Appl. Physiol., 1994. V. 76. P. 266–270.
44. Ferreira R, Neuparth M.J., Ascensão A., et al. // Eur. J. Appl. Physiol. 2006. V. 97 (3). P. 340–346.
45. Kawano F., Takeno Y., Nakai N., et al. // Am. J. Physiol. Cell. Physiol. 2008. V. 295 (2). P. 458–467.
46. Crameri R.M., Langberg H., Magnusson P., et al. // J. Physiol. 2004. V. 558. P. 333–340.
47. Kadi F., Charifi N., Denis C., et al. // Pflügers Arch. 2005. V. 451 (2). P. 319–327.
48. Adams G.R., Haddad F., Baldwin K.M. // J. Appl. Physiol. 1999. V. 87 (5). P. 1705–1712.
49. Hill M., Wernig A., Goldspink G. // J. Anat. 2003. V. 203 (1). P. 89–99.
50. Allen D.G., Whitehead N.P., Yeung E.W. // J. Physiol. 2005. V. 567 (3). P. 723–735.
51. Husmann I., Soulet L., Gautron J., Martelly I., Barritault D. // Cytokine Growth Factor Rev. 1996. V. 7 (3). P. 249–258.
52. Kästner S., Elias M.C., Rivera A.J., Yablonka-Reuveni Z.// J. Histochem. Cytochem. 2000. V. 48 (8). P. 1079–1096.
53. Anderson J.E. // Mol. Biol. Cell. 2000. V. 11 (5). P. 1859–1874.
54. Olguin H.C., Olwin B.B. // Dev. Biol. 2004. V. 275 (2). P. 375–388.
55. Yamada M., Sankoda Y., Tatsumi R., et al. // Int. J. Biochem. Cell. Biol. 2008. V. 40 (10). P. 2183–2191.
56. Rosenblatt J.D., Parry D.J. // J. App.l Physiol. 1992. V. 73 (6). P. 2538–2543.
57. Machida S., Booth F.W. // Proc. Nutr. Soc. 2004. V. 63 (2). P. 337–340.
58. Adi S., Bin-Abbas B., Wu N.Y., Rosenthal S.M. // Endocrinology. 2002. V. 143 (2). P.511–516.
59. Chakravarthy M.V., Abraha T.W., Schwartz R.J., et al. //J. Biol. Chem. 2000. V. 275 (46). P. 35942–35952.
60. Sartorelli V., Fulco M. // Sci. STKE. 2004. V. 244. P. 11.
61. Goldspink G. //Physiology (Bethesda). 2005. V. 20. P. 232–238.
62. Jacquemin V., Furling D., Bigot A., et al. // Exp. Cell. Res. 2004. V. 299 (1). P. 148–158.
63. McCroskery S., Thomas M., Maxwell L., Sharma M., Kambadur R. // J. Cell. Biol. 2003. V. 162 (6). P. 1135–1147.
64. O'Connor R.S., Pavlath G.K., McCarthy J.J., Esser K.A. // J. Appl. Physiol. 2007. V.103(3). P.1107.
65. Wada K.I., Katsuta S., Soya H. // Japan. J. Physiol. 2003. V. 53 (2). P. 145–150.
66. Dupont-Versteegden E.E., Murphy R.J., Houlé J.D., Gurley C.M., Peterson C.A. // Am. J. Physiol. 1999. V. 277. P. 89–97.
67. Li P., Akimoto T., Zhang M., et al. // Am. J. Physiol. Cell Physiol. 2006. V. 290 (6). P. 1461–1468.
68. Florini J.R., Ewton D.Z., Coolican S.A. // Endocr. Rev. 1996. V. 17 (5). P. 481–517.
69. Barton-Davis E.R., Shoturma D.I., Musaro A., et al. // Proc. Natl. Acad. Sci. 1998. V. 95 (26). P. 15603 –15607.
70. Barton-Davis E.R., Shoturma D.I., Sweeney H.L. // Acta Physiol. Scand. 1999. V. 167 (4). P. 301–305.
71. Kurosaka M., Naito H., Ogura Y., et al. // J. Sports Science and Medicine. 2009. V. 8. P. 51–57.
72. Delp M.D., Pette D. // Cell Tissue Res. 1994. V. 277 (2). P. 363–371.
73. Martins K.J., Murdoch G.K., Shu Y., et al. // Pflügers Arch. 2009. V. 458 (2). P. 325–335.
74. Giordano C., Rousseau A.S., Wagner N., et al. // Pflügers Arch. 2009. V. 458 (5). P. 901–913.
75. Ohira, Y., Jiang B., Roy R. R., et al. // J. Appl. Physiol. 1992. V. 73. P. 51 – 57.
76. Falempin M., Mounier Y. // Acta Astronaut. 1998. V. 42 (1–8). P. 489–502.
77. Ohira Y., Yoshinaga T., Yasui W., et al // J. Appl. Biomechanics. 2000. V. 16. P. 80–87.
78. Tatsumi R., Liu X., Pulido A., et al. // Am. J. Physiol. Cell. Physiol. 2006. V. 290 (6). P. 1487–1494.
79. Gordon S.E., Westerkamp C.M., Savage K.J., et al. // Can. J. Physiol. Pharmacol. 2007. V. 85 (6). P. 646–651.
80. Tarakina M.V., Turtikova O.V., Nemirovskaia T.L., Kokontsev A.A., Shenkman B.S. // Tsitologiya. 2008. V. 50 (2). P.140-146.
81. Kartashkina N.L., Turtikova O.V., Kuznetsov S.L., Kalamkarov G.R., Bugrova A.E., Orlov O.I., Nemirovskaya T.L. // Doklady RAN. In print.

Bioinformatic Analysis, Molecular Modeling of Role of Lys65 Residue in Catalytic Triad of D-aminopeptidase from *Ochrobactrum anthropi*

I.G. Khaliullin[1,2], D.A. Suplatov[1], D.N. Shalaeva[1], M. Otsuka[3], Y. Asano[3], V.K. Švedas[1*]
[1]Faculty of Bioengineering and Bioinformatics, Lomonosov Moscow State University
[2]Department of Chemistry, Lomonosov Moscow State University
[3]Biotechnology Research Center, Toyama Prefectural University, Japan
*E-mail: vytas@belozersky.msu.ru
Received 23.04.2010

ABSTRACT **A bioinformatic and phylogenetic study has been performed on a family of penicillin-binding proteins including D-aminopeptidases, D-amino acid amidases, DD-carboxypeptidases, and β-lactamases. Significant homology between D-aminopeptidase from *Ochrobactrum anthropi* and other members of the family has been shown and a number of conserved residues identified as S62, K65, Y153, N155, H287, and G289. Three of those (Ser62, Lys65, and Tyr153) form a catalytic triangle – the proton relay system that activates the generalized nucleophile in the course of catalysis. Molecular modeling has indicated the conserved residue Lys65 to have an unusually low pKa value, which has been confirmed experimentally by a study of the pH-profile of D-aminopeptidase catalytic activity. The resulting data have been used to elucidate the role of Lys65 in the catalytic mechanism of D-aminopeptidase as a general base for proton transfer from catalytic Ser62 to Tyr153, and *vice versa*, during the formation and hydrolysis of the acyl-enzyme intermediate.**
KEYWORDS **D-aminopeptidase, penicillin-binding protein family, bioinformatic analysis, catalytic mechanism.**

INTRODUCTION

D-aminopeptidase from *Ochrobactrum anthropi* possesses a unique structural organization, high stereospecificity, and shows catalytic activity towards a wide range of D-alanine derivatives [1]. It is a member of the serine hydrolases superfamily and acts as a homodimer, with each subunit consisting of three structural domains. One of those – a catalytic domain – has the so called β-lactamase fold [2]. Sequence comparison has revealed a strong evolutionary relationship of D-aminopeptidase with DD-carboxypeptidase and β-lactamase [3].

The catalytic mechanism of D-aminopeptidase has not been discussed in the literature; however, suggestions concerning other enzymes of the family – D-amino acid amidase from *Ochrobactrum anthropi*, as well as -lactamases and penicillin-binding proteins, can be taken into account. Different views on the catalytic mechanism of penicillin-binding proteins are presented, and several residues in close proximity to the catalytic serine are considered as potential candidates for the role of general base in the course of the enzymatic reaction [4- 6]. While choosing between them, it is important to look at the pH-profile of enzyme activity and possible pK shifts of the residue due to its environment, since the general base is bound to act in deprotonated form.

It is important that molecular modeling of the deacylation step has been performed for reactions catalyzed by DD-peptidase R61 from *Streptomyces sp.* and class C β-lactamase P99 from *Enterobacter cloacae* by means of QM/MM methods [7]. It revealed the leading role of the active site tyrosine residue in the deacylation of the catalytic serine of those enzymes.

Yet, an analysis of the literature shows that a comprehensive view on the catalytic mechanism of D-aminopeptidase is still lacking. In this work, we aim to use bioinformatics and molecular modeling to elucidate the role of the Lys65 residue in the catalytic triad of D-aminopeptidase from *Ochrobactrum anthropi*.

MATERIALS AND METHODS

Experimental study

D-aminopeptidase was purified according to a procedure described earlier [1]. The colorimetric substrate – D-alanine *p*-nitroanilide (D-Ala-*p*NA) – was produced by Bachem. Tris(hydroxymethyl)methylamine (Tris) of research-grade purity produced by SERVA Electrophoresis was used to prepare buffer solutions.

Kinetic assays were performed using progress curve analysis. The studies were carried out in a spectrophotometric cuvette of 500 μl and optical path length of 1 cm thermostated at 25°C. Enzymatic hydrolysis was initiated by adding a small amount of the enzyme solution to the reaction mixture containing the substrate in a concentration approximately 4 times higher than its K_M. Changes in absorption were reg-

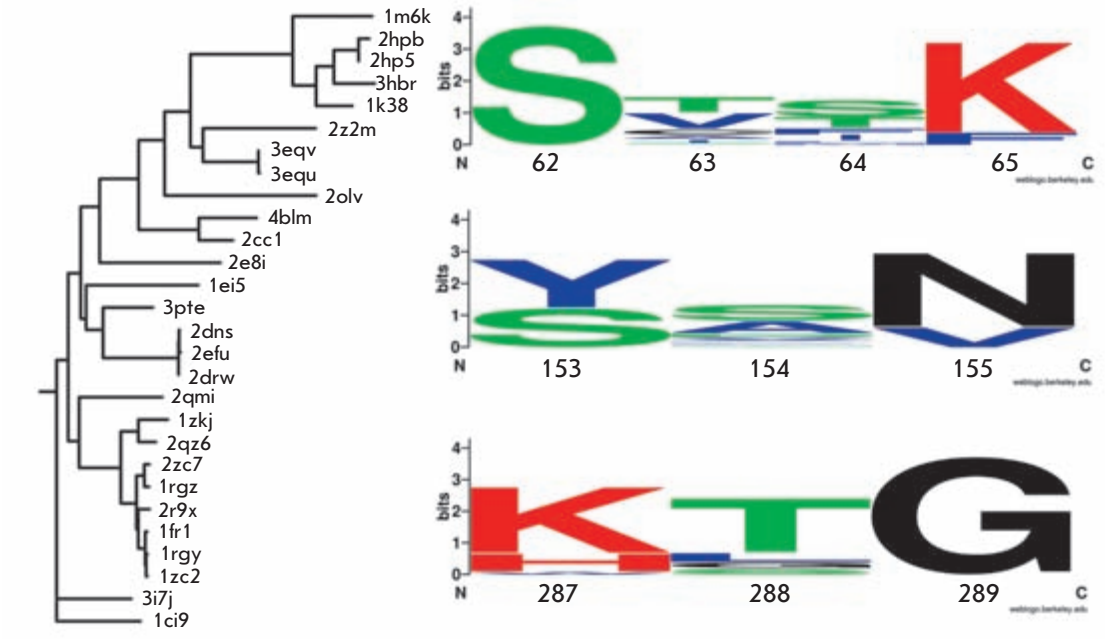

Fig. 1. Phylogenetic tree based on structural alignment of penicillin-binding proteins and primary structure motives containing important catalytic residues: Ser62 and Lys65 (SXXK), Tyr153 ([YS]XN) and His287 ([KH]XG). Leaves are named according to PDB databank accession numbers.

istered by a Shimadzu UV-1601 spectrophotometer in the Kinetics mode at 450 nm. The final levels of absorption were not higher than 2 in all of the assays.

To maintain the set pH value in the reaction mixture, the enzymatic reactions were carried out in a 0.1 M Tris-HCl buffer. A Hamilton Slimtrode pH-sensitive electrode was used in the preparation of the buffer solutions.

The progress curves obtained were processed by data linearization in $t/ln(p_\infty/(p_\infty-p)) - p/ln(p_\infty/(p_\infty-p))$ coordinates, where t is time, p – current concentration of the product, and p_∞ – the final concentration of the product. This anamorphosis allows to determine the value of the K_M/V_{max} and $1/V_{max}$ ratio as the line's slope and y-intercept, respectively. The nonlinear regression of the V_{max}/K_M dependence on pH and the computation of experimental pKa values were performed using SciDAVis software [8].

Bioinformatics

Homology search. In all homology search procedures, a sequence or structure of D-aminopeptidase from *Ochrobactrum anthropi* (PDB entry 1EI5) was used as a query.

The sequence-based homology search was carried out using the PSI-BLAST [9] algorithm v. 2.2.18 to scan a "non-redundant" protein sequence database. The resulting sample was filtered with a 95% pairwise identity threshold to eliminate redundancy and then aligned using t_coffee [10], mafft [11], and probcons [12] joined together by the consistency-based statistics implemented in t_coffee.

The structure-based homology search was carried out by scanning the PDB protein structure databank using the SSM [13] procedure. Hits were discriminated in case of high secondary structure elements mismatch with the 1EI5 structure. The resulting sample of three-dimensional structures was aligned using the MUSTANG [14] software.

Bioinformatic analysis. The phylogenetic analysis of sequence and structural alignment was performed using the phylip package [15]. The phylograms were constructed using distance-based methods with the neighbor-joining algorithm. The bioinformatic analysis was carried out using the original ZEBRA v. 3.2 software with a statistical threshold level of 2.2×10^{-43}.

Visualisation. The Jalview [16] program was used to look through multiple sequence alignments. Visualization of three-dimensional structures and a structure-based multiple alignment was done using PyMol [17]. Generation of phylogenetic trees was done using phylip [15]. Generation of sequence patterns logotypes was done with the WebLogo [18] Internet service.

RESULTS AND DISCUSSIONS

Bioinformatic analysis of enzymes homologous to D-aminopeptidase

Data related to the penicillin-binding protein family including D-aminopeptidases, D-amino acid amidases, and alkaline D-peptidases were collected and analyzed. The UniProt protein sequence database and PDB protein structures databank were screened *a priori* to identify all significant sequences and structure-based homologs of D-aminopeptidase. The resulting set of 734 sequence homologs and 24 structural homologs was sampled and filtered to acquire the most informative set. As a result of structural alignment, a significant similarity of the active site regions of D-aminopeptidase, alkaline D-peptidases, D-amino acid amidases, and β-lactamases was shown for both the sequence and structure levels (fig. 1).

The following residues were identified as conserved in the active site of penicillin-binding proteins using the original

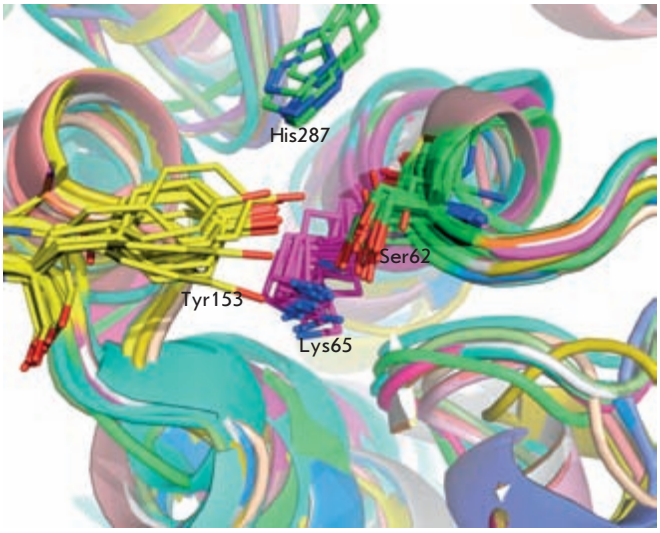

Fig. 2. An active site fragment of the structural alignment of penicillin-binding proteins – structural homologs of D-aminopeptidase from Ochrobactrum anthropi. Location of four conserved active site residues — Ser62, Lys65, Tyr153, His287— conserved in D-aminopeptidase, as well as in other members of the family, is shown.

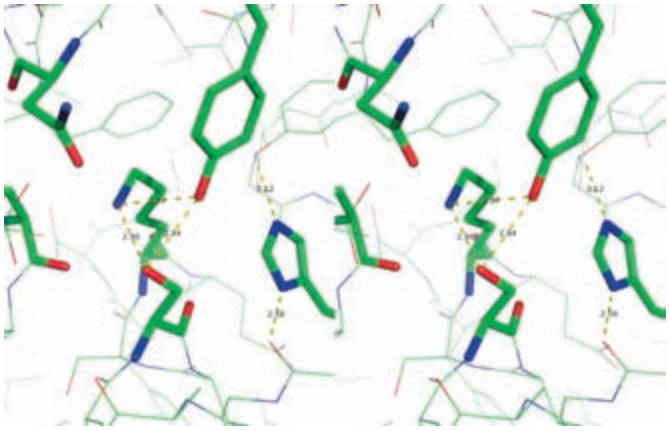

Fig. 3. Stereo view of the D-aminopeptidase active site and spatial organization of catalytic triad. The S62, K65, Y153, N155, H287, and D225 residues are highlighted.

ZEBRA software developed in our laboratory: 287H, 153Y, 155N, 289G, 273G, 293G, 270Y, 65K, 224G, 62S, 68T, 294W, 64S, 151Y, 228I, 60I, and 288G (numbered according to the 1EI5 structure and sorted in decreasing significance). Considering that the conservation of a residue in a protein structure indicates an evolutionary pressure on that position and thus underlines its functional or structural importance [19], we suggest that such residues are important to the D-aminopeptidase catalytic mechanism. A common alpha-beta domain identified as a "three-layer sandwich" by CATH [20] structure classification was shown to contain active site residues in all studied penicillin-binding proteins (fig. 2).

D-aminopeptidase structure analysis

The D-aminopeptidase structure (PDB entry 1EI5) analysis reveals a pair of amino acid residues, Tyr153 and Lys65, located in near proximity and in approximately equal distance to the catalytic Ser62's Oγ atom. All three residues form a nearly equilateral triangle in the enzyme active site (fig. 3). Such a location of residues implements a special organization of the proton relay system when the hydrogen atom of the serine's hydroxyl-group is directed toward the center of the triangle and shared among all of the residues of the catalytic triad. The specific organization of this catalytic triangle is based on the irregular properties of the Lys65 residue capable of accepting a proton in neutral and slightly alkaline media, which lends high reactivity to the Ser62 residue at the formation of the acyl-enzyme intermediate.

A considerably lower pKa value of the Lys65 residue equal to 7.8, compared to the ionization of regular lysine residues in proteins with pKa 10-11, was observed upon calculation

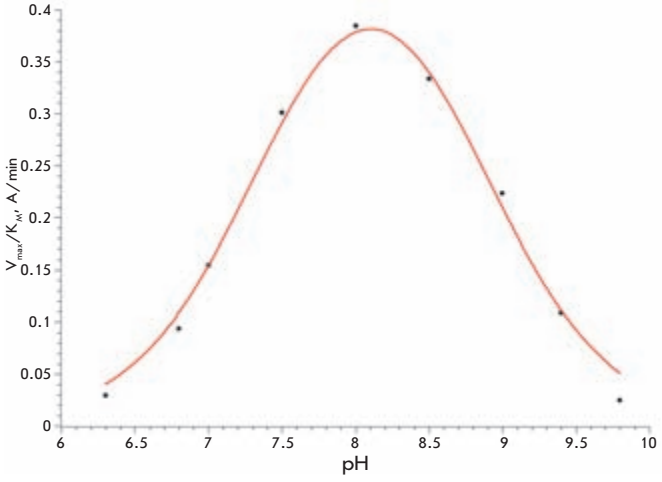

Fig. 4. pH-profile of D-aminopeptidase catalytic activity. The theoretical curve was calculated according to the equation $v = v_0/(1+[H^+]/K_1+K_2/[H^+])$, where v_0, pK_1 and pK_2 values are equal to 0.53, 7.4 and 8.8, respectively.

of the ionization properties of D-aminopeptidase active site residues by the PROPKA QSAR method [21]. A high-evaluated pKa value of the Tyr153 residue equal to 11.85 should be noted as well.

Experimental pH-profile of D-aminopeptidase catalytic activity

Experimental data are in good agreement with the results obtained by molecular modeling and shed light on the role of the Lys65 residue in the functioning of the catalytic triad. The pH-profile of the D-aminopeptidase catalytic activity has

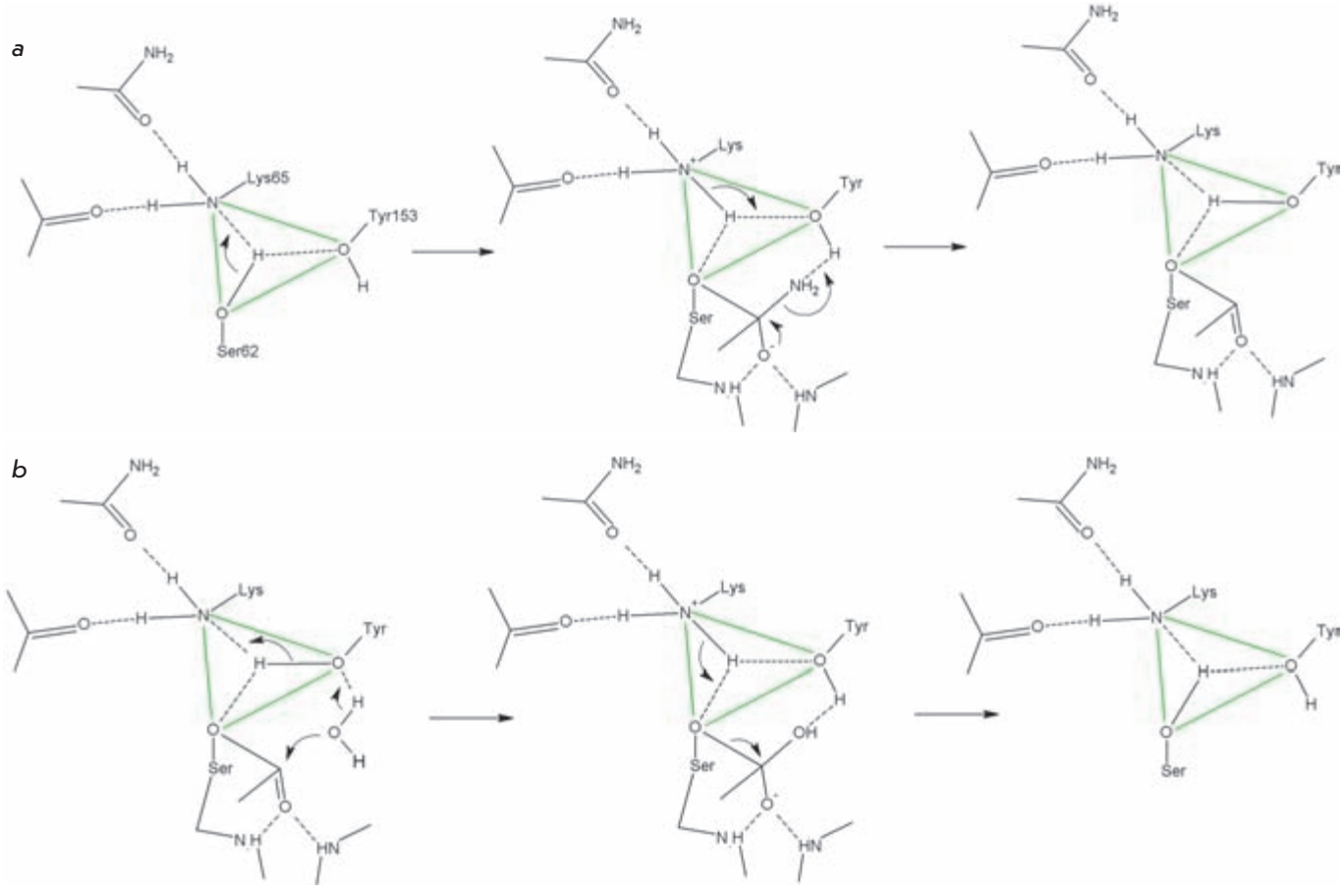

Fig. 5. Schematic presentation of acylation (a) and deacylation (b) of the Ser62 residue in the catalytic mechanism of D-aminopeptidase: (a) organization of catalytic triad and its role in the formation of the first tetrahedral intermediate followed by the formation of acyl-enzyme are shown; (b) nucleophile (water molecule) binding, activation, nucleophilic attack followed by formation of the second tetrahedral intermediate and regeneration of a free enzyme are shown.

a bell-shaped form with a pKa value of 7.4 and a pKb value of 8.8 (fig. 4). On the basis of the molecular modeling and the experimental study, the amino acid residue with a pKa of 7.4 was referred to Lys65.

Proposed catalytic mechanism of D-aminopeptidase

Just as in the case of other serine hydrolases, the reaction catalyzed by D-aminopeptidase follows a 3-step kinetic scheme with the formation of a covalent acyl-enzyme intermediate and its subsequent hydrolysis or transfer of the acyl group to an external nucleophile. Because of the extremely low pKa value of its terminal amino group, the Lys65 residue plays a specific role in the D-aminopeptidase catalytic mechanism (fig. 5):

Being uncharged at the pH-optimum of the enzymatic reaction, the Lys65 residue acts as a general base, while the Oγ atom of Ser62 attacks the carbonyl group of a substrate: Lys65 assumes a proton from the attacking OH-group when the first tetrahedral intermediate is formed at the acylation step.

At the decomposition of the first tetrahedral intermediate followed by the formation of the acyl-enzyme and release of the first reaction product, its leaving group gathers a proton donated by the OH-group of Tyr153, whose acidity is increased due to the proximity of a positively charged Lys65 residue, and at the same time the formed oxyanion of Tyr153, being stronger base, captures a proton from the Lys65 residue.

At the deacylation step, the water molecule (or molecule of another nucleophile) is activated through the concerted action of two bases - Tyr153 and Lys65. Protons are transferred by the proton relay system from the nucleophile to Tyr153 and from Tyr153 to Lys65, and a nucleophilic attack occurs, followed by the formation of the second tetrahedral intermediate.

At the decomposition of the second tetrahedral intermediate followed by the release of the second reaction product, the Lys65 residue cedes a proton to the Ser62 oxyanion and the enzyme returns to its initial state.

CONCLUSIONS

The bioinformatic and phylogenetic analysis of the penicillin-binding protein family including D-aminopeptidases was carried out, and the conserved residues were identified. Three of them – catalytic Ser62, Lys65, and Tyr153 – form a catalytic triangle – a specific proton relay system that captures/cedes a proton in the course of catalytic events and makes possible the activation of the generalized nucleophile in the D-aminopeptidase catalysis. Molecular modeling showed that a conserved residue (Lys65) possess an unusually low pKa value, which was confirmed by an experimental pH-profile of the D-aminopeptidase catalytic activity. The specific role of the Lys65 residue in a catalytic mechanism of D-aminopeptidase was proposed at the formation and hydrolysis of the acyl-enzyme intermediate. ●

This work was supported by the Russian Foundation for Basic Research and Japanese Society for the Promotion of Science (grant № 09-08-92104).

REFERENCES

1. Asano Y., Nakazawa A., Kato Y., Kondo K. // J. Biol. Chem. 1989. V. 264. P. 14233–14239.
2. Bompard-Gilles C., Remaut H., Villeret V., et al. // Structure. 2000. V. 8. P. 971–980.
3. Asano Y., Kato Y., Yamada A., Kondo K. // Biochemistry. 1992. V. 31. P. 2316–2328.
4. Okazaki S., Suzuki A., Komeda H., et al. // J. Mol. Biol. 2007. V. 368. P. 79–91.
5. Massova I., Kollman P. // J. Comput. Chem. 2002. V. 23. P. 1559–1576.
6. Ke Y., Lin T. // Biophys. Chem. 2005. V. 114. P. 103–113.
7. Gherman B., Goldberg S., Cornish V., Friesner R. // J. Am. Chem. Soc. 2004. V. 126. P. 7652–7664.
8. SciDAVis: a free application for scientific data analysis and visualization. http://scidavis.sourceforge.net/
9. Altschul S., Madden T., Schäffer A., et al. // Nucleic Acids Res. 1997. V. 25. P. 3389–3402.
10. Notredame C., Higgins D., Heringa J. // J. Mol. Biol. 2000. V. 302. P. 205–217.
11. Katoh K., Asimenos G., Toh H. // Methods Mol. Biol. 2009. V. 537. P. 39–64.
12. Do C., Mahabhashyam M., Brudno M., Batzoglou S. // Genome Res. 2005. V. 15. P. 330–340.
13. Krissinel E., Henrick K. // Acta Cryst. 2004. V. D60. P. 2256–2268.
14. Konagurthu A., Whisstock J., Stuckey P., Lesk A. // Proteins. 2006. V. 64. P. 559–574.
15. Felsenstein J. 2005. PHYLIP (Phylogeny Inference Package) version 3.6. Distributed by author. Department of Genome Sciences, University of Washington, Seattle, USA.
16. Waterhouse A., Procter J., Martin D., Clamp M., Barton G. // Bioinformatics. 2009. V. 25. P. 1189–1191.
17. The PyMOL Molecular Graphics System, Version 1.0r1, Schrödinger, LLC. http://www.pymol.org/
18. Crooks G., Hon G., Chandonia J., Brenner S. // Genome Research. 2004. V. 14. P. 1188–1190.
19. Koonin E., Galperin M. Sequence - Evolution - Function: Computational Approaches in Comparative Genomics. Kluwer Academic Publishers, 2003. P. 461.
20. Pearl F., Bennett C., Bray J., et al. // Nucleic Acids Res. 2003. V. 31. P. 452–455.
21. Li H., Robertson A., Jensen J. // Proteins. 2005. V. 61. P. 704–721.

Development of Recombinant Vaccine against A(H1N1) 2009 Influenza Based on Virus-like Nanoparticles Carrying the Extracellular Domain of M2 Protein

R.Y. Kotlyarov[1], V.V. Kuprianov[1], A.I. Migunov[2], L.A. Stepanova[2], L.M. Tsybalova[2], O.I. Kiselev[2], N.V. Ravin[1]*, K.G. Skryabin[1]
[1] Centre "Bioengineering" Russian Academy of Sciences
[2] Research Institute of Influenza, Russian Academy of Medical Sciences
E-mail: nravin@biengi.ac.ru
Received 23.04.2010

ABSTRACT **The conventional vaccines currently being used to deal with influenza are based on a virus obtained in chicken embryos or its components. The high variability of the major immunogenic surface proteins – hemagglutinin and neuraminidase–require the development of strain-specific vaccines that match the antigenic specificity of a newly emerging virus. Recombinant vaccines based on single viral proteins that could be easily produced in standard expression systems are attractive alternatives to traditional influenza vaccines. We constructed recombinant nanosized virus-like particles based on a nuclear antigen of the hepatitis B virus. These particles expose on the surface the extracellular domain of the M2 protein of the highly pathogenic A(H1N1) 2009 influenza virus. The methods of production of these virus-like particles in *Escherichia coli* and their purification were developed. Experiments on animals show that M2sHBc particles are highly immunogenic in mice and provide complete protection against the lethal influenza challenge.**
KEYWORDS **influenza, vaccine, M2 protein, nanoparticle, HBc antigen.**
ABBREVIATIONS **M2e – extracellular domain of Influenza virus M2 protein, HBc – nuclear antigen of hepatitis B virus, M2sHBc – hybrid protein including M2e of the swine flu virus and HBc, PCR – polymerase chain reaction, , PBS-phosphate buffered saline, TMB – tetramethylbenzidine, LD_{50} – dose corresponding to 50% lethality rate, ELISA – enzyme-linked immunosorbent assay, FCS – fetal calf serum**

INTRODUCTION:

Influenza is the most common viral disease in humans and animals. Type A influenza viruses vary in their degrees of pathogenicity. In recent years, the H5N1strain has caused local outbreaks of the disease with a high morbidity rate in Southeast Asia. The H1N1 virus originating in swine was behind the flu pandemic that lasted from 2009 to 2010, with an unexpectedly high morbidity rate among middle-aged and high-risk individuals. Given its large amount of phenotypic attributes and its phylogenic origin, the H1N1 virus is akin to the virus that was deemed responsible for the Spanish Flu epidemic that lasted between 1918 and 1920. These characteristics provide evidence of a possible return of a highly pathogenic virus into circulation throughout the human population. The current influenza vaccines are based on a virus obtained from chicken embryos, or from its components [1]. The high variability of the viral surface proteins, hemagglutinin and neuraminidase, leads to the appearance of an epidemic strain every 1-2 years [2], which requires the development of a "standard" strain-specific vaccine at the same rate.

One of the potential causes of antigen variability in the human influenza virus is its recombination (reassertion) with animal flu viruses, which can lead to the appearance of a new, highly pathogenic recombinant virus unfamiliar to the human immune system and, therefore, carrying the risk of a pandemic. At the same time, the development of a traditional vaccine for new strains requires a relatively extended period of time (6 to 9 months), during which the appearance of the new pandemic-causing strain could claim many casualties. As previously stated, the novel pathogenic strain responsible for the 2009 pandemic belongs to the H1N1 class, based on sequences coding of its hemagglutinin and neuraminidase.

Recombinant vaccines are alternatives to traditional methods, and they are based on specific viral proteins. The formulation of these novel vaccines may be achieved in standard producing organisms, such as bacteria or yeast. The use of recombinant vaccines not only eliminates the industry's dependence on chicken embryos and addresses the general safety concerns associated with vaccines based on the whole pathogen [3], but also creates an opportunity for the development of "universal" vaccines with the use of conservative viral proteins. Moreover, this type of approach allows to produce these vaccines at high speed while "overlapping" the antigen properties of several pandemic viruses.

Table 1. Sequence comparison of extracellular domains of M2 proteins of influenza strains of human and animal origins. Amino acids that change relative to the human influenza M2e consensus sequence are underlined.

Host	Strain	M2e peptide sequence
Swine/human	A/California/04/2009	SLLTEVETPTRSEWECRCSDSSD
Human	Consensus sequence	SLLTEVETPIRNEWGCRCNDSSD
Human	A/PR/8/34	SLLTEVETPIRNEWGCRCNGSSD
Avian	A/Chicken/Kurgan/05/2005	SLLTEVETPTRNEWECRCSDSSD
Avian	A/Duck/ Potsdam1402-6/1986	SLLTEVETPTRNGWECKCSDSSD

W. Fiers *et al.* (University of Ghent) analyzed the possibility of developing a universal influenza vaccine based on the extracellular domain of the M2 protein of the influenza virus [4, 5]. M2 is a small transmembrane protein (97 amino acid residues) present in small amounts within the virion, yet it is expressed effectively in the infected cells [6, 7]. An important property of M2 is the conservation of its sequence. The sequence of its extracellular domain (23 amino acid residues), M2e, remains practically unchanged for all type A viruses, which have been extracted from humans since 1933 [4, 8, 9]. However, M2 exhibits a low immunogenicity, and after infection, the immune response against it is practically not activated [10].

The solution to the problem of the low immunogenicity of M2 lies in the protein attaching to the nanosized carrier particle. Such a nanovaccine, when imitating a pathogen, possesses high immunogenicity and is effectively recognized by the human immune system. W. Friers *et al.* used virus-like particles produced by the HBc antigen of the hepatitis B virus as a carrier for the M2e peptide [4, 11]. Mice immunization by M2eHBc particles produced in *E. coli* provided 100% protection against the lethal influenza infection [4]. Besides the HBc, virus-like particles based on the human papilloma virus can be used as carriers of the M2e [12], as well as bacteriophages Qβ [13], the papaya mosaic virus [14], and the cowpea mosaic virus [15].

As mentioned above, the sequence of M2e is highly conserved in all human viral strains of Type A influenza; however, in animal strains it differs significantly [16, 17]. The M2e of the swine flu virus A/California/04/2009(H1N1), which was responsible for the 2009 pandemic, differs from the M2e of the human strain in 4 out of 23 amino acid residues (Table 1). Such differences may determine the specificity of vaccines based on M2e. In this work, we constructed recombinant particles (M2sHBc-particles) which carry the M2e viral peptide of the swine flu A/California/04/2009(H1N1) and showed that immunization with such nanoparticles provides full protection of vaccinated mice against the lethal challenge by swine flu virus A/California/04/2009(H1N1). At the same time, protection against the avian flu infection, strain A/Duck/Potsdam1402-6/1986 or human strain A/PR/8/34, proved only partial, which emphasizes the necessity of taking into account the sequence differences of M2e of influenza strains of different origins when developing universal influenza vaccines.

EXPERIMENTAL PART

Construction of expression vector pQE-M2sHBc and *E. coli* producer strain.

The gene that codes for the hybrid protein M2sHBc was synthesized using a three-step PCR. During the first step, the portion of the M2HBc sequence was obtained as a result of PCR with the primers M2F3 (C GAA TGG GAA TGC CGT TGC AGC GAT AGC AGC GAT GAC CCT) and HBC-R2 (A GGA TCC TCA GCA AAC AAC AGT AGT CTC CGG AAG) and DNA copy of the hepatitis B virus genome as a template. During the second step, the obtained fragment was used as a template for the PCR with the primers M2sF1 (GAA ACC CCG ACC CGT AGC GAA TGG GAA TGC CGT TGC AGC) and HBC-R2. During the third step, a full-sized gene, M2sHBc, was obtained as a result of the PCR amplification with the primers M2sF2 (CTC ATC AGC CTG CTG ACC GAA GTG GAA ACC CCG ACC CGT AGC) and HBC-R2. The fragment obtained, 525 bp, was digested with the restriction enzymes PagI and BamHI, whose recognition sites were entered into the sequence of primers M2sF2 and HBC-R2, respectively, and cloned into the expression vector pQE60 (Qiagen) using sites for NcoI and BamHI. The expression vector pQE-M2sHBc was used in further work. Sequencing verified the absence of the PCR-specified mutations in the synthesized gene.

To obtain the producing strain of M2sHBc, plasmid pQE-M2sHBc was introduced into the *E. coli* strain DLT1270 by transformation. Strain DLT1270, a derivative of the DH10B [18], contained the repressor gene for the lactose operon *lacI* integrated into a chromosome.

Isolation and purification of the M2sHBc-particles

Strain DLT1279/pQE-M2sHBc was grown in LB-broth until the midpoint of the logarithmic growth phase (OD_{600} = 0.5) at 37 ^{0}C, then IPTG was added to 1mM, and the culture was left to continue to grow for 16 hours at 30 ^{0}C. Cells from the producing strain were collected by centrifugation at 3,000 rpm for 30 minutes and were re-suspended in a 50 mM Tris-HCl buffer pH 8.0, which contained 0.5M NaCl, 15mM EDTA, and 20% sucrose, calculating 1ml of buffer per 50ml of culture. Cell suspension was treated with lysozyme (1mg/ml) for 15 min at 4 ˚C; afterwards, the cells were lysed by sonication. Polyethylene glycol (50% weight/volume) was added to the lysate solution (1/20 volume) and incubated for 30 min at 4 ˚C. Next, it was centrifuged for 20 minutes at 13,000 rpm.

Table 2. Evaluation of immunogenicity and protectivity of the candidate vaccine based on the M2e peptide of the swine influenza virus.

Group of mice	Number of mice	First immunization	Second immunization	Third immunization	Influenza virus challenge		
					A/Duck/ Potsdam/1402-6/1986 (H5N2)	A/California/ 04/2009 (H1N1)	A/PR/8/34
Experimental (M2sHBc)	60	60 mice with TiterMax Gold Adjuvant 50 μg/mice s.c.*	60 mice with Freund's incomplete adjuvant 50 μg/mice s.c.	60 mice with Freund's incomplete adjuvant 50 μg/mice s.c.	20 mice 5 LD/50	20 mice 5 LD/50	10 mice 5 LD/50
Control	40	PBS	PBS	PBS	15 mice 5 LD/50	15 mice 5 LD/50	10 mice 5 LD/50
* - subcutaneous injection							

A fifth of the volume of the concentrated solution of ammonium sulfate was added to the supernatant, mixed and left to stand for 30 min at 4 ˚C. The produced protein precipitate was suspended in 1ml of the same buffer and precipitated with ammonium sulfate a second time under the same conditions. The produced precipitate was dissolved in a 1ml 50mM Tris-HCl buffer with pH 8.0, which contained 0.5 M NaCl, 15mM EDTA, and 20% sucrose. The obtained preparation of M2sHBc particles contained, according to the SDS-PAGE, about 90% of the M2sHBc protein with a concentration of ~ 0.5 mg/ml.

Mice Immunization

To study the immunogenicity and the protectivity of the candidate vaccine, the immunization scheme was applied with the use of the TiterMax Gold Adjuvant (Sigma) at first immunization and the incomplete Freund's adjuvant (Sigma) at the following immunizations. Second immunization was conducted three weeks after the first, and the third was done the following week. The immunization outline is shown in Table 2.

Sera were collected 2 weeks after the third immunization, and the antibody titers were determined in the pooled sera of mice of each group (3-5 mice). As negative control, the serum of nonimmunized mice was used. As positive control, monoclonal antibodies to the M2e peptide strain A/Duck/Potsdam/1402-6/1986 (H5N2) were used: they were provided by P.G. Sveshnikov (Russian Research Center of Molecular Diagnostics and Therapy).

Synthetic Peptides

As a standard for the determination of M2e antibody synthetic peptides G-11-1 (SLLTEVETPTRNEWECRCSDSSD, corresponding to M2e of strain A/Chicken/Kurgan/05/2005), G19 (SLLTEVETPTRNGWECKCSDSSD, corresponding to the M2e of strain A/Duck/Potsdam1402-6/1986), G26 (SLLTEVETPTRSEWECRCSDSSD, corresponding to the M2e of strain A/California/04/2009), and G18 (SLLTEVETPIRNEWGCRCNDSSD, corresponding to M2e of strain A/PR/8/34) were used.

ELISA for the titer determination of specific antibodies

For ELISA, 96-well plates with a high sorption capacity (Greiner, Germany) were covered with synthetic peptides G-11-1, G19, G26, and G18 with a concentration of 5 mg/ml (in the carbonate buffer, pH 9.5-9.6) and kept overnight at 4 ˚C. Plates were treated with a blocking buffer (0.01 M PBS pH 7-7.4) with 5% FCS for 1 hour at room temperature and washed 3 times with PBS-Tween. The pooled mice sera from each group were analyzed in duplicates. 100 μl of 2-time serum dilutions were added to the well plates (starting with 1:400) in the blocking buffer then incubated for 1 hour at room temperature. As a conjugate, rabbit polyclonal anti-mice IgG (Abcam, Great Britain) were used in a 1:8,000 dilution, marked with a horseradish peroxidase. TMB was used as a substrate. The reaction was monitored by UV-Vis spectroscopy at 450 nm. The last dilution of the serum, which had an optical absorption at least twice higher than that of nonimmunized mice, was taken as an antibodies titer.

Viruses and mice infection

For the infection of the animals immunized by the candidate vaccines, the following influenza viruses, adapted to the mice, were used: A/Duck/Potsdam/1402-6/1986(H5N2), A/California/04/2009 (H1N1), and A/PR/8/34 (H1N1). The virus was administered intranasally in a total volume of 50 μl containing $5LD_{50}$ to mice anesthetized by ether. The animals were observed daily after infection. The protective properties of the candidate vaccine were evaluated based on two parameters: determination of body weight dynamics and mice survival after infection.

RESULTS AND DISCUSSION

Design and production of M2sHBc nanoparticles

The Hepatitis B nuclear antigen is one of the most effective carriers of antigen determinants. Monomers of this protein, consisting of 183 amino acid residues, self-assemble into icosahedral particles with a 34 nm diameter, made of 240 subparti-

cles organized in dimeric blocks [19]. Two HBc antigen regions can be used for the presentation of foreign peptides on the surface of the HBc particles – the protein N-terminus and the immunodominant loop located between the 75th and 85th amino acid residues of the protein [20-22]. Based on our experience, the introduction of the foreign sequence into the immunodominant loop results, in most cases, in the disturbance of the assembly and/or the solubility of the particles. Therefore, as a site for the introduction of the M2e peptide for the construction of the hybrid protein M2sHBc, the N-terminus of HBc was used. The HBc sequence contains an arginine-rich C-terminal domain, which binds viral DNA during the viron assembly. When expressed in *E. coli*, this domain binds bacterial RNA [23], whose presence in the preparation is undesired. Since the C-terminal domain (150 – 183 amino acid residues) is not necessary for the assembly of the particles [24], it was removed and replaced by a cysteine residue, whose introduction increases the stability of HBc particles [16]. Therefore, our hybrid protein M2sHBc comprises, starting from the N-terminus, the sequence of M2e peptide of the swine flu virus A/California/04/2009 (H1N1), the sequence of HBc antigen from the 4th to 149th amino acid residues, and the C-terminal cysteine.

The gene coding for the hybrid protein M2sHBc was synthesized using three-stage PCR with the HBc sequence as a template. During each stage, the sequences encoding the regions of M2e were added to the 5'-end of the synthetic gene. The obtained synthetic gene M2sHBc was cloned in the expression vector pQE60 (Qiagen) under the control of the promoter, inducible by IPTG. The hybrid protein is well expressed in *E. coli* (Figure 1A) and mainly present in the soluble fraction. The assembly of M2sHBc in virus-like nanoparticles was confirmed by electron microscopy of a purified specimen (Figure 1B).

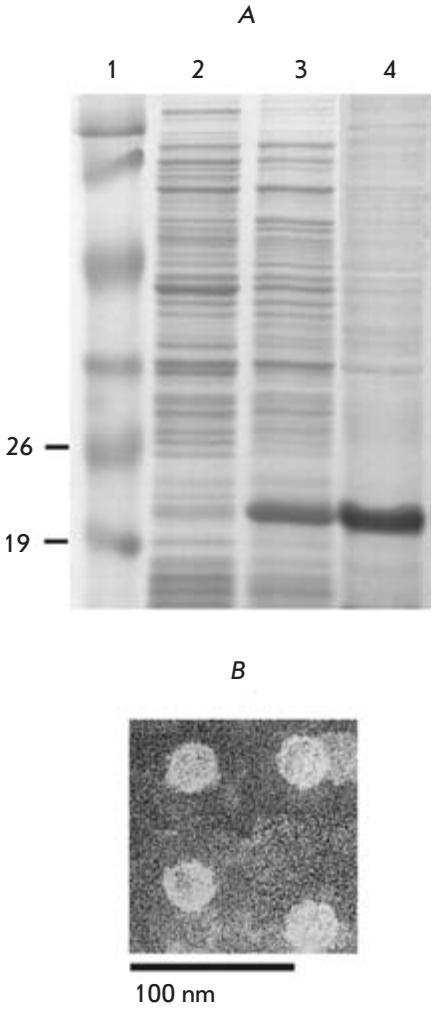

Fig. 1. Expression and purification of M2sHBc particles. (A) SDS-PAGE analysis of protein samples. 1 - molecular weight marker, kDa. 2 - protein sample from the strain DLT1270/ pQE-M2sHBc before the induction of M2sHBc expression. 3 - the same as in line 2, but after 16h induction of M2sHBc expression. 4 - purified M2sHBc particles (B) Electron microscopy of M2sHBc particles.

Immunogenicity of the M2sHB particles

Mice immunization with the purified preparation of M2sHBc particles was done to characterize their immunogenicity and protectivity. The test group that consisted of 60 animals was immunized subcutaneously, using TiterMax Gold Adjuvant (Sigma) for the first vaccine introduction, and the Freund's adjuvant (Sigma) for the consecutive immunizations. To test the immunogenicity of the candidate vaccine, the mice sera were analyzed two weeks after the first and the third immunizations and antibody titers were determined in the pooled mice sera from each group (3-5 mice). To perform ELISA, we used four synthetic peptides whose sequences corresponded to the M2e of the swine flu virus A/California/04/2009, two strains of avian flu, and a human strain, A/PR/8/34. The results obtained (Table 3) show that after three immunizations the serum antibodies of isotope IgG are produced in high tit-

Table 3. Titers of IgG antibodies against M2e in sera of immunized mice.

Serum samples	Titers of antibodies recognizing synthetic M2e peptides			
	G-26	G-19	G-11-1	G-18
After first immunization	1600	1600	800	800
After third immunization	51200	51200	51200	6400
Positive control (monoclonal antibodies against G19 peptide, clone D2)	>51200	>51200	>51200	1600
Negative control (sera of nonvaccinated mice)	<400	<400	<400	<400

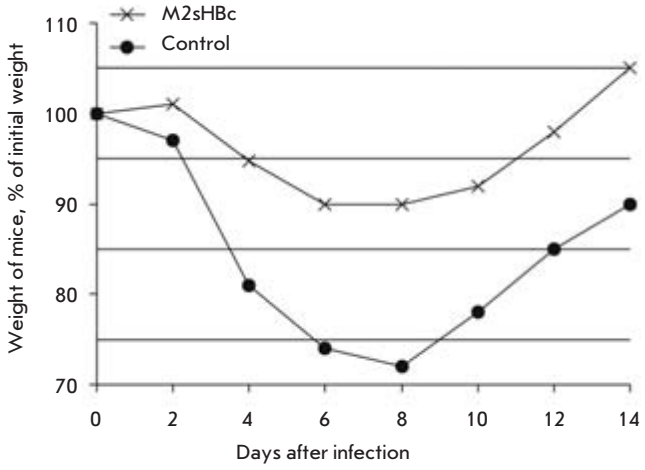

Fig. 2. Dynamics of body weight of mice after challenge with influenza virus A/California/04/2009 (H1N1). Data in the control are shown for survived mice.

ers. These antibodies bind both synthetic peptides G-26 of the swine flu A/California/04/2009 (H1N1), the sequence of which matched one in M2sHBc used for the immunization, as well as synthetic peptides, the sequences of which correspond to the M2e of heterological strains of the avian and human influenza.

Protective action of the candidate vaccine

In order to evaluate the effectiveness of the vaccine, mice in both the experimental and control groups were challenged with three influenza strains adapted to mice: A/Duck/Potsdam/1402-6/1986 (H5N2), A/California/04/2009 (H1N1), and A / PR / 8 / 34 (H1N1). Viruses were administered intranasally at a dose of 5 LD50.

Figure 2 shows the body weight loss dynamics of animals after infection with 5 LD50 of the swine flu virus A/California/4/2009, which could indicate the severity of the disease. The weight of the immunized animals dropped after infection (to 90% of the initial weight), but to a much lesser extent than that of mice in the control group (up to 70% of the initial weight). These results indicate that immunization with can-

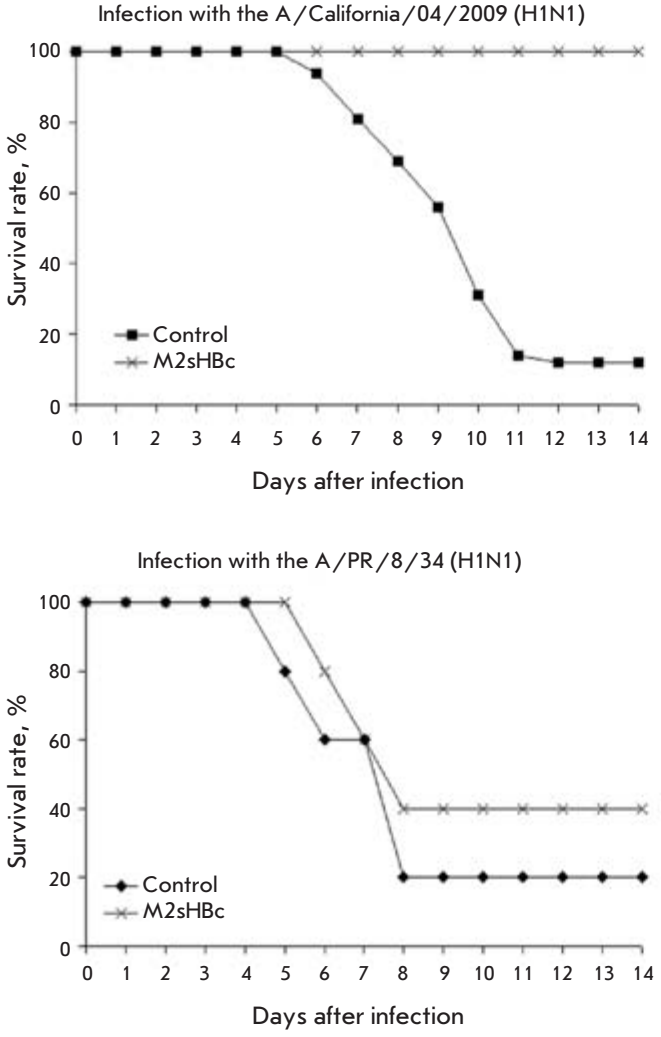

Fig. 3. Survival of mice immunized with M2sHBc, followed by a potentially lethal challenge with different mouse-adapted influenza strains.

didate vaccines will not prevent influenza infection, but that it will reduce the morbidity.

The dynamics of mice death after infection with various influenza strains are shown in Fig. 3. The results suggest that M2sHBc provides complete protection after a triple immunization. Over the entire period of observation, all of the animals in this group survived, whereas in the control group of mice subjected to these same infection conditions only 12% of animals survived. Partial protection against infection was observed against influenza strains in which the amino acid sequence of the M2e peptide differs from the one used in the preparation for immunization. Thus, 60% of immunized animals survived upon infection with the avian flu A/Duck/Potsdam/1402-6/1986 as opposed to 12% in the control group (statistical significance $P < 0.006$, Fisher test). When infected with a "human" influenza strain A/PR/8/34, the survival rate of animals was 40% in the experimental group and 20% in the control.

Prospects for the development of universal influenza vaccines based on M2e

The conservation of an amino acid sequence of the M2 protein has become a basis for the development of a universal influenza vaccine. Since practically all type A influenza viruses isolated from the human population have the same sequence of M2e, the prospects for the creation of such a vaccine are real [5]. However, strains of animal origin, such as the "swine flu" virus, that have appeared in recent years have differences in the M2e peptide sequence, and, as shown through our results, the effectiveness of an M2e-based vaccine against heterologous strains of influenza is lower. One of the ways to create a M2e vaccine effective against a wide range of influenza strains, both human and animal, can be through the inclusion of several copies of M2e peptide sequences corresponding to different types of M2e into the M2sHBc particles.

CONCLUSIONS

The purpose of this study was to develop a recombinant candidate vaccine against a new, highly pathogenic strain of the influenza A virus: the swine flu H1N1. We used an approach intended to design a nanovaccine in which an extracellular domain of the M2 protein of the influenza virus was introduced on the surface of the virus-like particles formed by a nuclear antigen of hepatitis B. Our data show that the hybrid protein M2sHBc was efficiently expressed in *E. coli* and self-assembled in nanosized virus-like particles. Mice immunization with M2sHBc particles generates an effective immune response against M2e, and it ensures immunity against an influenza virus strain that has an identical M2e peptide sequence. Thus, M2sHBc particles can be used as a basis for the development of a recombinant vaccine against the modern pandemic swine flu H1N1 and other viruses whose appearance is expected in the coming years. ●

REFERENCES

1. Nicholson K., Webster R., Hay A. Textbook of Influenza. Oxford: Blackwell Science, 1998.
2. Webster R., Bean W., Gorman O., Chambers T., Kawaoka Y. // Microbiol. 1992. Rev. 56. P. 152–179.
3. Webby R., Perez D., Coleman J., et al. // Lancet. 2004. V. 363. P. 1099–1103.
4. Neirynck S., Deroo T., Saelens X., et al. // Nat. Med. 1999. V. 5. P. 1157–1163.
5. Schotsaert M., De Filette M., Fiers W., Saelens X. // Expert Rev Vaccines. 2009. V. 8(4). P. 499–508.
6. Lamb R., Zebedee S., Richardson C. // Cell. 1985. V. 40. P. 627–633.
7. Pinto H., Holsinger J., Lamb A. // Cell. 1992. V. 69. P. 517–528.
8. Fiers W., De Filette M., Birkett A., Neirynck S., Min Jou W. // Virus Res. 2004. V. 103. P. 173–176.
9. Ito T., Gorman, O., Kawaoka Y., Bean W., Webster, R. // J. Virol. 1991. V. 65. P. 5491–5498.
10. Feng J., Zhang M., Mozdzanowska K., et al. // Virol. J. 2006. V. 3. P. 102.
11. De Filette M., Min Jou W., Birkett A., et al. // Virology. 2005. V. 337 (1). P. 149–161.
12. Ionescu R., Przysiecki C., Liang X., et al. // J. Pharm. Sci. 2006. V. 95 (1). P. 70–79.
13. Bessa J., Schmitz N., Hinton H., et al. // Eur. J. Immunol. 2008. V. 38 (1). P. 114–126.
14. Denis J., Acosta-Ramirez E., Zhao Y., et al. // Vaccine. 2008. V. 26 (2728) P. 3395–3403.
15. Meshcheriakova Iu.A., El'darov M.A., Migunov A.I. et al. // Mol. Biol. (Mosk). 2009. V. 43 (4). P. 741-750.
16. De Filette M., Fiers W., Martens W., et al. // Vaccine. 2006. V. 24 (4446) P. 6597–6601.
17. Tompkins S., Zhao Z., Lo C., et al. // Emerg. Infect. Dis. 2007. V. 13 (3) P. 426–435.
18. Grant S., Jessee J., Bloom F., Hanahan D. // Proc. Natl Acad. Sci. USA. 1990. V. 87. P. 4645–4649.
19. Wynne S., Crowther R., Leslie A. // Mol. Cell. 1999. V. 3. P. 771–780.
20. Kratz P., Bottcher B., Nassal M. // Proc. Natl. Acad. USA. 1999. V. 96. P. 1915–1920.
21. Murray K., Shiau A.L. // Biol. Chem. 1999. V. 380. P. 277–283.
22. Pumpens P., Grens E. // Intervirology. 2001. V. 44. P. 98–114.
23. Wingfield P., Stahl S., Williams R., Steven A. // Biochemistry. 1995. V. 34. P. 4919– 4932.
24. Zheng J., Schodel F., Peterson D. // J. Biol. Chem. 1992. V. 267. P. 9422–9429.

Effects of Myosin "Essential" Light Chain A1 on the Aggregation Properties of the Myosin Head

D. I. Markov[1], O. P. Nikolaeva[2], D. I. Levitsky[1,2]*
[1] Bach Institute of Biochemistry, Russian Academy of Sciences
[2] Belozersky Institute of Physico-Chemical Biology, Lomonosov Moscow State University
*E-mail: levitsky@inbi.ras.ru
Received 24.05.2010

ABSTRACT **We compared the thermal aggregation properties of two isoforms of the isolated myosin head (myosin subfragment 1, S1) containing different "essential" (or "alkali") light chains, A1 or A2. Temperature dependencies for the aggregation of these two S1 isoforms, as measured by the increase in turbidity, were compared with the temperature dependencies of their thermal denaturation obtained from differential scanning calorimetry (DSC) experiments. At relatively high ionic strength (in the presence of 100 mM KCl) close to its physiological values in muscle fibers, we have found no appreciable difference between the two S1 isoforms in their thermally induced aggregation. Under these conditions, the aggregation of both S1 isoforms was independent of the protein concentration and resulted from their irreversible denaturation, which led to the cohesion of denatured S1 molecules. In contrast, a significant difference between these S1 isoforms was revealed in their aggregation measured at low ionic strength. Under these conditions, the aggregation of S1 containing a light chain A1 (but not A2) was strongly dependent on protein concentration, the increase of which (from 0.125 to 2.0 mg/ml) shifted the aggregation curve by ~10 degrees towards the lower temperatures. It has been concluded that the aggregation properties of this S1 isoform at low ionic strength is basically determined by intermolecular interactions of the N-terminal extension of the A1 light chain (which is absent in the A2 light chain) with other S1 molecules. These interactions seem to be independent of the S1 thermal denaturation, and they may take place even at low temperature.**
KEYWORDS **myosin subfragment 1, "essential" light chains, aggregation, thermal denaturation, differential scanning calorimetry**

INTRODUCTION

Cyclic interaction of the heads of myosin molecules with actin filaments accompanied by ATP hydrolysis underlies the molecular mechanism of biological motility in its various forms (from the events of intracellular transport to muscle contraction). It has been revealed that the myosin head is an example of a molecular motor which is able to fulfill its functions even when isolated [1]. A single myosin head, which is usually referred to as subfragment 1 (S1), is composed of two major structural domains known as the motor (or catalytic) domain and the regulatory domain. The motor domain is a globular structure containing both the ATPase active site and actin-binding site, whereas the regulatory domain is a long α-helix stabilized by noncovalent interactions with two other polypeptides, which are also known as essential and regulatory myosin light chains [2]. The present concept of the myosin motor function includes the rotation of the regulatory domain relative to the motor domain. During this rotation, the regulatory domain acts as a "lever arm" which amplifies and transmits conformational changes occurring in the motor domain during ATP hydrolysis. It has also been shown that the length of the "lever arm" (i.e., the regulatory domain) affects the amplitude of myosin head movement along the actin filament [3, 4].

The essential light chains associated with the regulatory domain of the myosin head are known to have two isoforms (a "long" one and a "short" one). Myosin from the cardiac muscle contains only the long light chain, whereas in a smooth muscle only the short chain is present. In fast skeletal muscle there are two kinds of the light chains, usually referred to as alkali light chains and designated A1 and A2 for the long and the short isoforms, respectively. These light chains are nearly identical, with the only exception being an additional N-terminal sequence of extra 41 residues present in A1 isoform. This N-terminal extension contains multiple Ala-Pro repeats, as well as some lysine residues [5]. The presence of the N-terminal extension remains unclear in terms of function and is subjected to extensive investigation. For example, it has recently been shown that mutations in this region tend to be associated with a type of severe congenital disorder known as hypertrophic cardiomyopathy [6].

S1 prepared by the chymotryptic digestion of skeletal-muscle myosin lacks the regulatory light chain but does contain the essential light chain [7]. Since the myosin of skeletal muscles contains alkali chains of both types, such an S1 preparation is essentially a mixture of myosin heavy chains complexed with either A1 or A2 (S1(A1) and S1(A2), respectively). These S1 species can be separated by means of ion-

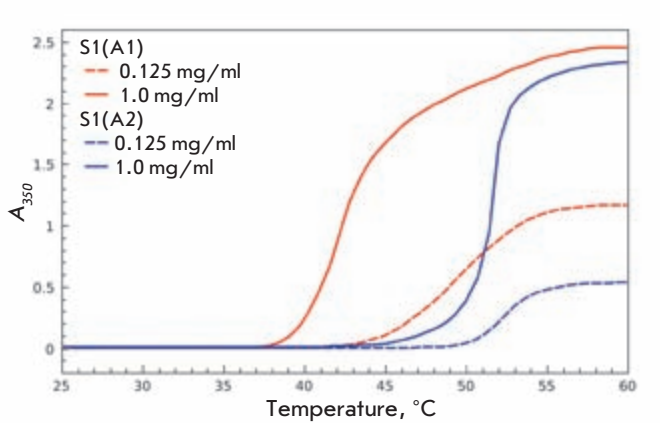

Fig.1. Temperature dependencies of the S1(A1) and S1(A2) thermal aggregations measured as an increase in apparent optical density at 350 nm at high (1 mg/ml) and low (0.125 mg/ml) protein concentrations. Other conditions are as follows: 20 mM Hepes, pH 7.3, 1 mM $MgCl_2$.

exchange chromatography [7] and used for a comparative functional analysis of A1 and A2 light chains, as well as for investigating the role of the N-terminal extension in A1. It was shown that, at low ionic strength, the S1(A1) affinity to actin greatly exceeds that of S1(A2) [8, 9] and N-terminal extension is involved in an additional interaction of A1 with actin filaments [10–13]. It is noteworthy that this interaction is merely observed at a low ionic strength, which is far from its physiological value and is shown to decrease markedly at 120 mM ionic strength [9].

Another intriguing feature of A1 N-terminal extension is its putative ability to interact with the globular motor domain of the myosin head. The possibility of this interaction was suggested by one of us more than 15 years ago [14] and was subsequently confirmed in works by other authors [15–17]. One recent study has revealed an interaction between the A1 N-terminal extension and the SH3 domain located near the N-terminus of the heavy chain (residues 35–80) [17]. The authors hypothesize that such a binding might play a significant role in the actin-myosin interaction, facilitating the straightening of the N-terminal extension into an antenna-like structure which is able to reach the surface of the actin filament.

Another interesting difference between the two S1 isoforms was revealed in earlier studies. Namely, it was shown that, at low ionic strength, S1(A1) aggregates at a substantially lower temperature than S1(A2) [18, 19]. It seems possible that, due to its semirigid extended structure, the A1 N-terminal segment can participate not only in intramolecular interactions, but also in intermolecular interactions with the motor domains of other S1 molecules. However, it should be noted that all previous experiments on S1 isoforms aggregation were carried out at very low ionic strengths and high protein concentrations [18, 19]. Unfortunately, nobody has undertaken a more thorough investigation of the thermal aggregation of S1 isoforms and the role of A1 N-terminal extension in this process. Therefore, a reasonable question arises: can intermolecular (or intramolecular) interactions of A1 N-terminal extension with the S1 motor domain affect S1 thermal aggregation at nearly physiological values of ionic strength? This is not a straightforward question, since a combined preparation of two S1 isoforms undergoes intensive thermal aggregation at the heat shock temperature (43°C) under salt conditions close to those in muscle fiber (100 mM KCl) [21]. In order to answer this question, in this study we performed a comparative analysis of the temperature dependencies of S1(A1) and S1(A2) aggregation at various ionic strengths and protein concentrations. We also compared the S1 thermal aggregation profiles with the temperature dependencies of its thermal denaturation obtained by differential scanning calorimetry (DSC).

EXPERIMENTAL PROCEDURES

S1 was prepared by the digestion of rabbit skeletal myosin with α-chymotrypsin [7]. S1(A1) and S1(A2) preparations were obtained by ion exchange chromatography on a column of SP-trisacryl [22]. S1 concentration was estimated spectrophotometrically using the extinction coefficient $E^{1\%}$ at 280 nm of 7.5 cm^{-1}. The absorption spectra of S1 isoforms were recorded on a Cary-100 spectrophotometer (Varian Inc.).

The temperature dependencies of S1-isoform aggregation were registered as an increase in the apparent optical density at 350 nm. The measurements were conducted on a Cary-100 spectrophotometer (Varian Inc.) equipped with a Biomelt thermostatted cell holder. The S1 samples were heated at a constant rate of 1 °C/min from 25 °C up to 65 °C. All measurements were carried out in a 20 mM Hepes-KOH buffer (pH 7.3) containing 1 mM $MgCl_2$ in the presence or absence of 100 mM KCl.

Thermal denaturation studies on S1(A1) and S1(A2) were carried out by means of DSC on a DASM-4M differential scanning microcalorimeter (Institute for Biological Instrumentation, Russian Academy of Sciences (RAS), Pushchino, Russia) as described earlier [21, 23, 24]. Samples containing S1 isoforms (1.5 mg/ml) were heated at a 1 °C/min rate from 15 °C to 75 °C in a 20 mM Hepes-KOH (pH 7.3) containing 1 mM $MgCl_2$ in the presence or absence of 100 mM KCl. In order to check the reversibility of thermal denaturation after the first scan and subsequent cooling, protein samples were reheated. The thermal denaturation of both S1 isoforms was fully irreversible.

RESULTS AND DISCUSSION

First of all, we were able to reproduce our longstanding results [19] comparing the thermal aggregation profiles of the two S1 isoforms at a high protein concentration (1 mg/ml) and a low ionic strength (in the absence of KCl). Figure 1 shows that, under these conditions, the S1 isoforms substantially differ in the character of their thermal aggregation: S1(A1) aggregates at a much lower temperature than S1(A2) does. This difference between the isoforms becomes less pronounced at lower protein concentrations as is seen in Fig.1. Under these conditions, the half-maximum of increase in optical density for S1(A2) remains nearly the same (52–53 °C), while this parameter for S1(A1) shifts from 42.5 to 50 °C as the protein concentration is decreased from 1 mg/ml to 0.125 mg/ml. Thus, a decrease in protein concentration at low ionic strength strongly affects S1(A1) thermal aggregation.

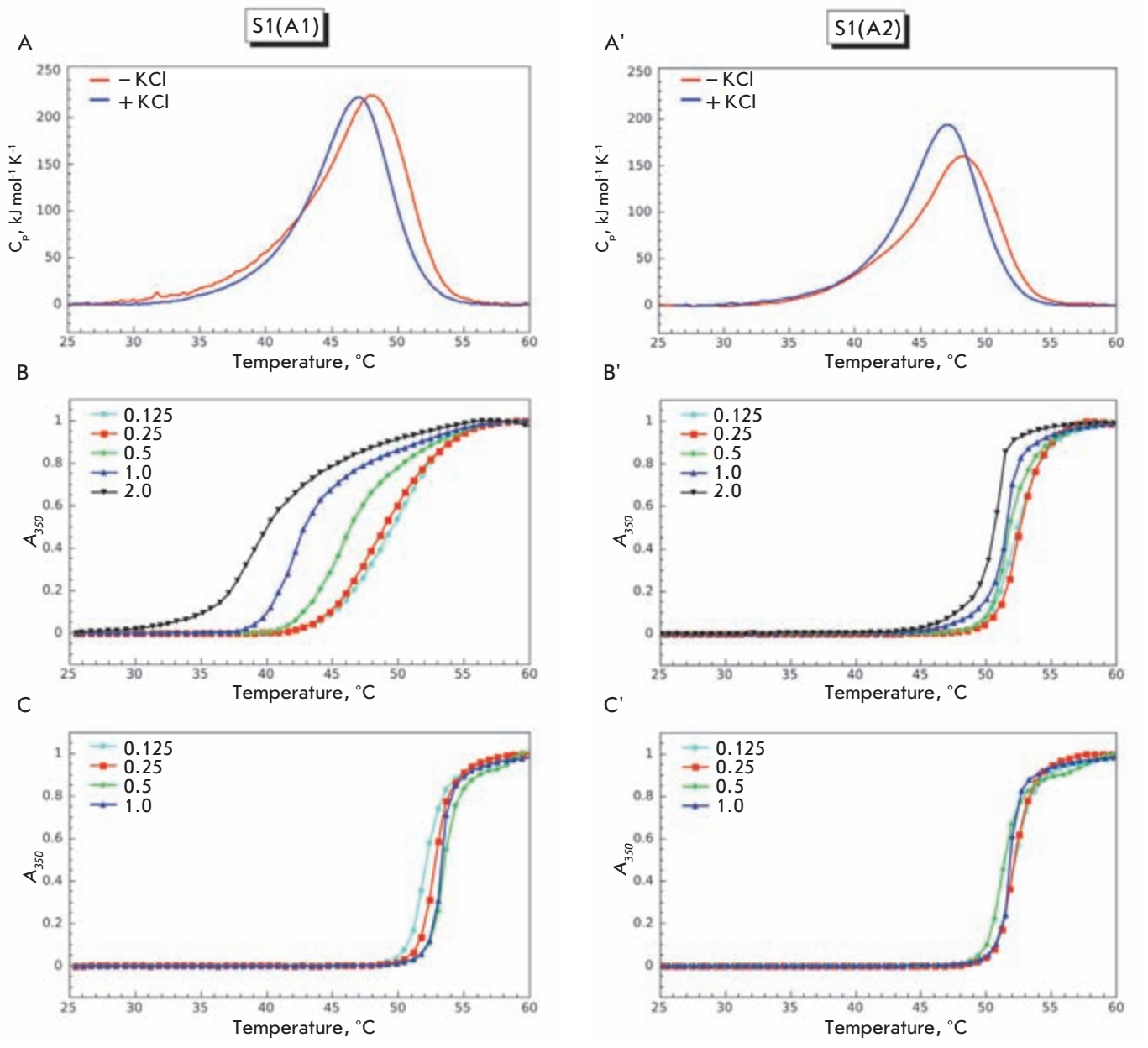

Fig. 2. Thermal denaturation and aggregation of isoforms S1(A1) (A–C) and S1(A2) (A`–C`). (A, A`) DSC curves obtained in the presence or absence of 100 mM KCl. (B, B`, C, C`) normalized temperature dependences of thermal aggregation of S1 isoforms obtained at various protein concentrations marked in each plot in the absence of KCl (B, B`) or in the presence of 100 mM KCl (C, C`). All experiments were performed at a heating rate of 1 °C/min. Other conditions are as follows: 20 mM Hepes, pH 7.3, 1 mM $MgCl_2$.

At the same time, the thermal aggregation of S1(A2) does not exhibit a strong dependence on protein concentration.

In subsequent experiments, we compared the normalized temperature dependencies of S1(A1) and S1(A2) aggregation obtained at different protein concentrations in the absence or presence of 100 mM KCl with the DSC profiles, which reflect thermal denaturation of the S1 isoforms under the same conditions. It is important to note that all the experiments were performed at the same heating rate (1 °C/min) and under similar salt conditions. However, the protein concentration remained constant (1.5 mg/ml) in DSC experiments, since earlier it had been shown that the variation in the protein concentration in the range of 0.5–2.0 mg/ml does not affect the temperature maximum of S1 heat-sorption curves [19]. Therefore, a comparison of the temperature dependencies of thermal denaturation and aggregation seems reasonable.

The addition of KCl did not appreciably affect the thermal denaturation of both S1 isoforms, shifting the temperature maximum of the heat-sorption curve by 1.1 ˚C towards lower temperatures (from 48 to 46.9 ˚C in the case of S1(A1) or from 48.1 to 47 ˚C in the case of S1(A2); see Figs. 2A and 2A'). On the contrary, the salt concentration largely affected the thermal aggregation profile of S1(A1) but not S1(A2). If there was a low ionic strength, we observed a clear dependence of aggregation on the S1(A1) concentration. When the concentration increased from 0.125 to 2.0 mg/ml, the aggregation curve shifted by ~10˚C towards lower temperatures (from ~ 50 to ~ 40 ˚C; Fig. 2B). Such effects were not observed in the presence of 100 mM KCl. In this case, the thermal aggregation of S1(A1) was almost independent of protein concentration: when the concentration of S1(A1) increased from 0.125 to 1.0 mg/ml, the temperature of the half-maximum increase in optical density was constant and equal to 52 ± 0.5 ˚C (Fig. 2C). In the case of S1(A2), heat aggregation was independent of both protein concentration and ionic strength (Figs. 2B`, 2C`) and did not differ from S1(A1) aggregation at a high ionic strength (Fig. 2C).

From a comparison of thermal aggregation curves for S1 isoforms and the DSC profiles, which reflect their thermal denaturation, some conclusions can be drawn. First of all, the aggregation of S1(A2) is a result of its thermal denaturation. It seems possible that thermal denaturation of its more thermostable motor domain [14, 19] is responsible for the aggregation, since the denaturation of this domain has been shown to limit the aggregation of S1(A2). This is also applicable to the S1(A1) thermal aggregation at a high ionic strength (Fig. 2C). However, S1(A1) aggregation at a low ionic strength appears to be different (Fig. 2B), because it is characterized by the absence of any correlations between S1(A1) aggregation and denaturation. We assume that under these conditions S1(A1) aggregation is not determined by the protein thermal denaturation and can be at least partially explained by additional interactions between the A1 N-terminal extension and other S1 molecules. Obviously, the probability of such interactions must increase at higher protein concentrations and higher temperatures. Therefore, this could explain the unusual aggregation profile observed in the case of S1(A1) at low ionic strength (Fig. 2B). At high ionic strength, the intermolecular interactions of the A1 N-terminal extension should be weakened, which explains the observed similarity between the S1(A1) and S1(A2) aggregation profiles in the presence of 100 mM KCl (Fig. 2C, 2C`).

When thoroughly analyzing the S1(A1) aggregation curves obtained at low ionic strength (Fig. 2B), one may notice that, at high protein concentrations, aggregation starts at relatively low temperatures (below 38 ˚C). Therefore, we can suggest that, at low ionic strength, S1(A1) aggregation based on the intermolecular interactions of the A1 N-terminal extension can occur slowly at a low temperature. Actually, we have observed noticeable opalescence in S1(A1) preparations which disappeared after the addition of 100 mM KCl. (It is noteworthy that, in thermal aggregation experiments, these opalescent S1(A1) preparations had been preliminarily subjected to ultracentrifugation.) These observations were confirmed by experimental results shown in Figure 3. As is seen, keeping the S1(A1) preparation overnight at 4 ˚C leads to an increase

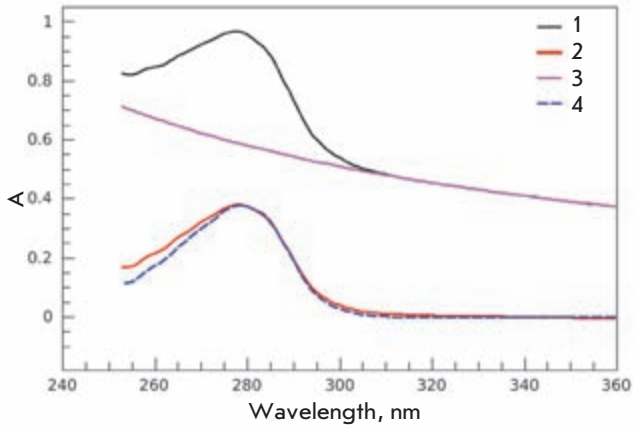

Fig. 3. Absorption spectra of a S1(A1) preparation (1 mg/ml), stored at 4 ˚C at low ionic strength (20 mM Hepes, pH 7.3, 1 mM $MgCl_2$) measured before (*1*) and after (*2*) addition of KCl up to a concentration of 100 mM. Curve *3* was obtained by extrapolation of the long-wavelength part of S1(A1) absorption spectrum into its short- wavelength region, and it reflects light-scattering of the S1(A1) preparation at low ionic strength in the entire wavelength range. Curve *4* was obtained by subtracting curve *3* from curve *1*.

in light scattering in the range of 320–360 nm, i.e. where proteins do not absorb (Fig.3, curve *1*). The opalescence fully disappears after the addition of 100 mM KCl (Fig.3, curve *2*). Extrapolating from the high wavelength range of the S1(A1) absorption spectrum, we were able to deduce the wavelength dependence of the sample's light scattering within the whole range of wavelengths (255–360 nm). Subtracting this curve (Fig 3, curve *3*) from the measured S1(A1) absorption spectra yielded curve *4*, which corresponds to the S1(A1) spectra with no impact of light scattering. The latter was indistinguishable from the S1(A1) spectra measured in the presence of 100 mM KCl (Fig.3, curve *2*).

The results of this experiment clearly show that S1(A1) aggregation based on intermolecular interactions of the A1 N-terminal extension at low ionic strength can even take place during the storage of an S1(A1) preparation in a fridge. This aggregation is reversible, because the forming aggregates can be easily dissolved at a high ionic strength. At this point, the reversible aggregation strongly differs from thermal denaturation-induced irreversible aggregation, which is accompanied by the cohesion of denatured protein molecules.

Therefore, the described experiments lead to the conclusion that the difference in the aggregation properties of the S1 isoforms is based on an additional interaction between the A1 N-terminal extension, which is absent in A2 light chain, and other S1 molecules. These interactions occur only at low ionic strength and are suppressed at a high ionic strength. These interactions take place even at a low temperature, though the probability of their formation increases at higher temperatures. To all appearances, these intermolecular interactions reflect the ability of the A1 N-terminal extension to bind to the motor domain of the same S1 molecule. Such an interaction is supposed to play an important role in the mechanism of

muscle contraction [16, 17]. However, it should be noted that all previous studies on the intramolecular interactions of the A1 myosin light chain were performed at a low ionic strength (~25 mM) [17], which is far from its physiological values. We can suggest that the probability of these intramolecular interactions should increase during the ATPase reaction. This could be due to the A1 N-terminal extension being brought into close proximity with the S1 motor domain, which could possibly occur as a consequence of the rotation of the regulatory domain relative to the motor domain. This, in turn, would decrease the probability of intermolecular interactions of the A1 N-terminal segment, which should affect the aggregation properties of S1(A1) when intermediate states of the ATPase reaction are modeled in an experiment. These assumptions need to be experimentally confirmed, which is among the goals of future studies in this field.

CONCLUSIONS

In this study we have shown that, at a relatively high ionic strength (close to that in the muscle fiber), the presence of an additional N-terminal segment in the myosin A1 light chain does not affect the aggregation properties of the isolated myosin head (S1). Under these conditions, S1 thermal aggregation follows its thermal denaturation and is caused by the cohesion of denatured protein molecules. A noticeable influence of the A1 N-terminal segment on the S1 aggregation is observed only at a relatively low ionic strength. Under these conditions, the intermolecular interactions of the A1 N-terminal extension appear to be the main factor underlying the aggregation properties of S1. These intermolecular interactions of the A1 N-terminal segment reflect its ability to form intramolecular interactions, which are thought to play an important role in muscle contraction. Presumably, under certain conditions (e.g., during the ATPase reaction, which is accompanied by considerable conformational changes in the myosin head), intramolecular interactions of the A1 N-terminal segment can take place in muscle fibers even at a relatively high ionic strength. ●

This work was supported by the Russian Foundation for Basic Research (grant 09-04-00266), the Program "Molecular and Cell Biology" of the Russian Academy of Sciences, and a grant from the President of the Russian Federation (grant MK 2965.2009.4).

REFERENCES

1. Levitsky D.I. // Biochemistry (Moscow). 2004. V. 69. № 11. P. 1177–1189.
2. Rayment I., Rypniewski W.P., Schmidt-Base K., et al. // Science. 1993. V. 261. P. 50–58.
3. Rayment I. // J. Biol. Chem. 1996. V. 271. P. 15850–15853.
4. Uyeda T.Q., Abramson P.D., Spudich J.A. // Proc. Natl. Acad. Sci. USA. 1996. V. 93. P. 4459–4464.
5. Frank G., Weeds A.G. // Eur. J. Biochem. 1974. V. 44. P. 317–334.
6. Hernandez O.M., Jones M., Guzman G., Szczesna-Cordary D. // Am. J. Physiol. Heart Circ. Physiol. 2007. V. 292. P. H1643–H1654.
7. Weeds A.G., Taylor R.S. // Nature. 1975. V. 257. P. 54–56.
8. Wagner P.D., Slayter C.S., Pope B., Weeds A.G. // Eur. J. Biochem. 1979. V. 99. P. 385–394.
9. Chalovich J.M., Stein L.A., Greene L.E., Eisenberg E. // Biochemistry. 1984. V. 23. P. 4885–4889.
10. Sutoh K. // Biochemistry. 1982. V. 21. P. 3654–3661.
11. Trayer I.P., Trayer H.R., Levine B.A. // Eur. J. Biochem. 1987. V. 164. P. 259–266.
12. Hayashibara T., Miyanishi T. // Biochemistry. 1994. V. 33. P. 12821–12827.
13. Andreev O.A., Saraswat L.D., Lowey S., et al. // Biochemistry. 1999. V. 38. P. 2480–2485.
14. Levitsky D.I. Domain Structure of the Myosin Head // Soviet Scientific Reviews. Section D – Physico-chemical Biology. Harwood Acad. Publishers GmbH. 1994. V. 12. № 1. 53 p.
15. Pliszka B., Redowicz M.J., Stepkowski D. // Biochem. Biophys. Res. Commun. 2001. V. 281. P. 924–928.
16. Borejdo J., Ushakov D.S., Moreland R., et al. // Biochemistry. 2001. V. 40. P. 3796–3803.
17. Lowey S., Saraswat L.D., Liu H., et al. // J. Mol. Biol. 2007. V. 371. P. 902–913.
18. Mrakovcic-Zenic A., Oriol-Audit C., Reisler E. // Eur. J. Biochem. 1981. V. 115. P. 565–570.
19. Levitsky D.I., Nikolaeva O.P., Vedenkina N.S., et al. // Biomed. Sci. 1991. V. 2. № 2. P. 140–146.
20. Abillon E., Bremier L., Cardinaud R. // Biochim. Biophys. Acta. 1990. V. 1037. P. 394–400.
21. Markov D.I., Pivovarova A.V., Chernik I.S., et al. // FEBS Lett. 2008. V. 582. № 10. P. 1407–1412.
22. Trayer H.R., Trayer I.P. // Biochemistry. 1988. V. 27. P. 5718–5727.
23. Nikolaeva O.P., Orlov V.N., Bobkov A.A., Levitsky D.I. // Eur. J. Biochem. 2002. V. 269. № 22. P. 5678–5688.
24. Shakirova L.I., Mikhailova V.V., Siletskaya E.I., et al. // J. Muscle Res. Cell Motil. 2007. V. 28. P. 67–78.

Influence of Ion Strength and pH on Thermal Stability of Yeast Formate Dehydrogenase

V. I. Tishkov[1,2,3]*, S. V. Uglanova[1,4], V. V. Fedorchuk[1], S. S. Savin[2,3]
[1]Department of Chemical Enzymology, Faculty of Chemistry, Lomonosov Moscow State University
[2]Innovations and High Technologies MSU Ltd.
[3]Bach Institute of Biochemistry, Russian Academy of Sciences
[4]Emanuel Institute of Biochemical Physics, Russian Academy of Sciences
*E-mail: vitishkov@gmail.com

ABSTRACT **The kinetics of the thermal inactivation of recombinant wild-type formate dehydrogenase from *Candida boidinii* yeast was studied in the temperature range of 53–61°C and pH 6.0, 7.0, and 8.0. It was shown that the loss of the enzyme's activity proceeds via a monomolecular mechanism. Activation parameters $\Delta H^{\neq}$ and $\Delta S^{\neq}$ were calculated based on the temperature relations dependence of inactivation rate constants according to the transition state theory. Both parameters are in a range that corresponds to globular protein denaturation processes. Optimal conditions for the stability of the enzyme were high concentrations of the phosphate buffer or of the enzyme substrate sodium formate at pH = 7.0.**

KEYWORDS **formate dehydrogenase, *Candida boidinii*, thermal inactivation, ionic strength, stabilization**
ABBREVIATIONS **FDH – NAD+-dependent formate dehydrogenase, PseFDH – FDH from *Pseudomonas* sp.101 bacteria, PseFDH GAV – mutant FDH from Pseudomonas sp.101 GAV version, CboFDH – FDH from *Candida boidinii* yeast**

INTRODUCTION

NAD^+-dependent formate dehydrogenase (EC 1.2.1.2, FDH) belongs to the superfamily of D-specific dehydrogenases of 2-hydroxyacids [1]. Because of the simplicity of the catalyzed reaction, which is a simple transfer of the hydride ion in the active site between the formate and the C4 atom of the nicotinamide ring with no acidic-basic catalysis involved, FDH is used as a model system for studying the enzyme catalytic mechanism of the whole superfamily.

The most thoroughly studied FDHs are the ones derived from bacterium *Pseudomonas* sp.101 (PseFDH) and from yeast *Candida boidinii* (CboFDH). Studies of both of these enzymes started almost simultaneously in the early 1970s. There is now a large number of mutant forms of these enzymes [2], and their quaternary structure has been determined using X-ray analysis [3–5]. Plant FDHs, which are localized in the mitochondria, are also an interesting topic for research. *Escherichia coli* strains which produce recombinant plant FHDs from *Arabidopsis thaliana* and soy *Glycine max* have been constructed in our laboratory [6]. Crystals of these FHDs were obtained very recently, and the structures of the enzymes have been mapped [7].

One of the most important characteristics of an enzyme is its thermal stability. This is a very important parameter for the practical use of an enzyme. We have conducted systematic studies of the thermal inactivation of the wild-type *Pseudomonas* sp.101 FDH, as well as that of mutant forms of this enzyme at various temperatures, pH, and concentrations of a phosphate buffer [2, 8]. We were able to show that an increase in the solution's ionic strength causes the observed inactivation rate constant to reach its maximum and that an elevated (several fold) stability of the enzyme can be observed at high concentrations of the phosphate buffer [8]. There are no such data for yeast *C. boidinii* FDH in the available literature; however, indirect data indicate that the effect of the surrounding solution on the stability of CboFDH may be even stronger. For instance, the half-time inactivation period of the enzyme is a few days during storage at +4°C in a 0.1 M phosphate buffer, pH7.0; that is why CboFDH samples should be stored in 40% glycerol at −20°C. However, the enzyme can remain activitve for several weeks during the synthesis of *L*-tert-leucine at a temperature of 25–30°C in a flow membrane reactor [9]. This process involves a high concentration of the CboFDH substrate ammonium formate, which suggests that the presence of the substrate stabilizes the enzyme.

The aim of this work was to carry out a systematic study of the stability of recombinant wild-type CboFDH at increased temperatures and pH 6.0–7.0, as well as at varying concentrations of phosphate buffer and the substrate of the enzyme, sodium formate.

EXPERIMENTAL PROCEDURES

For this work we used a preparation of recombinant formate dehydrogenase originating from wild-type *Candida boidinii yeast*. Cultivation of *E. coli* (BL21(DE3)/pCboFDH) cells expressing the *C. boidinii FDH* was performed at 25°C in 250 ml or 1l shaker flasks with baffles using 50 or 250 ml of medium, respectively. The medium consisted of 16 g/l

tryptone, 10 g/l of yeast extract, 1 g/l of sodium chloride, 1.5 g/l of H2NaPO4, 1 g/l of HK2PO4, 100 micrograms/ml of ampicillin, and 25 micrograms/ml of chloramphenicol. The volume of the bacterial inoculate was equal to 10–15% of the medium volume. Lactose was used for the unduction of FDH biosynthesis and an inducer was added to a final concentration of 20 mg/ml when absorbance of the cell suspension at 600 nm (A_{600}) reached the value 0.5–0.7 . The cells were then grown in maximum aeration overnight. Then, the cells were spun down on a Beckman J-21 (United States) centrifuge at 8000 rpm for 20 minutes at 4°C. Recombinant CboFDH was then purified according to the standard protocol developed for *Pseudomonas* sp.101 FDH [10]. The enzyme purification procedure involved the destruction of the 10% w/v cell suspension in a 0.1 M potassium-phosphate buffer, 0.02 M EDTA, and pH 8.0 using a Braun Sonic ultrasound disintegrator (Germany) at 0°C, the precipitation of some of the ballast proteins with ammonium sulfate (35% of saturation), hydrophobic chromatography on a Fast Protein Liquid Chromatography (FPLC) apparatus (Pharmacia Biotech, Sweden) using a column with Phenyl Sepharose Fast Flow from the same company, and gel filtration on a Sephacryl S200 column. The obtained preparations were at least 95% pure as assayed by an analytical gel electrophoresis in a 12% polyacrylamide gel in denturating conditions.

Formate dehydrogenase activity assay

FDH activity was measured spectrophotometrically by monitoring the accumulation of NADH at a wavelength of 340 nm (ε_{340} = 6220 $M^{-1} cm^{-1}$) on a Schimadzu UV 1601PC spectrophotometer at 30°C in a 0.1 M sodium–phosphate buffer, pH 7.0. Saturated NAD^+ and formate concentrations in the cuvette were 1.5 мМ and 0.3 M, respectively.

Study of the thermal inactivation of recombinant CboFDH

The thermal stability of the enzyme was assayed in a sodium phosphate buffer at a given concentration in the 0.01–1.5 M (pH 6.0–8.0) range and supplemented by 0.01 M EDTA and, depending on the type of experiment, 0.1–2.5 M of sodium formate. Each experiment used a series of 1.5 ml plastic tubes with 100 microliters of the enzyme solution (0.2–0.25 mg/ml). The tubes were placed into a preheated water thermostat (53–61°C, accuracy ±0.1°C). The tubes were taken out at regular intervals, transferred into an ice bath for 5 min, and then spun down for 2 min at 12 000 rpm in an Eppendorf 5415D centrifuge. The remaining FDH activity was assayed as described above. The thermal inactivation rate constant k_{in} was determined as the slope of the plot of a natural logarithm of the remaining activity value versus time (semilogarithmic coordinates $\ln(A/A_0) - t$) using the linear regression method available in the Origin 7.0 software package.

RESULTS AND DISCUSSION

Effect of pH on the Thermal Inactivation Rate of Recombinant *C. boidinii FDH*.

Previous studies of bacterial FDH from *Pseudomonas* sp.101 at temperatures above 37°C [2, 8] have demonstrated the following:

(1) The thermal inactivation of the enzyme is irreversible;
(2) The time-course of loss of enzymatic activity fits the kinetics of a first order reaction;
(3) The observed first order inactivation rate constant does not depend on the concentration of the enzyme, which means that the inactivation of bacterial FDH at high temperatures is, in fact, a true monomolecular process.

The thermal inactivation of recombinant CboFDH was studied at a temperature interval of 53–61°C and pH values of 6.0, 7.0, and 8.0. Figure 1 shows the dependence of the remaining enzymatic activity on time at various temperatures in a 0.1 M phosphate buffer, pH 6.0.

As can be seen in Fig. 1, the relations are linear in semilogarithmic coordinates ($\ln(A/A_0) - t$). The slope of the lines (which is the inactivation rate constant k_{in}) does not depend on the concentration of the enzyme in a range of 0.08–1.5-mg/ml. The linear character of the relation between the remaining enzymatic activity and time in semilogarithmic coordinates and the constant value of the observed inactivation rate constant at various enzyme concentrations indicate that the thermal inactivation of CboFDH, like that of bacterial enzymes, is a monomolecular process, which means that it is a single-stage process with no preceding dissociation of the dimeric enzyme into its separate subunits.

A study of the loss of activity of CboFDH at pHs 7.0 and 8.0 showed that the thermal inactivation of the enzyme is also a monomolecular process. Table 1 shows the values of the observed first-order inactivation rate constants for *C. boidinii yeast FDH* in a 0.1 M sodium–phosphate buffer at a varying pH.

Bacterial FDH are notably more stable than CboFDH. For instance, at pH 7.0 and 61°C, the inactivation rate constant for CboFDH was 2.26 × 10^{-3} sec^{-1}, while the appropriate constant for wild-type PseFDH at this temperature was 1.3 × 10^{-4} sec^{-1} [2], which is almost 20-fold less.

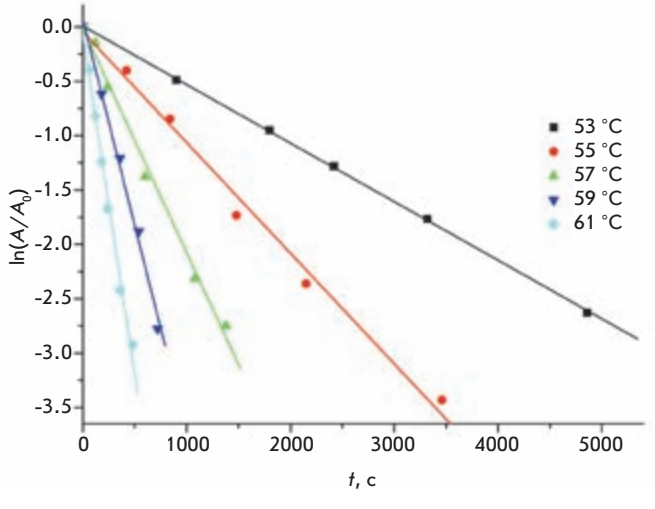

Fig. 1. Dependence of CboFDH residual activity on time as plot $\ln(A/A_0) - t$ at different temperatures. 0.1M sodium phosphate buffer, pH 6.0.

Table 1. Observed inactivation rate constants for recombinant formate dehydrogenase from *C.boidinii* in a 0.1M sodium phosphate buffer at different pHs.

pH	$k_{in}\cdot10^6$, s^{-1}				
	53°C	55°C	57°C	59°C	61°C
6.0	539 ± 4	1020 ± 50	2070 ± 80	3800 ± 200	6200 ± 200
7.0	28 ± 1	97 ± 3	370 ± 20	1050 ± 50	2260 ± 90
8.0	290 ± 9	1000 ± 10	2570 ± 40	6350 ± 200	12000 ± 400

Table 2. Activation parameters for the thermal inactivation of CboFDH at different pHs.

pH	$\Delta H^{\neq}$, kJ·mole^{-1}	$\Delta S^{\neq}$, J·K^{-1}mole^{-1}
6.0	280 ± 9	500 ± 30
7.0	500 ± 30	1360 ± 90
8.0	420 ± 30	1240 ± 80

Activation Parameters of the CboFDH Thermal Inactivation Process

The fact that the yeast FDH is inactivated via a monomolecular process at the studied temperatures and pH range makes it possible to use the transition state theory to analyze this process.

According to the trasition state theory, the equation that describes the relation between the observed first-order rate constant and the temperature can be represented thus:

$$k = \frac{k_B T}{h}\exp\left(-\frac{\Delta G^{\neq}}{RT}\right) = \frac{k_B T}{h} e^{\frac{\Delta S^{\neq}}{R}} e^{-\frac{\Delta H^{\neq}}{RT}}, \qquad (1)$$

where k_B and h are the Boltzmann and Plank constants, respectively; R is the universal gas constant, and T is the temperature in Kalvin degrees; and $\Delta G^{\neq}$, $\Delta H^{\neq}$, and $\Delta S^{\neq}$ are the changes of activation energy, enthalpy, and entropy, respectively.

Equation (1) can be transformed into the following linear form:

$$\ln\left(\frac{k}{T}\right) = \ln\left(\frac{k_B}{h}\right) + \frac{\Delta S^{\neq}}{R} - \frac{\Delta H^{\neq}}{RT} = const - \frac{\Delta H^{\neq}}{R}\frac{1}{T},$$

where $const = \ln\left(\frac{k_B}{h}\right) + \frac{\Delta S^{\neq}}{R}$.

As can be seen in Fig. 2, the experimentally determined dependences between the observed inactivation rate constants and temperature in $\ln(k_{ин}/T) - 1/T$ coordinates fit into straight lines, which means that these relations can be described by the trasition state-theory equation. Values of $\Delta H^{\neq}$ were determined from the slope of the lines in Fig. 2.

The value of $\Delta S^{\neq}$ can be calculated by approximating the line in Fig. 2 onto the zero point of the ordinate axis. However, this procedure will result in serious errors, since one has to do an approximation to a very large distance, the value $\ln(k_B/h)$ must also be subtracted from the value of intercept. The $\Delta S^{\neq}$ can be obtained much more accurately from the slope of the plot relating $\Delta G^{\neq}$ and T according to the following equation:

$$\Delta G^{\neq} = \Delta H^{\neq} - T\Delta S^{\neq}.$$

A calculation of the activation free energy involves the following expression:

$$\Delta G^{\neq} = RT\left[\ln\left(\frac{k_B}{h}\right) - \ln\left(\frac{k}{T}\right)\right] = RT\ln\left(\frac{k_B T}{kh}\right).$$

The values of $\Delta H^{\neq}$ and $\Delta S^{\neq}$ for three pH values are presented in Table 2.

In most cases the inactivation of the enzyme at high temperatures is caused by the denaturation of the protein globule. Thermal denaturation is a cooperative process, and it must be accompanied by increases in both the $\Delta H^{\neq}$ and $\Delta S^{\neq}$ values. These increases are much larger (tenfold or more) than the similar ones seen in chemical reactions, which can be seen for the obtained $\Delta H^{\neq}$ and $\Delta S^{\neq}$ values for the thermal inactivation of CboFDH (Table 2). Notably, similar values of activation parameters were obtained during a study of thermal inactivation for various bacterial formate dehydrogenases [8].

As is clear from these data, pH has a significant effect on the thermal inactivation of *C. boidinii* FDH. The enzyme is most stable at pH 7.0. An increase or decrease in the pH value causes the rapid destabilization of the protein globule, which in turn causes a 3–20-fold increase in k_{in}, depending on the temperature (Table 1). Notably, the relation between the temperature and k_{in} upon a varying pH is somewhat different. The relation changes quickly at pH 7.0 and is slower at pH 6.0 (Fig. 2). This seems to be due to the altered ioni-

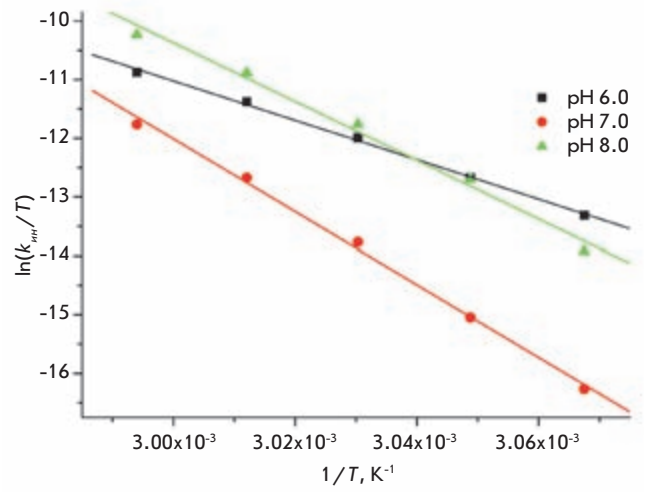

Fig. 2. Temperature dependence of the first order inactivation rate constant for recombinant wild-type CboFDH at different pH values in coordinates **$\ln(k_{ин}/T) - 1/T$.** 0.1M sodium phosphate buffer.

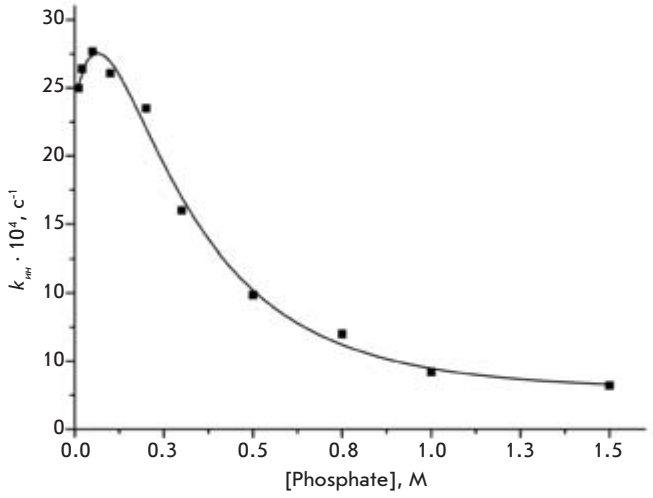

Fig. 3. Influence of sodium phosphate buffer concentration on the inactivation rate constant of CboFDH. 0.01 – 1.5M sodium phosphate buffer, pH 7.0, 61°C.

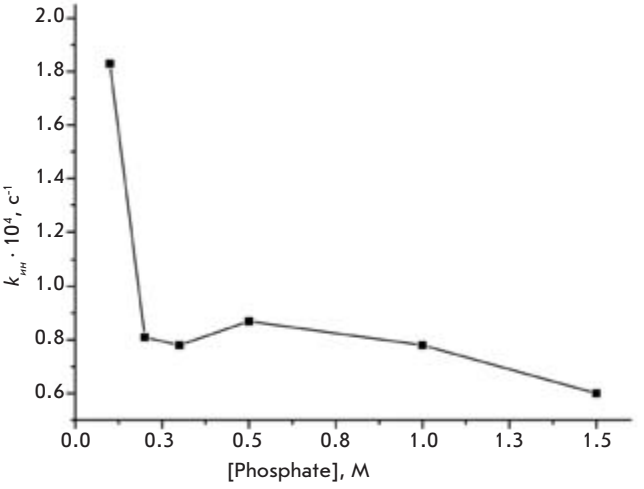

Fig 4. Influence of the sodium phosphate buffer concentration on the inactivation rate constant of PseFDH GAV. 0.1 – 1.5M sodium phosphate buffer, pH 8.0, 61°C.

zation of charged groups in the protein globule (such as the loss of a positive charge by a histidine residue at pH ≥7.0 or the appearance of a positive charge on a histidine residue at pH ≤7.0), which leads to a decrease in the number of oppositely charged groups taking part in electrostatic interactions or creates repulsive interactions between residues with the same charge. For instance, according to an X-ray analysis, the ND1 atom of the His57 residue of CboFDH is located at a distance of 2.82 Å from the NZ atom of the amino group of the Lys2 residue of the same subunit, and the distance between the ND1-atom of the His126 residue of one subunit and the NE-atom of the guanidine group of the Arg136 of another subunit is 3.61 Å (structure 2FSS.PDB). The apo form of a CboFDH molecule might contain four electrostatic bonds between His residues and the carboxy groups of Asp and Glu residues. The distance between the interacting entities is less than 4 Å. Moreover, it is important to bear in mind that alterations in even a single group's ionization can cause considerable conformational changes in a protein globule.

The Dependence of CboFDH Thermal Stability on Concentration of Phosphate Ions

As was mentioned above, electrostatic interactions play a very important role in the formation of native protein conformation. The effectiveness of these interactions is weakened in solutions with a high ionic strength. In order to analyze the effect that electrostatic interactions have on the stability of *C. boidinii yeast FDH*, we analyzed the thermal inactivation of the enzyme in solutions with varying concentrations of phosphate. We chose the phosphate ion because of its large size, which prevents it from penetrating the protein globule. Therefore, it should only disrupt the ionic interactions on the protein surface and thus have no effect on the structure of the protein globule itself. For comparison, we performed the same analysis with mutant FDH from *Pseudomonas* sp.101 GAV (PseFDH) at pH 8.0.

Figure 3 shows the relationship between the inactivation rate constant of the *C. boidinii* FDH and the concentration of the phosphate buffer at pH 7.0. At first, increasing the ionic strength of the solution lowers the stability of the enzyme, which can be attributed to an increase in the dielectric permittivity of the solution and the disruption of electrostatic interactions. However, a further increase in the salt concentration causes the enzyme stability to increase (approximately seven- fold in the overall stabilization). A similar relation is seen at pH 8.0; however, the stabilization effect is much more pronounced, almost 100-fold.

The effect of high concentrations of the phosphate buffer on the thermal stability of recombinant wild-type PseFDH has been studied before [8]. For this enzyme, the maximum value of the inactivation rate constant was observed at a higher concentration of the phosphate buffer (0.2 M), the destabilization effect was stronger (two-fold) compared to the CboFDH (about 11%), and high concentrations of the phosphate buffer (>1 M) did not have any stabilizing effect when compared to lower concentrations (0.05 M).

Figure 4 shows the relationship between the inactivation rate constant and the concentration of the phosphate ion for the mutant FDH from *Pseudomonas* sp.101, GAV version (PseFDH GAV) at pH 8.0 and 61°C. The increase in the salt concentration causes only weak stabilization in the case of PseFDH GAV: only 3-fold, as compared to 100-fold for CboFDH at pH 8.0. However, PseFDH GAV is much more stable as it is; even a 100-fold increase in CboFDH stability is not enough to render it as stable as the bacterial enzyme.

The data on the effect that an increase in the phosphate buffer concentration has on the inactivation rate constant of the wild-type CboFDH and an analysis of the quaternary structure allow us to explain the dramatic stabilization effect of CboFDH in a 0.1 M phosphate buffer due to the Arg-178Ser mutation observed in [11]. This substitution increases enzyme stability more than three-fold [2]. The mechanism behind this stabilization is as follows. Two more Arg residues are located near the latter residue in positions 174 and 182 (Fig. 5*A*). Their positively charged guanidine groups are situated 4.05 Å and 4.78 Å from Arg178, respectively. These are relatively large distances, and the repulsive forces will not

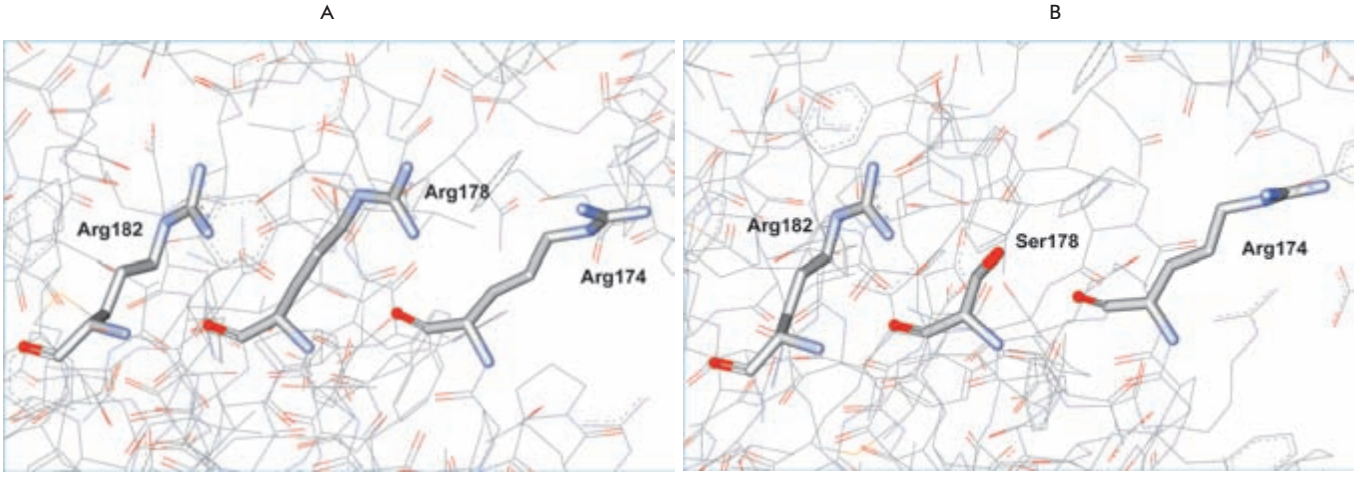

Fig. 5. (A) Spatial orientation of amino acid residues Arg174, Arg178, and Arg184 in apo form of formate dehydrogenase from *C.boidinii* (PDB structure 2FSS.PDB). (B). Removal of electrostatic repulsion and the production of a new hydrogen bond in CboFDH due to the amino acid change Arg178Ser.

be too significant in the case of only one pair of positive residues; however, there are two pairs of such residues, so the effectiveness of the repulsion is improved dramatically. The Arg178Ser substitution diminishes the electrostatic repulsion between the positive charges, and a new hydrogen bond is formed between the Arg182 and Ser178 residues (Fig. 5B), which is the reason for the high stability of an enzyme with this substitution. Increasing the concentration of the phosphate buffer masks the positive charges with the negatively charged phosphate ions.

A comparison of bacterial, plant, yeast, and fungi FDH amino acid sequences indicates that arginine residues which correspond to the CboFDH Arg174 and 182 residues are conserved in all of the above-mentioned enzymes (see Fig. 1 in ref. [2]). Moreover, the Arg174 residue is part of the **(G/A) AGIRG region, which is a "fingerprint" sequence fo coenzyme binding** domain in dehydrogenases. An X-ray analysis for *Pseudomonas* sp.101 [3] and *Moraxella* sp.C2 FDH showed that the arginine residue from the signature region (Arg202 in bacterial enzymes) is involved in the binding of NAD^+, interacting with its pyrophosphate group. It is obvious that substituting these two conserved Arg residues (especially Arg174) should disrupt the enzyme's catalytic functions. In yeast and fungi, the Arg178 residue of FDH is completely conserved. However, bacteria and higher plant FDH have either Ala or Leu residues, respectively, in the position corresponding to Arg178 in the amino acid sequence of CboFDH. The reason that nature "chose" to put a disadvantageous arginine residue into this position in yeast and fungi FDH remains unclear, and further investigation is needed to provide an answer to this question.

THE DEPENDENCE OF CBOFDH THERMAL STABILITY ON SODIUM FORMATE CONCENTRATION

Formate dehydrogenase is widely used in dehydrogenase catalyzed synthesis of chiral compounds as a coenzyme regenerating catalyst, and high concentrations (up to 2-3 M) of formate-ion, substrate of FDH, are used to achive high turnover of coenzyme. This is why we decided to examine CboFDH thermal inactivation kinetics upon varying sodium formate concentrations at two pH values: 7.0 and 8.0 (Fig. 6) since these are the values which are most often used for enzymatic synthesis processes involving dehydrogenases. As can be seen in Fig. 6, the dramatic stabilization of the enzyme is observed at high concentrations of sodium formate. This effect is especially notable at concentrations of sodium formate reaching 1.5 M. As in the case of the relation between the inactivation rate constant and the concentration of the phosphate ion, the stabilization effect is more pronounced at pH 8.0 than at pH 7.0 (Fig. 6).

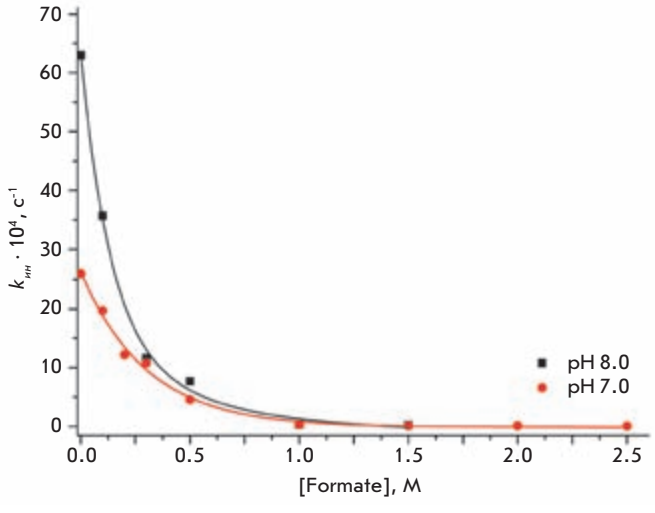

Fig. 6. Influence of the sodium formate concentration on the inactivation rate constant of CboFDH in a 0.1M sodium phosphate buffer at pH 7.0 and 61°C and at pH 8.0 and 59°C.

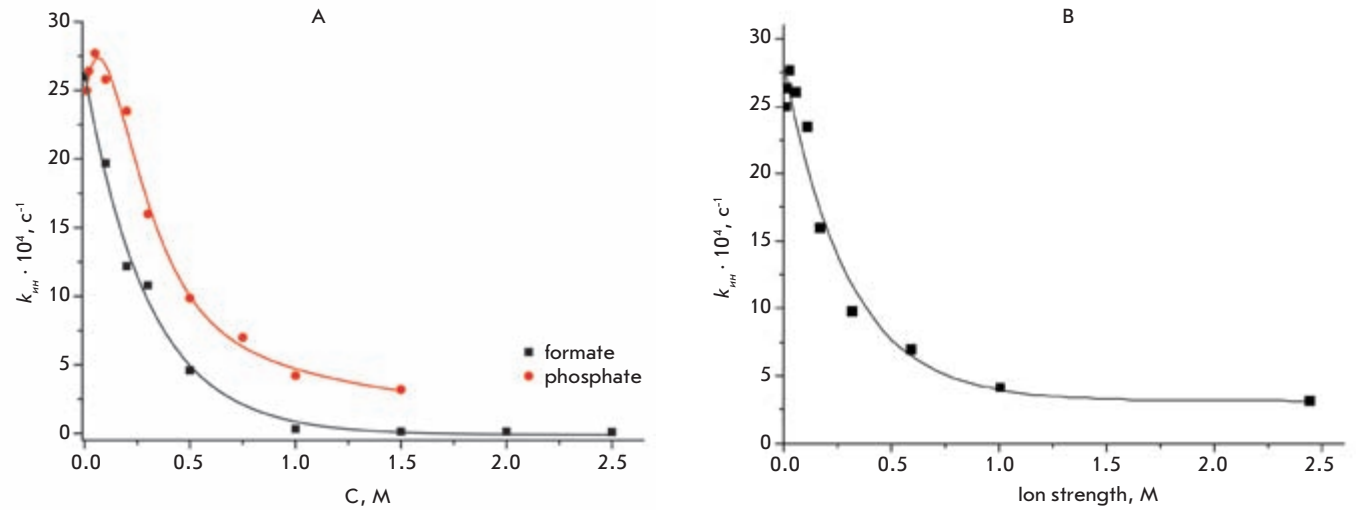

Fig 7 (A) Influence of the concentrations of the sodium phosphate buffer and sodium formate on the inactivation rate constant of CboFDH. pH 7.0 and 61°C. (B) Influence of the sodium phosphate buffer concentration presented as the ion strength value on the inactivation rate constant of CboFDH at pH 7.0 and 61°C.

A comparison of the relations between the inactivation rate constants and the phosphate and formate concentrations (Fig. 7*A*) obtained at pH 7.0 and 61°C shows that formate is better than phosphate at stabilizing CboFDH; moreover, achieving this stabilization requires much lower concentrations of substrate. However, a recalculation of the phosphate concentration for the according ionic strength indicates that the relation between the inactivation rate constant and ionic strength is identical, and this relation can be described as a simple exponent, just as in the case of the formate ion (Fig. 7B). This fact suggests a universal CboFDH stabilization effect under the influence of ionic strength. The more effective stabilization in the case of formate is most likely due to the fact that the formate ion is smaller and can thus penetrate deeper into the protein globule or bind specifically.

The data on CboFDH stabilization at high concentrations of formate can be used in practice for the enzymatic synthesis of chiral compounds. Moreover, CboFDH can be stored in buffer solutions with high salt concentrations at +4°C without a significant loss of activity, as compared to the usual conditions, −20°C in 40% glycerine. The high salt concentration also lowers the concentration of oxygen in the solution, which gives the enzyme additional protection from inactivation due to the oxidation of sulfhydryl groups of cystein residues. In our case, preparations of recombinant wild-type CboFDH were stored for 9 months with no loss of activity in a solution of ammonium sulfate (35% of saturated solution) and a 0.1 M phosphate buffer, pH 7.0 at a temperature of 4°C.

In conclusion, we must note that the results of a direct comparison between the thermal stability of bacterial and yeast FDH, based on a study of inactivation kinetics, are in agreement with the thermal stability data determined for these enzymes by differential scanning calorimetry, which were also obtained in our laboratory [12] and used the same preparations of recombinant CboFDH as those used in this work.

Thus, in this work, the first systematic study of the thermal stability of recombinant *C. boidinii* formate dehydrogenase was performed. The resulting data allowed a direct comparison between this enzyme and the FDH from *Pseudomonas* sp.101 bacterium. The obtained data indicate that the inactivation mechanism for these enzymes is identical, but the effect of the surroundings on their stability differs. ●

This work was supported by the Russian Foundation for Basic Research (grant № 08-04-01589-a).

REFERENCES

1. Vinals C., Depiereux E., Feytmans E. // Biochem. Biophys. Res. Commun. 1993. V. 192. P. 182–188.
2. Tishkov V.I., Popov V.O. // Biomol. Eng. 2006. V. 23. P. 89–110.
3. Lamzin V.S., Dauter Z., Popov V.O., et al. // J. Mol. Biol. 1994. V. 236. P. 759–785.
4. Filippova E.V., Polyakov K.M., Tikhonova T.V., et al. // Kristallographia. 2006. V. 51. P. 627–631.
5. Schirwitz K., Schmidt A., Lamzin V.S. // Protein Sci. 2007. V. 16. P. 1146–1156.
6. Sadykhov E.G., Serov A.E., Yasnyi I.E, et al. // Vestnik MGU. 2 Ed. Khimia. 2006. V. 47. P. 31–34.
7. Shabalin I.G., Serov A.E., Skirello O.E. et al. // Crystallography Reports . 2010. V.55. №5. P.855-859
8. Fedorchuk V.V., Galkin A.G., Yasny I.E. *et al.* // Biochemistry (Moscow). 2002. V. 67. P. 1145–1151.
9. Bommarius A.S., Schwarm M., Stingl K., et al. // Tetrahedron-Asymmetry. 1995. V. 6. P. 2851–2888.
10. Rojkova A.M., Galkin A.G., Kulakova L.B., et al. // FEBS Lett. 1999. V. 445. P. 183–188.
11. Felber S. Optimierung der NAD-abhängigen Formiatdehydrogenase aus *Candida boidinii* für den Einsatz in der Biokatalyse: PhD Thesis. Düsseldorf: Heinrich-Heine University of Düsseldorf, 2001. URL: http://diss.ub.uni-duesseldorf.de/ebib/diss/file?dissid=78
12. Sadykhov E., Serov A., Voinova N., et al. // Appl. Biochem. Microbiol. 2006. V. 42. P. 236–240.

Anionic Lipids: Determinants of Binding Cytotoxins from Snake Venom on the Surface of Cell Membranes

A.G. Konshina[1]*, I.A. Boldyrev[1], A.V. Omelkov[2], Yu.N. Utkin[1], R.G. Efremov[1]
[1] Shemyakin and Ovchinnikov Institute of Bioorganic Chemistry, Russian Academy of Sciences
[2] Faculty of Technology of Organic Substances and Chemical Pharmaceutical Compounds, Mendeleev University of Chemical Technology of Russia
*E-mail: nastya@nmr.ru
Received 19.05.2010.

ABSTRACT **The cytotoxic properties of cytotoxins (CTs) from snake venom are mediated by their interaction with the cell membrane. The hydrophobic pattern containing the tips of loops I–III and flanked by polar residues is known to be a membrane-binding motif of CTs. However, this is not enough to explain the difference in activity among various CTs which are similar in sequence and in 3D structure. The mechanism of further CT–membrane interaction leading to pore formation and cell death still remains unknown. Published experimental data on the specific interaction between CT and low molecular weight anionic components (sulphatide) of the bilayer point to the existence of corresponding ligand binding sites on the surface of toxin molecules. In this work we study the membrane-lytic properties of CT I, CT II (*Naja oxiana*), and CT 4 (*Naja kaouthia*), which belong to different structural and functional types (P- and S-type) of CTs, by measuring the intensity of a fluorescent dye, calcein released from liposomes containing a phosphatidylserine (PS) lipid as an anionic component. Using molecular docking simulations, we find and characterize three sites in CT molecules that can potentially bind the PS polar head. Based on the data obtained, we suggest a hypothesis that CTs can specifically interact with one or more of the anionic lipids (in particular, with PS) contained in the membrane, thus facilitating the interaction between CTs and the lipid bilayer of a cell membrane.**
KEYWORDS **cytotoxins, phosphatidylserine, lipid membranes, molecular docking, fluorescent spectroscopy**
ABBREVIATIONS **CT — cytotoxin, PS — phosphatidylserine, PKC — protein kinase C, SGC—sulphatide, POPC — palmitoyl oleyl phosphatidylcholine, 6-CF — 6-carboxyfluorescein, L/P — lipid/protein ratio, DPC — dodecylphosphocholin, NMR — nuclear magnetic resonance, hPS — phosphatidylserine polar head, PDB — Protein Data Bank**

INTRODUCTION

One of the features of cytotoxins (CTs, sometimes called cardiotoxins) from snake venom is their toxicity to cells of various types [1]. CTs are small basic proteins from the three-finger toxin group. The secondary structure of CTs consists of two β-sheets that have 2 and 3 antiparallel β-strands and is stabilized with 4 disulphide bonds. The major differences between the amino acid sequence and the 3D structure of members of this large CT group occur in irregular loop segments, primarily in loops I and II. Depending on the presence of the conservative residues S28 (S-type) or P30 (P-type) in loop II, CTs exhibit different functional activities [2]. For a long time, CTs were believed to interact with the cell membrane in a nonspecific way. P-type CTs interact with the bilayer more actively than S-type CTs due to the more hydrophobic loop II, resulting in an extended hydrophobic region on the toxin's surface formed by the hydrophobic tips of the three loops. The amphiphilic properties of CT molecules (the hydrophobic ends of loops I–III are flanked with cationic residues) enable their embedding into the lipid bilayer, creating porous defects in the membrane [3–6] and leading to the cell death. Several models of the mechanism of bilayer damage by CT and lysis have been proposed [7]. It was shown later that some CTs, for instance the CT A3 (*Naja atra*), can penetrate inside the cell and interact with cell organelles, mitochondria [8], and lysosomes [9].

The biological activity of CTs is very diverse. In particular, they can modify the function of various membrane proteins, such as protein kinase C (PKC), Na^+, K^+-ATPase, and integrins. Therefore, the hypotheses about the specific CT targets and molecular mechanisms of toxin-membrane interaction are of interest and have been actively discussed [7, 10–12].

Based on NMR and X-ray data, a search for potential CT targets revealed a series of anionic low molecular weight ligands (heparin-derived oligosaccharides, ATP derivatives, and sulphatide) that interact with certain sites on the toxin's surface [13–17]. Fluorescent spectroscopy studies on liposomes of various composition combined with *in vivo* experiments using monoclonal antibodies indicate a specific CT target—a polar head of a glycolipid sulphatide (hSGC)—located on the surface of a rat's cardiomyocyte membrane,

which mediates the toxic activity of CT A3 [17]. Taking into account the fact that CTs affect various cell types and that toxins effectively lyse model membranes containing no glycolipids [5, 18, 19], one can expect CT to be able to interact nonspecifically with other anionic membrane lipids, including the most common one, phosphatidylserine (PS). Although this lipid is normally localized in the inner leaflet of the cell membrane, when the bilayer is damaged in certain pathologies, PS is present in the outer leaflet and can be accessible to CT molecules. Some experimental data indirectly support the possibility that there is competition for a site on the membrane's surface between CT and other PS-binding molecules (PKC, thionin) [10, 20, 21].

In this work we assumed that PS is a specific target mediating CT cell toxicity and studied the interaction of S-type (CT I from *Naja oxiana*) and P-type (CT II from *Naja oxiana* and CT 4 from *Naja kaouthia*) cytotoxins with palmitoyl oleyl phosphatidylcholine (POPC) membranes, including those containing PS and SGC. It should be noted that the primary structure of CT 4 (*N. kaouthia*) is identical to that of CT A3 (*N. atra*). Using fluorescent spectroscopy, we studied the lytic activity of the selected CTs on liposomes of various composition. In order to identify sites in a CT molecule capable of binding PS, we performed molecular docking simulations of the PS polar head using 3D models of toxins active with respect to PS-containing liposomes. Based on the results obtained, we hypothesized that toxins interact with the bilayer *via* a two-stage specific mechanism, the molecular determinants of which are the polar heads of the anionic lipids, which interact with specific CT sites.

EXPERIMENT

Fluorescent Spectroscopy: CT Lytic Activity on PS-Containing Liposomes of Various Composition

CT I and CT II were extracted from *N. oxiana* venom following the technique described in [22]. CT 4 was extracted from *N. kaouthia* venom using the technique proposed in [23] and refined by reverse phase chromatography. The toxin's structure was confirmed by mass-spectrometry using peptide mapping after the trypsin hydrolysis of the reduced pyridylethylated toxin derivative. Liposomes were prepared using SGC and PS extracted from bovine brain in the Laboratory of Lipid Chemistry, Institute of Bioorganic Chemistry, Russian Academy of Sciences (IBC RAS), and synthetic POPC (Avanti Polar Lipids, United States). Liposomes of the following composition were prepared: POPC, POPC/PS5%, POPC/PS20%, POPC/PS35%, POPC/PS50%, POPC/PS70%, POPC/SGC5%, and POPC/SGC50%. Lipid solutions in chloroform/methanol (1:1) at appropriate concentrations were mixed, evaporated, and dried in vacuum. The lipid films were hydrated with a buffer containing 50 mM tris-HCl (pH 7.8), 30 mM NaCl, 4 mM EDTA, and 100 mM calcein. The suspension was incubated for several hours, subjected to 10 freeze/thaw cycles, and then forced through a 100-nm polycarbonate filter (NucleoPore, USA) 20 times using a mini-extruder (Avanti Polar Lipids, United States). The external dye was eliminated by gel filtration using a Sepharose CL-4B column equilibrated with a buffer containing 50 mM tris-HCl (pH 7.8), 110 mM NaCl, and 4 mM EDTA. In addition, the activity of CT 4 with respect to SGC-containing liposomes (POPC/SGC50%) was measured under the conditions described in [6] (buffer: 10 mM tris-HCl (pH 7.4), 75 mM NaCl; 50 mM 6-carboxyfluorescein (6-CF) as fluorophore; lipid/protein ratio (L/P) ~62).

The level of liposome membrane damage by CTs was estimated from spectrophotometric measurements of the amount of fluorophore released from inside the liposomes, I, upon adding an aliquot of the toxin solution into the quartz cuvette with the liposome sample. The value of I (%) was calculated using the following equation:

$$I = 100 \text{ x } (F - F_0) / (F_t - F_0),$$

where F_0 is the fluorescent signal from liposomes without the toxin (background level); F is the fluorescent signal from liposomes in the presence of the toxin; and F_t is the fluorescent signal after the liposomes have been destroyed with a detergent (Triton X-100).

The L/P ratio in all experiments was 100, unless otherwise stated. The fluorescent signal was measured at 517 nm, with excitation at 494 nm, and the spectral slit width for excitation and emission was 3 and 5 nm, respectively. For each experiment, the kinetics of the fluorescent signal was monitored (for about 40 min) and the final measurements were taken when I reached a plateau. For reproducibility control, all measurements were repeated 2–3 times. All measurements were performed at room temperature using HITACHI F4000 (Japan) spectrofluorimeter.

Molecular Docking of PS Polar Head in CT II and CT 4

Molecular docking simulations using GOLD 2.0 software [24] were performed to identify PS binding sites on the surface of CT molecules.

In our simulations, we used a crystallographic model of the 3D structure of CT A3 from *N. atra* venom (PDB code: 2BHI) [17] and NMR models of CT II in hydrated state (PDB code: 1CB9, models 1, 14 and 18) [25] and in the presence of dodecylphosphocholine (DPC) micelles (PDB code: 1FFJ, models: 1 and 10) [4].

In order to account for the receptor's conformational mobility, we used a series of 3D models representing the dynamic behavior of the toxins in media of different polarities. Starting from experimental toxin models, we obtained representative sets of corresponding 3D models of CT 4 and CT II by molecular dynamics simulations in aqueous media and by Monte Carlo conformational search for finding low-energy states in the presence of the implicit membrane (data not published).

The phosphatidylserine polar head (hPS) used in the simulations included all atoms of this lipid's polar head group with CH_3 groups, instead of fatty acid residues (Fig. 1a). hPS docking simulations were performed for 16 and 15 spatial models of CT 4 and CT II, respectively.

For each CT model, 50 complexes (docking solutions) were obtained, among which 10 with the best "gold score" criterion [26] (TOP10) were used for further analysis. Thus, for CT 4 and CT II, 160 and 150 TOP10 solutions in total were selected, respectively. We made decisions about hPS binding sites at CT by analyzing the localization of hPS on the toxins

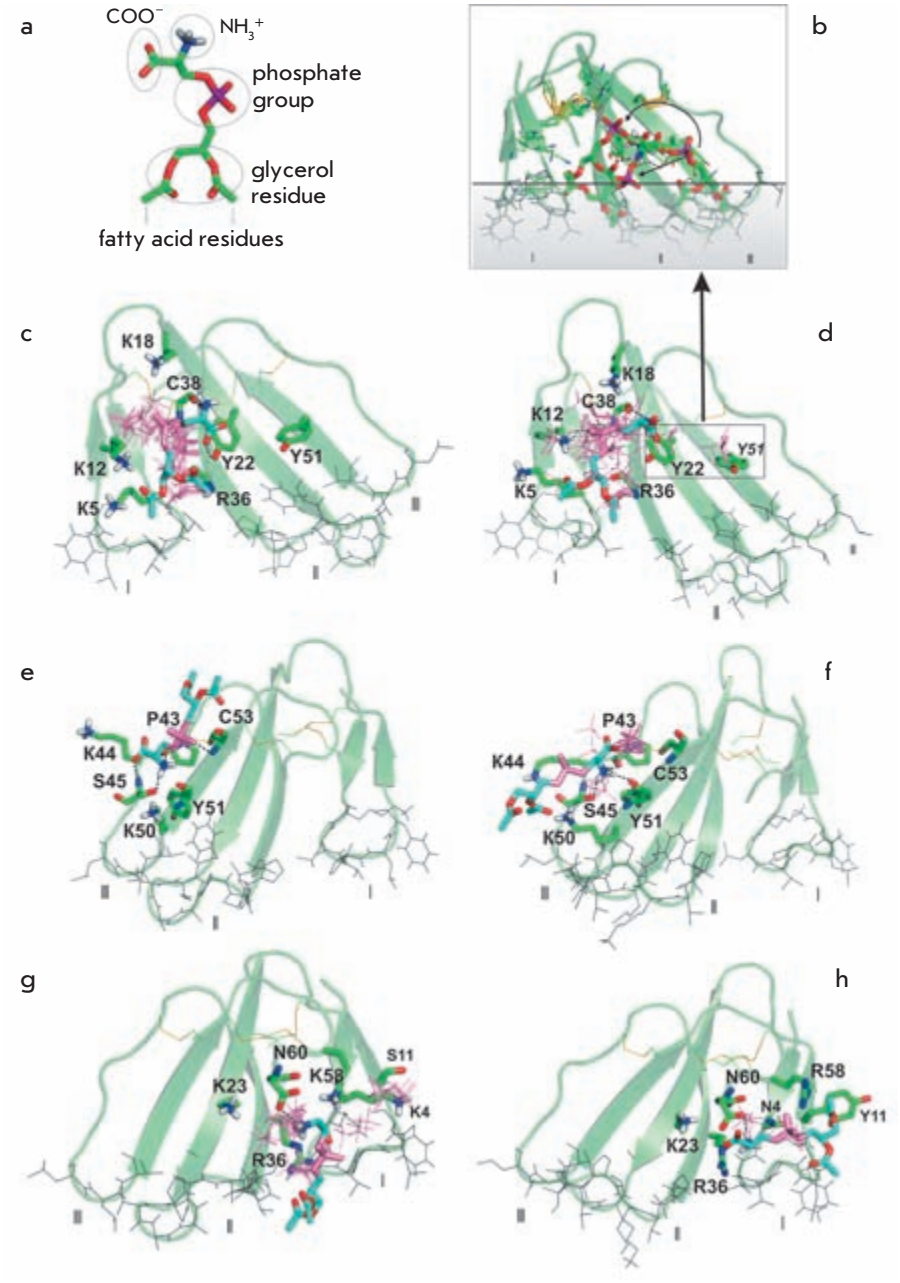

Fig. 1. (a) 3D model of the PS polar head (hPS) used in molecular docking simulations. Functional groups are indicated. (b–h): Molecular docking solutions for hPS bound in the M site of (b, d) CT 4 and (c) CT II, in the L3 site of (e) CT II and (f) CT 4, and in the L1 site of (g) CT II and (h) CT 4. 3D models of the toxins are shown in a ribbon representation. The membrane binding hydrophobic residues of loops I–III (designated with roman numbers), backbone and/or side chain atoms of the site-forming residues, and one of the preferred conformations of hPS in the related sites are displayed as stick diagrams. To demonstrate the diversity of hPS positions in the sites, the corresponding locations of the hPS phosphate group are also shown in stick representation for other docking solutions from the TOP10 set. Amino acid residues forming the sites are marked with a one-letter code, with a residue number and a standard coloring scheme for the atom types. The phosphate group and carbon atoms of hPS are pink and cyan, respectively. (b) Different positions of hPS in the site M_Y51 of CT 4 found among the TOP10 docking solutions. A hypothetical migration path of hPS from the M_Y51 site towards the M site is shown by arrows. The phospholipid bilayer is depicted as the shadow region under the horizontal line. The location of CT 4 relative to the membrane's interface (the horizontal line) corresponds to the proposed mode of CT binding to the lipid membrane.

molecule's surface and the frequency of occurrence of corresponding complexes in the TOP10 solutions. The hPS surface is polar; therefore, hydrogen bonds and electrostatic forces contribute most to the lipid-toxin complex energy. The docking solution sets were analyzed with respect to the number and distribution of hydrogen bonds and ionic contacts (those with distances between ionic groups below 6 Å) in order to identify the key residues involved in the interaction with hPS in most of the complexes.

The presence of hydrogen bonds and ionic interactions was estimated using the PLATINUM [27] and GROMACS 3.3.1 [28] software packages.

RESULTS

Fluorescence Measurements: CT-Induced Release of Dye from Liposomes

Dependence of CT activity on a type of minor (5%) anionic lipid (PS, SGC). In this work, we estimated the lytic activity of P- and S-type toxins, namely CT II (*N. oxiana*), CT 4 (*N. kaouthia*), and CT I (*N. oxiana*) by the amount of organic dye calcein released from POPC, POPC/PS5%, and POPC/SGC5% liposomes. CT I (S-type) shows almost no activity with respect to both neutral liposomes (POPC) and those con-

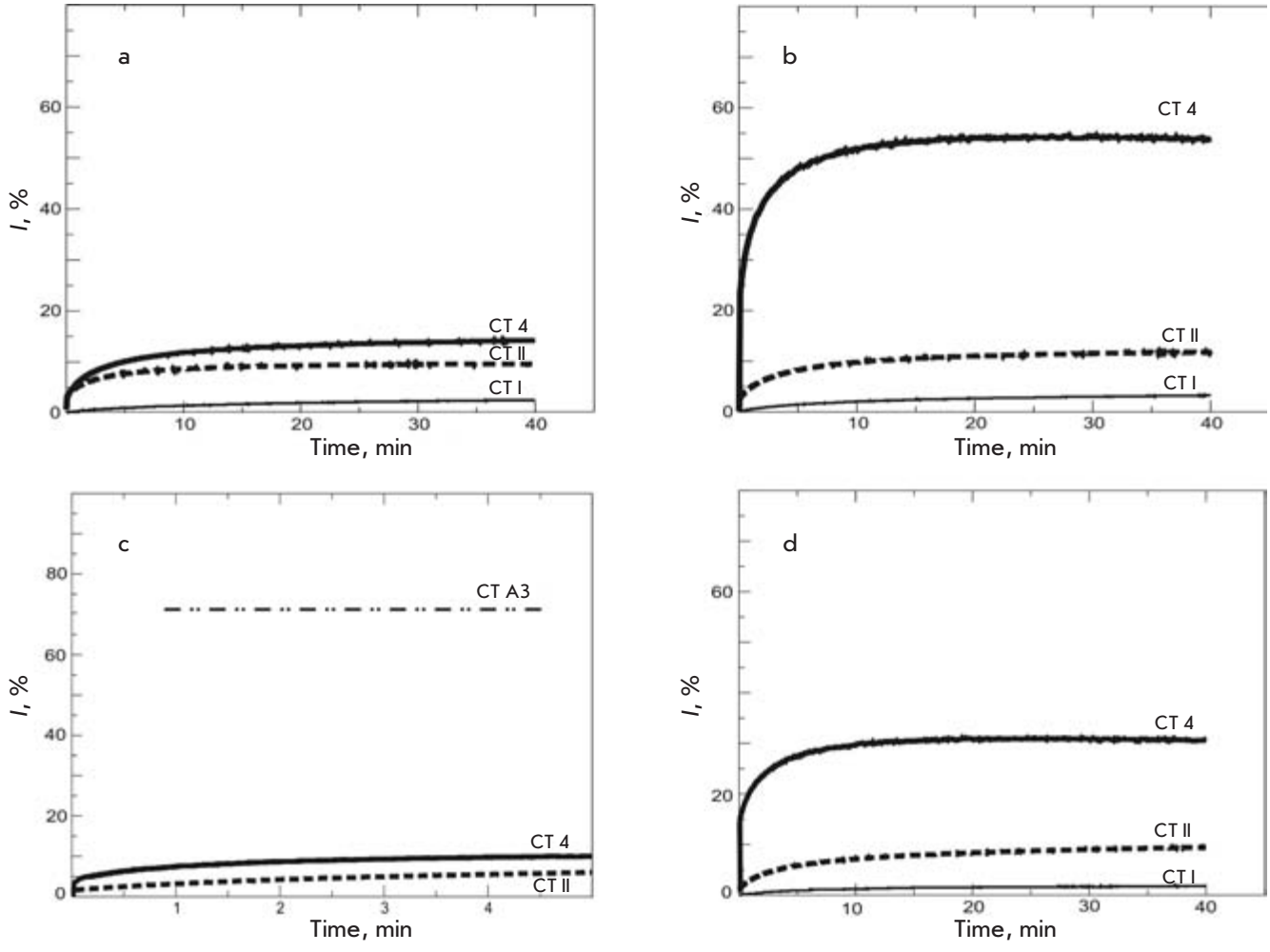

Fig. 2. CT-induced release of fluorescent dye calcein from liposomes of different compositions: (a) pure POPC; (b) POPC/PS5%, and (d) POPC/SGC5% after addition of CT I, CT II (*Naja oxiana*), and CT 4 (*Naja kaouthia*). (c) Kinetics of 6-CF fluorescence during the initial few minutes after addition of CT II and CT 4. For this measurement, (c) the experimental conditions, such as buffer composition, fluorophore and lipid/protein concentrations (10/0.16 μM) in the sample correspond to those in [6]. The data for 6-CF release induced by CT A3 (*Naja atra*) reported in [6] are shown as (_ .. _).

taining minor quantities of anionic lipids (PS, SGC) (Fig. 2): in all cases intensity of the released calcein, *I*, was below 5%. In experiments with CT II (P-type), the release intensity of dye was higher (compared to the results obtained with CT I), average *I* values being below 10% regardless of the liposome composition (Fig. 2).

Fluorescence measurements showed that CT 4 had the strongest damaging effect on all the liposome types studied (Fig. 2). With this toxin, a clear trend is visible: its activity depends on the presence and type of the anionic component in the liposome. Thus, the value of *I* for neutral liposomes was only ~10%, whereas for SGC-containing vesicles it was 30%. The highest CT 4 activity was measured for POPC/PS5% liposomes, with dye release reaching 50%. It should be noted that there was also a significant difference in the activity of individual toxins with respect to the anionic lipids in liposomes. For instance, CT II does not differentiate between PS- and SGC-containing liposomes, while the lytic activity of CT 4 with respect to POPC/PS vesicles is almost twice as high as that with respect to SGC-containing ones (Figs. 2 b, d).

It is interesting that we did not find a specific interaction between SGC molecules and CT 4 (which is identical to CT A3 from *N. atra* venom). Moreover, when we reproduced the experimental conditions described in [6] (see the Experiment section), the value of *I* after a few minutes of incubation was less than 10%, unlike the >70% reported in [6] (Fig. *2 c*). The authors of [6] used 6-CF fluorofore, which, due to its lower molecular charge, is prone to spontaneously releasing from liposomes (A.V. Feofanov, private communication).

CT-induced permeability of POPC liposomes with different PS content. We measured *I* for the interaction of CT I, CT II,

and CT 4 with POPC liposomes containing varying amounts of PS (20, 35, 50, and 70%) and studied the dependence of the lytic efficiency on the anionic lipid concentration. The latter turned out to be similar for all three toxins; in particular, there was a maximum in *I* at 20% PS (Fig. 3) for all CTs. The toxicity trend CT 4 > CT II > CT I stays the same for all liposome types at the given lipid/protein ratio (L/P = 100). The lytic effect of CT 4 and, especially, CT II increases drastically for liposomes POPC/PS20% (over 90 and 70%, respectively). At lower (5%) and higher (35% and more) PS contents, the drop in the activity curve *I* is more pronounced for CT II than for CT 4. CT I shows low lytic activity in the entire range of PS contents in the liposomes, with a weak maximum at PS20% (Fig. 3).

To explain the observed effects, we assumed a uniform distribution of PS in the liposomes and calculated the number of PS molecules per toxin molecule in liposomes of various composition that were 1000 Å in diameter. It appeared that the number of PS molecules for liposomes, with respect to which CTs show the maximum activity, is the same as the number of potential binding sites for the lipid head found in molecular docking simulations. In the case of complete toxin binding at L/P = 100, the liposome charge is compensated in the POPC/PS20% liposomes. Thus, there are 10–12 PS molecules (on average, 3.5 PS at the toxin's binding site) per each toxin molecule. There are 50–60 lipids in total per each toxin, and 16–18 lipids are located in direct proximity to the contact region with toxin.

For comparison, in the POPC/PS5% liposomes, charge compensation occurs at very low CT concentrations (L/P ~300); therefore, at a higher toxin content (L/P = 100), some CT molecules may not bind to the membrane. However, even if there is complete CT binding to the POPC/PS5% liposome surface, there may not be a single PS molecule at the toxin/lipid contact region (on average, there are 0.8 PS molecules per surface area in contact with a toxin molecule).

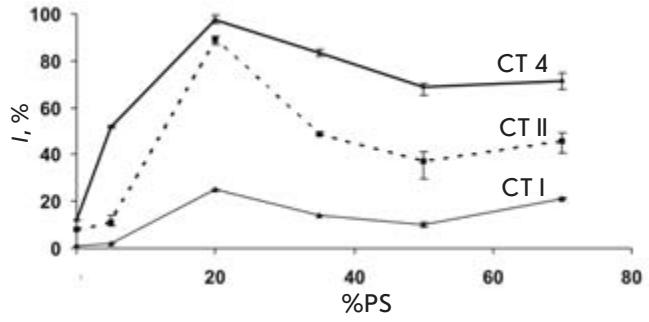

Fig. 3. Dependence of the CT-induced calcein release, *I* (%), on the PS content (in %) in the POPC liposomes. The fluorescence measurements were performed 10 min after the addition of the toxins. The values of *I* are calculated (see the Experiment section) and averaged for 2–3 measurements.

Molecular Docking

As a result of molecular docking simulations of hPS into 3D models of CT 4 and CT II, three hPS binding sites (referred to further as M, L3, and L1) consisting mainly of conservative residues were found on the surfaces of both toxins. One feature of the complexes that were formed is the multivariant positioning of the ligand in the sites (Fig. 1), which is due to the presence of several donor–acceptor groups capable of forming hydrogen bonds in both the ligand and the receptor.

The M site. The M site is the most frequently occurring one among the TOP10 docking solutions; it is present in 75 and 60% of solutions for CT 4 and CT II, respectively (Fig. 4). The site M includes a "lysine" cluster (K5, K12, K18, K35) surrounding the polar surface (the site's bed), which is formed by the backbone atoms of the residues L6, R36, G37, C38 and Y22 OH-group (Figs. 1c, 1d). In more than 60% of solutions for both toxins, there are three or more hydrogen bonds between key residues of the site M (K12, Y22, R36, and C38) and hPS and, usually, several ionic contacts.

The mobility of side chains of lysine residues makes site M compatible with different hPS conformations (Figs. 1c, 1d). This site is present in the TOP10 docking solutions for most CT 4 and CT II models, including the toxin structures determined experimentally.

In contrast to CT II, in the TOP10 set for CT 4, there is a group of solutions (further referred to as M_Y51) in which the Y51 residue's hydroxyl group is involved in binding of the lipid head (Figs. 1b, 2d). In most M_Y51 solutions (10 out of 16 complexes), the hPS tail is oriented towards the tip of loop III (Fig. 1b). In the other M_Y51 solutions, the hPS glycerine group is oriented towards loop I with fewer hydrogen bonds with the ligand. Therefore, in this group of solutions, the ligand's position is intermediate between those in the M_Y51 and M sites. In this case, Y22 is a key residue with which the ligand interacts (*via* the hydrogen bond) during the supposed migration from the M_Y51 to the M site (Fig. 1b).

The L3 and L1 sites. In addition to the major (in the number of solutions) site M, there are two sites in the TOP10 set, L1

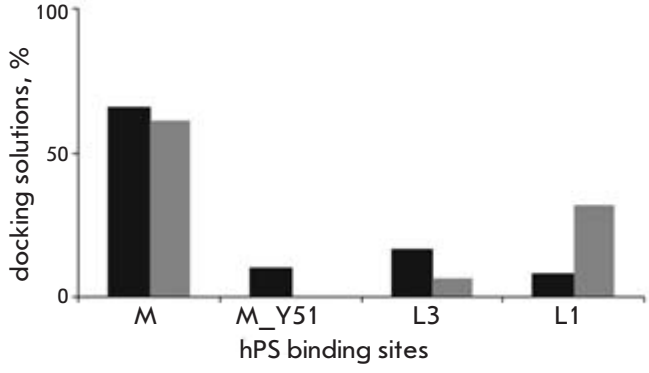

Fig. 4. Distribution histogram of docking solutions for the hPS binding sites (M, M_Y51, L3, L1) in CT II (grey) and CT 4 (black) molecules. The best scoring solutions (TOP10) for both toxins are presented.

and L3, located on the concave side of the CT molecule surface near loops I and III, respectively. The frequency at which these sites occur among the TOP10 docking solutions is different for CT II and CT 4 (Fig. 4).

The L3 site is formed by the bakbone atoms of the P43, Y51, C53, and S45 conservative residues, as well as by the side chain of the S45 residue. In most of the CT–hPS complexes, P43 and Y51 carbonyl groups and the S45 OH-group fix the position of the ligand's NH_3^+ group by forming a hydrogen bond (Figs. 1e, 1f**)**. In some solutions, the hPS glycerine residue is oriented towards the tips of loops I–III and the K44 and K50 side chains are near the hPS phosphate group (Fig. 1f).

The site L1 and CT 4/CT II represents a region with high electrostatic potential containing side chains of the N4/K4, K23, R36, R58/K58, and N60 residues, which form favorable electrostatic contacts with hPS. In most docking solutions obtained for CT II and CT, the hPS NH_3^+ group is located near the N60 residue, forming a hydrogen bond with the side chain carboxyl or carbonyl group (Figs. 1g, 1h). The hPS molecule accommodates various orientations with respect to the toxin molecule and suggested bilayer, including those corresponding to the lipid position in the bilayer (Fig. 1g).

DISCUSSION

The functional activity of cytotoxins arises from their interaction with the cell membrane; however, the mechanism of this interaction at the molecular level is still unknown. The oligomerisation of CTs necessary for forming pores in the membrane [5, 6] takes place not in solution, but apparently in the vicinity of the membrane; the details of this process and the geometry of the supramolecular complex are unclear. Understanding the initial stages of the toxin-membrane interaction is extremely important for understanding the entire mechanism of cytotoxic activity.

The data obtained in this study on the release of calcein from the POPC, POPC/PS5%, and POPC/SGC5% liposomes, depending on the CT type (P- or S-), correlate with the hypothesis that the properties of the membrane-binding motif (tips of loops I–III) influence the CT lytic activity with respect to the cell membranes. P-type CTs are known to more actively interact with the bilayer [2, 29, 30]. Indeed, both of the P-type CTs studied, CT II and CT 4, demonstrated more pronounced lipolytic behavior (on POPC/PS5% and POPC/SGC5%) than CT I, for which intensity of the released dye did not exceed 5%. It has been suggested that, due to the presence of polar residues in loop II (S28 and D29 in CT I) of the S-type CTs, their interaction with the bilayer involves fewer residues, primarily those of loop I [2, 31]. For identical bilayer embedding geometry, the calculated free energy of binding is higher for CT I than for CT II [30].

The experiments also showed that all the toxins studied were most active with respect to PS-containing liposomal membranes, and that the dye-release dependencies on the PS content were of dome shape and with the highest lysis intensity for the POPC/PS20% liposomes. An estimation of the number of PS molecules in 1000-Å diameter liposomes at L/P = 100 suggests that the lysis intensity peak can be reached when there are no less than three PS molecules on the surface of the bilayer in contact with the toxin during embedding. Under such conditions, the difference in the intensity of the released dye for CT 4 and the significantly less active CT II is minimal (90 and ~70%) compared to the case of liposomes with a PS content other than 20%. We can speculate that the optimum PS content for lysis that ensures the involvement of all three toxin sites is very important for the efficiency of toxin–membrane interaction. The weak response observed for the nearly inactive CT I is, perhaps, due to the fact that that this toxin does not embed deep enough into the bilayer and/or because of the different binding geometry involving only one or two loops, resulting in a lower availability of sites for binding with PS.

The drastic decrease of the POPC/PS5% lysis efficiency indicates that the mechanism that binds the highly basic toxin with the anionic membrane includes nonspecific electrostatic attraction. As a result, due to the low membrane charge density and too few PS molecules as potential ligands (less than one per toxin–membrane contact region), the CT does not embed into the bilayer efficiently.

The observed decrease in CT 4 and CT II activity with respect to liposomes with PS contents of 35% and higher is most likely caused by a change in the bilayer's properties, in particular, by an increase in the lipid packing density near the interface. For instance, the formation of mini-clusters of PS molecules becomes more probable. According to the data of molecular dynamics simulations for bilayers containing 20 and 50% PS, in the latter case there are twice as many hydrogen bonds between PS polar heads near the interface (data not published).

The estimated number of PS molecules in the POPC/PS20% liposomes interacting with CTs is the same as the number of the toxin PS-binding sites predicted by molecular docking simulations. It should be also noted that the embedding of the hydrophobic tips of loops I–III of the toxins studied into the lipid bilayer has been confirmed by NMR data on CT II [4] and CT A3 (*N. atra*) [6] in micelles.

The M site (residues K5, K12, K18, Y22, R36, and C38), presents in most docking solutions, is identical to the sulphatide-binding pocket located on the convex side of the toxin molecule [17]. Indeed, the results of a chemical modification of lysine and tyrosine residues suggest that the site's key residues, such as Y22 and K12, significantly influence the functional activity of CTs [32, 33]. Judging by the number of intermolecular hydrogen bonds and ionic contacts in the docking solutions, the M site has the best potential for forming a stable complex with the ligand. Formation of the CT A3-SGC complex in of a membrane-mimicking environment [17] indicates that other anionic components in the membrane can bind to the M site. At the same time, the superimposition of CT docking models, according to the mode by which they are embedded into the bilayer, indicates different availabilities of the sites for the PS head. For instance, the M site residues do not directly interact with the bilayer. In order to reach the M site, the lipid molecule must overcome the energy barrier so that the acyl part of the lipid will penetrate the polar interfacial zone.

It is interesting that, in the M_Y51 docking models for CT 4, the lipid binding site assumes a hydrogen bond between the lipid NH_3^+ group and OH groups of both tyrosine residues, Y22 and Y51, the phosphate group being near the mem-

Fig. 5. Sequence alignment for CT I, CT II, CT 4, and CT A3. The β-strands are indicated by *b*. Amino acid substitutions between CT A3 and CT 4 are underlined.

brane's surface. Therefore, we can expect that lipids reach the M_Y51 site faster than they reach the M site. Moreover, the existence of M_Y51 solutions differing in the involvement of the M site's key residues and the orientation of the lipid's glycerin residue can indicate a possible migration path of the lipid head from the M_Y51 site to the M site.

There is no direct experimental evidence of the existence of the L3 and L1 sites revealed by docking simulations. On the other hand, the L3 site located near loop III has a structure similar to that of the M site: the backbone atoms of this site's residues (P43, Y51, and C53) form hydrogen bonds with the lipid's polar head, which is additionally supported by an electrostatic interaction with the ionic groups of lysine residues (K44 and K50). Recently, a consensus sequence L/PKSSLL based on a peptide sequence alignment (related to antibodies neutralizing *N. atra* venom) revealed by phage display has been proposed as an epitope involved in the action of CT A3 from *N. atra* venom [34]. This epitope corresponds to a fragment of the loop III sequence and contains the L3 site residues (P43–S45). The L3 site is the least available for PS in the bilayer, taking into account the CT-membrane binding mode. It is possible that, during later stages of embedding, when CT penetrates deeper and this site becomes more available, binding an additional lipid strengthens the CT-membrane interaction.

In contrast, among docking solutions for the L1 site (a polar cluster comprised mainly of charged residues at the base of loops I and II) there are models of complexes with hPS in the membrane–water interfacial zone (in case CT loops embed into the membrane). This indicates the availability of this site for the bilayer hPS. There have been reports of NMR studies showing that some L1 site residues take part in dATP binding [16].

It is interesting to note that just five amino acid substitutions turn CT II into the much more lytically active CT 4 (Fig. 5); the total charge of the molecule (+9) is the same for both CTs. It is not surprising therefore that, along with a high sequence homology and similar 3D structure, the docking results for the two CTs are also very similar, differing only in the frequency at which the sites occur among the docking solutions. Four out of five amino acid substitutions are localized near the L1 site (more frequently in the case of CT II), and three of them—in the areas most important for the toxin—are in loops I and II. Thus, the positive charge in CT II (K4/N4 in CT II/CT 4) is transferred to loop II (H31/K31 in CT II/CT 4) in CT 4. On the one hand, this disturbs the hydrophobic pattern of loop II; on the other hand, lysine residues are known to anchor at the interface by interacting with the lipid phosphate groups [35], which may reduce the protein dissociation constant. A correlation has been found between the presence of a positive charge at the tip of loop II and CT hemolytic activity [36]. Although the K4/N4 and K58/R58 substitutions in toxins are localized relatively far from the membrane surface (assuming that the CT embeds with the tips of loops I–III), both residues are parts of the L1 site and form a hydrogen bond and/or ionic contact with the lipid's serine head in the docking solutions. The S11/Y11 substitution increases the hydrophobicity of the CT 4's loop I by enabling the coupling of the F10 and Y11 aromatic residues, which can act as a good hydrophobic anchor. We can speculate that, due to the less favorable binding conditions in the M_Y51 site (manifested by the absence of this site among the TOP10 solutions for CT II), the availability of the M site for the anionic lipid head is less for CT II. The local conformational differences between CT II and CT 4 can also contribute to the rearrangement of the hPS binding locations for the L1 and L3 sites. At the same time, it is obvious that the simulation data are not sufficient for a qualitative estimation of the possible changes of the lipid binding constants for the predicted sites and, therefore, for a detailed explanation of the differences in the CT II and CT 4 activities.

Also, we would like to note that our experiments on the release of calcein from the POPC/SGC5% liposomes and reproducing the experimental conditions described in [6], where 6-CF was used as fluorophore, did not reveal any high affinity of CTs (in particular, CT 4) with respect to SGC, which was in disagreement with the data published in [6]. At the same time, the existence of the X-ray CT A3-SGC complex confirms that various anionic components in the membrane can bind to the M site, and experiments with SGC-specific antibodies and enzymes reveal a dependence between the CT A3 functional activity and the presence of SGC in the membrane [17]. This glycolipid is present in low concentration in the outer membrane leaflet of rat cardiomyocytes, hence the big interest in SGC as a potential CT target. The low reproducibility of the results achieved on model membranes, in addition to the importance of technical details (e.g., the nature of dye), emphasizes the need to exercise caution when extrapolating to cells the results obtained using model systems. The functional activity of a toxin is likely to arise due to a number of factors that are not at all limited to the affinity to various membrane components.

In conclusion, based on the data on fluorescence intensity of a due released from anionic liposomes with a varying content of an anionic lipid as a measure of CT 4, CT I, and CT II activity, as well as the results of molecular docking of hPS into CT 4 and CT II, our hypothesis is that there are specific lipid binding sites of various affinities on the toxin surface. The concept of a CT binding to the membrane surface in two stages (initially via electrostatic and then *via* hydrophobic interaction), specific complexes of toxin with the anionic lipid's polar heads being the determinants of the process, provides qualitative insight into the dependence that the fluorescent dye release has on the PS content in the POPC liposomes. ●

This work was supported by the Russian Foundation for Basic Research and Programs of the Presidium of RAS "Molecular and Cell Biology" and "Fundamental Research in Nanotechnologies and Nanomaterials."

REFERENCES

1. Dufton M.J., Hider R.C. // Pharmacol. Ther. 1988. V. 36. P. 1–40.
2. Chien K.Y., Chiang C.M., Hseu Y.C., et al. // J. Biol. Chem. 1994. V. 269. P. 14473–14483.
3. Dauplais M., Neumann J.M., Pinkasfeld S., et al. // Eur. J. Biochem. 1995. V. 230. P. 213–220.
4. Dubovskii P.V., Dementieva D.V., Bocharov E.V., et al. // J. Mol. Biol. 2001. V. 305. P. 137–149.
5. Forouhar F., Huang W.N., Liu J.H., et al. // J. Biol. Chem. 2003. V. 278. P. 21980–21988.
6. Tjong S.C., Wu P.L., Wang C.M., et al. // Biochemistry. 2007. V. 46. P. 12111–12123.
7. Kumar T., Jayaraman G., Lee C., et al. // J. Biomol. Struct. & Dyn. 1997. V. 15. P. 431–463.
8. Wang C.H., Wu W. // FEBS Lett. 2005. V. 579. P. 3169–3174.
9. Feofanov A.V., Sharonov G.V., Astapova M.V., et al. // Biochem. J. 2005. V. 390. P. 11–18.
10. Chiou S.H., Raynor R.L., Zheng B., et al. // Biochemistry. 1993. V. 32. P. 2062–2067.
11. Raynor R.L., Zheng B., Kuo J.F. // J. Biol. Chem. 1991. V. 266. P. 2753–2758.
12. Wu P.L., Lee S.C., Chuang C.C., et al. // J. Biol. Chem. 2006. V. 281. P. 7937–7945.
13. Lee S. C., Guan H. H., Wang C. H., et al. // J. Biol. Chem. 2005. V. 280. P. 9567–9577.
14. Sue S. C., Brisson J. R., Tjong S. C., et al. // Biochemistry. 2001. V. 40. P. 10436–10446.
15. Tjong S.C., Chen T.S., Huang W.N., et al. // Biochemistry. 2007. V. 46. P. 9941–9952.
16. Jayaraman G., Krishnaswamy T., Kumar S., et al. // J. Biol. Chem. 1999. V. 274. P. 17869–17875.
17. Wang C.H., Liu J.H., Lee S.C., et al. // J. Biol. Chem. 2006. V. 281. P. 656–667.
18. Dufourcq J., Faucon J.F., Bernard E., et al. // Toxicon. 1982. V. 20. P. 165–174.
19. Chen K.C., Kao P.H., Lin S.R., et al. // Toxicon. 2007. V. 50. P. 816–824.
20. Osorio e Castro V.R., Vernon L.P. // Toxicon. 1989. V. 27. P. 511–517.
21. Osorio e Castro V.R., Rogers A., Vernon L.P. // J. Nat. Toxins. 2001. V. 10. P. 255–268.
22. Feofanov A.V., Sharonov G.V., Dubinnyi M.A., et al. // Biokhimya (Moscow). 2004. V. 69. P. 1410–1421.
23. Kukhtina V.V., Weise K., Osipov A.V., et al. // Bioorg. Khim. 2000. V. 26. P. 803-807.
24. Jones G., Willett P., Glen R.C., et al. // J. Mol. Biol. 1997. V. 267. P. 727–748.
25. Dementieva D.V., Bocharov E.V., Arseniev A.S. // Eur. J. Biochem. 1999. V. 263. P. 152–162.
26. Jones G., Willett P., Glen R.C. // J. Mol. Biol. 1995. V. 245. P. 43–53.
27. Pyrkov T.V., Chugunov A.O., Krylov N.A., et al. // Bioinformatics. 2009. V. 25. P. 1201–1212.
28. Lindahl E., Hess B., van der Spoel D. // J. Mol. Model. 2001. V. 7. P. 306–317.
29. Dubovskii P.V., Lesovoy D.M., Dubinnyi M.A., et al. // Eur. J. Biochem. 2003. V. 270. P. 2038–2046.
30. Dubovskii P.V., Lesovoy D.M., Dubinnyi M.A., et al. // Biochem. J. 2005. V. 387. P. 807–815.
31. Efremov R.G., Volynsky P.E., Nolde D.E., et al. // Biophys. J. 2002. V. 83. P. 144–153.
32. Gatineau E., Toma F., Montenay-Garestier T., et al. // Biochemistry. 1987. V. 26. P. 8046–8055.
33. Gatineau E., Takechi M., Bouet F., et al. // Biochemistry. 1990. V. 29. P. 6480–6489.
34. Wang P.C., Loh K.S., Lin S.T., et al. // Biochem. and Biophys. Res. Commun. 2009. V. 387. P. 617–622.
35. Désormeaux A., Laroche G., Bougis P.E., et al. // Biochemistry. 1992. V. 31. P. 12173–12182.
36. Hider R.C., Khader F. // Toxicon. 1982. V. 20. P. 175–179.

2D-gel Electrophoresis As a Tool to Investigate the Composition of CD95 DISC

D. Riess, I. Lavrik*
Division of Immunogenetics, German Cancer Center, Heidelberg, Germany
E-mail: i.lavrik@dkfz-heidelberg.de
Received 25.05.2010

ABSTRACT Stimulation of CD95 (APO-1/Fas) leads to apoptosis induction in multicellular organisms. CD95-mediated apoptosis starts with the formation of the protein complex at the receptor CD95 (APO-1/Fas), which was named DISC (death-inducing signaling complex). In this work, the composition of the CD95 DISC in two different cell types was analyzed using proteomics approaches. Using 2D gels, the composition of the CD95 DISC was analyzed in the so-called Type I and Type II cells, which are characterized by different kinetics of apoptosis. The detailed analysis of the CD95 DISC performed by 2D gels demonstrated that, besides the well-established components of the CD95 DISC, which are present in both cell types (CD95, FADD and procaspase-8), there are a number of differential spots detected at the CD95 DISC of Type I *versus* Type II cells. Taken together, this work demonstrates the differential composition of the CD95 DISC of Type I *versus* Type II cells.
KEYWORDS apoptosis, receptor CD95, 2D-gel electrophoresis

INTRODUCTION

Apoptotic cell death is common to multicellular organisms and can be triggered by a number of factors, including UV- or γ-irradiation, chemotherapeutic drugs, growth factor withdrawal, and signaling from death receptors (1, 2).

The death receptor family comprises the following receptors: TNF-R1, CD95 (APO-1/Fas), DR3, TRAIL-R1, TRAIL-R2, DR6, EDA-R, and NGF-R (2). It is considered that, for efficient signal transduction, death receptors have to form oligomers, probably trimers (1-3). The cytoplasmic part of the death receptors contains the so-called death domains (DD), which play the central role in the transduction of the apoptotic signal. DDs can undergo homotypic oligomerization with other molecules containing DD. In this way, adaptor molecules can bind to the receptors, forming a receptor-signaling complex.

CD95/APO-1/Fas-mediated apoptosis is one of the most studied apoptotic signaling pathways (1, 3). The CD95 DISC formation occurs within seconds after the binding of CD95L to CD95 (3-5). All interactions at the CD95 DISC are based on homotypic interactions. First, FADD (Fas-associated DD) binds to the DISC *via* DD interactions. The FADD molecule also contains DED (Death effector domain), which allows recruitment of procaspase-8 into the receptor complex *via* DED interactions. Procaspase-8 undergoes autocalytic activation at the DISC with the generation of the active form of caspase-8 (Fig. 1). This results in the activation of the effector caspases-3 and -7, which is followed by the cleavage of the apoptotic substrates, leading to cell death (2) (Fig. 1).

Two CD95 signaling pathways have been identified so far (4) (Fig. 1). Type I cells are characterized by high levels of CD95 DISC formation and increased amounts of active caspase-8, which activates downstream effector caspases-3 and -7. Type II cells are characterized by lower levels of CD95 DISC formation and, thus, lower levels of active caspase-8. In this case, signaling requires an additional amplification loop that involves the cleavage of the Bcl-2-family protein Bid by caspase-8 to generate truncated (t)Bid and subsequent (t) Bid-mediated release of cytochrome C from mitochondria. The release of cytochrome C from mitochondria results in apoptosome formation, followed by activation of procaspase-9, which in turn cleaves downstream effector caspases. Among T and B cell lines, Type I cells comprise: B cell lines SKW6.4, Raji, BJABs and T cell line Hut78, as well as peripheral T cells. It has been shown that Type II cells comprise T cell lines CEM and Jurkat (4).

The nature of the different kinetics of caspase-8 activation at the DISC in Type I and Type II cells is not established yet and, probably, might be due to the different protein composition of the CD95 DISC of Type I *versus* Type II cells. The goal of this study was to verify this hypothesis and to compare the protein pattern of the CD95 DISC of Type I cells *versus* Type II cells with proteomics approaches using 2D gels.

2D gels are based on the separation of proteins in the first direction based on their isoelectric point (pI), which is followed by the separation of proteins in the second direction based on their molecular mass (M_r) (6). This approach plays a very important role in proteomics studies. The 2D gels approach is also applied with different modifications, which allows to analyze protein complexes of different complexities. We used the approach with immobilized pH-gradients (IPG), which has been shown to possess high reproducibility (7). In this work, we have analyzed the composition of the CD95 DISC in a pI interval ranging from 3 to 10 and developed conditions for 2D gels in a pI range from 6 to 11. Our work has shown different protein compositions of the CD95 DISC immunoprecipitated from Type I *versus* Type II cells.

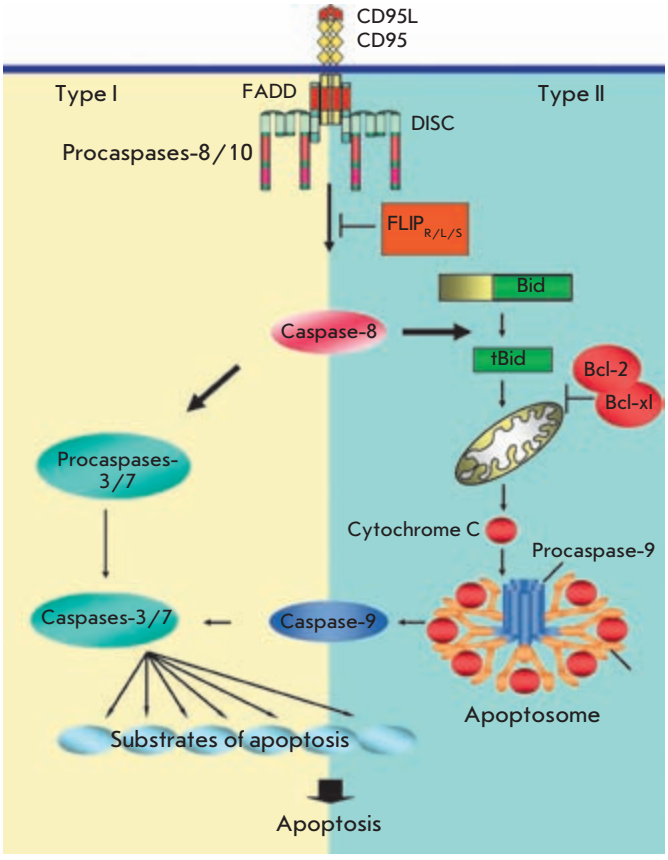

Figure 1. Scheme of Type I and Type II apoptotic pathways. In the CD95 pathway, stimulation with CD95L of CD95 leads to formation of the death-inducing signaling complex (DISC), where activation of procaspase-8 and procaspase-10 takes place. Caspase-8-mediated apoptosis occurs in different ways in type I *vs.* type II cells. Type I cells are characterized by high levels of DISC formation and increased amounts of active caspase-8 (left-hand side). Caspase-8 cleaves and thereby activates the downstream effector caspase-3, caspase-6, and caspase-7. In type II cells, there are lower levels of CD95 DISC formation and, therefore, lower levels of active caspase-8 (right-hand side). In this case, signaling requires an amplification loop that involves the cleavage by caspase-8 of the Bcl-2-family protein Bid to generate truncated (t) Bid and a subsequent tBid-mediated release of cytochrome C (cyt C) from mitochondria. The release of cyt C from mitochondria results in apoptosome formation, followed by the activation of initiator procaspase-9, which in turn cleaves downstream effector caspases. Type II CD95 signaling might be blocked by Bcl-2 family members such as Bcl-2 and Bcl-x_L. Activation of procaspase-8 at the DISC can be blocked by c-FLIP proteins.

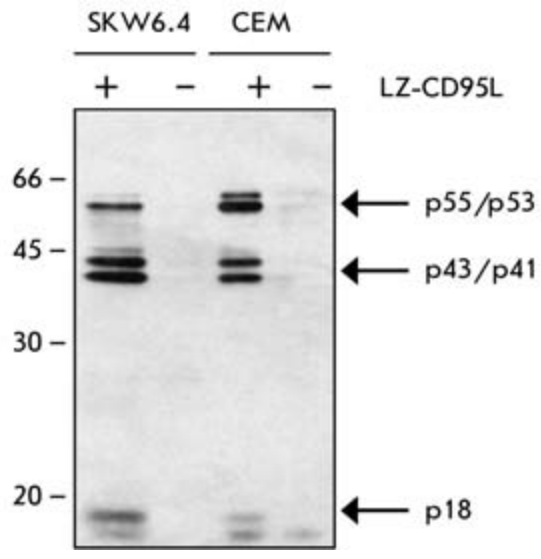

Figure 2. Control of the CD95 DISC formation using Western Blot. CD95 DISC formation (1/10 of the amount of protein loaded on 2D gels) was analyzed using 1D gels with subsequent Western Blot analysis using monoclonal antibodies C15 against caspase-8. The position of procaspase-8 (p55/p53) and its cleavage products p43/p41, p18, and p10 is indicated.

MATERIALS AND METHODS

Cell lines

The B lymphoblastoid cell line SKW6.4 and the T cell line CEM were maintained in RPMI 1640 (Life Technologies, Germany), 10 mM HEPES (Life Technologies, Germany), 50 μg/ml Gentamycin (Life Technologies, Germany), and 10% fetal calf serum (Life Technologies, Germany) in 5% CO_2.

Antibodies and reagents

Anti-CD95 polyclonal antibodies C20 were purchased from Santa Cruz Biotechnology (Heidelberg, Germany). CD95L was prepared as described in (8). The anti-FADD mAb 1C4 (mouse IgG1) recognizes the C-terminus of FADD. The anti-caspase-8 mAb C15 and mAb C5 (mouse IgG2b and IgG2a, respectively) recognize the p18 subunit of caspase-8 and the p10 subunit of caspase-8 (9). Anti-APO-1 is an agonistic monoclonal antibody recognizing an epitope on the extracellular part of CD95 (APO-1/Fas) (10). Horseradish peroxidase-conjugated goat anti-mouse IgG1, -2a, and -2b were from Southern Biotechnology Associates (United Kingdom). [^{35}S] Met and [^{35}S]Cys were purchased from Amersham. All the other chemicals used were of analytical grade and purchased from Merck (Germany) or Sigma (Germany).

Preparation of total cellular lysates

1 x 10^8 cells were washed twice in 1 x PBS and subsequently lysed in buffer A (20 mM Tris/HCl, pH 7.5, 137 mM NaCl, 2 mM EDTA, 1 mM phenylmethylsulfonyl fluoride (Sigma, Germany), protease inhibitor cocktail (Roche, Switzerland), 1% Triton X-100 (Serva, Germany) and 10% glycerol) (stimulation condition) or lysed without treatment (unstimulated). The total cellular lysates were subsequently analyzed by Western Blot.

DISC analysis by immunoprecipitation and Western Blot

5 x 10^7 SKW6.4 cells or 7 x 10^7 CEM cells were treated with 1 μg/ml of LZ-CD95L at 37°C for the indicated periods of time, washed twice in 1 x PBS, and subsequently lysed in buffer A (stimulation condition) or lysed without treatment (unstimu-

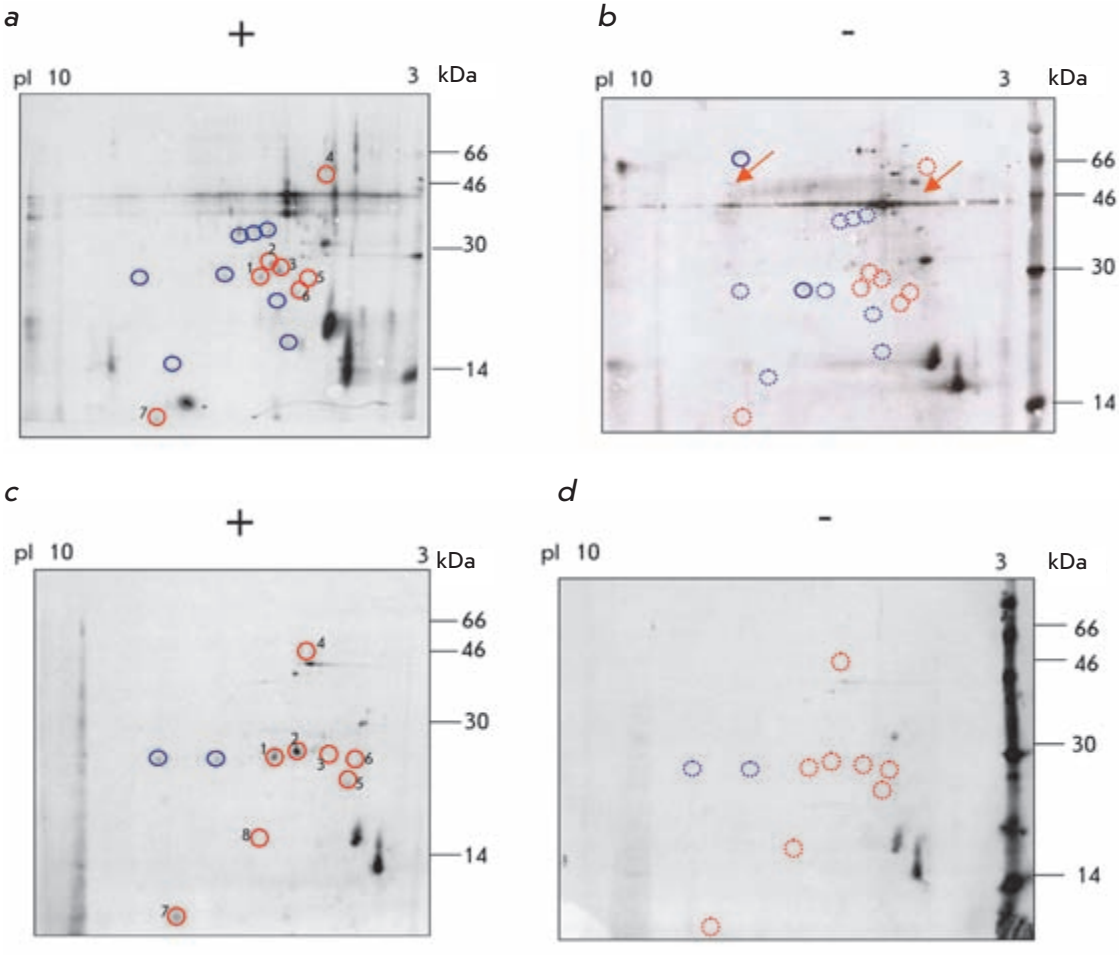

Figure 3. The analysis of the CD95 DISC in Type I cells (SKW6.4) and Type II cells. 5 x 10^7 of SKW6.4 cells were stimulated with LZ-CD95L (a) or left untreated (b). 7 x 10^7 of CEM cells were stimulated with LZ-CD95L (c) or left untreated (d). CD95 DISC immunoprecipitations were analyzed using 2D gels in the pI range from 3 to 10. The autoradiograms were exposed for 4 weeks. One out of three representative experiments is shown. CD95 position is indicated. All main components of the CD95 DISC are indicated with numbers. Differential spots are shown with a solid line. The disappearance of the spot is shown with a dashed line.

○ Characterized proteins of the DISC
1,2–FADD, CAP1 and CAP2
4-Procaspase-8 (CAP4 = p55)
3, 5, 6- Cleavage products of procaspase-8 (CAP3, CAP5=p26 and CAP6=p24)
7- Caspase-8 (p10)
○ Non-characterized proteins of the DISC

lated). The CD95 DISC was immunoprecipitated overnight with 2 μg of anti-APO-1 and protein A sepharose beads (11). Protein A sepharose beads were washed five times with 20 volumes of lysis buffer. The immunoprecipitates were analyzed on the 12% PAGE. Subsequently, the gels were transferred to the Hybond nitrocellulose membrane (Amersham Pharmacia Biotech., Germany), blocked with 5% nonfat dry milk in PBS/Tween (PBS plus 0.05% Tween 20) for 1 h, washed with PBS/Tween, and incubated with the primary antibodies in PBS/Tween at 4°C overnight. Blots were developed with a chemoluminescence method following the manufacturer's protocol (Perkin Elmer Life Sciences, Germany).

Labeling of the cells with [^{35}S]

5 x 10^7 SKW6.4 cells or 7 x 10^7 CEM cells were incubated for one hour at 37°C in RPMI media without methionine and cysteine. Afterwards, [^{35}S]Met and [^{35}S]Cys were added to the cells, and cells were cultured 24 h before performing the experiments.

2D-gels

To perform isoelectrofocusing (IEF) of the lysates, 10 μλ of total cellular lysates were added to 340 μλ of the buffer B (9M urea, 2% CHAPS, 18 mM DTT, 0.001% bromphenol blue, 0.5 % IPG buffer (Amersham)) or buffer C (9M urea, 2% NP-40, 18 mM DTT, 0.001% bromphenol blue, 0.5 % IPG buffer (Amersham)).

To perform isoelectrofocusing (IEF) of the immunoprecipitates, proteins after immunoprecipitation were eluted from protein A sepharose beads for 30 minutes at room temperature using buffer B.

After isoelectrofocusing, IPG stripes were equilibrated for 20 minutes in the buffer D: 50 mM tris-HCl, pH 8.8,6 M urea,

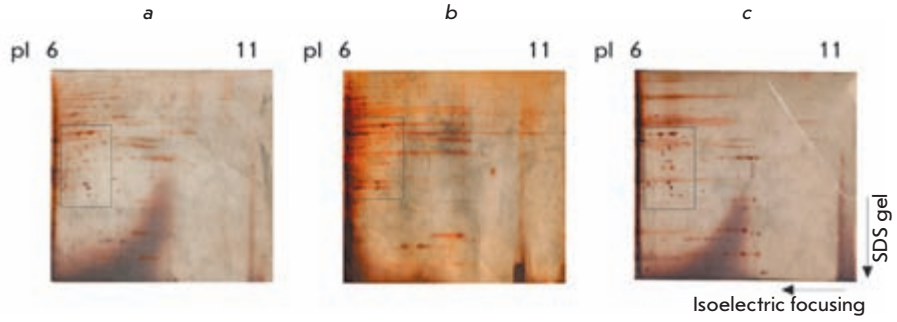

Figure 4. Optimization of isoelectrofocusing conditions. We performed isoelectrofocusing of the cellular lysates obtained from 10^7 of SKW6.4 cells. Afterwards, the samples were loaded on a 12 % PAGE. The proteins were detected using silver stain. The composition for the buffers for electrofocusing was as follows: (a, c) 9 M urea, 2 % CHAPS, 18 mM DTT, 0.001 % bromphenol blue, and 0.5 % of IPG buffer from Amersham. (b) 9 M urea, 2 % NP-40, 18 mM DTT, 0.001 % bromphenol blue, and 0.5 % of IPG buffer from Amersham. Isoelectrofocusing has been performed: (a, b) 12 h - dehydration, 1 h-500 V, 1 h-1000 V, 1 h- 3000 V, 8000 V until 60000 Vh. (c) 12 h- dehydration, 1 h -100 V, 1 h – 150 V, 1 h – 300 V, 1 h – 400 V, 1 h – 500 V, 1 h – 1000 V, 1 h – 3000 V, 8000 V to until 180000 Vh.

30% glycerol, 65 mM DTT, 0.001% bromphenol blue, which was followed with the incubation in buffer D containing 2.5% of iodoacetamide. Afterwards, IPG stripes were fixed with 0.5% agarose at 12% SDS-PAGE, which was followed by electrophoresis in the second direction. Afterwards, gels were analyzed using autoradiography or Western Blot. In some cases, the gels were stained using the SiverQuest Silver Staining Kit from Invitrogen.

RESULTS AND DISCUSSION

Analysis of the CD95 DISC using 2D gels at a pI range from 3 to 10

To undertake the proteomics analysis of the CD95 DISC composition, we selected two cell lines: B lymphoblastoid cells SKW6.4 as Type I cells and T cell line CEM as Type II cells. Both cell lines were characterized in detail in previous works and were demonstrated to possess typical features of Type I (SKW6.4 cells) *versus* Type II cells (CEM cells) (4).

To analyze the CD95 DISC composition, SKW6.4 and CEM cells were first cultured with [^{35}S]Met and [^{35}S]Cys for one day. Afterwards, cells were stimulated with LZ-CD95L. CD95 DISC was immunoprecipitated using monoclonal antibodies anti-APO-1. Anti-APO-1 antibodies recognize the extracellular domain of CD95 and have been used for the CD95 DISC immunoprecipitation in previous works (10, 11, 12). Immunoprecipitates were analyzed using 2D gels.

To control the immunoprecipitation, a tenth of the sample which was used for 2D gels was loaded onto the 1D gels and controlled using Western Blot and specific antibodies against procaspase-8 (Fig. 2). This analysis demonstrated the presence of procaspase-8, as well as its cleavage products p43/p41 at the DISC, showing the specificity of the methods used.

The composition of the CD95 DISC after immunoprecipitation was first analyzed using 2D gels with a pI range varying from 3 to 10 (Fig. 3). The 2D gel analysis of the CD95 DISCs of Type I *versus* Type II cells revealed the presence of spots with a pI and molecular mass corresponding to the main proteins of the CD95 DISC described in previous works (5, 13). The following proteins were detected: CD95, FADD, which is present in two forms: CAP1 (cytotoxicity-associated protein 1) and CAP2 (non-phosphorylated and phosphorylated FADD, respectively), procaspase-8 (CAP4) and its cleavage products CAP3, p26/p24, p18, and p10. In the DISC of both Type I and Type II cells, new non-characterized proteins were detected, as can be seen at corresponding 2D gels (Fig. 3). Interestingly, the molecular masses and pI of the new proteins of the CD95 DISC were different in Type I *versus* Type II cells, which indicates the differential composition of the CD95 DISC in these two cell types.

Analysis of the CD95 DISC using 2D gels at a pI range from 6 to 11

Since the resolution of the 2D gels at the region above the pI is relatively low, the proteins with basic pIs might not be detected using this approach. Therefore, we decided to analyze the protein composition of the DISC at a pI range varying from 6 to 11.

It was shown that isoelectrofocusing at a pI range varying from 6 to 11 is complicated due to the electroosmotic flow of water and migration of the DTT in the direction of the anode (14). This makes it difficult to obtain 2D gels of high quality at a pI range varying from 6 to 11. Therefore, first we had to optimize the conditions of isoelectrofocusing in a pI range from 6 to 11. First, lysates of SKW6.4 cells were prepared, and isoelectrofocusing was carried out using different detergents: e.g. CHAPS and NP-40. In addition, different protocols for isoelectrofocusing were utilized (Fig. 4). The quality of the 2D gels was judged according to the number of spots and their resolution.

The detergent CHAPS (Fig. 4a) provided a much better resolution in comparison with the detergent NP-40 (Fig. 4b). Isoelectrofocusing which was performed in experiments presented in Figs. 4a and 4b comprised four regimes: 500V, 1000V, 3000V, and 8000V. To improve the quality of the 2D gels, we also applied conditions for isoelectrofocusing with

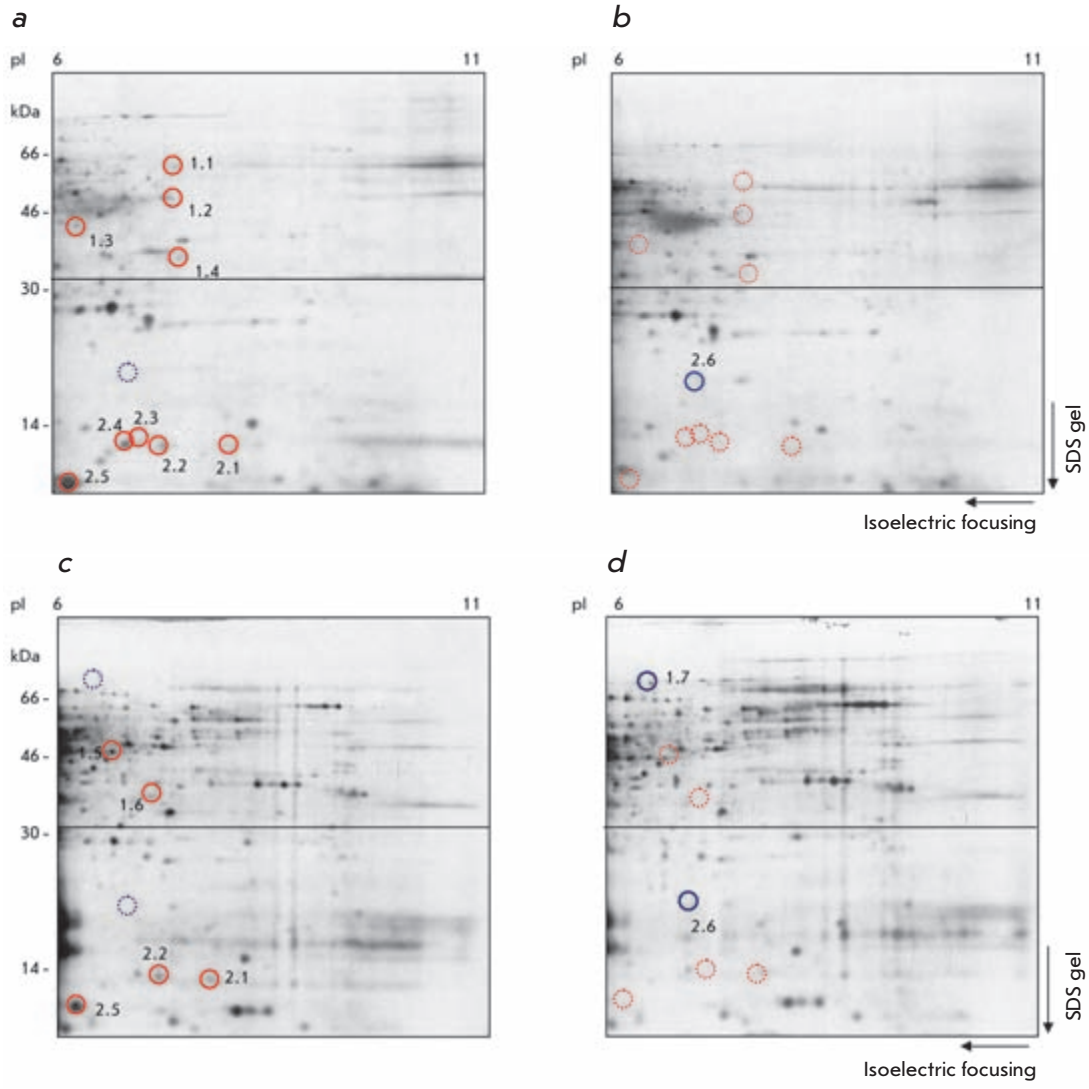

Figure 5. Analysis of the CD95 DISC in Type I cells (SKW6.4) and Type II cells (CEM). 5 x 10^7 of SKW6.4 cells were stimulated with LZ-CD95L (a) or left untreated (b). 7 x 10^7 of CEM cells were stimulated with LZ-CD95L (c) or left untreated (d). CD95-DISC was analyzed using 2D gels in the pI range from 6 to 11. The autoradiograms were exposed for 4 weeks. One out of three representative experiments is shown. Differential spots are shown with a solid line. The disappearance of the spot is shown with a dashed line.

eight regimes of focusing from 100V up to 8000V and a longer time of isoelectrofocusing (Fig. 4c). Apparently, these conditions resulted in a much better resolution of the 2D gels (Fig. 4c). Therefore, for the next experiments we used detergent CHAPS and conditions for isoelectrofocusing as shown in Fig. 4c.

For the comparative analysis of the CD95 DISC of Type I *versus* Type II cells in this pI range, we also selected SKW6.4 cells as Type I cells and CEM cells as Type II cells. Experiments were performed similarly as described above for the analysis for a pI varying from 3 to 10. The SKW6.4 and CEM cells were cultured with [^{35}S]Met and [^{35}S]Cys for 24 hours. To induce the formation of the CD95 DISC, cell cultures were treated with LZ-CD95L. This was followed by the immunoprecipitation of the CD95 DISC using monoclonal antibodies anti-APO-1 and 2D gel analysis at a pI range from 6 to 11.

The analysis of 2D gels revealed a number of new proteins present in the CD95 DISC of Type I cells (Fig. 5a), as well as in Type II cells (Fig. 5b). All proteins with a molecular mass of more than 30 kDa are identified with numbers from 1.1 to 1.7. All proteins with a molecular mass lower than 30 kDa are identified with numbers from 2.1 to 2.7 (Fig. 5). The molecular masses and pIs of the new proteins of the CD95 DISC of Type I and Type II cells were different, with the exception of the spot 2.5, which was observed in both cell types. Therefore, we were able to demonstrate that the protein composition of the CD95 DISC in Type I cells is different from the CD95 DISC in Type II cells also in a pI range from 6 to 11.

To control the immunoprecipitation, a tenth of the CD95 DISC immunoprecipitation was loaded on the 1D gel. This was followed by Western Blot with the specific antibodies against established components of the CD95 DISC as was demonstrated in Fig. 2. In addition, we analyzed 2D gels using Western Blot and we detected the presence of already known components of the CD95 DISC: CD95 (Fig. 6a, b) and active caspase-8, p10 (Fig. 6c). The comparison of the pI and molecular mass of the active caspase-8 at the Western Blot

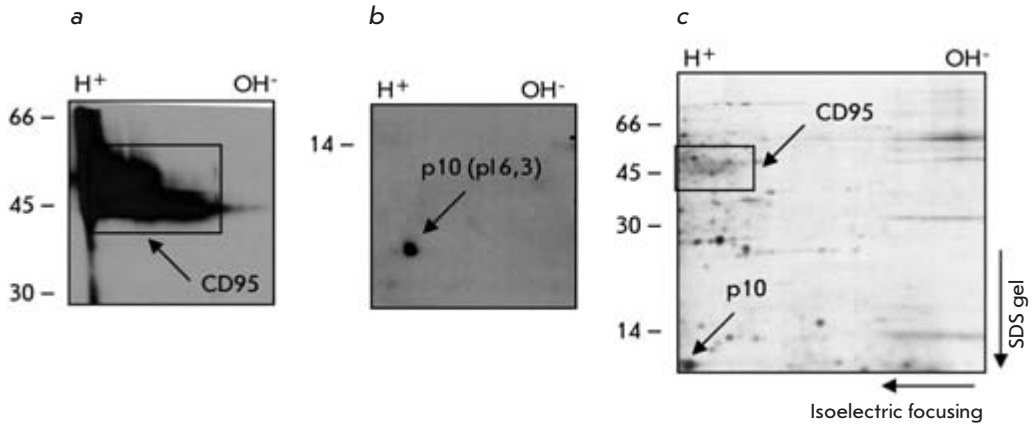

Figure 6. Analysis of the 2D gels using Western Blot. CD95 DISC, immunoprecipitated from SKW6.4, was analyzed using 2D gels with Western Blot and specific antibodies C20 against CD95 (a), specific antibodies C15 against caspase-8 (b). The position of caspase-8 and CD95 is shown at autoradiogram (c).

with spots at autoradiogramms showed that the protein 2.5 corresponds to the active caspase-8 (Fig. 6d). Thus, we, for the first time, had established the conditions for 2D gels in a pI range varying from 6 to 11 needed to analyze the proteins associated with CD95.

CONCLUSIONS

Therefore, the application of 2D gel electrophoresis has allowed us to analyze the composition of the CD95 DISC in Type I *vs*. Type II cells. Notably, 2D gel analysis has revealed the differential spots at the 2D gel of Type I *vs*. Type II cells, which confirms the hypothesis that the differential kinetics of caspase-8 activation in Type I *vs*. Type II cells is based on the different protein compositions of the CD95 DISC. At the moment, we are attempting to identify new proteins using mass-spectrometry analysis. ●

REFERENCES
1. Krammer P.H. // Nature. 2000. V. 407. P. 789–795.
2. Lavrik I.N., Golks A., Krammer P.H. // J. Cell Science. 2005. V. 11. P. 265–267.
3. Peter M., Krammer P.H. // Cell Death and Diff. 2003. V. 10. P. 26–35.
4. Scaffidi C., Fulda S., Srinivasan A., et al. // EMBO J. 1998. V. 17. P. 1865–1687.
5. Kischkel F.C., Hellbardt S., Behrmann I., et al. // EMBO J. 1995. V. 14. P. 5579–5588.
6. O'Farrel P.H. // J. Biol. Chem. 1975. V. 250. P. 4007–4021.
7. Gorg A., Postel W., Gunter S. // Electrophoresis. 1998. V. 9. P. 531–546.
8. Walczak H., Miller R.E., Ariail K., et al. // Nat. Medicine. 1999. V. 5. P. 157–163.
9. Scaffidi C., Medema J.P., Krammer P.H., Peter M.E. // J. Biol. Chem. 1997. V. 272. P. 26953–26958.
10. Trauth B.C., Klas C., Peters A.M., et al. // Science. 1989. V. 245. P. 301–305.
11. Lavrik I.N., Golks A., Baumann S., Krammer P.H. // Blood. 2006. V. 108. P. 110–117.
12. Golks A., Brenner D., Fritsch C., Krammer P.H., Lavrik I.N.// J. Biol Chem. 2005. V. 280. P. 14507–14513.
13. Golks A., Brenner D., Schmitz I., et al. // Cell Death and Diff. 2005. V. 13. P. 489–498.
14. Gorg A. // Methods Mol. Biol. 1999. V. 112. P. 197–209.

Derivation of Induced Pluripotent Stem Cells from Fetal Human Skin Fibroblasts

S. P. Medvedev[1], A. A. Malakhova[1], E. V. Grigor'eva[1], A. I. Shevchenko[1], E. V. Dementyeva[1], I. A. Sobolev[1], I. N. Lebedev[2], A .G. Shilov[1], I. F. Zhimulev[3], S. M. Zakian[1,4]*

[1]Institute of Cytology and Genetics, Siberian Branch, Russian Academy of Sciences

[2]Research Institute of Medical Genetics, Siberian Branch, Russian Academy of Medical Sciences

[3]Institute of Chemical Biology and Fundamental Medicine, Siberian Branch, Russian Academy of Sciences

[4]Research Center of Clinical and Experimental Medicine, Siberian Branch, Russian Academy of Medical Sciences

* E-mail: zakian@bionet.nsc.ru

Received 10.04.2010

ABSTRACT **The isolation and study of autologous human stem cells remain among the most urgent problems in cell biology and biomedicine to date. Induced pluripotent stem cells can be derived from human somatic cells by the overexpression of a number of genes. In this study we reprogrammed fetal human skin fibroblasts by transduction with retroviral vectors carrying murine *Oct4*, *Sox2*, *Klf4*, and *c-Myc* cDNAs. As a result, cells with the protein expression and gene transcription pattern characteristic of human embryonic stem cells were derived. These induced pluripotent cells are capable of differentiation *in vitro* into the ectoderm, mesoderm, and endoderm derivatives.**

KEYWORDS **induced pluripotent stem cells, reprogramming, retroviral vectors**

ABBREVIATIONS **ESCs – embryonic stem cells, HEFs – human embryonic fibroblasts, iPSCs – induced pluripotent stem cells, PCR – polymerase chain reaction, RT-PCR – reverse transcription-polymerase chain reaction**

Induced pluripotent stem cells are a unique model for studies in many fields of biomedicine, such as the molecular basis of human cell pluripotency and reprogramming (processes occurring in early embryogenesis) [1]. Broad prospects are opening up for the application of induced pluripotent stem cells in toxicology and pharmacology, as well as in regenerative medicine [2–4].

In this work we intended to prepare stable lines of pluripotent cells from human embryonic fibroblasts (HEFs) by their transduction with retroviral vectors carrying murine *Oct4, Sox2, Klf4,* and *c-Myc* genes.

The MA N1 HEF line (ninth week of gestation) was used as the starting cell population. The fibroblasts were transduced with retroviruses prepared by the cotransfection of the constructs pMXs-Oct4, pMXs-Sox2, pMXs-Klf4, and pMXs-c-Myc carrying the murine *Oct4, Sox2, Klf4, and c-Myc* cDNAs [5] and a plasmid carrying the vesicular stomatitis virus (VSV) glycoprotein G (VSV-G) into the cells of the Phoenix HEK293 packaging line carrying the viral *Gag* and *Pol genes*. The retroviral vector carrying a pMX-GFP construct (Cell Biolabs, United States) encoding the green fluorescent protein (GFP) was used as the control. About 1 million fibroblasts were used in the experiment. Two days (48 h) after transduction, the cells were seeded onto the feeder (mitotically inactive murine fibroblasts treated with mitomycin C) grown in a medium for human ESC containing 0.5mM of 2-propylvaleric acid (valproic acid, VPA). At the second week after transduction, about 500 granular cell colonies appeared that differ in morphology from fibroblasts. However, these colonies were negative when stained for alkaline phosphatase (AP), one of the markers of pluripotent cells. It is likely that these cells corresponded to early reprogramming stages [6]. We continued selecting ESC-like clones by morphology for 15–30 days after transduction. The scheme of the experiment is shown in Fig. 1. Of the 200 clones subjected to the following cultivation, AP-positive ones began to appear. Totally, we obtained 18 stable ESC-like lines, four of which (hiPS-A24, hiPS-A29, hiPS-21L, and hiPS-30L) were characterized in detail. Cells of these lines have a high nucleus-cytoplasm ratio; form dense colonies, i.e., demonstrate morphological features of human ESC (Fig. *2A*); and are AP-positive (Fig. *2B*). Using PCR, we ensured that all four lines contained inserts of the used retroviral constructs (pMXs-Oct4, pMXs-Sox2, pMXs-Klf4, and pMXs-c-Myc). Using immunocytochemistry, we found that these cells expressed the following pluripotent cell markers: TRA-1-60, TRA-1-81, and SSEA-4 surface antigens, as well as NANOG and OCT4 transcription factors (Fig. *3*). Using RT-PCR, we examined a transcription of 25 gene markers of human ESCs (Fig. *4A*). All four clones were very similar in their expression pattern to the human ESC HUES9 line taken as a positive control. iPSCs derived from ESFs express the robust pluripotent cell markers, such as the genes *OCT4, NANOG, SOX2, FGF4, REX1, DNMT3B, NODAL, etc.* (Fig. *4A*). The only difference was found in the transcription of the *GDF3 gene*. Of

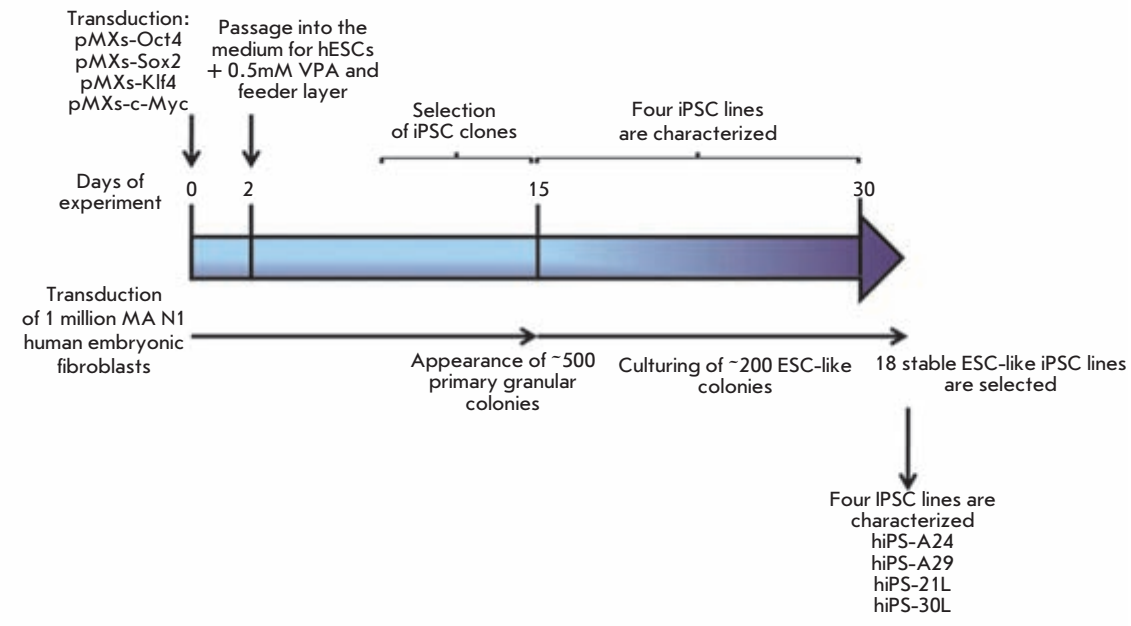

Fig. 1. Schematic representation of an experiment on the preparation of induced pluripotent stem cells from human embryonic fibroblasts.

the four tested iPSC lines, this gene is only transcribed in hiPS-21L. Among the 25 gene markers, the transcription of *KLF4* and *c-MYC* is only observed in MA N1 fibroblasts (Fig. *4A*). *The iPSCs* hiPS-A24, hiPS-A29, hiPS-21L, and hiPS-30L cells form embryoid bodies in suspension culture (F*ig. 4B*). An RT-PCR assay of the cells formed during the growth of embryoid bodies showed the presence of markers characterizing the derivatives of all three germ layers: ectoderm (*MAP2, PAX6, and GFAP*), mesoderm (*BRACHYURY*), and endoderm (*SOX17, FOXA2, CK8, CK18, and AFP*) (F*ig. 4C*). An immunocytochemical analysis of cells from disaggregated embryoid bodies revealed various cell derivatives expressing ectodermal (β-III-tubulin and GFAP), mesodermal (collagen I and fibronectin), and endodermal (α-fetoprotein and cytokeratin 18) markers (F*ig. 5*). Cells were also found that express both endodermal and mesodermal markers GATA6, as well as those expressing the protein nestin, which is a marker of both ectodermal and mesodermal derivatives (F*ig. 5*). Thus, we have shown that the obtained human iPSCs possess a broad differentiation potential *in vitro*. Karyotyping of the obtained iPSC lines showed a normal chromosomal set46, XY.

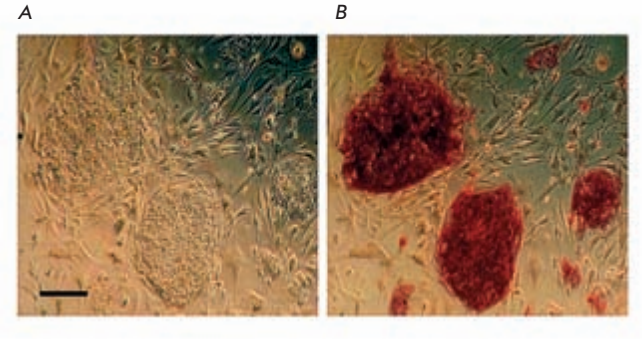

Fig. 2. (A) morphology of iPSC colonies derived from hEFs; (B) staining of the iPSC colonies demonstrating the expression of alkaline phosphatase (one of the pluripotent cell markers). Scale 100 μm.

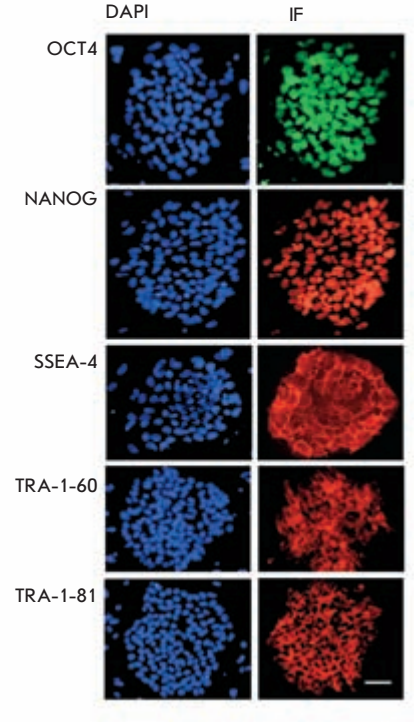

Fig. 3. Immunocytochemical staining (IF) of iPSC colonies with antibodies against the transcription factors OCT4 (green) and NANOG (red) and against the surface antigens SSEA-4, TRA-1-60, and TRA-1-81 (red). Cell nuclei are counterstained with DAPI (blue). Scale 100 μm.

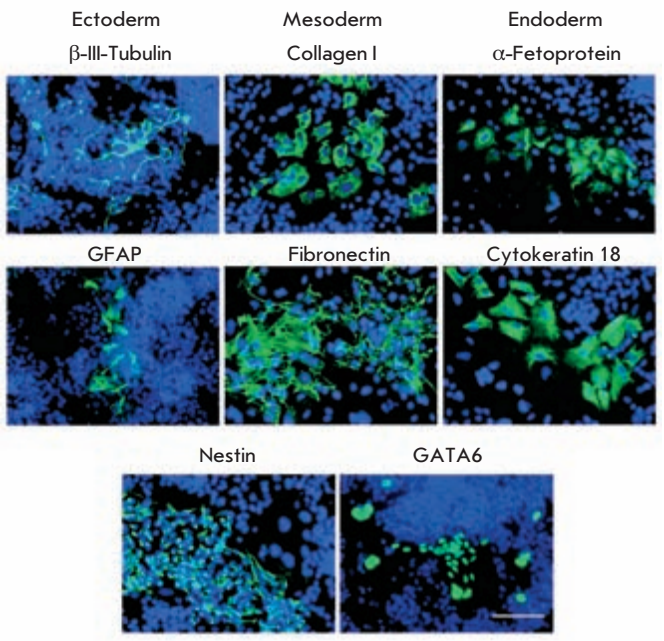

Fig. 5. Expression of gene markers characterizing three germ layers (ectoderm, mesoderm, and endoderm) in spontaneous differentiation of iPSC in embryoid bodies. Scale 100 μm.

Thus, we have shown that the expression of the murine *Oct4*, *Sox2*, *c-Myc*, and *Klf4* genes in human cells can result in their reprogramming with the formation of stable iPSC clones that are very similar in their features to human ESCs. Reprogramming fibroblasts using retroviral constructs is a replicable method allowing the accumulation of a great amount of pluripotent cell clones in a relatively short time. ●

This study was supported by the Russian Academy of Sciences' Presidium Program "Molecular and Cell Biology."

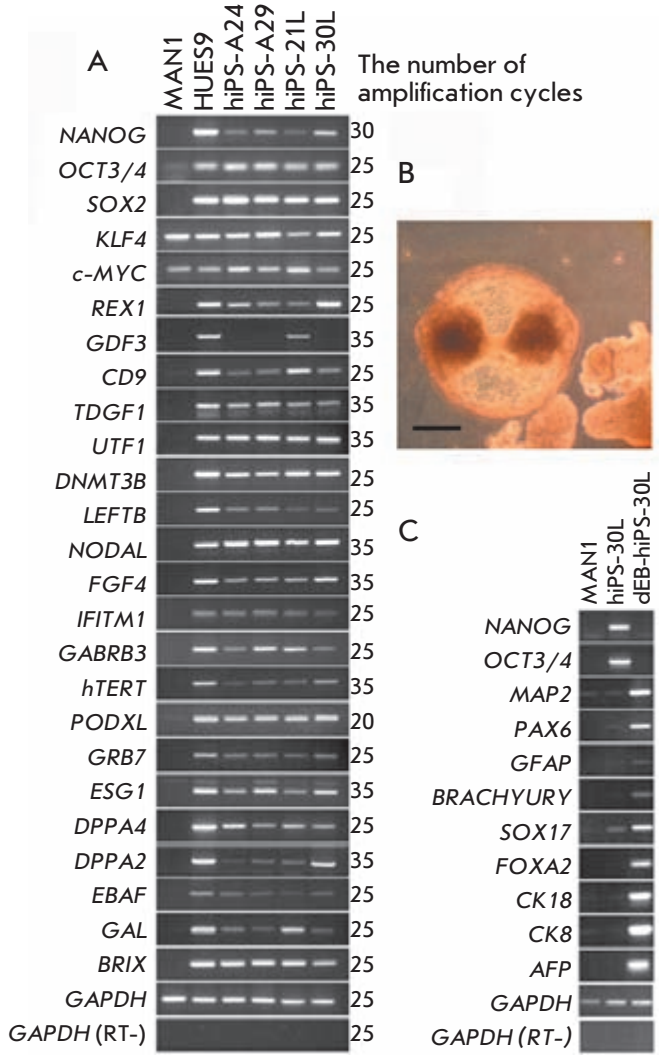

Fig. 4. (A) RT-PCR assay of gene transcripts, which are the markers of human embryonic stem cells, in embryonic fibroblasts (MA N1), human embryonic stem cells (HUES9), and four iPSC lines: hiPS-A24, hiPS-A29, hiPS-21L, and hiPS-30L; (B) embryoid bodies formed following the passage of hiPS-30L iPSC cells in suspension culture, scale 100 μm; (C) RT-PCR assay of gene transcripts, which are the markers of three germ layers (ectoderm, mesoderm, and endoderm), following the differentiation of the hiPS-30L clone via the embryoid body formation.

REFERENCES

1. Yamanaka S. // Cell. 2009. V. 137. P. 13–17.
2. Park I.H., Arora N., Huo H., et al. // Cell. 2008. V. 134. P. 877–886.
3. Ebert A.D., Yu J., Rose F.F., Jr., et al. // Nature. 2009. V. 457. P. 277–280.
4. Lee G., Papapetrou E.P., Kim H., et al. // Nature. 2009. V. 461. P. 402–406.
5. Takahashi K., Yamanaka S. // Cell. 2006. V. 126. P. 663–676.
6. Takahashi K., Tanabe K., Ohnuki M., et al. // Cell. 2007. V. 131. P. 861–872.

Acta Naturae is a new international journal on life sciences based in Moscow, Russia. Our goal is to present scientific work and discovery in molecular biology, biochemistry, biomedical disciplines and biotechnology. *Acta Naturae* is also a periodical for those who are curious in various aspects of biotechnological business, intellectual property protection and social consequences of scientific progress.

For more information and subscription
please contact us at info@biorf.ru

GENERAL RULES

Actae Naturae publishes experimental articles and reviews, as well as articles on topical issues, short reviews, and reports on the subjects of basic and applied life sciences and biotechnology.

The journal is published by the Park Media publishing house in both Russian and English.

The journal *Acta Naturae* is on the list of the leading periodicals of the Higher Attestation Commission of the Russian Ministry of Education and Science

The editors of *Actae Naturae* ask of the authors that they follow certain guidelines listed below. Articles which fail to conform to these guidelines will be rejected without review. The editors will not consider articles whose results have already been published or are being considered by other publications.

The maximum length of a review, together with tables and references, cannot exceed 60,000 symbols (approximately 40 pages, A4 format, 1.5 spacing, Times New Roman font, size 12) and cannot contain more than 16 figures.

Experimental articles should not exceed 30,000 symbols (20 pages in A4 format, including tables and references). They should contain no more than ten figures. Lengthier articles can only be accepted with the preliminary consent of the editors.

A short report must include the study's rationale, experimental material, and conclusions. A short report should not exceed 12,000 symbols (8 pages in A4 format including no more than 12 references). It should contain no more than four figures.

The manuscript should be sent to the editors in electronic form: the text should be in Windows Microsoft Word 2003 format, and the figures should be in TIFF format with each image in a separate file. In a separate file there should be a translation in English of: the article's title, the names and initials of the authors, the full name of the scientific organization and its departmental affiliation, the abstract, the references, and figure captions.

MANUSCRIPT FORMATTING

The manuscript should be formatted in the following manner:

- Article title. Bold font. The title should not be too long or too short and must be informative. The title should not exceed 100 characters. It should reflect the major result, the essence, and uniqueness of the work, names and initials of the authors.
- The corresponding author, who will also be working with the proofs, should be marked with a footnote *.
- Full name of the scientific organization and its departmental affiliation. If there are two or more scientific organizations involved, they should be linked by digital superscripts with the authors' names. Abstract. The structure of the abstract should be very clear and must reflect the following: it should introduce the reader to the main issue and describe the experimental approach, the possibility of practical use, and the possibility of further research in the field. The average length of an abstract is 20 lines (1,500 characters).
- Keywords (3 – 6). These should include the field of research, methods, experimental subject, and the specifics of the work. List of abbreviations.
- INTRODUCTION
- EXPERIMENTAL PROCEDURES
- RESULTS AND DISCUSSION
- CONCLUSION

  The organizations that funded the work should be listed at the end of this section with grant numbers in parenthesis.
- REFERENCES

  The in-text references should be in brackets, such as [1].

RECOMMENDATIONS ON THE TYPING AND FORMATTING OF THE TEXT

- We recommend the use of Microsoft Word 2003 for Windows text editing software.
- The Times New Roman font should be used. Standard font size is 12.
- The space between the lines is 1.5.
- Using more than one whole space between words is not recommended.
- We do not accept articles with automatic referencing; automatic word hyphenation; or automatic prohibition of hyphenation, listing, automatic indentation, etc.
- We recommend that tables be created using Word software options (Table → Insert Table) or MS Excel. Tables that were created manually (using lots of spaces without boxes) cannot be accepted.
- Initials and last names should always be separated by a whole space; for example, A. A. Ivanov.
- Throughout the text, all dates should appear in the "day.month.year" format, for example 02.05.1991, 26.12.1874, etc.
- There should be no periods after the title of the article, the authors' names, headings and subheadings, figure captions, units (s – second, g – gram, min – minute, h – hour, d – day, deg – degree).
- Periods should be used after footnotes (including those in tables), table comments, abstracts, and abbreviations (mon. – months, y. – years, m. temp. – melting temperature); however, they should not be used in subscripted indexes (T_m – melting temperature; $T_{p.t}$ – temperature of phase transition). One exception is mln – million, which should be used without a period.
- Decimal numbers should always contain a period and not a comma (0.25 and not 0,25).
- The hyphen ("-") is surrounded by two whole spaces, while the "minus," "interval," or "chemical bond" symbols do not require a space.
- The only symbol used for multiplication is "×"; the "×" symbol can only be used if it has a number to its right. The "·" symbol is used for denoting complex compounds in chemical formulas and also noncovalent complexes (such as DNA·RNA, etc.).

- Formulas must use the letter of the Latin and Greek alphabets.
- Latin genera and species' names should be in italics, while the taxa of higher orders should be in regular font.
- Gene names (except for yeast genes) should be italicized, while names of proteins should be in regular font.
- Names of nucleotides (A, T, G, C, U), amino acids (Arg, Ile, Val, etc.), and phosphonucleotides (ATP, AMP, etc.) should be written with Latin letters in regular font.
- Numeration of bases in nucleic acids and amino acid residues should not be hyphenated (T34, Ala89).
- When choosing units of measurement, SI units are to be used.
- Molecular mass should be in Daltons (Da, KDa, MDa).
- The number of nucleotide pairs should be abbreviated (bp, kbp).
- The number of amino acids should be abbreviated to aa.
- Biochemical terms, such as the names of enzymes, should conform to IUPAC standards.
- The number of term and name abbreviations in the text should be kept to a minimum.
- Repeating the same data in the text, tables, and graphs is not allowed.

GUIDENESS FOR ILLUSTRATIONS

- Figures should be supplied in separate files. Only TIFF is accepted.
- Figures should have a resolution of no less than 300 dpi for color and half-tone images and no less than 500 dpi.
- Files should not have any additional layers.

REVIEW AND PREPARATION OF THE MANUSCRIPT FOR PRINT AND PUBLICATION

Articles are published on a first-come, first-served basis. The publication order is established by the date of acceptance of the article. The members of the editorial board have the right to recommend the expedited publishing of articles which are deemed to be a priority and have received good reviews.

Articles which have been received by the editorial board are assessed by the board members and then sent for external review, if needed. The choice of reviewers is up to the editorial board. The manuscript is sent on to reviewers who are experts in this field of research, and the editorial board makes its decisions based on the reviews of these experts. The article may be accepted as is, sent back for improvements, or rejected.

The editorial board can decide to reject an article if it does not conform to the guidelines set above.

A manuscript which has been sent back to the authors for improvements requested by the editors and/or reviewers is reviewed again, after which the editorial board makes another decision on whether the article can be accepted for publication. The published article has the submission and publication acceptance dates set at the beginning.

The return of an article to the authors for improvement does not mean that the article has been accepted for publication. After the revised text has been received, a decision is made by the editorial board. The author must return the improved text, together with the original text and responses to all comments. The date of acceptance is the day on which the final version of the article was received by the publisher.

A revised manuscript must be sent back to the publisher a week after the authors have received the comments; if not, the article is considered a resubmission.

E-mail is used at all the stages of communication between the author, editors, publishers, and reviewers, so it is of vital importance that the authors monitor the address that they list in the article and inform the publisher of any changes in due time.

After the layout for the relevant issue of the journal is ready, the publisher sends out PDF files to the authors for a final review.

Changes other than simple corrections in the text, figures, or tables are not allowed at the final review stage. If this is necessary, the issue is resolved by the editorial board.

FORMAT OF REFERENCES

The journal uses a numeric reference system, which means that references are denoted as numbers in the text (in brackets) which refer to the number in the reference list.

For books: the last name and initials of the author, full title of the book, location of publisher, publisher, year in which the work was published, and the volume or issue and the number of pages in the book.

For periodicals: the last name and initials of the author, title of the journal, year in which the work was published, volume, issue, first and last page of the article.

Bressanelli S., Tomei L., Roussel A., et al // Proc. Natl. Acad. Sci. USA. 1999. V. 96. P.13034–13039 (If there are more than five authors). If there are less than five authors, all the authors must be listed.

References to books which have Russian translations should be accompanied with references to the original material listing the required data.

References to doctoral thesis abstracts must include the last name and initials of the author, the title of the thesis, the location in which the work was performed, and the year of completion.

References to patents must include the last names and initials of the authors, the type of the patent document (the author's rights or patent), the patent number, the name of the country that issued the document, the international invention classification index, and the year of patent issue.

The list of references should be on a separate page. The tables should be on a separate page, and figure captions should also be on a separate page.

The following e-mail addresses can be used to contact the editorial staff: vera.knorre@gmail.com, actanaturae@gmail.com, tel.: (495) 727-38-60, (495) 930-80-05

I International Scientific Practical Conference

Postgenomic Methods of Analysis in Biology, Laboratory and Clinical Medicine

November 17-19, 2010

Organizers

Federal Agency for Medicine and Biology;
Scientific Research Institute of Physical-Chemical Medicine;
Lomonosov Moscow State University;
Park-Media Publishing Company

Conference sponsors:

Ministry of Education and Science of the Russian Federation;
Russian Academy of Medical Sciences;
Siberian Branch, Russian Academy of Sciences.

Among other issues, the conference will feature

The performances of Russian and foreign scientists (statements);
Seminars and free discussions;
Lectures and reports;
An exhibition;
A host of other issues.

Location:

Moscow, Lomonosov MSU, building 51.

CONTACT INFORMATION:

Tel.: +7 (495) 930 8850, 930 8707

E-mail: info@postgenom.ru

www.postgenom.ru